UNIVERSITÉ PARIS-EST

Thèse présentée pour obtenir le grade de

Docteur de l'Université Paris-Est

Spécialité : Sciences et Techniques de l'Environnement

par

Yi Hong

Ecole Doctorale : SCIENCES, INGENIERIE ET ENVIRONNEMENT

Modélisation distribuée à base physique du transfert hydrologique des polluants routiers de l'échelle locale à l'échelle du quartier.

Thèse soutenue le 3 janvier 2017 devant le jury composé de :

Jean-Luc Bertrand-Krajewski	*Rapporteur*
Victor Jetten	*Rapporteur*
Ludovic Leclercq	*Examinateur*
Fabrice Rodriguez	*Examinateur*
Stephane Cordier	*Examinateur*
Minh-Hoang Le	*Examinateur*
Céline Bonhomme	*Co-encadrante de thèse*
Ghassan Chebbo	*Directeur de thèse*

Remerciements

A l'heure d'écrire ces remerciements, je suis ravi que finalement, je puisse profiter de ces lignes pour remercier toutes les personnes qui ont fait de cette expérience unique dans ma vie.

J'aimerais tout d'abord remercier mes deux encadrants de thèse. Monsieur Ghassan Chebbo, coordinateur du programme OPUR (Observatoire des Polluants URbains), a été mon directeur de thèse. Je souhaite le remercier pour m'avoir fait découvrir ce programme de recherche très actif pour échanger des idées avec ses membres scientifiques et opérationnels. Je lui adresse mes sincères remerciements pour ses idées scientifiques enrichissantes, son soutien, ses encouragements, sa bonne humeur et sa gentillesse. Madame Céline Bonhomme, co-coordinatrice du projet Trafipollu, a été ma co-encadrante de thèse. Je souhaite la remercier pour m'avoir permis d'intégrer ce projet de recherche complet et passionnant. Je tiens à lui exprimer ma plus profonde gratitude pour sa disponibilité pour répondre à mes interrogations et mes incertitudes, pour son investissement très important à mes côtés pour me guider, pour le temps consacré aux améliorations des articles et du manuscrit de thèse et pour ses nombreux conseils. De plus, je voudrais exprimer un remerciement spécial à mes encadrants pour avoir surmonté les difficultés liées aux perturbations externes (notamment la fin de ma deuxième année de thèse) par leur confiance en moi et leurs encouragements. Grâce à eux j'ai appris beaucoup, non seulement en modélisation, mais également en persévérance et en rigueur.

J'adresse mes remerciements à l'ensemble des membres de mon jury: M. Jean-Luc Bertrand-Krajewski et M. Victor Jetten, qui m'ont fait l'honneur de bien vouloir y participer en tant que rapporteurs, ainsi que M. Ludovic Leclercq, M. Fabrice Rodriguez, M. Stephane Cordier et M. Minh-Hoang Le qui a accepté de participer à l'évaluation de ce travail.

Un grand merci à M. Minh-Hoang Le (LHSV), M. Victor Jetten, et M. Bastrian Bout (ITC, Pays-Bas), pour leurs aides précieuses au développement des modèles..

Je tiens à remercier les différents partenaires du projet Trafipollu de nous avoir fourni des données. Je remercie B. Soleilhan (IGN) et V. Bousquet (IGN-Conseil) pour les données SIG; F. Mahe et F. Dugay (AirParif), C. Seigneur et L. Thouron (CEREA) pour les données atmosphériques; B. Béchet (IFSTTAR), D. Ramier (CEREMA), M. Saad et P. Dubois (LEESU) pour les données mesurées.

Je suis également reconnaissant envers tous les thésards et l'équipe du personnel du LEESU. Je ne pourrai jamais oublier les gâteaux dans le cafétéria, les petits dessins sur les tableaux et sur les portes, les plats internationaux lors des Leesuriales, les séances de sport (tennis, PingPong, etc.), les dîners doctorants, les photos sur le groupe Twitter, etc... Merci: Claire, Yujie, Neng, Annick, Natalie, Saja, Mohamad, Damien, Kelsey, Denis ...

最后，我要特别感谢我的爱人苏真珍，是她一直以来的鼓励、支持和宽容让我始终能够用饱满的热情和积极的态度去面对攻读博士过程中的各种艰难险阻。衷心感谢我的父亲洪志贵，母亲步长华，他们一直是我最坚强的后盾，给予我最坚定的支持，让我即使出国在外，也完全没有后顾之忧。爸爸妈妈，我爱你们！希望你们永远健康快乐！

Résumé

Le développement des réseaux séparatifs entraîne le transfert fréquent de polluants urbains vers les milieux récepteurs (plans d'eau, rivières, etc.). La compréhension des processus de production et de lessivage des polluants dans le milieu urbain est pourtant incomplète à l'heure actuelle. Afin de répondre aux questions liées à la gestion des eaux urbaines, l'amélioration des connaissances des processus physiques est nécessaire, tant au niveau des surfaces urbaines que les réseaux d'assainissement. Pour cela, la modélisation du transfert hydrologique des polluants en milieu urbain peut être un outil précieux.

Cette thèse a pour objectif de développer et d'analyser des modèles distribués à base physique pour simuler les flux de polluants routiers (Matières En Suspension (MES), Hydrocarbures, Métaux) dans un environnement urbain. Elle s'inscrit dans le cadre du projet ANR "Trafipollu" et bénéficie des résultats expérimentaux mis en œuvre dans ce projet pour la calibration et validation des modèles utilisés. Le travail de thèse s'articule autour de deux échelles de modélisation : l'échelle locale et l'échelle du quartier.

A l'échelle locale, le code FullSWOF (volumes finis, schéma numérique d'ordre 2) couplé au modèle d'érosion d'Hairsine and Rose (1992a; 1992b) et des données géographiques très détaillées (résolution spatiale centimétrique) ont été utilisés et adaptés afin d'améliorer nos connaissances des processus physiques du lessivage des polluants sur les surfaces urbaines. La comparaison aux mesures en continu permet d'évaluer la performance d'une modélisation physique pour représenter les variations spatiales et temporelles des processus de transferts des polluants sur les surfaces urbaines. Les analyses des résultats obtenus permettent de constater la prédominance des effets d'arrachement liés à la pluie sur les processus d'entrainement par l'advection sur la majeure partie du bassin versant routier. L'utilisation d'un modèle d'érosion pour modéliser le transport particulaire en zone urbaine est une innovation importante de cette thèse.

A l'échelle du quartier, la deuxième étape du travail consiste à coupler séquentiellement le modèle TREX (Velleux, England, et al., 2008) avec le modèle CANOE (Alison, 2005), nommé "TRENOE" plateforme. En changeant différentes options de mise en œuvre et de configurations du modèle, l'adaptation de la précision numérique et l'utilisation de données détaillées d'occupation du sol semblent être les facteurs clés pour une telle modélisation. Par ailleurs, ce couplage a montré des problèmes de fond tels que la modélisation du schéma numérique des

flux en surface (seulement dans 4 directions), ainsi que l'utilisation de l'équation USLE pour simuler l'érosion en milieu urbain, ne comprenant pas d'impact des gouttes de pluie pour la modélisation.

Pour remédier à ces défauts, la plateforme opensource LISEM-SWMM est développée en couplant le modèle LISEM (De Roo, Wesseling, et al., 1996), modèle d'érosion développé initialement pour le milieu naturel, et le modèle SWMM (Rossman, 2010). Pour la première fois, la modélisation hydrologique s'appuie aussi sur l'utilisation de sorties de modèles atmosphériques pour les dépôts des particules fines (PM10), hydrocarbures et métaux. Les résultats montrent que l'emploi de modèles totalement distribués peut arriver à reproduire de manière très fine les dynamiques des particules, des hydrocarbures et des métaux. Même si à ce stade la plateforme développée nécessite des améliorations pour adapter aux utilisations dans le champ opérationnel, ceci constitue une avancée pour le domaine de modélisation du transfert hydrologique des polluants routiers en milieu urbain.

Mots Clés

Modélisation distribuée à base physique; Modélisation intégrée;

Modélisation du lessivage sur les surfaces urbaines; Modélisation 2D - 1D;

Qualité des eaux pluviales urbaines; Polluants liés au trafic routier;

Données Lidar haute résolution; Occupation du sol urbain;

Arrachement liés aux gouttes de pluie; Entrainement par le ruissellement;

Analyse de sensibilité; Dépositions atmosphériques.

Abstract

Nowadays, the increasing use of separate stormwater systems causes a frequent transport of urban pollutants into receiving water bodies (lakes, rivers). However, current studies still lack of the knowledge of urban build-up and wash-off processes. In order to address urban management issues, better understanding of physical mechanism is required not only for the urban surfaces, but also for the sewer systems. In this context, the modelling of hydrological transfer of urban pollutants can be a valuable tool.

This thesis aims to develop and assess the physically-based and distributed models to simulate the transport of traffic-related pollutants (suspended solids, hydrocarbons, heavy metals) in urban stormwater runoffs. This work is part of the ANR "Trafipollu" project, and benefit from the experimental results for model calibration and validation. The modelling is performed at two scales of the urban environment: at the local scale and at the city district scale.

At the local scale of urban environment, the code FullSWOF (second-order finite volume scheme) coupled with Hairsine and Rose model (1992a; 1992b) and detailed monitoring surveys is used to evaluate urban wash-off process. Simulations over different rainfall events represent promising results in reproducing the various dynamics of water flows and particle transfer on the urban surfaces. Spatial analysis of wash-off process reveals that the rainfall-driven impacts are two orders of magnitude higher than flow-drive effects. These findings contribute to a significant improvement in the field of urban wash-off modelling. The application of soil erosion model to the urban context is also an important innovation.

At the city district scale, the second step consists of coupling the TREX model (Velleux, England, et al., 2008) and the CANOE model, named "TRENOE" platform. By altering different options of model configurations, the adequate numerical precision and the detailed information of landuse data are identified as the crucial elements for achieving acceptable simulations. Contrarily, the high-resolution topographic data and the common variations of the water flow parameters are not equally significant at the scale of a small urban catchment. Moreover, this coupling showed fundamental problems of the model structure such as the numerical scheme of the overland flow (only 4 directions), and the empirical USLE equations need to be completed by raindrop detachment process.

To address these shortcomings, the LISEM - SWMM platform is developed by coupling the open-source LISEM model (De Roo, Wesseling, et al., 1996), which is initially developed for soil erosion simulations, and the SWMM model (Rossman, 2010). For the first time, the hydrological model is also supported by the simulations

of atmospheric dry deposits of fine particles (PM10), hydrocarbons and heavy metals. The performance of water flow and TSS simulations are satisfying with the calibrated parameters. Considering the hydrocarbons and heavy metals contents of different particle size classes, simulated event mean concentration of each pollutant is comparable to local in-situ measurements. Although the platform at current stage still needs improvements in order to adapt to the operational applications, the present modelling approach contributes to an innovative technology in the field of modelling of hydrological transfer of the traffic-related pollutants in urban environment.

Key words

Physically based and distributed modelling;

Integrated modelling;

Urban wash-off modelling;

2D - 1D modelling;

Urban stormwater quality;

Traffic - related pollutants;

High-resolution LiDAR data;

Detailed urban landuse;

Raindrop - driven detachment;

Flow - driven detachment;

Sensitivity analysis;

Atmospheric deposition.

Sommaire

Chapitre 1. Contexte de la thèse

1.1. L'hydrologie urbaine

Aujourd'hui, 54% de la population mondiale vivent dans les villes, une proportion qui devrait passer à 66% en 2050 (ONU, 2014). Cet afflux massif d'habitants implique une expansion rapide des zones urbaines. La forte tendance de l'urbanisation se traduit donc par une imperméabilisation importante des sols naturels, qui modifie les mécanismes du ruissellement pluvial en surface, tant du point de vue quantitatif (débit, volume) que qualitatif (pollutions urbaines).

En milieu urbain, la présence de surfaces imperméables et de réseaux d'assainissement sont des facteurs fondamentaux du fonctionnement hydrologique du bassin versant. Les impacts de ces deux phénomènes sur le cycle de l'eau en milieu urbain ont été beaucoup étudiés par de nombreux chercheurs et ingénieurs (Bressy et al., 2012; Elliott and Trowsdale, 2007; Fletcher et al., 2013; Petrucci et al., 2014; Zoppou, 2001). Les effets de l'urbanisation sont généralement les suivants:

- Augmentation des débits de pointe par temps de pluie;
- Augmentation des volumes de ruissellement;
- Diminution du temps de réponse du bassin versant;
- Diminution de l'infiltration vers la nappe;
- Augmentation des charges polluantes, notamment pour les métaux lourds et les Hydrocarbures Aromatiques Polycycliques (HAPs);
- Dégradation de la qualité des milieux récepteurs.

L'hydrologie urbaine a pour objectif de développer et d'améliorer les systèmes de gestion des eaux urbaines, afin (i) de protéger les populations contre les risques sanitaires; (ii) de protéger la ville contre les inondations; (iii) de protéger les milieux aquatiques contre les rejets polluants.

1.2 Pollution des eaux de ruissellement urbaines

Depuis les années 1990, les eaux de ruissellement en milieu urbain sont considérées comme une source importante de pollution des milieux aquatiques (Estebe et al., 1997; Fisher et al., 1999). D'après la Directive Cadre sur l'Eau (DCE) 2000/60/CEE, une liste de 33 substances ou groupes de substances prioritaires dans les eaux pluviales a été établie le 7 février 2000. Cette liste comprend 10 pesticides

(par exemple, Alachlore, Chlorfenvinphos, etc.), 4 métaux (par exemple, Nickel, Plomb, etc.), et 19 substances organiques diverses (par exemple, Hydrocarbures Aromatiques Polycycliques (HAPs), Phtalates, Polychlorobiphényles (PABs), etc.) (Legret and Pagotto, 1999; Sabin et al., 2005; Zgheib et al., 2012). Les impacts des rejets urbains de temps de pluie sur les masses d'eau réceptrices dépendent de la nature, des concentrations et des effets cumulés de plusieurs contaminants. Les sources possibles des polluants dans les eaux de ruissellement sont présentées dans le Tableau 1.1:

Tableau 1.1 Les origines des polluants dans les eaux de ruissellement.

	Déchets	Entretien	Freinage	Pneus	Carrosserie	Carburant	Dépôts atmosphériques
Solides	■		■	■	■		■
Cadmium	■			■			■
Chrome	■			■	■		■
Cuivre	■		■	■	■		■
Fer	■			■	■		■
Plomb	■				■		■
Nickel	■			■	■		■
Zinc	■		■	■	■		■
HAPs				■		■	■
PCB	■						■
Pesticides	■	■					
Nutriments	■	■					■
Autres polluants	■	■					■

Les travaux de recherche effectués pour la caractérisation des effluents de temps de pluie ont montré que les concentrations de MES sont le vecteur principal des polluants des rejets urbains par temps de pluie (Aryal et al., 2010; Bressy et al., 2012; Chebbo, 1992; Gasperi et al., 2014a). Parmi les différents contaminants, la plupart des HAPs, Chrome (Cr), Cuivre (Cu), Fer (Fe) et Nickel (Ni) sont associés aux MES. Par contre, les concentrations de Zinc (Zn) et Cadmium (Cd) en phase dissoute et particulaire dans les eaux pluviales sont très variables.

Par ailleurs, les nutriments (azote et phosphore) qui sont souvent sous forme dissoute, sont des facteurs essentiels causant des phénomènes d'eutrophisation dans les milieux aquatiques. Dans un milieu urbain, les nutriments proviennent généralement des engrais utilisés pour les jardins, les pelouses, les terrains de sport (golf, tennis, football). En revanche, le trafic automobile est une origine secondaire

d’azote dans les eaux de ruissellement (Wakida and Lerner, 2005; Waschbusch et al., 1999). Par conséquent, les contaminants azotés et phosphorés ne sont pas étudiés dans cette thèse.

1.2.1 Polluants liés au trafic routier

Les émissions dues au trafic routier représentent une source importante de polluants des eaux de ruissellement dans les villes et les zones périurbaines (Fletcher et al., 2013; Petrucci et al., 2014; Shorshani et al., 2013). Par ailleurs, les réseaux d'assainissement séparatifs sont fréquemment utilisés dans les zones urbaines. Ils transportent les eaux de ruissellement vers le milieu aquatique. Une conséquence du transport de ces polluants liés au trafic routier est la dégradation des milieux récepteurs ainsi que de l'écosystème aquatique (Shirley Clark, 2007). Conformément à la DCE (2000/60/CEE), la réduction des micropolluants est un des objectifs principaux pour les zones urbaines. Il est donc essentiel de mieux comprendre les processus de génération et de transport des polluants liés au trafic routier lors des événements pluvieux.

Les polluants principaux tels que les particules, ETMs, et HAPs sont d'abord émis dans l'atmosphère avec le trafic (Gunawardena et al., 2013); ensuite, ces polluants dans la phase atmosphérique se dispersent et se déposent sur les surfaces en formant des dépôts secs ou humides (Huston et al., 2009); enfin, ces contaminants diffus peuvent être entraînés par le ruissellement des eaux pluviales. Les polluants des eaux de ruissellement ne sont cependant pas seulement reliés au degré de contamination atmosphérique et d'autres processus contribuent à la contamination des surfaces et des effluents urbains (Gasperi et al., 2014a). En particulier, le trafic automobile génère aussi des particules grossières (par exemple, abrasion de la surface routière) qui ont des temps de vol faibles et ne sont pas comptabilisées dans les polluants d’origine atmosphérique. Les surfaces urbaines sont aussi réceptrices d’autres sources de contamination directe, par les passants, les animaux domestiques, l’entretien des voiries et espaces verts. Enfin, les dépôts atmosphériques ne sont pas uniquement dus au trafic routier, mais sont également dus à l’intégration à grande échelle de toutes les sources de contamination (industries, chauffage urbain).

Les contaminants émis par le trafic automobile peuvent être regroupés en deux catégories: forme dissoute et particulaire. Concernant les HAP et les métaux, de nombreuses études montrent une prédominance de la fraction particulaire (Bressy et al., 2012; Gasperi et al., 2014b; Kafi et al., 2008). Les particules vectrices de contaminants peuvent être de différentes tailles. Les particules grossières sont déposées directement sur les surfaces. Les particules fines sont pour certaines dispersées dans l'atmosphère et pour d’autres déposées directement sur les

surfaces urbaines. Les particules atmosphériques sont ensuite déposées lors du temps sec (dépôts secs) mais aussi lessivées pendant la pluie (dépôts humides). Comme les particules de tailles inférieures à 10 μm (notées PM10) sont à l'origine de nombreuses pathologies humaines (par exemple, inflammations, maladies coronariennes et pulmonaires), la séparation des particules fines et grossières est habituellement basée sur le critère de 10 μm.

En flux massique, les dépôts secs de polluants atmosphériques sont prédominants par rapport aux dépôts humides (Chu et al., 2008; Gunawardena, 2012). Au contraire, les dépôts humides, bien que parfois supérieurs aux dépôts secs en flux instantanés, sont finalement négligeables devant les dépôts secs, compte tenu de la durée annuelle de pluie comparée à la durée de temps sec. Le transfert des polluants émis par le trafic automobile dans le milieu urbain est illustrée dans la figure 1.1.

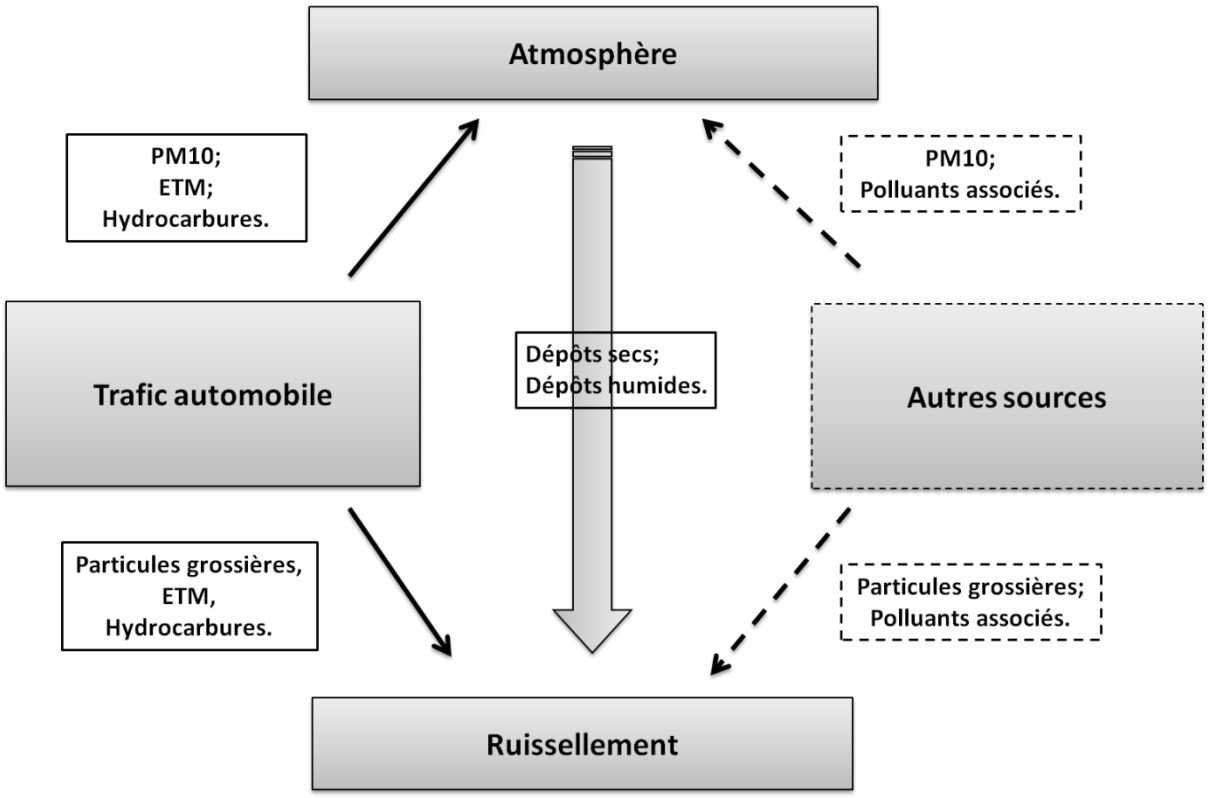

Fig. 1.1 Transfert des polluants liés au trafic dans le milieu urbain.

1.3 Contexte de développement: le projet ANR-Trafipollu

Dans le cadre de l'étude des polluants liés au trafic routier, le projet Trafipollu a été sélectionné par l'appel d'offre de l'ANR-VBD 2012 (Ville et Bâtiment Durable) et a été lancé en Avril 2013. L'origine du projet Trafipollu est le projet « Ville Numérique »

(2009 - 2014) qui visait à produire des outils numériques pour améliorer la connaissance et la gestion de la ville.

L'objectif principal du projet Trafipollu est de développer des outils de modélisation permettant de réaliser des cartographies caractérisant la dynamique et la localisation des polluants générés par le trafic en milieu urbain. La résolution spatiale et temporelle de ces cartographies varie selon les échelles considérées (de l'échelle locale à l'échelle urbaine). Pour atteindre cet objectif, le projet comporte d'abord une expérimentation de grande ampleur. Cette expérimentation comprend des observations multi-milieux (trafic, air, eau, sol), sur un même site fortement circulé et à des échelles de temps et d'espace très fines. Les observations réalisées doivent permettre de calibrer et d'évaluer les modèles proposés.

Plus généralement, l'objectif du projet est de mettre en œuvre des chaînes de modélisation à différentes échelles urbaines (rue, quartier et ville), afin de prévoir (i) le comportement du trafic, (ii) les émissions de polluants associés, (iii) la dispersion des polluants dans l'atmosphère, (iv) le dépôt des polluants sur les surfaces urbaines, et (v) leur transfert sur les surfaces urbaines (sols, chaussées) et dans le réseau d'assainissement.

Ce projet est organisé en 4 work-packages : WP1 : Couplage multi-physiques à l'échelle local : étude fine des polluants en bordure de voirie (responsable : C. Bonhomme - ENPC/LEESU) ; WP2 : Etude fine des polluants associés au trafic à l'échelle d'un quartier ou d'un aménagement structurant (responsable : Katia Chancibault - IFSTTAR/IRSTV) ; WP3 : Analyse des pollutions associées au trafic à l'échelle de l'agglomération (responsable : C. Seigneur - ENPC/CEREA) ; WP4 : Données (responsable : B. Soheilian - IGN/MATIS).

Cette thèse s'inscrit de manière transversale dans les WP1 (échelle locale) et WP2 (échelle du quartier).

Référence

Aryal, R., Vigneswaran, S., Kandasamy, J., Naidu, R., 2010. Urban stormwater quality and treatment. Korean J. Chem. Eng. 27, 1343–1359. doi:10.1007/s11814-010-0387-0

Bressy, A., Gromaire, M.-C., Lorgeoux, C., Saad, M., Leroy, F., Chebbo, G., 2012. Towards the determination of an optimal scale for stormwater quality management: Micropollutants in a small residential catchment. Water Res. 46, 6799–6810. doi:10.1016/j.watres.2011.12.017

Chebbo, G., 1992. Solides des rejets pluviaux urbains : caractérisation et traitabilité. Ecole Nationale des Ponts et Chaussées,, France.

Chu, C.-C., Fang, G.-C., Chen, J.-C., Yang, I.-L., 2008. Dry deposition study by using dry deposition plate and water surface sampler in Shalu, central Taiwan. Environ. Monit. Assess. 146, 441–451. doi:10.1007/s10661-007-0090-8

Elliott, A.H., Trowsdale, S.A., 2007. A review of models for low impact urban stormwater drainage. Environ. Model. Softw., Special section: Advanced Technology for Environmental Modelling 22, 394–405. doi:10.1016/j.envsoft.2005.12.005

Estebe, A., Boudries, H., Mouchel, J., Thevenot, D., 1997. Urban runoff impacts on particulate metal and hydrocarbon concentrations in river seine: Suspended solid and sediment transport. Water Sci. Technol. 36, 185–193. doi:10.1016/S0273-1223(97)00600-8

Fisher, T.S., Hayward, D.G., Stephens, R.D., Stenstrom, M.K., 1999. Dioxins and Furans Urban Runoff. J. Environ. Eng. 125, 185–191. doi:10.1061/(ASCE)0733-9372(1999)125:2(185)

Fletcher, T.D., Andrieu, H., Hamel, P., 2013. Understanding, management and modelling of urban hydrology and its consequences for receiving waters: A state of the art. Adv. Water Resour. 51, 261–279. doi:10.1016/j.advwatres.2012.09.001

Gasperi, J., Geara, D., Lorgeoux, C., Bressy, A., Zedek, S., Rocher, V., El Samrani, A., Chebbo, G., Moilleron, R., 2014a. First assessment of triclosan, triclocarban and paraben mass loads at a very large regional scale: Case of Paris conurbation (France). Sci. Total Environ. 493, 854–861. doi:10.1016/j.scitotenv.2014.06.079

Gasperi, J., Gromaire, M.-C., Moilleron, R., Caupos, E., Varrault, G., Bonhomme, C., Bressy, A., Lemaire, B., Vinçon-Leite, B., Chebbo, G., 2014b. Micropolluants dans les eaux pluviales et les eaux usées : de leur caractérisation à leur traitement. Presented at the Workshop 02/10 INTERZA - Micropolluants au sein des ZA : Mesures, traitements et changements de pratiques.

Gunawardena, J., Egodawatta, P., Ayoko, G.A., Goonetilleke, A., 2013. Atmospheric deposition as a source of heavy metals in urban stormwater. Atmos. Environ. 68, 235–242. doi:10.1016/j.atmosenv.2012.11.062

Gunawardena, J.M.A., 2012. Relating vehicle generated pollutants to urban stormwater quality. Queensland university of Technology.

Huston, R., Chan, Y.C., Gardner, T., Shaw, G., Chapman, H., 2009. Characterisation of atmospheric deposition as a source of contaminants in urban rainwater tanks. Water Res. 43, 1630–1640. doi:10.1016/j.watres.2008.12.045

Kafi, M., Gasperi, J., Moilleron, R., Gromaire, M.C., Chebbo, G., 2008. Spatial variability of the characteristics of combined wet weather pollutant loads in Paris. Water Res. 42, 539–549. doi:10.1016/j.watres.2007.08.008

Legret, M., Pagotto, C., 1999. Evaluation of pollutant loadings in the runoff waters from a major rural highway. Sci. Total Environ. 235, 143–150. doi:10.1016/S0048-9697(99)00207-7

ONU, 2014. Perspectives de l'urbanisation mondiale. L'Organisation des Nations unies.

Petrucci, G., Gromaire, M.-C., Shorshani, M.F., Chebbo, G., 2014. Nonpoint source pollution of urban stormwater runoff: a methodology for source analysis. Environ. Sci. Pollut. Res. Int. 21, 10225–10242. doi:10.1007/s11356-014-2845-4

Sabin, L.D., Lim, J.H., Stolzenbach, K.D., Schiff, K.C., 2005. Contribution of trace metals from atmospheric deposition to stormwater runoff in a small impervious urban catchment. Water Res. 39, 3929–3937. doi:10.1016/j.watres.2005.07.003

Shirley Clark, R.P., 2007. Annotated Bibliography of Urban Wet Weather Flow Literature From 1996 Through 2006.

Shorshani, M.F., Bonhomme, C., Petrucci, G., André, M., Seigneur, C., 2013. Road traffic impact on urban water quality: a step towards integrated traffic, air and stormwater modelling. Environ. Sci. Pollut. Res. 21, 5297–5310. doi:10.1007/s11356-013-2370-x

Wakida, F.T., Lerner, D.N., 2005. Non-agricultural sources of groundwater nitrate: a review and case study. Water Res. 39, 3–16. doi:10.1016/j.watres.2004.07.026

Waschbusch, R.J., Selbig, W.R., Bannerman, R.T., 1999. Sources of phosphorus in stormwater and street dirt from two urban residential basins in Madison, Wisconsin, 1994-95. Presented at the National Conference on Tools for Urban Water Resource Management and Protection proceedings, February 710, 2000, DIANE Publishing., Chicago.

Zgheib, S., Moilleron, R., Chebbo, G., 2012. Priority pollutants in urban stormwater: Part 1 – Case of separate storm sewers. Water Res. 46, 6683–6692. doi:10.1016/j.watres.2011.12.012

Zoppou, C., 2001. Review of urban storm water models. Environ. Model. Softw. 16, 195–231. doi:10.1016/S1364-8152(00)00084-0

Chapitre 2. Objectifs et plan du manuscrit de thèse

2.1 Objectifs et méthodes de la thèse

Cette thèse a deux objectifs principaux :

- développer des modèles distribués à base physique pour simuler les flux de polluants routiers (Matières En Suspension, Hydrocarbures, Métaux) dans un environnement urbain à deux échelles spatiales (locale et quartier).
- analyser les sorties de modèle obtenues pour améliorer la connaissance sur les processus dominants vis-à-vis de la production et du transfert des contaminants par temps de pluie.

Elle s'inscrit dans le cadre du projet ANR « Trafipollu » et bénéficie des résultats expérimentaux mis en œuvre dans ce projet pour l'implémentation, la calibration et la validation des modèles utilisés.

La première étape du travail consiste en un travail de modélisation à l'échelle locale, en utilisant des données géographiques très détaillées (résolution spatiale centimétrique) produites par l'IGN. Le code FullSWOF (SWE[1], volumes finis, schéma numérique d'ordre 2) (Delestre et al., 2014) couplé à un module d'érosion de type Hairsine and Rose (1992a, 1992b) (Le et al., 2015) a été adapté au contexte urbain. Pour la première fois, la comparaison des résultats de modélisation aux données expérimentales nous permet de démontrer la pertinence de ce type d'approche pour représenter les processus de transfert des polluants en zone urbaine. L'analyse physique des résultats obtenus permet d'identifier les processus dominants (arrachement par la pluie, mobilisation par l'advection liée au flux d'eau lors du ruissellement), ce qui permet d'approfondir la compréhension des processus physiques liés au transfert des polluants en zone urbaine.

La deuxième étape du travail consiste à coupler séquentiellement un code open-source 2-D hydrologique en surface avec un modèle 1-D d'écoulement pour le réseau afin de modéliser à l'échelle évènementielle le transfert des contaminants par temps de pluie. La première tentative a consisté à coupler le modèle TREX (Velleux et al., 2008) avec le modèle commercial CANOE (Lhomme et al., 2004). L'absence

[1] Shallow Water Equations (SWE), aussi appelées les équations de Barré de Saint Venant constituent un système d'équations différentielles partielles hyperboliques qui décrit l'écoulement d'un fluide en contact avec une surface.

d’un schéma numérique totalement satisfaisant et de processus physiques de surface liées à la mobilisation par les gouttes de pluie dans le modèle TREX nous a conduit à développer une nouvelle plateforme totalement open source en couplant les modèles LISEM (De Roo et al., 1996) et SWMM (Rossman, 2010). Pour cette dernière plateforme, un couplage avec des données d’entrée provenant de simulations des dépôts atmosphériques (Airparif, Trafipollu) et de données expérimentales issues du projet a été réalisé. L’intégration des données issues de modèles atmosphériques et l’utilisation de nouveaux modèles d’érosion pour simuler la qualité des eaux urbaines à l’échelle d’un quartier constituent l’originalité de cette seconde partie de thèse.

2.2 Plan du document

Ce manuscrit correspond à une thèse "sur articles". Après une introduction du contexte et des objectifs de la thèse (Chapitres 1 - 2), le reste de cette dissertation est organisé comme suit:

La Partie I (Chapitres 3 - 4) constitue une étude bibliographique sur la modélisation hydrologique en milieu urbain. Dans le **Chapitre 3**, nous faisons une synthèse de l'état actuel des connaissances sur les modèles hydrologiques urbains tant pour les simulations quantitatives, que pour les simulations qualitatives. Plus généralement, le **Chapitre 4** apporte une vision globale des usages de la modélisation hydrologique en milieu urbain.

La partie II (Chapitres 5 - 6) est consacrée à la modélisation distribuée du milieu urbain à base physique à l'échelle locale. Dans le **Chapitre 5**, nous présentons d'abord les démarches expérimentales afin d'obtenir les données détaillées (pluies, débits, turbidités, topographies, polluants, etc.) de la zone urbaine. Les configurations du modèle FullSWOF sur le bassin urbain à l'échelle locale, ainsi que les calibrations et les analyses de sensibilités du modèle sont également décrites. Dans le **Chapitre 6**, nous analysons les résultats du modèle et les données de l'expérimentation pour indiquer des rôles de détachement par la pluie et par les ruissellements dans les processus de lessivage des particules, nous réalisons pour la première fois des analyses spatiales et détaillées des processus physiques du lessivage des polluants en milieu urbain par temps de pluie.

La **partie III** (Chapitre 7 - 9) est consacrée aux couplages de différents modèles 2D-1D à l'échelle du quartier. Dans le **Chapitre 7**, nous couplons des modèles TREX et CANOE pour simuler les transferts de l'eau et de polluants à l'échelle du quartier et nous analysons l'influence de différents facteurs du modèle (structure, précision numérique, paramètres, données d'entrée) sur les résultats obtenus. Le **Chapitre 8** est dédié à l'évaluation de l'importance des données détaillées, telles que les données de télédétection et les données de haute résolution de l'occupation du sol,

dans la modélisation 2D-1D en milieu urbain. Dans le **Chapitre 9**, nous présentons une approche de modélisation intégrée couplant l'air, l'hydrologie de surface et dans les réseaux pour simuler le transfert des polluants urbains liés au trafic routier, les simulations des concentrations des polluants (métaux, HAPs) à l'exutoire du basin-versant urbain seront comparées avec les données mesurées.

Enfin dans la **partie IV**, nous concluons par une synthèse des principaux résultats et nous proposons des questions perspectives pour le travail dans le futur.

Les principaux résultats de cette thèse ont été publiés dans les articles suivants:

Hong, Y., Bonhomme, C., Le, M.-H., Chebbo, G., 2016a. A new approach of monitoring and physically-based modelling to investigate urban wash-off process on a road catchment near Paris. Water Res. 102, 96–108. doi:10.1016/j.watres.2016.06.027

Hong, Y., Bonhomme, C., Le, M.-H., Chebbo, G., 2016b. New insights into the urban washoff process with detailed physical modelling. Sci. Total Environ. 573, 924–936. doi:10.1016/j.scitotenv.2016.08.193

Hong, Y., Bonhomme, C., Bouf, B., Jetten, V., Chebbo, G., (submitted). Integrating atmospheric deposition, soil erosion and sewer transport models to assess the transfer of traffic-related pollutants in urban areas. Enviromental Model. Softw.

Hong, Y., Bonhomme, C., Chebbo, G., (submitted). Development and assessment of the physically-based 2D/1D model “TRENOE” for urban stormwater quantity and quality modelling. Water.

Hong, Y., Bonhomme, C., Soheilian, B., Chebbo, G., (submitted). Is the high-resolution topographic and landuse data really necessary? A new attempt of urban 2D-surface and 1D-drainage modelling. Water Sci. Technol.

Référence

De Roo, A.P.J., Wesseling, C.G., Ritsema, C.J., 1996. Lisem: A Single-Event Physically Based Hydrological and Soil Erosion Model for Drainage Basins. I: Theory, Input and Output. Hydrol. Process. 10, 1107–1117. doi:10.1002/(SICI)1099-1085(199608)10:8<1107::AID-HYP415>3.0.CO;2-4

Delestre, O., Cordier, S., Darboux, F., Du, M., James, F., Laguerre, C., Lucas, C., Planchon, O., 2014. FullSWOF: A Software for Overland Flow Simulation, in: Gourbesville, P.,

Cunge, J., Caignaert, G. (Eds.), Advances in Hydroinformatics. Springer Singapore, Singapore, pp. 221–231.

Hairsine, P.B., Rose, C.W., 1992a. Modeling water erosion due to overland flow using physical principles: 1. Sheet flow. Water Resour. Res. 28, 237–243. doi:10.1029/91WR02380

Hairsine, P.B., Rose, C.W., 1992b. Modeling water erosion due to overland flow using physical principles: 2. Rill flow. Water Resour. Res. 28, 245–250. doi:10.1029/91WR02381

Le, M.-H., Cordier, S., Lucas, C., Cerdan, O., 2015. A faster numerical scheme for a coupled system modeling soil erosion and sediment transport. Water Resour. Res. 51, 987–1005. doi:10.1002/2014WR015690

Lhomme, J., Bouvier, C., Perrin, J.-L., 2004. Applying a GIS-based geomorphological routing model in urban catchments. J. Hydrol., Urban Hydrology 299, 203–216. doi:10.1016/j.jhydrol.2004.08.006

Rossman, lewis A., 2010. Storm water management model user's manual version 5.0. National risk management research and development U.S. environmental protection agency, Cincinnati, OH 45268.

Velleux, M.L., England, J.F., Julien, P.Y., 2008. TREX: Spatially distributed model to assess watershed contaminant transport and fate. Sci. Total Environ. 404, 113–128. doi:10.1016/j.scitotenv.2008.05.053

PARTIE I. Synthèse bibliographique

Chapitre 3. Etat de l'art de la modélisation en hydrologie urbaine

La maîtrise des polluants urbains, dans le but de préserver et de reconquérir la qualité des écosystèmes aquatiques, constitue un enjeu important pour les gestionnaires. Face à ces besoins, la mise au point de méthodes de surveillance et d'outils d'évaluation des flux de polluants s'avèrent nécessaires. Au vu de la multiplicité des phénomènes en jeu et de la difficulté de réalisation et du coût des campagnes de mesures exhaustives (en tous les points de déversement), la modélisation apparaît comme un outil fondamental pour la conception, la planification et la gestion en hydrologie urbaine.

3.1 Qu'est-ce qu'un modèle hydrologique ?

Depuis les années 1960, les modèles ont été utilisés de plus en plus dans le domaine de la modélisation hydrologique. Néanmoins, le terme de « modèle » recouvre une grande variété de définitions et de concepts selon l'objectif auquel on l'applique (Clarke, 1973). Les modèles hydrologiques étudiés dans cette thèse sont caractérisés par: (a) représentation des caractéristiques des milieux urbains/naturels par des données numériques, (par exemple, les topographies, les occupations du sols, les réseaux d'assainissement, etc.); (b) représentation des processus hydrauliques et hydrologiques par des équations mathématiques, (par exemple, les équations de St-Venant pour le ruissellement, les équations de Green and Ampt (1911) pour l'infiltration, etc.); (c) implémentation de ces équations par des schémas numériques appropriés (par exemple, différences finies, volumes finis, etc.).

3.2 Classification des modèles hydrologiques

En milieu urbain, les processus hydrauliques et hydrologiques, tels que les précipitations, le ruissellement, l'infiltration, l'évapotranspiration, l'écoulement dans le réseau d'assainissement, la génération et le transport des polluants sont distribués dans le temps et l'espace. Ces divers aspects ont conduit les hydrologues à proposer différents critères pour catégoriser les modèles hydrologiques urbains (Chocat, 1997; Fletcher et al., 2013; Refsgaard, 1997; Salvadore et al., 2015; Zoppou, 2001). Selon les différentes représentations des relations entre les variables, des processus, du temps et de l'espace, les modèles hydrologiques urbains peuvent être classés selon le schéma proposé dans la Fig. 3.1.

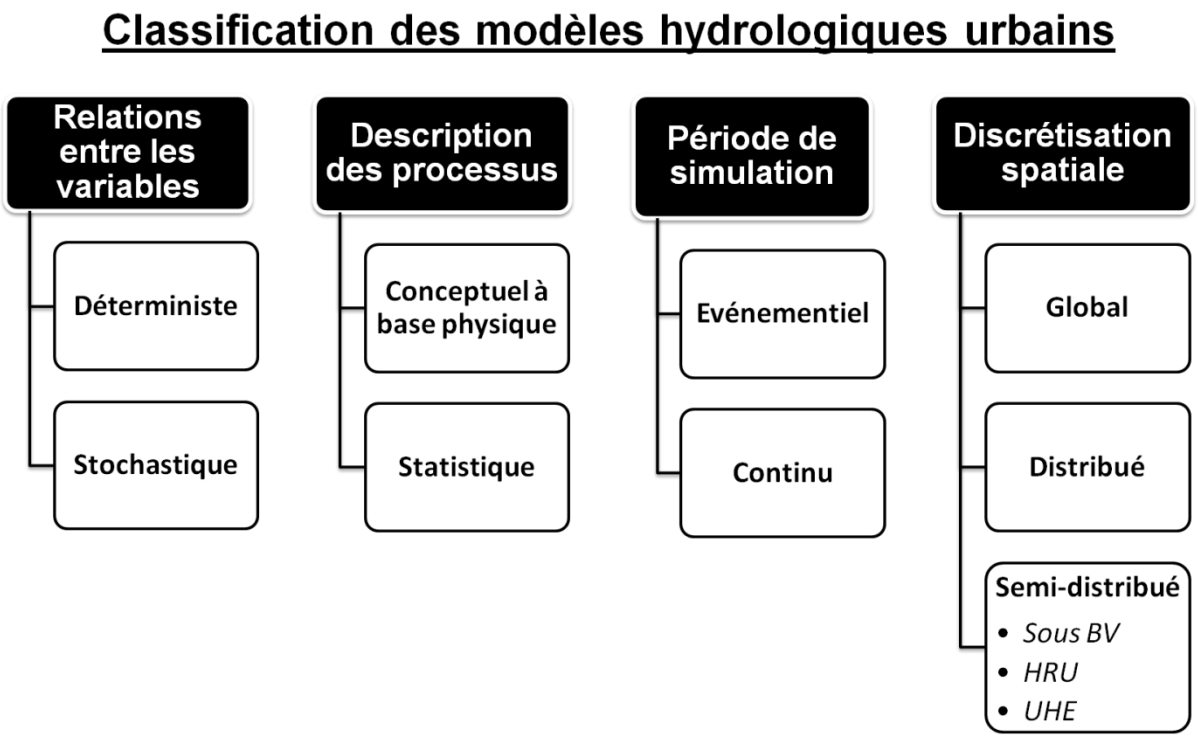

Fig. 3.1 Classification des modèles hydrologiques urbains.

3.2.1 Classification selon la relation entre les variables d'entrée et de sortie

Selon la relation entre les variables d'entrée et de sortie dans le modèle hydrologique, les modèles peuvent être déterministes ou stochastiques.

Les modèles déterministes sont constitués de relations "de cause à effet" entre les variables d'entrée et de sortie. Les variables de sortie sont uniques avec des données d'entrée définies. Néanmoins, les modèles déterministes comportent des incertitudes attribuées aux erreurs de structure du modèle, des solutions numériques, de la variabilité du terrain urbain étudié, des paramètres et des données mesurées. Divers modèles de ruissellement sur des surface urbaines ou d'écoulement dans les réseaux appartiennent à cette catégorie.

Au contraire, les modèles stochastiques ou probabilistes sont constitués de relations entre les probabilités ou distributions de probabilité des variables d'entrée et de sortie. Dans ces modèles, les variables étudiées sont considérées comme aléatoires.

3.2.2 Classification selon la description des processus

Afin de décrire les processus de cheminement des gouttes de pluie tombées sur la surface jusqu'à l'exutoire, nous avons recours le plus souvent à une simplification qui

consiste à décomposer les phénomènes hydrologiques en différents processus qui peuvent être représentés séparément. Selon la description de ces processus, les modèles hydrologiques peuvent être distingués en modèles conceptuels à base physique ou modèles statistiques.

Les modèles conceptuel à base physique sont essentiellement déterministes et sont issus de théories physiques (par exemple, mécanique des fluides, thermodynamique...). Tous les processus élémentaires sont représentés par les lois physiques.

Les modèles statistiques cherchent à reproduire la dynamique des variables de sortie en fonction des variables d'entrée, sans tenter de décrire les processus élémentaires. Les formules utilisées dans le modèle sont souvent basées sur des équations empiriques.

3.2.3 Classification selon la période de simulation

Selon les objectifs recherchés à travers la modélisation, le comportement du basin-versant urbain peut être reproduit uniquement pour des événements particuliers ou en continu sur une période plus ou moins longue englobant des périodes de temps sec (hors événements). Nous distinguons ainsi les modèles événementiels et les modèles continus.

Les modèles événementiels s'attachent à reproduire les conséquences d'un événement pluvieux particulier. Ce genre de modèle nécessite de pouvoir préciser les conditions initiales des eaux et des polluants du bassin versant urbain.

Les modèles continus permettent, quant à eux, de suivre l'évolution des variables à plus long terme. En hydrologie urbaine, ce type des modèles est souvent utilisé pour simuler le fonctionnement sur le long terme d'ouvrages spéciaux comme des déversoirs d'orage, la mobilisation des solides dans les réseaux ou l'impact des eaux pluviales sur les milieux récepteurs.

3.2.4 Classification selon la discrétisation spatiale

La discrétisation spatiale est un critère souvent utilisé pour classifier différents modèles hydrologiques (Elliott and Trowsdale, 2007; Fletcher et al., 2013; Merritt et al., 2003; Salvadore et al., 2015). Selon les représentations de l'espace dans le modèle, les modèles hydrologiques peuvent être séparés en trois catégories: les modèles globaux (*lumped models*), les modèles semi-distribués, et les modèles distribués. Parmi ces trois catégories, les modèles semi-distribués peuvent être discrétisés en trois classes différentes: ils peuvent être basés sur les sous-bassins versants (sous BV), ou basés sur les *Hydrologic Response Unit* (HRU), ou basés sur les *Urban Hydrological Element* (UHE).

En général, les modèles globaux (*lumped models*) sont plus simples que les autres types de modèles, et sont utilisés surtout pour les cas où les données sont

limitées. Ce type de modèle simule des réponses hydrologiques seulement à l'exutoire du bassin-versant urbain. La variabilité spatiale interne des processus hydrauliques et hydrologiques est soit ignorée, soit prise en compte par l'intermédiaire de "valeurs moyennes".

Les modèles distribués résultent d'un découpage fin de la surface urbaine suivant des grilles à mailles régulières (carrées) ou irrégulières (triangulaires et de taille variable par exemple). Dans les modèles existants, les mailles carrées sont les plus souvent utilisées. Une connaissance géographique et physique détaillée de la zone urbaine est nécessaire pour la modélisation hydrologique distribuée. Cependant, ces modèles sont généralement couplés à un Modèle Numérique de Terrain (MNT) ou un Système d'Information Géographique (SIG).

Les modèles semi-distribués sont construits en considérant que certains composants du bassin-versant peuvent être globalisés. Ce type de modèle tient compte de la variabilité spatiale à travers des classes ayant des comportements hydrauliques ou hydrologiques supposés similaires. Par conséquence, les modèles semi-distribués nécessitent plus de données spatiales que les modèles globaux. Cependant, ils peuvent être utilisés dans les cas où les informations détaillées du SIG ou du MNT ne sont pas disponibles par rapport aux modèles distribués. Néanmoins, les modèles semi-distribués peuvent potentiellement calculer des réponses hydrauliques et hydrologiques détaillées si les séparations des composants sont fines. Tenant compte des différentes stratégies de regroupement des composants du bassin-versant urbain, les modèles semi-distribués peuvent être définis en plusieurs groupes, (i)soit basés sur les sous-bassins versants; (ii) soit basés sur les HRUs; (iii) soit basé sur les UHEs.

Les modèles basés sur les sous-bassins versants utilisent les données topographiques et/ou les données de réseaux d'assainissement pour délimiter différents sous bassins en milieu urbain. Les conditions hydrauliques et hydrologiques sont homogènes pour chaque sous-bassin. Par ailleurs, les modèles basés sur les HRUs (*Hydrologic Response Units*) regroupent différentes caractéristiques géomorphologiques pour définir les Unités de Réponse Hydrologique (HRUs). Par exemple, un type d'HRU peut être représenté par une combinaison d'une occupation du sol, une classe de pente (par exemple, < 2%), et un type du sol. Les HRUs ne sont donc pas géo-localisées, et cette méthode s'adapte mieux à la modélisation des grands bassins versants avec de nombreux types de géomorphologie, où les zones urbaines représentent des sous parties du bassin. De plus, les modèles basés sur les UHEs (*Urban Hydrological Element*) sont développés particulièrement pour décrire les systèmes hydrologiques urbains. Contrairement aux autres types de modèle, les concepts des modèles basés sur les UHEs sont légèrement différents d'un modèle à l'autre. L'idée en commun est d'identifier l'élément ou l'unité suffisamment petite, pour que les processus homogènes à l'échelle de l'élément soient capables de représenter l'hétérogénéité du bassin versant urbain.

3.2.5. Discussion sur les critères de classification

Dans les sections précédentes, nous avons présentés la classification des modèles hydrologiques urbains selon quatre différents aspects, tels que (i) les relations entre les variables, (ii) la description des processus, (iii) la période de simulation, et (iv) la discrétisation spatiale. Néanmoins, il faut noter que même si ces classifications couvrent la plupart des modèles existants, certains aspects restent assez ambigus.

La distinction entre les modèles conceptuels à base physique et statistiques est contestable selon plusieurs chercheurs et hydrologues (Beven, 1989; Zoppou, 2001). Ces avis contradictoires proviennent généralement de la difficulté à identifier clairement les lois physiques dans la recherche en l'hydrologie urbaine. Par exemple, Clarke (1973) a justifié que la loi de Darcy[2] est une loi physique, cependant, cette loi est basée sur les observations et les définitions empiriques. Dans ce contexte, les modèles hydrologiques peuvent également être catégorisés comme des modèles basés sur des processus (*process-based*) ou non (*non process-based*) (De Roo, 1998; Nearing, 1998). Néanmoins, il est difficile d'identifier explicitement les processus élémentaires pour que les mécanismes soient suffisamment représentés. Par conséquent, ce manuscrit continue à utiliser la notion des modèles "conceptuels à base physique" ou "statistiques". Les modèles à base physique écrits dans cette thèse signifient que les équations utilisées dans ce type des modèles sont basées sur les lois connues et largement appliquées (par exemple, équation de Barré de Saint-Venant, loi de Stokes, etc.).

De plus, la classification des modèles en globaux, distribués et semi-distribués est aussi discutable. En effet, les modèles distribués sont globaux à l'échelle de la maille, et les modèles semi-distribués sont globaux à l'échelle d'une sous-partie du bassin versant (Beven, 1989; Bonhomme and Petrucci, 2014; Refsgaard et al., 1990). Par conséquent, les modèles peuvent aussi être catégorisés en modèles basés sur des grilles (*grid-based*) ou pas (*non grid-based*) (Salvadore et al., 2015). Dans cette thèse, nous continuons à utiliser le terme de "modèles distribués", pour signifier que les processus simulés sont spatialement distribués sur les surfaces urbaines.

3.2.6 Classification des modèles existants

Dans la littérature, il existe déjà de nombreux modèles hydrauliques et hydrologiques pour simuler les transferts des eaux et des polluants en milieu urbain. Un certain nombre de modèles a été incorporé dans les logiciels commerciaux. Selon les critères que nous avons présentés dans les sections précédentes, le Tableau 3.1 présente les caractéristiques de quelques modèles connus pour la modélisation des eaux pluviales en milieu urbain.

[2] Loi de Darcy: une loi qui exprime le débit d'un fluide incompressible filtrant au travers d'un milieu poreux supposé isotrope à l'échelle de travail.

Tableau 3.1 Classification de quelques modèles pour la simulation des eaux pluviales en milieu urbain.

Modèles et Référence	Relations entre les variables	Description des processus	Période de simulation	Discrétisation spatiale
SWMM (Rossman, 2010)	Déterministe	Conceptuel	Evénementiel + Continu	Semi-distribué (Sous BV)
MUSIC (Dotto et al., 2011; Hamel et al., 2013)	Déterministe	Conceptuel	Evénementiel	Semi-distribué (Sous BV)
URBS (Rodriguez et al., 2008)	Déterministe	Conceptuel	Evénementiel + Continu	Semi-distribué (UHE)
CANOE (Lhomme et al., 2004)	Déterministe	Conceptuel	Evénementiel + Continu	Semi-distribué (Sous BV)
AVSWAT-X (Jeong et al., 2010; Larose et al., 2007)	Déterministe	Conceptuel	Continu	Semi-distribué (HRU)
CWD (Mackay and Last, 2010)	Déterministe	Statistique	Continu	Semi-distribué (UHE)
MIKE-SHE (DHI, 2008)	Déterministe	Conceptuel	Evénementiel + Continu	Distribué
InfoWORKS CS (Innovyze Ltd, 2011)	Déterministe	Conceptuel	Evénementiel + Continu	Distribué
Chen and Adams (2006)	Stochastique	Statistique	Evénementiel	Global
Aronica and Candela (2007)	Stochastique	Statistique	Evénementiel	Global

En outre, il faut noter que dans la pratique, certains processus dans les modèles hydrologiques urbains, surtout les processus concernant la modélisation de la qualité de l'eau, sont difficiles à représenter par les lois physiques connues. Dans ce cas là, la plupart des modèles urbains actuels (e.g. Hamel et al., 2013; Lhomme et al., 2004; Rossman, 2010) utilisent des approches de modélisation à la fois conceptuelle à base physique (quantité) et fois conceptuelle (qualité).

3.3 Modélisation de la qualité de l'eau en milieu urbain

Depuis les années 1970, de nombreux outils mathématiques de modélisation ont été développés afin de simuler la qualité de l'eau en milieu urbain. Pourtant, la

description des processus inclus dans les modèles d'aujourd'hui restent celle proposée par les pionniers (e.g. Sartor et al., 1974). Peu de connaissances nouvelles sur les mécanismes de génération et de transport des polluants par temps de pluie ont été intégrées dans les outils de modélisation. D'autre part, après 40 ans d'expérience, il apparaît que très peu de modèles de la qualité de l'eau sont utilisés dans les zones urbaines par les opérationnels. Trois raisons principales expliquent ce manque de confiance dans la modélisation de la qualité de l'eau:

- L'insuffisance des connaissances des processus à modéliser dans le milieu urbain.
- L'insuffisance des données disponibles pour les caler et les valider.
- Le manque de performance qui a été mis en évidence pour ces modèles.

Les modèles à base physique sont des outils prometteurs pour nous aider à améliorer les connaissances des processus physiques de transfert hydrologique des polluants en milieu urbain. Néanmoins, la plupart des modèles actuels (par exemple, les modèles SWMM, MUSIC, CANOE, etc.) utilisent des formules statistiques telles que les équations de Sartor et al. (1974), pour simuler la qualité de l'eau en milieu urbain. En utilisant ces formules, le lessivage des polluants est proportionnel au flux d'eau et à la masse initiale à l'échelle d'un bassin ou une sous-partie du bassin. Les mécanismes de transport, ainsi que la distribution spatiale des polluants (pollution diffuse) ne peuvent donc pas être représentés. Par conséquent, le travail présenté ici cherche à adapter les modèles distribués à base physique, qui sont initialement utilisés sous le domaine de l'érosion sur les bassins versants naturels, pour simuler les processus physiques de transferts des polluants en milieu urbain par temps de pluie.

3.3.1 Processus de transfert des polluants en milieu urbain

Depuis les débuts des années 1970, l'approche la plus souvent utilisée pour simuler les flux polluants en milieu urbain prend en compte quatre processus principaux: (i) accumulation des solides en temps sec sur les surfaces (*build-up*), (ii) lessivage et entraînement des solides en temps de pluie sur les surfaces (*wash-off*), (iii) transport des solides dans le réseau incluant la sédimentation et la remise en suspension, et enfin (iv) processus chimiques et biologiques des polluants dans le réseau. Pour les simulations en zones urbaines équipées des réseaux d'assainissement séparatifs, nous faisons l'hypothèse forte dans ce travail de thèse que les processus (iii) et (iv) peuvent être négligés.

Accumulation des solides sur les surfaces urbaines (build-up)

La pollution des eaux de ruissellement urbaines a pour origine d'une part le lessivage de l'atmosphère, et d'autre part le lessivage et l'érosion des surfaces urbaines. D'après Gunawardena et al. (2013) et Sabin et al. (2006), les dépôts secs

dominent les processus de dépositions atmosphériques. Le stock de polluants disponibles sur les surfaces en début de pluie résulte du dépôt des polluants au cours du temps sec précédant la pluie. Il dépend de facteurs tels que le type d'occupation du sol, la circulation, le nettoyage de la voirie, et les conditions météorologiques. Il en résulte une variabilité spatiale et temporelle importante dans le processus d'accumulation.

Dans l'étude de Sartor et al. (1974), la masse disponible des polluants tend vers une valeur limite au bout d'une dizaine de jours selon le type d'occupation de sol. Sur la base de ces constats, ces auteurs ont proposé un ajustement asymptotique (relation exponentielle) de la masse de stock accumulée en fonction de la durée de temps sec. Ces équations sont largement utilisées même dans les modèles actuels. Néanmoins, ces modèles d'accumulation ne sont pas liés aux caractéristiques physiques du système étudié, et ont été critiqués par plusieurs auteurs à cause de leurs faibles performances (e.g. Al Ali et al., 2016; Sage et al., 2015). En pratique, l'accumulation des solides pendant le temps sec est souvent estimée à partir de campagnes de mesures à l'échelle des bassins versants urbains. Les mesures des dépôts secs sont généralement faites ponctuellement et leur transposition sur une surface non uniforme engendrent des risques de non-représentativité. Dans quelques modèles, la source des polluants sur les surfaces est supposée illimitée, et par la suite il n'y a pas besoin de tenir compte de l'accumulation (Escrig et al., 2011; Guentzel et al., 1995; Scheerer et al., 2005).

Lessivage des solides en temps de pluie sur les surfaces (wash-off)

Les gouttes de pluie et les eaux de ruissellement peuvent provoquer l'arrachement et l'entraînement des solides accumulés par temps sec aux surfaces urbaines. Le lessivage des solides dépend de paramètres tels que l'intensité moyenne ou maximale de pluie, la hauteur et la durée de la pluie, le débit de pointe du ruissellement, le volume ruisselé, la topographie, la rugosité et les caractéristiques des solides, etc. (Aalderink et al., 1990; Barbé et al., 1996; Yuan et al., 2001).

Sartor et al. (1974) ont proposé pour la première fois un modèle pour simuler le lessivage des polluants sur la surface du milieu urbain. Il suppose que le processus de lessivage est proportionnel à la masse disponible des particules et à l'intensité de pluie et/ou au débit ruisselé sur la surface. Le modèle de Sartor et al. (1974), de type statistique, a été utilisé en premier lieu dans SWMM (Jewell and Adrian, 1978); il a ensuite été repris avec certaines modifications dans plusieurs autres modèles: MUSIC (Dotto et al., 2011; Hamel et al., 2013), CANOE (Lhomme et al., 2004), MOUSE (Thorndahl and Willems, 2008), InfoWORKS CS (Innovyze Ltd, 2011), MIKE-SHE (Refsgaard et al., 2010), etc.

Du fait qu'il est difficile de décrire de manière mécaniste la mobilisation des dépôts secs sur les surfaces urbaines lors des périodes inter-événement, très peu de modèles actuels intègrent des processus physiques de transfert des polluants par temps de pluie. Cependant, la plupart des modèles à base physique pour simuler la

qualité de l'eau a été développée et appliquée aux bassins versants naturels. En considérant que les théories physiques de transfert des solides en milieu urbain peuvent être analogues à celles dans les milieux naturels, nous pouvons appliquer les modèles de l'érosion aux zones urbaines pour simuler les processus physiques de lessivage sur les surfaces urbaines. Les différentes études sur le sujet s'accordent pour dire que le lessivage des particules déposées est dû à l'impact des gouttes de pluie, et à l'effet de la contrainte de cisaillement du ruissellement (Deletic et al., 1997; Kinnell, 2009; Shaw et al., 2006; Vaze and Chiew, 2003).

3.3.2 Modèles d'érosion

Bien que les équations d'accumulation et de lessivage des polluants (*build-up / wash-off*) sur les surfaces urbaines soient largement utilisées dans les modèles actuels, l'utilisation de ces équations conceptuelles est fréquemment assimilée à un modèle "boîte noire" (Al Ali et al., 2016; Bonhomme and Petrucci, n.d.; Sage et al., 2015). Il est donc nécessaire d'améliorer les connaissances sur les processus physiques de lessivage des polluants sur les surfaces urbaines, afin de proposer des nouvelles formules mathématiques et des techniques de modélisation avancées.

Tableau 3.2 Les deux formules fréquemment utilisés pour la modélisation de l'érosion.

Nom	Principe	Exemples des modèles
USLE (Foster et al., 1977; Wischmeier and Smith, 1978)	$A = RKLCSP$ Dans l'équation, A est les particules érodées par unité de la surface; *R, K, L, C, S et P* sont des facteurs empiriques pour représenter l'érodabilité des particules liée à la pluie (R), au sol (K), à la topographie (L et S), et au management agricole (C et P).	TREX (Velleux et al., 2008); WEPP (Laflen et al., 1991); CREAMS (Leonard et al., 1987);
Hairsine and Rose (1992a, 1992b)	$\frac{dc}{dt} = H\left[aP + \frac{F(\Omega - \Omega_0)}{J}\right] - d$ Dans l'équation, $\frac{dc}{dt}$ est le taux d'érosion par unité du temps; P est l'intensité de pluie; Ω *et* Ω_0 sont l'énergie et l'énergie limite de flux d'eau; d est la déposition; *H, a, J, F* sont des facteurs liés aux processus différents.	GUEST (Misra and Rose, 1996); FullSWOF (Delestre et al., 2014); Shaw et al. (2006); Vaze and Chiew (2003); Heng et al. (2011);

Comme la majorité des polluants liés au trafic routier (e.g. Cu, Fe, Ni, Cr, HAPs, etc.) est attachée aux particules, la mise en place de modèles d'érosion sur les surfaces urbaines est une tentative prometteuse dans le domaine de la modélisation de la qualité des eaux pluviales en milieu urbain. Plusieurs formules ont été développées pour décrire les processus de transport des solides dans différents modèles distribués. Dans les modèles actuels, deux types de formulations fréquemment utilisées sont (i) les équations de type USLE (*Universal Soil Loss Equation*) (Foster et al., 1977; Wischmeier and Smith, 1978); (ii) les équations de type Hairsine and Rose (1992a, 1992b). Les descriptions de ces deux méthodes ainsi que les exemples de modèle sont présentées dans le tableau 3.2.

Les équations de type USLE

L'équation USLE (Foster et al., 1977; Wischmeier and Smith, 1978) est initialement développée par le USDA (*United States Department of Agriculture*), puis largement utilisée dans le monde. L'équation prévoit le taux moyen annuel de l'érosion à long terme en milieu naturel, en fonction de la pluie, du type de sol, de la topographie, du système cultural et des pratiques de gestion. L'USLE prévoit uniquement l'importance des pertes en sédiment qui résultent des détachements par les ruissellements sur une pente simple, sans tenir compte des effets de goutte de pluie. En raison des limites reconnues de cette équation (e.g. Kinnell, 2010; Nearing, 1998), de nombreux auteurs ont proposé des versions modifiées ou révisées afin d'améliorer les formules de base de l'USLE. Par exemple la famille de RUSLE (Renard and Freimund, 1994) et le groupe d'USLE-M (Kinnell and Risse, 1998).

Les équations de type Hairsine and Rose(1992a, 1992b)

Basées sur le principe que les impacts de gouttes de pluie et les effets de la contrainte de cisaillement du ruissellement détachent les particules sur la surface, les équations de type de Hairsine and Rose (1992a, 1992b) (e.g. Deletic et al., 1997; Heng et al., 2011; Shaw et al., 2006; Vaze and Chiew, 2003) visent à améliorer la représentation physique des processus d'érosion par rapport aux équations USLE. Ces formules permettent de considérer séparément les trois processus d'érosion suivants: le détachement par la pluie, le détachement et le transport par le ruissellement, et le dépôt des sédiments. De plus, ces équations prennent en compte que les sédiments peuvent être classés en plusieurs classes en fonction de leur diamètre.

A part les deux types de modèles présentés dans les sections précédentes, plusieurs chercheurs ont construit des modèles d'érosion "à base physique" basés sur différents concepts ou leur données mesurées (e.g. Jetten and Roo, 2001; Nearing et al., 1989). Néanmoins, il faut aussi indiquer que les modèles d'érosion actuels contiennent toujours des relations empiriques sur un aspect ou un autre (Bryan, 2000; De Roo, 1998). Par exemple, les paramètres de l'équation USLE sont dérivés directement des données mesurées; ainsi, les valeurs de paramètres *H, a, J et F* de l'équation de Hairsine and Rose (1992a, 1992b) sont très variables dans les

différentes études publiées (e.g. Beuselinck et al., 2002; Heng et al., 2011; Hogarth et al., 2004; Jomaa et al., 2010; Misra and Rose, 1996; Proffitt et al., 1993). La demande importante en données reste une limitation sérieuse pour l'utilisation de ces modèles, d'autant plus que les données sont censées représenter une variabilité spatiale complexe.

Référence

Aalderink, R.H., Duin, E.H.S. van, Peels, C.E., Scholten, M.J.M., 1990. Some characteristics of runoff quality from a separated sewer system in Lelystad, The Netherlands.

Al Ali, S., Bonhomme, C., Chebbo, G., 2016. Evaluation of the Performance and the Predictive Capacity of Build-Up and Wash-Off Models on Different Temporal Scales. Water 8, 312. doi:10.3390/w8080312

Aronica, G.T., Candela, A., 2007. Derivation of flood frequency curves in poorly gauged Mediterranean catchments using a simple stochastic hydrological rainfall-runoff model. J. Hydrol. 347, 132–142. doi:10.1016/j.jhydrol.2007.09.011

Barbé, D.E., Cruise, J.F., Mo, X., 1996. Modeling the Buildup and Washoff of Pollutants on Urban Watersheds1. JAWRA J. Am. Water Resour. Assoc. 32, 511–519. doi:10.1111/j.1752-1688.1996.tb04049.x

Beuselinck, L., Hairsine, P.B., Govers, G., Poesen, J., 2002. Evaluating a single-class net deposition equation in overland flow conditions: SINGLE-CLASS NET DEPOSITION EQUATION. Water Resour. Res. 38, 15–1–15–10. doi:10.1029/2001WR000248

Beven, K., 1989. Changing ideas in hydrology — The case of physically-based models. J. Hydrol. 105, 157–172. doi:10.1016/0022-1694(89)90101-7

Bonhomme, C., Petrucci, G., 2014. Spatial Representation in semi-distributed modelling of water quantity and quality, in: 13th International Conference on Urban Drainage, Kuching, Malaysia.

Bonhomme, C., Petrucci, G., n.d. Should we trust build-up/wash-off water quality models at the scale of urban catchments? Water Res. doi:10.1016/j.watres.2016.11.027

Brun, S.., Band, L.., 2000. Simulating runoff behavior in an urbanizing watershed. Comput. Environ. Urban Syst. 24, 5–22. doi:10.1016/S0198-9715(99)00040-X

Bryan, R.B., 2000. Soil erodibility and processes of water erosion on hillslope. Geomorphology 32, 385–415. doi:10.1016/S0169-555X(99)00105-1

Chen, J., Adams, B.J., 2006. A framework for urban storm water modeling and control analysis with analytical models. Water Resour. Res. 42, W06419. doi:10.1029/2005WR004540

Chocat, B., 1997. Encyclopédie de l'hydrologie urbaine. Lavoisier.

Clarke, R.T., 1973. A review of some mathematical models used in hydrology, with observations on their calibration and use. J. Hydrol. 19, 1–20. doi:10.1016/0022-1694(73)90089-9

De Roo, A.P.J., 1998. Modelling runoff and sediment transport in catchments using GIS. Hydrol. Process. 12, 905–922. doi:10.1002/(SICI)1099-1085(199805)12:6<905::AID-HYP662>3.0.CO;2-2

Delestre, O., Darboux, F., James, F., Lucas, C., Laguerre, C., Cordier, S., 2014. FullSWOF: A free software package for the simulation of shallow water flows. ArXiv Prepr. ArXiv14014125.

Deletic, A., Maksimovic, C., Ivetic, M., 1997. Modelling of storm wash-off of suspended solids from impervious surfaces. J. Hydraul. Res. 35, 99–118. doi:10.1080/00221689709498646

DHI, 2008. MIKE by DHI Software. Reference Manuals for MIKE FLOOD.

Dotto, C.B.S., Deletic, A., McCarthy, D.T., Fletcher, T.D., 2011. Calibration and Sensitivity Analysis of Urban Drainage Models: Music Rainfall/Runoff Module and a Simple Stormwater Quality Model. Aust. J. Water Resour. 15, 85–94. doi:10.1080/13241583.2011.11465392

Elliott, A.H., Trowsdale, S.A., 2007. A review of models for low impact urban stormwater drainage. Environ. Model. Softw., Special section: Advanced Technology for Environmental Modelling 22, 394–405. doi:10.1016/j.envsoft.2005.12.005

Escrig, A., Amato, F., Pandolfi, M., Monfort, E., Querol, X., Celades, I., Sanfélix, V., Alastuey, A., Orza, J.A.G., 2011. Simple estimates of vehicle-induced resuspension rates. J. Environ. Manage. 92, 2855–2859. doi:10.1016/j.jenvman.2011.06.042

Fletcher, T.D., Andrieu, H., Hamel, P., 2013. Understanding, management and modelling of urban hydrology and its consequences for receiving waters: A state of the art. Adv. Water Resour. 51, 261–279. doi:10.1016/j.advwatres.2012.09.001

Foster, G.R., Meyer, L.T., Onstad, C.A., 1977. An Erosion Equation Derived from Basic Erosion Principles. Trans. ASAE 20, 0678–0682. doi:10.13031/2013.35627

Green, W.H., Ampt, G.A., 1911. Studies on Soil Phyics. J. Agric. Sci. 4, 1–24. doi:10.1017/S0021859600001441

Guentzel, J.L., Landing, W.M., Gill, G.A., Pollman, C.D., 1995. Atmospheric deposition of mercury in Florida: The fams project (1992–1994). Water. Air. Soil Pollut. 80, 393–402. doi:10.1007/BF01189689

Gunawardena, J., Egodawatta, P., Ayoko, G.A., Goonetilleke, A., 2013. Atmospheric deposition as a source of heavy metals in urban stormwater. Atmos. Environ. 68, 235–242. doi:10.1016/j.atmosenv.2012.11.062

Hairsine, P.B., Rose, C.W., 1992a. Modeling water erosion due to overland flow using physical principles: 2. Rill flow. Water Resour. Res. 28, 245–250. doi:10.1029/91WR02381

Hairsine, P.B., Rose, C.W., 1992b. Modeling water erosion due to overland flow using physical principles: 1. Sheet flow. Water Resour. Res. 28, 237–243. doi:10.1029/91WR02380

Hamel, P., Daly, E., Fletcher, T.D., 2013. Source-control stormwater management for mitigating the impacts of urbanisation on baseflow: A review. J. Hydrol. 485, 201–211. doi:10.1016/j.jhydrol.2013.01.001

Heng, B.C.P., Sander, G.C., Armstrong, A., Quinton, J.N., Chandler, J.H., Scott, C.F., 2011. Modeling the dynamics of soil erosion and size-selective sediment transport over nonuniform topography in flume-scale experiments. Water Resour. Res. 47, W02513. doi:10.1029/2010WR009375

Hogarth, W.., Rose, C.., Parlange, J.., Sander, G.., Carey, G., 2004. Soil erosion due to rainfall impact with no inflow: a numerical solution with spatial and temporal effects of sediment settling velocity characteristics. J. Hydrol. 294, 229–240. doi:10.1016/j.jhydrol.2004.02.014

Innovyze Ltd, 2011. InfoWorks 2D - Collection Systems Technical Review.

Jeong, J., Kannan, N., Arnold, J., Glick, R., Gosselink, L., Srinivasan, R., 2010. Development and Integration of Sub-hourly Rainfall–Runoff Modeling Capability Within a Watershed Model. Water Resour. Manag. 24, 4505–4527. doi:10.1007/s11269-010-9670-4

Jetten, V.G., Roo, A.P.J. de, 2001. Spatial Analysis of Erosion Conservation Measures with LISEM, in: Harmon, R.S., III, W.W.D. (Eds.), Landscape Erosion and Evolution Modeling. Springer US, pp. 429–445.

Jewell, T., Adrian, D., 1978. SWMM stormwater pollutant washoff functions. J. Environ. Eng. Div. ASCE.

Jomaa, S., Barry, D.A., Brovelli, A., Sander, G.C., Parlange, J.-Y., Heng, B.C.P., Tromp-van Meerveld, H.J., 2010. Effect of raindrop splash and transversal width on soil erosion: Laboratory flume experiments and analysis with the Hairsine–Rose model. J. Hydrol. 395, 117–132. doi:10.1016/j.jhydrol.2010.10.021

Kinnell, P.I.A., 2010. Event soil loss, runoff and the Universal Soil Loss Equation family of models: A review. J. Hydrol. 385, 384–397. doi:10.1016/j.jhydrol.2010.01.024

Kinnell, P.I.A., 2009. The influence of raindrop induced saltation on particle size distributions in sediment discharged by rain-impacted flow on planar surfaces. CATENA 78, 2–11. doi:10.1016/j.catena.2009.01.008

Kinnell, P.I.A., Risse, L.M., 1998. USLE-M: Empirical Modeling Rainfall Erosion through Runoff and Sediment Concentration. Soil Sci. Soc. Am. J. 62, 1667. doi:10.2136/sssaj1998.03615995006200060026x

Laflen, J.M., Elliot, W.J., Simanton, J.R., Holzhey, C.S., Kohl, K.D., 1991. WEPP: Soil erodibility experiments for rangeland and cropland soils. J. Soil Water Conserv. 46, 39–44.

Larose, M., Heathman, G.C., Norton, L.D., Engel, B., 2007. Hydrologic and Atrazine Simulation of the Cedar Creek Watershed Using the SWAT Model. J. Environ. Qual. 36, 521. doi:10.2134/jeq2006.0154

Leonard, R.A., Knisel, W.G., Still, D.A., 1987. GLEAMS: Groundwater Loading Effects of Agricultural Management Systems. Trans. ASAE 30, 1403–1418. doi:10.13031/2013.30578

Lhomme, J., Bouvier, C., Perrin, J.-L., 2004. Applying a GIS-based geomorphological routing model in urban catchments. J. Hydrol., Urban Hydrology 299, 203–216. doi:10.1016/j.jhydrol.2004.08.006

Mackay, R., Last, E., 2010. SWITCH city water balance: a scoping model for integrated urban water management. Rev. Environ. Sci. Biotechnol. 9, 291–296. doi:10.1007/s11157-010-9225-4

Merritt, W.S., Letcher, R.A., Jakeman, A.J., 2003. A review of erosion and sediment transport models. Environ. Model. Softw. 18, 761–799. doi:10.1016/S1364-8152(03)00078-1

Misra, R.K., Rose, C.W., 1996. Application and sensitivity analysis of process-based erosion model GUEST. Eur. J. Soil Sci. 47, 593–604.

Nearing, M., Foster, G., Lane, L., Finkner, S., 1989. A process-based soil erosion model for USDA-water erosion prediction project technology. Trans. ASAE 1587–1593.

Nearing, M.A., 1998. Why soil erosion models over-predict small soil losses and under-predict large soil losses. CATENA 32, 15–22. doi:10.1016/S0341-8162(97)00052-0

Proffitt, A.P.B., Hairsine, P.B., Rose, C.W., 1993. Modeling Soil Erosion by Overland Flow: Application Over a Range of Hydraulic Conditions. Trans. ASAE 36, 1743–1753. doi:10.13031/2013.28519

Refsgaard, J.C., 1997. Validation and Intercomparison of Different Updating Procedures for Real-Time Forecasting. Hydrol. Res. 28, 65–84.

Refsgaard, J.C., Storm, B., Abbott, M.B., 1990. Comment on 'A Discussion of Distributed Hydrological Modelling' by K. Beven, in: Abbott, M.B., Refsgaard, J.C. (Eds.), Distributed Hydrological Modelling. Springer Netherlands, Dordrecht, pp. 279–287.

Refsgaard, J.C., Storm, B., Clausen, T., 2010. Système Hydrologique Europeén (SHE): review and perspectives after 30 years development in distributed physically-based hydrological modelling. Hydrol. Res. 41, 355–377. doi:10.2166/nh.2010.009

Renard, K.G., Freimund, J.R., 1994. Using monthly precipitation data to estimate the R-factor in the revised USLE. J. Hydrol. 157, 287–306. doi:10.1016/0022-1694(94)90110-4

Rodriguez, F., Andrieu, H., Morena, F., 2008. A distributed hydrological model for urbanized areas – Model development and application to case studies. J. Hydrol. 351, 268–287. doi:10.1016/j.jhydrol.2007.12.007

Rossman, lewis A., 2010. Storm water management model user's manual version 5.0. National risk management research and development U.S. environmental protection agency, Cincinnati, OH 45268.

Sabin, L.D., Hee Lim, J., Teresa Venezia, M., Winer, A.M., Schiff, K.C., Stolzenbach, K.D., 2006. Dry deposition and resuspension of particle-associated metals near a freeway in Los Angeles. Atmos. Environ. 40, 7528–7538. doi:10.1016/j.atmosenv.2006.07.004

Sage, J., Bonhomme, C., Al Ali, S., Gromaire, M.-C., 2015. Performance assessment of a commonly used "accumulation and wash-off" model from long-term continuous road runoff turbidity measurements. Water Res. 78, 47–59. doi:10.1016/j.watres.2015.03.030

Salvadore, E., Bronders, J., Batelaan, O., 2015. Hydrological modelling of urbanized catchments: A review and future directions. J. Hydrol. 529, Part 1, 62–81. doi:10.1016/j.jhydrol.2015.06.028

Sartor, J.D., Boyd, G.B., Agardy, F.J., 1974. Water Pollution Aspects of Street Surface Contaminants. J. Water Pollut. Control Fed. 46, 458–467.

Scheerer, H., Hoche, H., Broszeit, E., Schramm, B., Abele, E., Berger, C., 2005. Effects of the chromium to aluminum content on the tribology in dry machining using (Cr,Al)N coated tools. Surf. Coat. Technol., PSE 2004Plasma Surface Engineering (PSE 2004) 200, 203–207. doi:10.1016/j.surfcoat.2005.02.112

Shaw, S.B., Walter, M.T., Steenhuis, T.S., 2006. A physical model of particulate wash-off from rough impervious surfaces. J. Hydrol. 327, 618–626. doi:10.1016/j.jhydrol.2006.01.024

Thorndahl, S., Willems, P., 2008. Probabilistic modelling of overflow, surcharge and flooding in urban drainage using the first-order reliability method and parameterization of local rain series. Water Res. 42, 455–466. doi:10.1016/j.watres.2007.07.038

Vaze, J., Chiew, F.H.S., 2003. Comparative evaluation of urban storm water quality models. Water Resour. Res. 39, 1280. doi:10.1029/2002WR001788

Velleux, M.L., England, J.F., Julien, P.Y., 2008. TREX: Spatially distributed model to assess watershed contaminant transport and fate. Sci. Total Environ. 404, 113–128. doi:10.1016/j.scitotenv.2008.05.053

Wischmeier, W., Smith, D., 1978. Agriculutral Handbook No. 537.

Yuan, Y., Hall, K., Oldham, C., 2001. A preliminary model for predicting heavy metal contaminant loading from an urban catchment. Sci. Total Environ. 266, 299–307. doi:10.1016/S0048-9697(00)00728-2

Zoppou, C., 2001. Review of urban storm water models. Environ. Model. Softw. 16, 195–231. doi:10.1016/S1364-8152(00)00084-0

Chapitre 4. Usages de la modélisation hydrologique urbaine

4.1 Deux utilisations principales de la modélisation hydrologique

Selon Grayson et al. (1992), les objectifs principaux de la modélisation hydrologique sont:

- Un outil de recherche, qui permet d'améliorer nos connaissances des processus physiques du système;
- Un outil opérationnel, qui peut être utilisé comme un outil de prédiction et de gestion.

En tant que modélisateur en hydrologie urbaine, il est important de distinguer ces deux différents objectifs, qui peuvent exiger des approches de modélisation différentes. Pour les objectifs de recherche, les modèles les plus détaillés avec les données à haute résolution sont souvent encouragés (Beck, 1987; Beven, 1989; Fletcher et al., 2013). Ces approches de modélisation peuvent éventuellement améliorer la connaissance des mécanismes en jeu. Néanmoins, ces types de modélisation nécessitent des données abondantes, et les temps de calculs sont relativement longs. Au contraire, pour les objectifs opérationnels, les gestionnaires des eaux urbaines préfèrent des outils faciles à utiliser, qui imposent des données d'entrée limitées et qui ont tout de même une bonne précision et de faibles niveaux d’incertitude. Afin de répondre à ces demandes, les avancements de la recherche sont réciproquement requis pour mieux comprendre les processus physiques ainsi que les améliorations des techniques de modélisation.

La modélisation de la qualité de l'eau en milieu urbain se situe au croisement de ces deux objectifs. Contrairement à la modélisation quantitative, dont les processus physiques sont bien analysés et largement validés (par exemple les équations de Saint-Venant, (Green and Ampt, 1911), etc.), les mécanismes physiques de l'accumulation et du lessivage des polluants en milieu urbain sont très peu étudiés. Aujourd'hui, nous ne connaissons pas les variables primaires pour conduire les transferts des polluants dans un bassin-versant urbain (Vaze and Chiew, 2003). Ce phénomène exige des avancées dans la connaissance des processus physiques de transfert des polluants en zone urbaine. Par ailleurs, les prévisions de la qualité de l'eau par temps de pluie permettent de savoir quand et où les charges de polluants sont importantes dans un milieu urbain, ces informations sont précieuses pour

concevoir et planifier des démarches de gestion afin de contrôler les pollutions hydrologiques en milieu urbain. Les deux objectifs de la modélisation hydrologiques sont illustrés dans la figure 4.1.

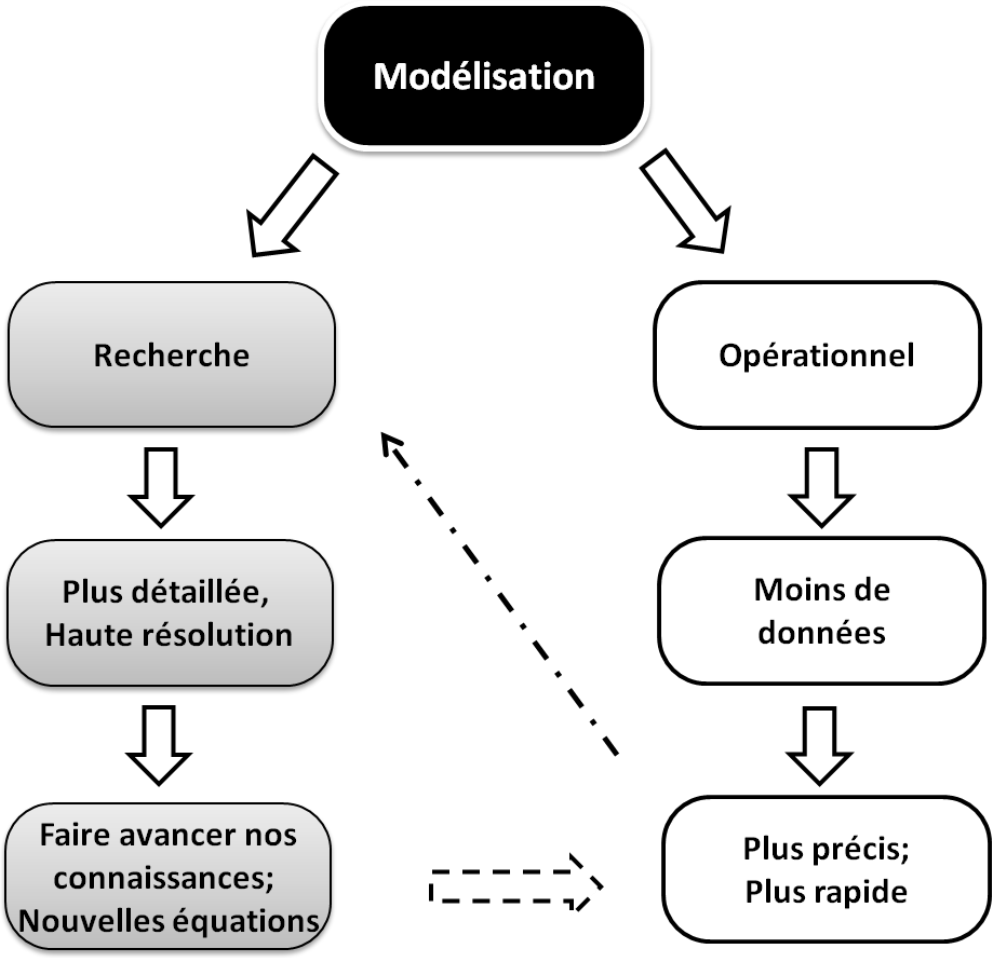

Fig. 4.1 Les deux objectifs de la modélisation hydrologique

4.2 Données géographiques et la télédétection

Depuis les dix dernières années, les développements rapides des techniques de cartographie numérique, telles que les Systèmes d'Information Géographique (SIG), ont conduit à une forte croissance des modélisations hydrologiques distribuées à base physique.

Les données SIG conviennent particulièrement à la modélisation en hydrologie urbaine parce qu'elles sont capables de représenter la variabilité spatiale (e.g. topographie), et les évolutions rapides des données urbaines (e.g. occupation du sol). Dans le cadre du projet Trafipollu, des données topographiques d'une résolution

centimétrique sont obtenues. D'après Salvadore et al. (2015), les plateformes SIG utilisées dans la modélisation hydrologique urbaine peuvent servir (i) au pré- et post-traitement des données d'entrée et des paramètres; (ii) à la gestion et l'affichage des données spatiales; (iii) à l'identification des sous BV, des HRUs ou des UHEs; (iv) à l'intégration des données de télédétection; et (v) peuvent être utilisées pour coupler différents modèles.

L'utilisation des données de télédétection est également supportée par les plateformes de SIG. La télédétection par photo aérienne est la technique la plus souvent utilisée pour mesurer les topographies et l'occupation du sol à haute résolution (par la technique d'ortho-photos). Les données radar de précipitation sont aussi utilisées pour générer les données de pluie distribuées. De plus, les techniques de laser ou Lidar peuvent également être utilisées pour estimer les valeurs de paramètres telles que le LAI (*Leaf Area Index*) (Zhou et al., 2010), la rugosité de la surface (Vieux and Bedient, 2004), et la largeur du fond de rivière (Ogden et al., 2011).

4.3 Vers une approche intégrée pour la modélisation des systèmes environnementaux urbains

En raison de la complexité du milieu urbain, les applications des modèles hydrologiques urbains cherchent généralement à répondre aux questions liées aux composants élémentaires du système urbain (par exemple, les surfaces, les réseaux d'assainissement, etc.). Ces modèles ne donnent pas accès au fonctionnement d'ensemble des zones urbaines. Afin de résoudre les divers problèmes liés à l'environnement urbain, il est récemment proposé de fédérer le savoir-faire des chercheurs dans les différents domaines autour de l'hydrologie urbaine, dans l'intention de développer des modélisations intégrées pour la gestion des eaux et des polluants en milieu urbain. Ces modèles intégrés passent par des projets interdisciplinaires qui associent différentes communautés, telles que les sciences de l'ingénieur, économiques, politiques, sociologiques, anthropologiques, géographiques, historiques et d'aménagement urbain (Bach et al., 2014; Brown et al., 2009; Mitchell et al., 2004).

Du point de vue de la modélisation intégrée, les modèles distribués à base physique ont des avantages significatifs par rapports aux autres types de modèle pour la simulation des eaux de ruissellement. Ce type des modèles s'adapte bien à la conception modulaire de la modélisation hydrologique en milieu urbain (Abbott et al., 1986; Refsgaard et al., 2010). Comme les processus physiques sont bien décris à l'échelle de la maille géo-localisée, les autres composants urbains, tels que les réseaux d'assainissement, le trafic, les milieux aquatiques, l'atmosphère, etc., peuvent être couplés avec un modèle 2D existant.

4.4 Incertitudes des modèles hydrologiques urbains

En vue d'utiliser les modèles pour la prédiction des réponses hydrauliques ou hydrologiques en milieu urbain, il faut indiquer les incertitudes du modèle associé aux différents aspects. D'après la littérature (Dotto et al., 2012; Refsgaard et al., 2007), quatre types d'incertitudes peuvent être identifiés dans la modélisation en hydrologie urbaine:

- Incertitudes liées à l'environnement urbain lui-même. Ce sont des conséquences de la variabilité spatio-temporelle des phénomènes en milieu urbain (e.g. précipitation, trafic, activités humaines, etc.), qui introduisent des fonctions aléatoires dans les processus physiques.
- Incertitudes liées aux données d'entrée. A cause des techniques d'acquisition des données et des méthodes d'interprétation et d'interpolation utilisées, des incertitudes peuvent apparaitre systématiquement. Les techniques de télédétection peuvent potentiellement réduire ces incertitudes, mais elles sont coûteuses et ces techniques ne peuvent pas être appliquées aux grandes échelles.
- Incertitudes liées à la structure du modèle. L'incapacité du modèle de représenter les processus physiques est à l'origine de ce type d'incertitude.
- Incertitudes liées aux paramètres du modèle.

Aujourd'hui, de nombreuses méthodes ont été développées pour calculer les incertitudes liées à la modélisation hydrologique (Beck, 1987; Beven et al., 2000; Dotto et al., 2012; Refsgaard et al., 2007). Afin d'appliquer les modèles pour des objectifs opérationnels, les analyses des incertitudes devront être adressées aux utilisateurs.

Référence

Abbott, M.B., Bathurst, J.C., Cunge, J.A., O'Connell, P.E., Rasmussen, J., 1986. An introduction to the European Hydrological System — Systeme Hydrologique Europeen, "SHE", 2: Structure of a physically-based, distributed modelling system. J. Hydrol. 87, 61–77. doi:10.1016/0022-1694(86)90115-0

Bach, P.M., Rauch, W., Mikkelsen, P.S., McCarthy, D.T., Deletic, A., 2014. A critical review of integrated urban water modelling – Urban drainage and beyond. Environ. Model. Softw. 54, 88–107. doi:10.1016/j.envsoft.2013.12.018

Beck, M.B., 1987. Water quality modeling: A review of the analysis of uncertainty. Water Resour. Res. 23, 1393–1442. doi:10.1029/WR023i008p01393

Beven, K., 1989. Changing ideas in hydrology — The case of physically-based models. J. Hydrol. 105, 157–172. doi:10.1016/0022-1694(89)90101-7

Beven, K., Freer, J., Hankin, B., Schulz, K., 2000. The use of generalised likelihood measures for uncertainty estimation in high order models of environmental systems. Nonlinear Nonstationary Signal Process. 115–151.

Brown, R.R., Keath, N., Wong, T.H.F., 2009. Urban water management in cities: historical, current and future regimes. Water Sci. Technol. 59, 847–855. doi:10.2166/wst.2009.029

Dotto, C.B.S., Mannina, G., Kleidorfer, M., Vezzaro, L., Henrichs, M., McCarthy, D.T., Freni, G., Rauch, W., Deletic, A., 2012. Comparison of different uncertainty techniques in urban stormwater quantity and quality modelling. Water Res. 46, 2545–2558. doi:10.1016/j.watres.2012.02.009

Fletcher, T.D., Andrieu, H., Hamel, P., 2013. Understanding, management and modelling of urban hydrology and its consequences for receiving waters: A state of the art. Adv. Water Resour. 51, 261–279. doi:10.1016/j.advwatres.2012.09.001

Grayson, R.B., Moore, I.D., McMahon, T.A., 1992. Physically based hydrologic modeling: 2. Is the concept realistic? Water Resour. Res. 28, 2659–2666. doi:10.1029/92WR01259

Green, W.H., Ampt, G.A., 1911. Studies on Soil Phyics. J. Agric. Sci. 4, 1–24. doi:10.1017/S0021859600001441

Mitchell, D.A., von Meien, O.F., Krieger, N., Dalsenter, F.D.H., 2004. A review of recent developments in modeling of microbial growth kinetics and intraparticle phenomena in solid-state fermentation. Biochem. Eng. J. 17, 15–26. doi:10.1016/S1369-703X(03)00120-7

Ogden, F.L., Raj Pradhan, N., Downer, C.W., Zahner, J.A., 2011. Relative importance of impervious area, drainage density, width function, and subsurface storm drainage on flood runoff from an urbanized catchment. Water Resour. Res. 47, W12503. doi:10.1029/2011WR010550

Refsgaard, J.C., Storm, B., Clausen, T., 2010. Système Hydrologique Europeén (SHE): review and perspectives after 30 years development in distributed physically-based hydrological modelling. Hydrol. Res. 41, 355–377. doi:10.2166/nh.2010.009

Refsgaard, J.C., van der Sluijs, J.P., Højberg, A.L., Vanrolleghem, P.A., 2007. Uncertainty in the environmental modelling process – A framework and guidance. Environ. Model. Softw. 22, 1543–1556. doi:10.1016/j.envsoft.2007.02.004

Salvadore, E., Bronders, J., Batelaan, O., 2015. Hydrological modelling of urbanized catchments: A review and future directions. J. Hydrol. 529, Part 1, 62–81. doi:10.1016/j.jhydrol.2015.06.028

Vaze, J., Chiew, F.H.S., 2003. Comparative evaluation of urban storm water quality models. Water Resour. Res. 39, 1280. doi:10.1029/2002WR001788

Vieux, B.E., Bedient, P.B., 2004. Assessing urban hydrologic prediction accuracy through event reconstruction. J. Hydrol., Urban Hydrology 299, 217–236. doi:10.1016/j.jhydrol.2004.08.005

Zhou, Y., Wang, Y., Gold, A.J., August, P.V., 2010. Modeling watershed rainfall–runoff relations using impervious surface-area data with high spatial resolution. Hydrogeol. J. 18, 1413–1423. doi:10.1007/s10040-010-0618-9

PARTIE II. Modélisation distribuée à base physique à l'échelle locale

Dans cette partie, nous présentons la modélisation du transfert de l'eau et de polluants en milieu urbain à l'échelle locale. Dans le cadre du projet ANR-Trafipollu, le modèle distribué à base physique FullSWOF (Delestre et al., 2014) est couplé avec un module sédimentaire (modèle Hairsine and Rose (1992a, 1992b)), afin de décrire les processus physiques de lessivage sur les surfaces urbaines. Ces avancées ont permis de mettre au point une nouvelle génération de modèles hydrologiques pour les polluants des bassins versants urbains. Elles ont notamment permis d'évaluer séparément l'importance des effets d'arrachement liés aux gouttes de pluie et les effets d'entrainement par advection. Le modèle est appliqué sur un bassin versant routier situé sur la commune du Perreux-sur-Marne, autour du boulevard d'Alsace Lorraine (RD 34), dans le département du Val de Marne à 12 km à l'est de Paris. Le bassin versant routier est constitué d'un tronçon de chaussée et représente une surface de 2661 m². Les chapitres 5 - 6 présentent les configurations, les calibrations et les validations du modèle FullSWOF. Ils intègrent également une analyse de sensibilité et une analyse détaillée des processus physiques en jeu.

- **Chapitre 5**

Dans le Chapitre 5, nous proposons une nouvelle approche d'expérimentation et de modélisation physique de lessivage sur les surfaces urbaines.

Dans le cadre du projet Trafipollu, les données détaillées du bassin versant local, telles que les données topographiques de résolution centimétrique, les données pluviométriques, les masses de dépôts secs sur les surfaces urbaines, et les analyses granulométriques des matières en suspension (MES) dans l'eau de ruissellement sont mesurées et collectées. Des mesures en continu de débits et de turbidité sont mises en place dans un avaloir qui représente l'exutoire du bassin versant local. Les résultats des expérimentations montrent que seules les particules fines de dépôts secs sur les surfaces urbaines peuvent être transférées à l'exutoire du bassin versant pendant les pluies. Ils montrent aussi que la plupart des Hydrocarbures Aromatiques Polycycliques (HAPs) se trouvent dans la phase particulaire.

Basé sur ces observations, le modèle FullSWOF a été appliqué à l'échelle locale, avec l'hypothèse que les contaminants tels que les métaux et les HAPs sont associés à une seule classe de particules (D50 = 15 μm). Les modélisations ont portées sur 6 événements représentatifs des 56 événements observés pendant la période du 20/09/2014 au 27/04/2015. La méthode des effets élémentaires (*elementary effects*, également connue sous le nom de *Morris*) (Campolongo et al., 2007; Morris, 1991) a été utilisée pour les analyses de sensibilité des six paramètres étudiés. Les résultats de simulations ont montré que le modèle distribué à base physique est capable de représenter les dynamiques des flux d'eau et des concentrations de MES à l'échelle locale du bassin-versant urbain. Les résultats d'analyses de sensibilité indiquent que la vitesse de chute de particules et les stocks

initiaux en sédiments sur la surface sont les paramètres les plus influents pour les simulations qualitatives en milieu urbain par temps de pluie.

- **Chapitre 6**

Afin d'approfondir le travail précédent, le Chapitre 6 présente une analyse détaillée des processus physiques de lessivage sur les surfaces urbaines.

En plus des expérimentations réalisées dans le Chapitre précédent, les mesures des hauteurs d'eau à la surface de la chaussée sont enregistrées en continu pour un site à l'échelle locale du bassin-versant urbain. Les simulations quantitatives du modèle sont donc validées en comparant les données simulées et mesurées des hauteurs d'eau à 0 - 0.5 mm. Les résultats obtenus confirment que les variations spatiales et temporelles des flux d'eau sur les surfaces urbaines peuvent être représentées par le modèle distribué à base physique.

Par conséquent, nous pouvons essayer de décrire les mécanismes physiques du lessivage sur les surfaces urbaines en analysant les différentes variables obtenues par la modélisation. Les simulations appliquées permettent de représenter les solides en 3 classes particulières en se basant sur les mesures granulométriques de MES dans les eaux de ruissellement (D50 = 7 μm, 70 μm, et 250 μm). L'analyse des résultats locaux indique que la plupart des particules fines (> 90%) sur les surfaces peuvent être lessivées au début d'un événement de pluie, environ 10% - 20% des particules de taille intermédiaire sont lessivées lors de la seconde partie de la pluie, et presque aucune particule grosse ne peut être transférée jusqu'à l'exutoire du bassin. Les analyses spatiales des processus du lessivage montrent que (i) les concentrations de MES sur les surfaces des chaussées et des trottoirs sont plus sensibles à l'intensité de pluie que celles sur les surfaces des caniveaux; (ii) les particules grosses sont accumulées sur les surfaces des caniveaux lors du temps de pluie; (iii) concernant les forces d' entrainement du lessivage, l'impacts des gouttes de pluie est de deux ordres de grandeur supérieur à l'effet des contraintes de cisaillement; (iv) les détachements par les gouttes de pluie se réduisent considérablement par l'augmentation des hauteurs d'eau; et (v) les détachements avec les contraintes de cisaillement se produisent uniquement sur les surfaces des caniveaux.

Chapitre 5. A new approach of monitoring and physically-based modelling to investigate urban wash-off process on a road catchment near Paris

Yi Hong[1], Celine Bonhomme[1], Minh-Hoang Le[2], Ghassan Chebbo[1,3]

[1] University Paris-Est, Ecole des Ponts ParisTech, LEESU, 6-8 Avenue Blaise Pascal, 77455 Champs-sur- Marne cedex 2, France.

[2] Université Paris-Est, Ecole des Ponts ParisTech, Laboratoire Saint-Venant, 6 Quai Watier, 78400 Chatou, France

[3] Université Libanaise, faculté de génie, campus rafic hariri, Hadat, Lebanon

* *Corresponding author: yi.hong@leesu.enpc.fr*

*(Article publié dans le journal "**Water Research**")*

DOI: 10.1016/j.watres.2016.06.027

Abstract:

Nowadays, the increasing use of vehicles is causing contaminated stormwater runoff to drain from roads. The detailed understanding of urban wash-off processes is essential for addressing urban management issues. However, existing modelling approaches are rarely applied for these objectives due to the lack of realistic input data, unsuitability of physical descriptions, and inadequate documentation of model testing. In this context, we implement a method of coupling monitoring surveys with the physically-based FullSWOF (Full Shallow Water equations for Overland Flow) model (Delestre et al., 2014) and the process-based H-R (Hairsine-Rose) model (Hairsine and Rose, 1992a, 1992b) to evaluate urban wash-off process on a road catchment near Paris (Le Perreux sur Marne, Val de Marne, France, 2661 m²). This work is the first time that such an approach is applied for road wash-off modelling in the context of urban stormwater runoff. On-site experimental measurements have shown that only the finest particles of the road dry stocks could be transferred to the sewer inlet during rainfall events, and most Polycyclic Aromatic Hydrocarbons (PAHs) are found in the particulate phase. Simulations over different rainfall events represent promising results in reproducing the various dynamics of water flows and sediment

transports at the road catchment scale. Elementary Effects method is applied for sensitivity analysis. It is confirmed that settling velocity (V_s) and initial dry stocks (S) are the most influential parameters in both overall and higher order effects. Furthermore, flow-driven detachment seems to be insignificant in our case study, while raindrop-driven detachment is shown to be the major force for detaching sediment from the studied urban surface. Finally, a multiple sediment classification regarding the Particle Size Distribution (PSD) can be suggested for improving the model performance for future studies.

Keywords: physically based and distributed model; urban wash-off; Hairsine-Rose model; FullSWOF model; Sensitivity analysis;

1. Introduction

It is predicted that by 2050, 64% of the "developing world" and 86% of the "developed world" will be urbanized (Montgomery, 2008). This trend of rapidly increasing urbanization requires better understanding of the urban wash-off phenomenon in order to develop more advanced management strategies.

Among the various substances of urban stormwater pollutants, suspended solids, heavy metals and Polycyclic Aromatic Hydrocarbons (PAHs) are widely considered as the major causes of contamination in receiving environments (Fletcher et al., 2013; Zoppou, 2001). Most of these heavy metals and PAHs are found in the particulate phase and associated with fine particles (Aryal et al., 2010; Bressy et al., 2012; Gasperi et al., 2014). Therefore, the studies of stormwater quality can focus on the urban sediment transport during stormwater events.

Numerous urban stormwater quality models exist, however, most of them are still unable to adequately reproduce urban wash-off dynamics (Dotto et al., 2012; Egodawatta et al., 2007; Elliott and Trowsdale, 2007). One of the major reasons is the lack of available and reliable local data. According to Duncan, (1995); Vaze and Chiew, (2003), accurate urban stormwater quality models require detailed spatial and temporal data of rainfall intensity, water runoff characteristics and pollutants' features (e.g. Weight, Size, Settling velocity). Since it is impossible to collect sufficient water runoff data over different temporal and spatial points of an urban catchment, the application of Full Shallow-Water equations with extremely high-resolution topographic data is a promising approach for representing stormwater runoff processes (Grayson et al., 1992a, 1992b). Another challenge of modelling urban stormwater quality is the shortage of physical descriptions of pollutant wash-off mechanisms. Until now, current urban wash-off models are generally based on

exponential wash-off functions (e.g. SWMM, M-QUAL, HSPE, STORM etc.), assuming the rate of particle loss on a catchment scale is directly proportional to the availability of the pollutants on the road surface and to the water flow. With these equations, urban spatial heterogeneities are neglected, leaving models to rely on extensive calibration of empirical wash-off coefficients, a fact that limits their predictive capacities (Tsihrintzis and Hamid, 1997). Thus, greater insight into the physical processes of particulate detachment and transport will provide a more detailed understanding of the movement of pollutants in urban landscapes.

Only very few studies have been performed for the physically-based modelling of urban wash-off processes. Shaw et al., (2006) proposed a saltation-type wash-off model in which particles were repeatedly detached from the impervious surface by raindrop impacts and were transported laterally by overland flow while settling back to the surface. Massoudieh et al., (2008) presented a wash-off model in which detachment and reattachment of contaminants were considered as rate-limited processes and the detachment rate was assumed to be a function of flow velocity by a power expression. These existing models have provided a basic perception of developing new mechanistic wash-off models for urban surfaces. However, the wash-off processes in the above models were not combined with two-dimensional water-flow simulations, and the detachments were only represented by single effects of raindrops impacts (Shaw et al., 2006) or flow power influences (Massoudieh et al., 2008). These inadequate assumptions limit the reliability of such physically-based models for stormwater quality modelling in urban areas (Deletic et al., 1997; Dotto et al., 2012; Wijesiri et al., 2015).

In this study, the Hairsine-Rose (H-R) model (Hairsine and Rose, 1992a, 1992b) coupled with the FullSWOF (Full Shallow-Water equations for Overland Flow) modelling system (Delestre et al., 2014; Le et al., 2015) is applied. Unlike other physically based approaches, the H-R model calculates raindrop-driven detachment, flow-driven detachment and deposition processes separately, with the net outcome being the difference between these process groups. The H-R model also simulates a deposited layer that differs from the original soil in its composition and detachability, which allows us to distinctively model urban dust and road pavement.

This study is the first time that the H-R model is applied and analyzed within the context of urban stormwater wash-off, using the example of a road catchment near Paris. With this new approach, our objective is to examine urban surface wash-off dynamics for several stormwater events. This approach couples detailed monitoring surveys and physically-based modellling, which may help to advance the understanding of stormwater wash-off mechanisms. The following sections will provide details on monitoring surveys for the road catchment, model configurations, and sensitivity analysis.

2. Materials and methods

2.1. Study site

A small urban road catchment near Paris (Le Perreux sur Marne, Val de Marne, France), including a segment of high traffic volume (more than 30,000 vehicles per day) and its adjacent sidewalk and parking zones, are selected for this study. A gutter is located between the road and the sidewalk, allowing water flow from the upper part of the catchment to the sewer inlet (FIG. 1). The total surface of the study basin is 2661 m²,where approximately 65% of the surface are roads, 30% are sidewalks, and 5% are gutters and parkings. The western section on a higher incline than the eastern side, with an average slope of less than 2%.

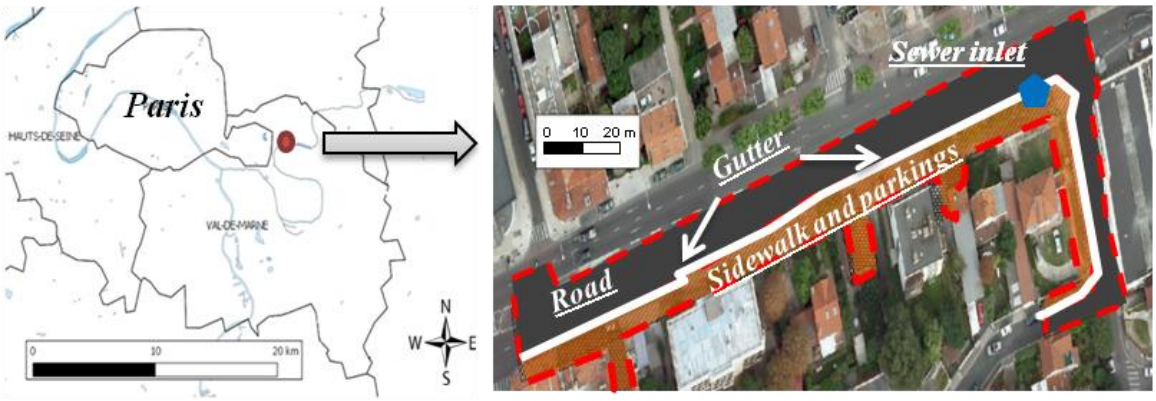

Fig. 1 Study area at Eastern Paris, France. The catchment is delineated by red dashed lines, the sewer inlet is located at the northeast side of the catchment. In this picture, road area is marked as grey, gutter area is marked as white, sidewalk and parking areas are marked as brown.

2.2. On-site monitoring and sampling

2.2.1. Rainfall measurements

A tipping-bucket rain gauge is installed on the roof of a building close to the road catchment (less than 150 meters). The pluviometer has a resolution of 0.1 mm. As the study area is quite small, rainfall is considered as homogeneous within the basin. Monitoring took place between September 20, 2014 and April 27, 2015, identifying different rainfall events by intervals longer than 90 minutes between two tipping records and total rainfall depth of each event of more than 1mm. It has to be noted that there is no street sweeping on the study road, thus the antecedent dry days between two rainfall events are the only factor that influence the deposited dry stocks.

2.2.2. Monitoring at the sewer inlet

The sewer inlet is equipped for continuous monitoring of discharge, turbidity and ability to perform samplings for the analysis of Particles Size Distribution (PSD) and the PAHs features (FIG. 2a). The flow is measured by a Nivus Flowmeter, using the cross correlation method in order to calculate flow speed for different layers in a full pipe, which increased the reliability of data. The water discharge is recorded with a 1 minute time interval inside the road inlet. At the same time, a multi-parameter probe (mini-probe OTT) is installed with the flowmeter, measuring turbidity with a 1minute time interval. For several rainfall events, a peristaltic pump (Watson Marlow) pumped 250 mL of water at regular volume intervals entering the inlet for the purpose of measuring mean TSS concentrations at the scale of rainfall event. The sampling bottles are located in a cabinet at the side of the road (FIG. 2b). The complete monitoring system is presented in FIG. 2c. The TSS-Turbidity relationship is therefore established based on samplings during 16 studied rainfall events, which follows a linear regression TSS=0.8533*Turbidity, with the R^2 equal to 0.97.

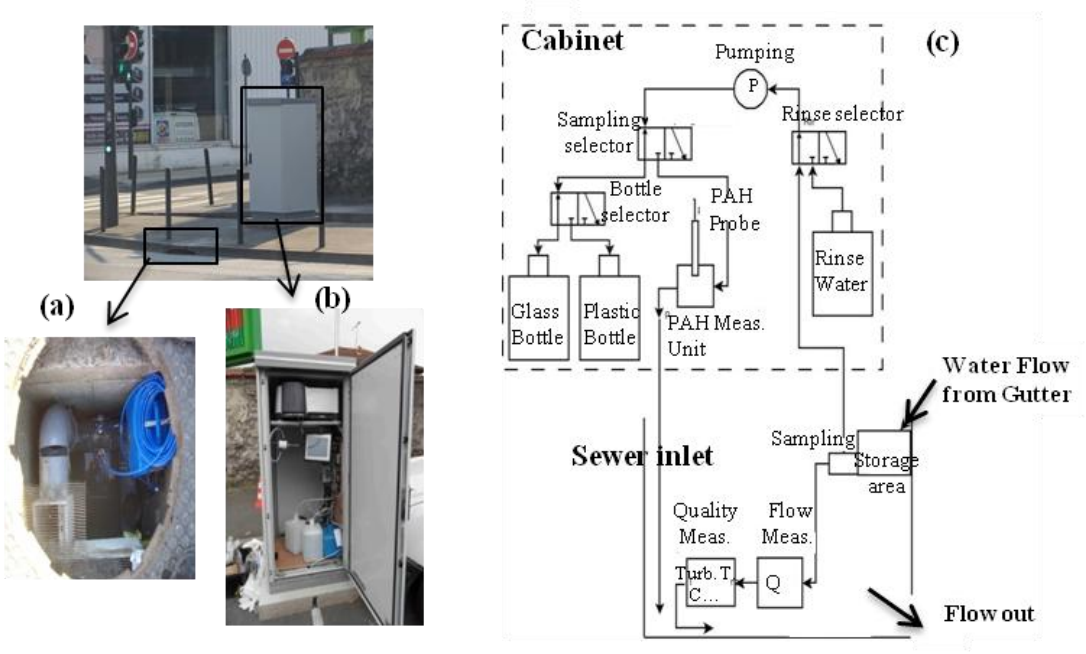

Fig. 2 (a) Monitoring equipments inside the sewer inlet; (b) Cabinet at the road side; (c) Flowchart of the monitoring system.

2.2.3. Road dust sampling

In the framework of the ANR (French National Agency for Research) Trafipollu project, the road dust sampling was carried out on theOctober 14th 2014. The detailed experimental protocol is described in (Bechet et al., 2015). The samples

were collected in dry-weather after a dry period of 2 days. A two-square meter surface was delimited with adhesive tape. After hand-brushing the surface, the road dust was dry-vacuumed using a vacuum cleaner (Rowenta ZR80)(Fig. 3b)). Road dust samples were collected in paper filters along the road: on the sidewalk, in the gutter and on the road (3 positions (noted as A, B, C) over 3 locations (marked as 1, 2, 3)).

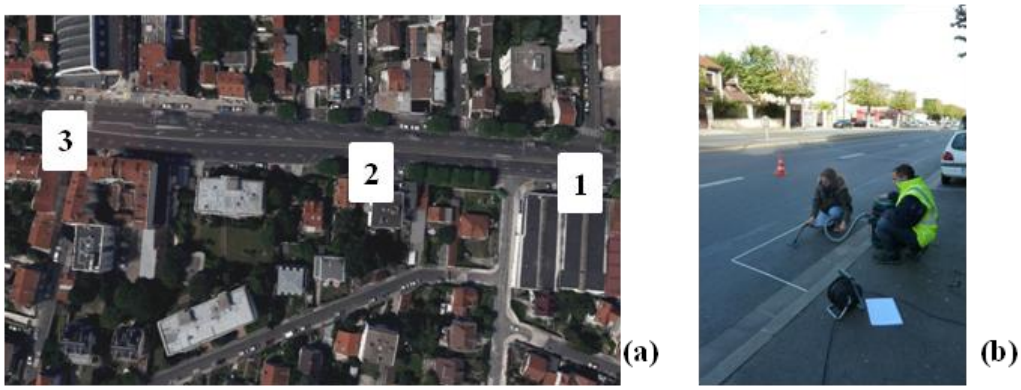

FIG. 3 (a) Location of sampling points along the road (Le Perreux, France); (b) road dust dry sampling by a vacuum cleaner in gutter (point 3).

2.3. Particle Size Distribution (PSD) analysis

For both dry samples (road dust) and wet samples (sewer inlet), particle size analysis is performed using a laser diffractometer for the fraction below 2mm (Malvern® Mastersizer 3000), while the volume distribution is calculated with the Mie (1908) light scattering theory. In order to compare the mass distribution of dry deposits and suspended solids in the stormwater, the total mass of either road dust or TSS load for the entire catchment is calculated independently. Assuming the uniform distribution of sediments throughout the road surface, the measurements of the deposit samples (2 m²) are used to calculate the total mass of road dust on the catchment surface (2661 m²). Likewise, the total mass of loaded TSS during a rainfall event can be calculated by multiplying the measured mean TSS concentration by the total volume of flow water for each event.

2.4. PAH chemical analysis

Particles are freeze-dried during 48 hours and then extracted by means of microwave-assisted digestion (Multiwave 3000, Anton Paar). PAHs samples are extracted using Methylene chloride/Methanol (90/10, v/v) and spiked with similar surrogate standards over a 30min cycle. Extracts are recovered by filtration, then the solvent is removed and the residue dissolved in 300µL heptane before purification. Thus, a 2.1g silica column is conditioned with 4mL heptane and the PAH fraction is

eluted with 10mL heptane/methylene chloride (80/20, v/v). 13 types of PAHs are analyzed with GC/MS (Focus DSQ, Thermo Fisher Scientific) using a RTX5SIL MS silica capillary column (60m long, 0.25mm internal diameter and 0.25µm film thickness, Restek). The molecules are detected by a quadripole mass analyzer operating in Selected Lon Monitoring mode (SIM).

2.5. High resolution topographic data

The accuracy of a process-based wash-off model depends on the accurate simulation of water flows. Therefore, precisely defined topographic data is adapted to the study site. In the framework of the ANR-Trafipollu project, topographical data of 1cm-resolution was collected by an on-vehicle LiDAR by the National Institute of Geography of France (IGN) (Hervieu and Soheilian, 2013; Paparoditis et al., 2012). In order to have the model apply with an adequate number of pixels, an aggregation of 1cm-resolution to 10cm-resolution is performed (FIG 4).

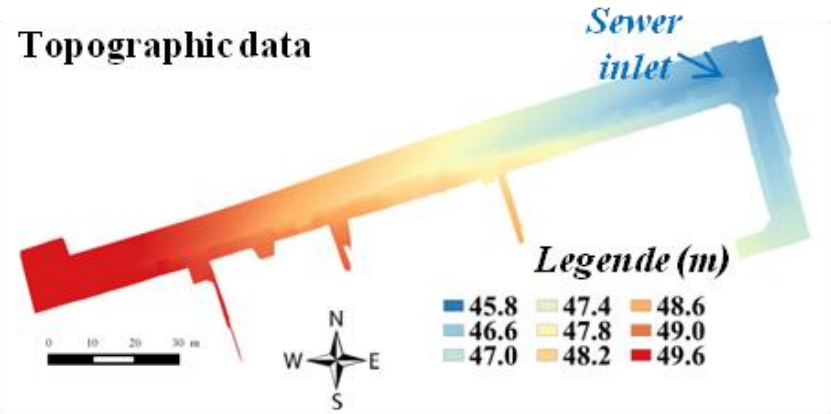

FIG. 4 Topographic data of 10cm-resolution for the model, (pixels 1833 x 515)

2.6. Model description

2.6.1. Water quantity modelling

The C++ code FullSWOF (Delestre et al., 2014) is applied for the water flow modelling in this study. The FullSWOF model uses a finite volume scheme to solve bidimensional Shallow-Water (SW) equations with topographical and friction source terms. The water infiltration process is represented by using the Green and Ampt model. Recently, (Le et al., 2015) recalled the studies of (Heng et al., 2009; Kim et al., 2013), and introduced a faster numerical scheme for coupling the Hairsine-Rose (H-R) model with SW equations. These authors introduced a numerical scheme for

coupling the H-R model with SW equations within the FullSWOF system, allowing the simulation of soil erosion and transport processes of sediments.

2.6.2. Wash-off modellling

In this study, it is supposed that sediments are represented by a single class of particles. This assumption is linked to experimental results obtained from urban dust analysis, which will be explained in the section below. This simplification greatly reduces the model complexity.

The H-R model allows particles to be present in one of three compartments: the flow itself (in the form of suspended solid), the deposited layer, or the original soil. Once sediments have been detached, particles can be suspended or return to the bed by deposition, forming a deposited layer from which they can be subsequently re-detached. Two types of wash-off processes are considered: the first one is due to rainfall impact; and the second one is due to the shear stress by overland flow. This presumption allows model to distinguish between the rates of detachment of the original cohesive soil and non-cohesive deposited sediments. In the case of urban catchment, the road asphalt is considered as a non-erodible original soil, while the road dust is the deposited layer. This consideration leads to a simplification of the initial H-R model by neglecting the terms of detachment on original soil (e, r). The processes represented in H-R model are illustrated in Fig. 5:

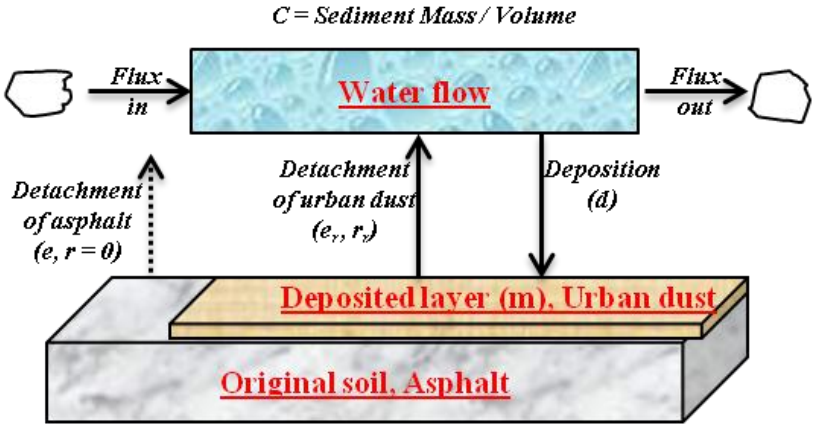

Fig. 5 Concept of Hairsine - Rose Model. C represents the TSS concentration in mass per unit volume; m refers to the deposited sediment mass per unit area; e and r stand for the rate of rainfall-driven and flow-driven detachment for original soil, respectively; er and rr mean respectively the rate of rainfall-driven and flow-driven detachment for the deposited layer; and d is the rate of TSS deposition from the water flow to the deposited layer.

The H-R model reflects the conservation of mass entering and exiting a cell, equations are written as below (1 - 2):

$$\frac{\partial hc}{\partial t} + \frac{\partial qc}{\partial x} = e_r + r_r - d \qquad (1)$$

$$\frac{dm}{d_t} = d - e_r - r_r \qquad (2)$$

Where *c* represents the TSS concentration in mass per unit volume; *m* refers to the deposited sediment mass per unit area; e_r and r_r means the rate of rainfall-driven and flow-driven detachment for deposited layer, respectively; *h* is the water-height and *q* is water flux which are computed from the SW equations; *and d* is the deposition. The terms e_r , r_r and *d* can be written by Eq.3 - 5:

$$e_r = a_d P \qquad (3)$$

$$r_r = \frac{\Omega_e}{\frac{\rho_s - \rho_w}{\rho_s} gh} \qquad (4)$$

$$d = v_s c \qquad (5)$$

Where,

- a_d is the detachability of the deposited sediment *(kg m^{-3})*;
- P is the rainfall intensity (*m/s*);
- Ω_e is the effective stream power *(W/m²);*
- ρ_s and ρ_w are the densities of sediment and water (*kg/m^3*);
- *h* is the water-heigh (*m*);
- *g* is the standard gravity (*m/s²*);
- v_s is the settling velocity of the single-class particle in water *(m/s)*.

According to Eq.3, the rate of rainfall detachment (e_r) is considered to be dependent on rainfall rate (*P*). In Eq. 4, since the cohesive strength of the deposited sediment is considered negligible, the resisting force of flow-driven detachment only depends on the immersed weight of sediments. The power expended in lifting the

sediment to some height in the flow is directly calculated by the rate of change of potential energy of the sediment. The detachability a_d and the effective stream power Ω_e can be written as Eq.6-8:

$$a_d = \begin{cases} a_{d0}\,, & h \le h_0 \\ a_{d0}\left(\frac{h_0}{h}\right)^b\,, & h > h_0 \end{cases} \qquad (6)$$

$$\Omega_e = F(\Omega - \Omega_0) \qquad (7)$$

$$\Omega = \rho_w g S_f q \qquad (8)$$

Where:

- a_{d0} is the initial detachability of deposited sediment *(kg m^{-3})*;
- h_0 is the threshold of flow depth, above which the detachability will decline (*m*);
- *b* is a positive constant.
- *F* is the effective fraction of excess stream power*;*
- Ω is the calculated total stream power *(W/m²);*
- Ω_0 is the threshold stream power below which there is no entrainment *(W/m²);*
- S_f is the friction slope which is calculated by Manning's equations;

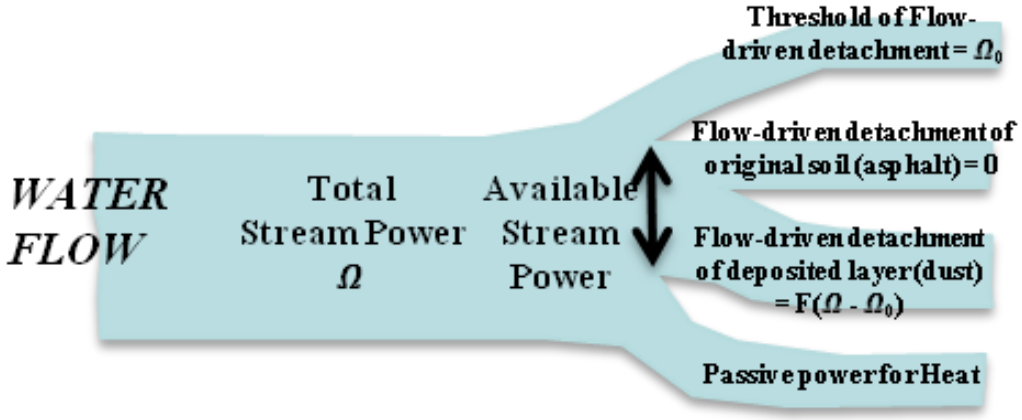

Fig. 6 Flow diagram of the redistribution of Total Stream Power.

Eq.6 illustrates that the raindrop impact detachability declines with the rise in flow depth when it is beyond a certain threshold. This principle was originally proposed by (Mutchler and Hansen, 1970), and revised by (Proffitt et al., 1991) for the H-R model. Eq.7-8 show that the rate of flow-driven detachment is due to the effective stream power (Ω_e), while the source and sinks of stream power in overland flow are shown in Fig. 6.

2.7. Model performance and sensitivity analysis

2.7.1. RMSD and PCC objective functions

Model's ability to replicate the TSS concentrations is first evaluated by the widely used Root-Mean-Square-Deviation objective function (*RMSD*) (Eq.9):

$$RMSD = \sqrt{\frac{\sum_{t=1}^{n}(Sim_t - Obs_t)^2}{n}} \qquad (9)$$

Where *n* is the total duration of the simulated rainfall duration, Sim_t and $Obs_t$are the simulated and observed TSS concentration at t^{th} minute.

However, Bennett et al., (2013); Gupta et al., (2009) summarized that when using the RMSD and its related Nash-Sutcliffe efficiency (NSE) criterion, the bias between the simulated and measured signals are systematically over-weighted, while the variability and the relative correlation are underestimated. Consequently, the RMSD coefficient assigns more importance to the highest TSS values, which have the most significant discrepancies between measurements and simulations, compared to other moderate fluctuations. As for the urban wash-off phenomenon, the first TSS concentration peaks are typically much more important than subsequent peaks, thus, using only the RMSD objective function could not truly evaluate the model's performance on the overall TSS dynamics. In this case, we introduced the Pearson's Correlation Coefficient (*PCC*) objective function as a complement (Eq.10):

$$PCC_T = \frac{\sum_{t=1}^{T}\left(Sim_t - \overline{Sim}\right)\left(Obs_t - \overline{Obs}\right)}{\sqrt{\sum_{t=1}^{T}\left(Sim_t - \overline{Sim}\right)^2}\sqrt{\sum_{t=1}^{T}\left(Obs_t - \overline{Obs}\right)^2}} \qquad (10)$$

Where t indicate t-th minute in the duration of the rainfall event, $\mathrm{Sim_t}$ and $\mathrm{Obs_t}$ are the simulated and observed TSS concentration at t^{th} minute, $\overline{\mathrm{Sim}}$ and $\overline{\mathrm{Obs}}$ are the mean simulated and observed TSS concentration.

2.7.2. The investigated parameters

Generally, the simplified H-R model needs to define three parameters concerning the raindrop impact detachment (a_{d0}, h_0, b), two parameters involving the flow-driven detachment (F, Ω_0), and two physical properties which are difficult to measure accurately (V_s, S).

Following (Mutchler and Hansen, 1970), most researchers (Heng et al., 2011; Proffitt et al., 1991; Torri et al., 1987) consider that $h_0 = 0.33\ D_R$, where D_R is the mean raindrop size. We use the same presumption in this study, with $D_R = 2\ mm$ for the Parisian region in France (Gloaguen and Lavergnat, 1995), the parameter is hence fixed as $h_0 = 0.7\ mm$.

As for the parameters a_{d0}, b, F, and Ω_0, their testing ranges are determined by following the investigations of (Beuselinck et al., 2002; Heng et al., 2011; Hogarth et al., 2004; Jomaa et al., 2010; Proffitt et al., 1991). These authors have investigated the optimized parameter values of the H-R model for several case studies. Although these parameter studies are based on erosion processes in natural soils, the physical interpretations of the indicated 4 parameters are related to the properties of sediment particles and water flows. Therefore, we could learn from the previous findings in order to set testing parameter ranges for urban wash-off modelling.

Table 1 Tested values of H-R parameters for the Elementary Effects (EE) method

Symbol	Units	Definition	Ranges
a_{d0}	kg/m^3	Initial detachability of deposited sediment	1500 - 4500
b	-	Positive constant	0.8 - 2
F	-	Effective fraction of excess stream power	0.01 - 0.03
Ω_0	W/m^2	Threshold stream power	0.15 - 0.35
V_s	m/s	Settling velocity	0.00001 - 0.001
S	kg/m^2	Uniformly initial dry stock	0.0001 - 0.01

The settling velocity (V_s) and the initial dry stock (S) are roughly estimated from the measured data. As it is difficult to obtain the exact values of these parameters, we make some assumptions from the observed values, which will be explained in the section below. The testing ranges of the 6 parameters are listed in Table 1.

2.7.3. Using Elementary-Effects (EE) Method for sensitivity analysis

The Elementary-Effects (EE) method (also known as Morris method) is applied for the Sensitivity Analysis (SA) (Campolongo et al., 2007; Morris, 1991). The major advantage of this screening method is that it has a lower computational cost compared to other global SA methods (Song et al., 2015). Thus the EE method is particularly suited for computationally expensive models such as the physically-based FullSWOF platform.

With the EE method, parameters are sampled using One-At-a-Time (OAT) design (Saltelli and Annoni, 2010). Each model input X_i, $i = 1, ..., k$, is assumed to vary across p selected levels in the parameter ranges. The parameter sampling space Ω is thus a k-dimensional p-level grid. Following a standard practice in sensitivity analysis, factors are assumed to be normalized in [0,1] for generating parameter samples, and then transformed to their actual values for simulations. For a given $\mathbf{X}=(x_1, x_2, ..., x_k)$, the elementary effect of the i-th parameter is defined as (Eq. 11):

$$d_i(\boldsymbol{X}) = \frac{y(x_1, \dots, x_{i-1}, x_i + \Delta, x_{i+1}, \dots, x_k) - y(\boldsymbol{X})}{\Delta} \qquad (11)$$

where Δ is the distance between two testing values of parameter x_i, and $y(\boldsymbol{X})$ is the objective function.

By setting different starting points $\boldsymbol{X}$ from Ω, we can obtain the distribution of elementary effects associated with the i-th input factor, denoted as F_i. Two sensitivity measures, the absolute mean (μ^*) and the standard deviation (σ) of the F_i can be calculated by Eqs (12) and (13) (Campolongo et al., 2007):

$$\mu_i^* = \frac{1}{r}\sum_{j=1}^{r} |d_i(j)| \qquad (12)$$

$$\sigma_i = \sqrt{\frac{1}{r-1}\sum_{j=1}^{r}\left[d_i(j) - \frac{1}{r}\sum_{j-1}^{r} d_i(j)\right]^2} \qquad (13)$$

where $d_i(j)$ is the elementary effect for i-th input factor using the j-th starting point, j=1,2,...,r; r is the number of repeated parameter sampling design, which is also named trajectories of sample points in the parameter space Ω. The number of r is commonly set between 10 and 40 (Campolongo et al., 2007; Saltelli and Annoni, 2010).

In this paper, we investigate the sensitivities of 6 parameters (k=6) for urban wash-off modelling. p=9 levels ({0, 0.125, ... , 0.875, 1}) and r=20 trajectories are set for parameter samplings. Following Campolongo et al., (2007), the starting points for the trajectories are generated with Latin Hypercube Sampling (LHS), while the Δ=0.5 for x_i < 0.5 and Δ=-0.5 for x_i>0.5. The RMSD and PCC objective functions are applied. In general, 20*(6+1)=140 simulations are performed for each rainfall events. The μ^* estimates the overall effect of each parameter on the output, while the σ estimates the higher order effects, such as nonlinearity and interactions between inputs, respectively.

3. Results and discussions

3.1. Field data treatment and analysis

3.1.1. Rainfall events selection

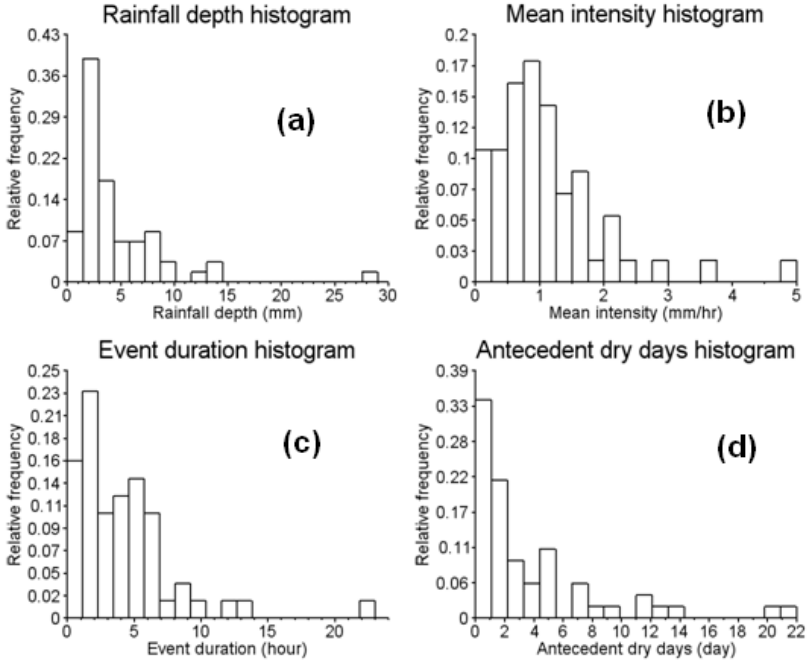

Fig. 7 Histogram of rainfall event characteristics over the entire period. Where (a) Rainfall depth; (b) Mean intensity; (c) Event duration; (d) Antecedent dry days.

56 rainfall events have been identified during the study period of September 20, 2014 to April 27, 2015. Analysis of rainfall depth, mean intensity, event duration and

antecedent dry days are performed for all the precipitation events in order to highlight their characteristics (Fig. 7).

According to the FIG. 7 (a)(b), we can observe that most rainfall events within the study area of Eastern Paris, are considered low. In fact, more than 88% of rainfall events have a rain depth of less than 8 mm, and nearly 89% of rainfall events have a mean intensity of smaller than 3 mm/hr. Additionally, FIG. 7 (c)(d) shows that event duration and antecedent dry days are a little more dispersed. However, most rainfall events observed are shorter than 7 hours (87%), while 88% of the events are preceded by a previous rainfall event by less than 8 days.

As the distributed FullSWOF model is implemented on a 10^6 pixel grid, the simulation is quite time-consuming. Therefore, we have to select several rainfall events which contain different characteristics in order to characterize the overall performance of the FullSWOF model within an urban context. Among the observed rainfall events, we selected 6 typical events for model application and performance evaluation, with the rainfall depths varying from 2 to 7.4 mm, the mean intensities differing from 0.8 to 2.9 mm/hr, durations varying from 0.7 to 8 hours, and antecedent dry days differing from 0.2 to 7.3 days. The summary of selected rainfall events is listed in Table 2:

Table 2 Summary of the 6 selected rainfall events.

Rainfall date	Rainfall depth (mm)	Mean intensity (mm/hr)	Max intensity (mm/hr)	Duration (hour)	Antecedent dry days (day)
10/06/2014	5.9	1.73	8.37	3.42	7.3
10/07/2014	2	2.86	20	0.7	0.2
11/14/2014	7.4	2.1	8.57	3.5	7.1
02/28/2015	4.6	2.05	5	2.2	2
04/02/2015	2.6	1	8.57	2.6	3.3
04/03/2015	6.9	0.84	5.63	8.1	0.9

3.1.2. Total mass and PSD of TSS and dry stocks

The total mass of TSS for several rainfall events and the total weight of road dry stocks over the entire catchment are approximated based on stormwater samplings and road dust samplings, respectively (FIG. 8a). Meanwhile, the mass distributions of the washed off particles and the dry deposits for the entire catchment are compared in FIG. 8b.

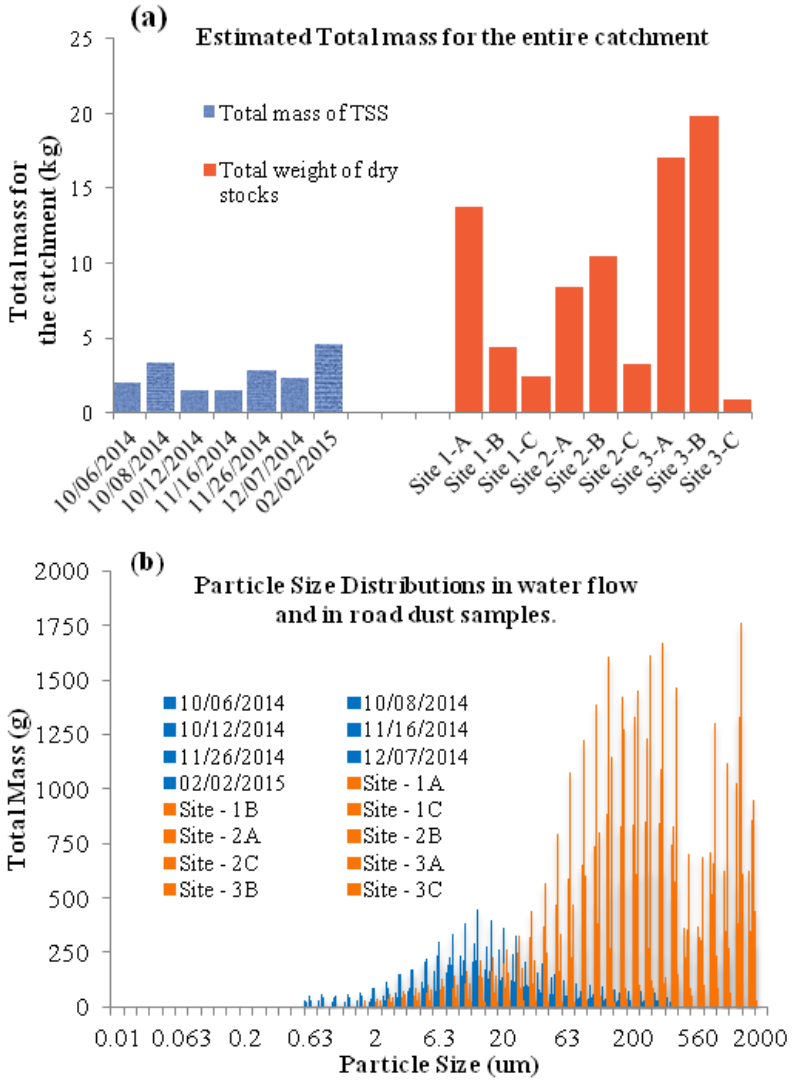

Fig. 8 Measurements of Total Suspended Solids (TSS) and road dust in water flow and dry stock samples, respectively. For (a) Estimated total mass of TSS (blue bars) and road dust (orange bars) for different rainfall events and sampling sites, respectively. (b) Mass distributions of TSS (blue bars) and road dust (orange bars) for different rainfall events and sampling sites, respectively.

Generally, the mass of washed-off particles collected in the sewer inlet is much lower than the estimated dry stocks, indicating that a large proportion of the deposited particles are not transferred into the sewer networks during the rainfall events. Moreover, the PSD of stormwater samples is quite different than that of surface dust samples. The TSS in surface runoffs contains most of fine particles (<50 um), which represent more than 90% of total TSS load. While the small particles are only shown in a limited portion (< 10%) of the surface dust samples. This phenomenon suggests that only the finest particles of road dry stocks could be transferred into the sewer inlet during the average rainfall events.

For the modelling approach, since the TSS concentration is derived from turbidity observations and the turbidimeter (mini-probe OTT) can only measure fine particles (< 2mm), we focus on this part of sediments. By homogenizing the estimated weight of road dust (FIG. 8a, orange bars) for the entire catchment (2661 m²), the testing range of initial dry stocks is set to 0.1 - 10 g/m². The settling velocity is calculated with the particle size using Cheng's (1997) equation. According to FIG. 8b (blue bars), the median diameter (d_{50}) of suspended solids in stormwater samples equals to 15um, while cumulative 10% and 90% points of diameter are d_{10}=5um and d_{90}=50um, respectively. Therefore, the tested range of settling velocity is calculated from the d_{10} and d_{90} of the Particle Size Distribution, equals to 0.00001 - 0.001 m/s.

3.1.3. Investigations of PAHs

In the framework of ANR-Trafipollu project, 13 types of PAHs (Fluorene, Phenanthrene, Benzos, etc.) have been found in 7 wet weather samples. The average percentages of investigated PAHs in particulate phases are presented in Fig. 9:

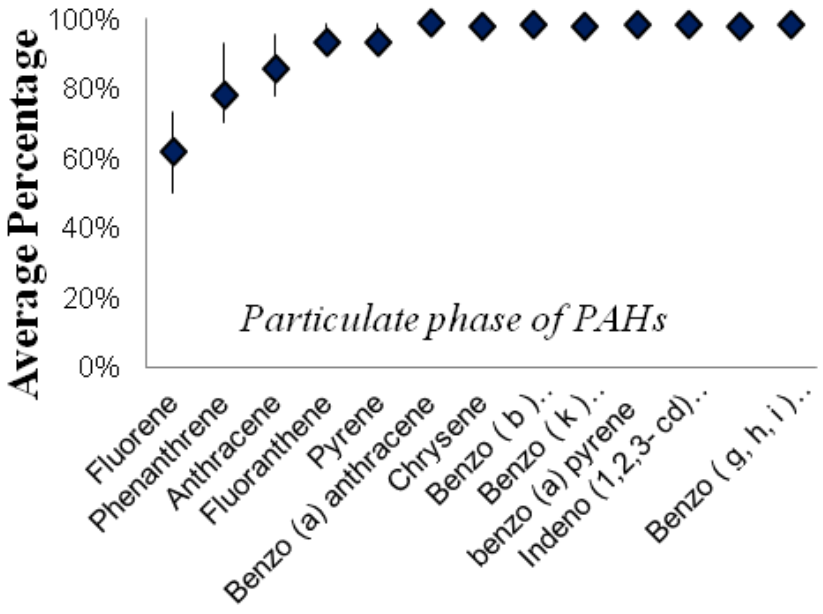

Fig. 9 Average percentage of PAHs in particulate phases in stormwater runoff samples.

As shown in Fig. 9, most PAHs have more than 90% are associated with suspended particles, while the particulate fraction of Fluorene and Phenanthrene are slightly smaller, yet still remaining between 60% and 80%. This finding confirms our assumption of using TSS concentration as the indicator for urban stormwater quality modelling.

3.2. Water flow simulations

An accurate water quantity simulation is required for water quality modelling. The trial and error procedure is performed for calibrating the Manning coefficient in order to correctly reproduce the water flow. The RMSD and the NSE is used to evaluate the model performance. An optimized Manning coefficient value of 0.05 is calibrated for the event of Feb. 28th 2015 and validated for the other 5 examined rainfall events. As seen in FIG. 10, the performance of the quantitative simulation is quite satisfying. Compared to our previous work with the SWMM model (Rossman, 2010), the NSE value is improved from 0.7 to 0.9. Therefore, the use of such a physically-based and distributed model integrating the full shallow-water equations is more accurate than using only Mannings' formula for the water flow simulation at the scale of a small road catchment.

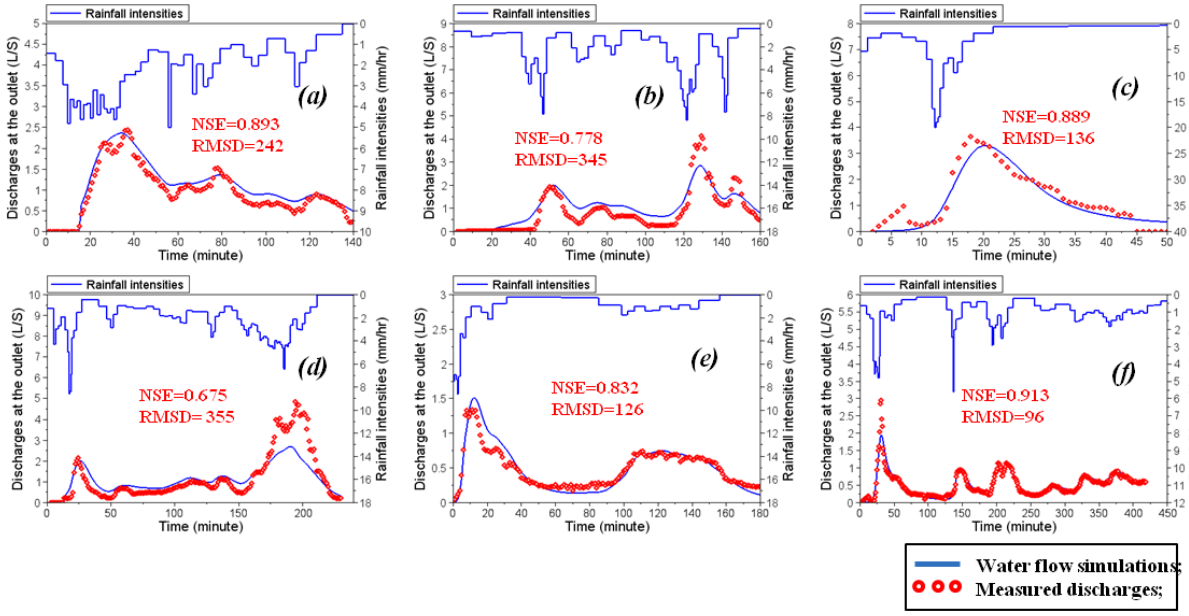

Fig. 10 Water flow simulations using NSE and RMSD as objective functions. The simulated discharges at the outlet (solid blue line) are compared with the measured data (red circles). Rainfall is plotted on the upper part. For events (a) Feb. 28th 2015, (b) Oct. 6th 2014, (c) Oct. 7th 2014, (d) Nov. 14th 2014, (e) April. 2th 2015, (f) April. 3th 2015.

3.3. Water quality simulations and parameter investigations.

The Elementary-Effects (EE) method with 20 trajectories of 6 parameters is performed for the 2 rainfall events of Oct. 7th 2014 and Feb. 28th 2015. The cost is *20*(6+1)=140* simulation runs for each event. The event of Oct. 7th 2014 has only

one runoff peak while the other event contains several. Moreover, the durations of these two events are relatively short (only 2.2 and 40min respectively), which require shorter simulation times compared to other precipitation events.

3.3.1. "Best-fitted" TSS simulations

The "best-fitted" TSS simulations with the 20 trajectories EE method are displayed in Fig. 11. Although the simulations are performed by using discrete parameter values with very limited calibration efforts, the results are quite promising for the road wash-off modelling. However, even though the performance of the model seems satisfying visibly, the NSE and RMSD criterion show poor outcomes, owing mainly to the significant deviation between the measured and simulated TSS concentrations. Since the objective of this study is to investigate the effects of parameter on TSS dynamics, the correlation coefficient (PCC) is a promising complement to assess model performance.

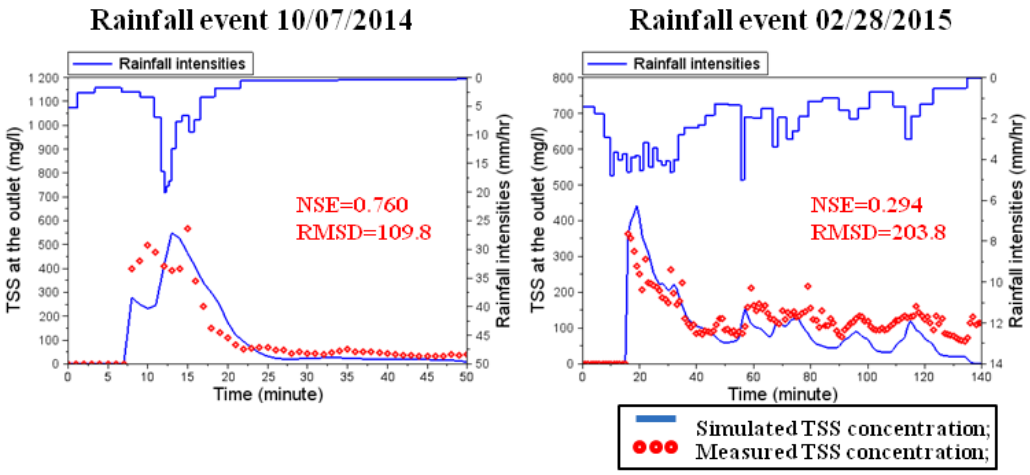

Fig. 11 Best-fitted TSS simulations using NSE and RMSD objective functions for the rainfall events of (a) Oct. 07th 2014 and (b) Feb. 28th 2015. The simulated TSS concentration at the sewer inlet (solid blue line) are compared with the measured data (red circles). Rainfall intensity is plotted on the upper part.

3.3.2. Sensitivity analysis of H-R parameters

The absolute mean (μ^*) and the standard deviation (σ) of the distribution of elementary effects related with each parameter are obtained using EE method with 20 trajectories. The RMSD and PCC objective functions are applied to calculate the discrepancies between the measured and simulated TSS concentrations at the sewer inlet. The EE sensitivity measures are shown graphically by scatter plots in Fig. 12,

which consist of the x- and y- axes the absolute mean (μ^*) and the standard deviation (σ), respectively.

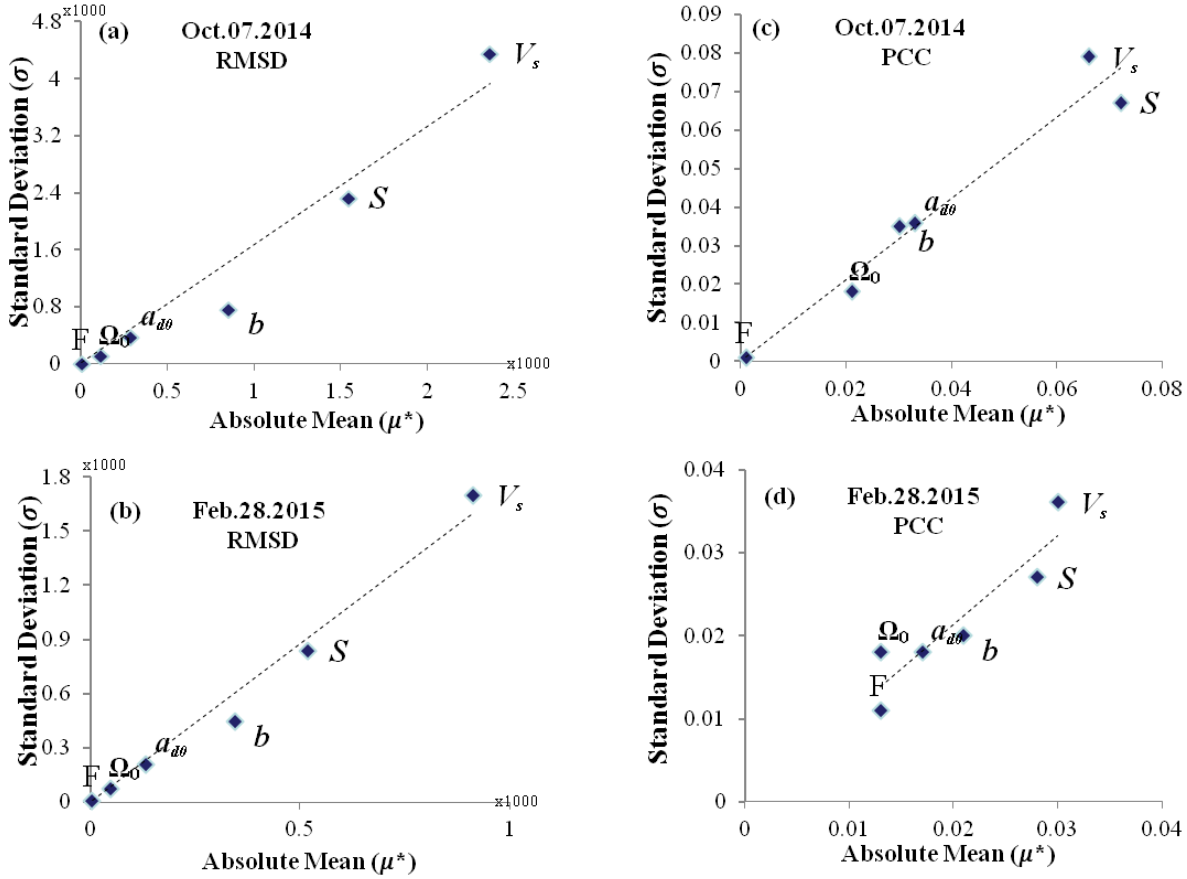

Fig. 12 Scatter plots representing the results of the sensitivity analysis using the Elementary Effect (EE) method. For (a) the rainfall event of Oct.07.2014 using RMSD; (b) the rainfall event of Feb.28.2015 using RMSD; (c) the rainfall event of Oct.07.2014 using PCC; (d) the rainfall event of Feb.28.2015 using PCC.

As illustrated in Fig.12, the settling velocity (V_s) is the most sensitive parameter and the initial dry stock (S) is the second influential factor for either of the two presented rainfall event using different objective functions. While the others are relatively less sensitive (b, a_{d0}, Ω_0 and F). This result is caused by our assumption to simulate only one deposited layer with FullSWOF. Since all the initially available particles can be easily detached during the rainfall events, the sedimentation process and the initial dry stocks are the driving factors controlling the amount of particles on the surface for further wash-offs.

Concerning the detachment process, the parameters related to the raindrop-driven process (b, a_{d0}) are much more important than that concerned with the flow-driven

process (Ω_0, F). Moreover, the Ω_0 and F seem to be insensitive to the TSS concentration at the sewer inlet. This finding suggests that the energy of simulated water flow rarely exceed the threshold of the stream power for initiating particle detachment. This implies that the wash-off process is predominately caused by raindrop impact for the investigated urban road catchment.

In addition to giving detailed information on the standard deviation (σ), the scatter plots also allow us to highlight possible interactions and nonlinear behaviours as well as identifying anomalies. According to Fig. 12, the parameter V_s has the largest standard deviation in all conditions. This observation indicate that the interaction of V_s with other parameters is more significant. Contrarily, the σ of the parameters *b* and *S* are relatively less significant compared to their μ^*. These two parameters are therefore more highlighted by their overall sensitivities. Moreover, it is shown in the FIG. 12(d) that using the PCC objective function, the standard deviation (σ) of Ω_0 becomes more important for the event of Feb 28 2015. Since the event of Feb 28 2015 is longer (2.2 hours) than the other one (40min) and contains several runoff and TSS concentration peaks after the first peak, the flow-driven process, which is linked to the parameters Ω_0 and F, may be more responsible for the fluctuations of TSS concentration in the latest part of the rainfall event.

3.3.3. Continuous effects of the settling velocity (Vs) on TSS

Since the V_s was confirmed to be the most influential parameter on TSS dynamics in our study, a continuous TSS correlation analysis is performed in order to continuously investigate the effects of the settling velocity on the model performance for 5 rainfall events. The selected events contain several runoff peaks and TSS concentrations. Therefore, we fixed all other parameter values as the best-fitted simulations, while the V_s is varied from its measured value (noted level 0, d_{50}=15um, V_s=0.0001 m/s) to a higher limit (noted level +1, d_{90}=50um, V_s=0.001 m/s) and a lower limit (noted level -1, d_{10}=5um, V_s=0.00001 m/s), separately. The results are displayed in Fig. 13:

As shown in Fig. 13, the effects of the settling velocity (V_s) on continuous TSS correlation are consistent for all studied rainfall events. For every tested value of V_s, the model is able to satisfactorily represent the dynamic trends until the first peak of TSS concentrations. However, it should be noted that the performance of the model is better with larger V_s values in simulating the fluctuations after the first peak. This phenomenon can be explained by the assumption of single-class particles. In fact, the model does not consider the change in sediment-size distribution which occurs throughout the rainfall event. Due to the preferential deposition of the coarsest particles in regards to the grain-size distribution of the transported sediment, the representative settling velocity changed continuously during the rainfall event. Thus, we can argue that the subsequent peaks of TSS concentration are mainly caused by

particles which are re-deposited after the occurrence of the first peak. In order to confirm this assumption, a detailed investigation of the road wash-off processes with different classes of sediment is suggested for the further studies.

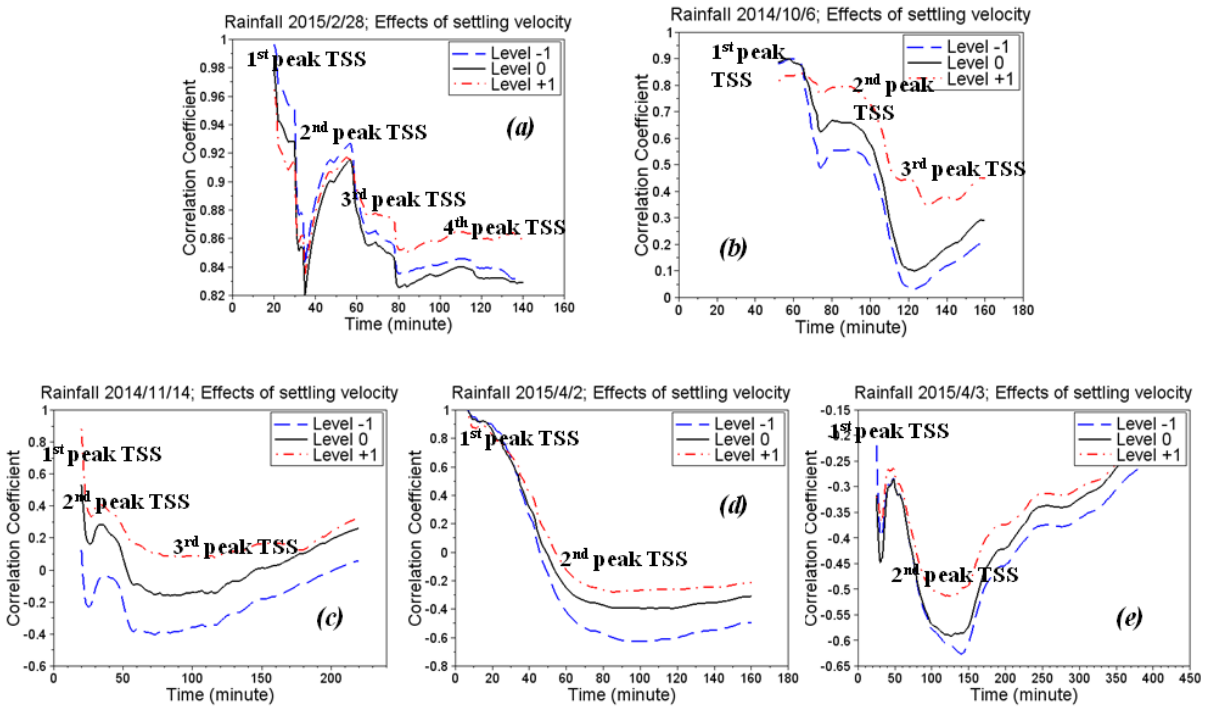

Fig. 13 Continuous Pearson's Correlation Coefficient (PCC) calculated from the simulated and observed TSS concentrations at the sewer inlet for different rainfall events, where (a) Feb. 28th 2015, (b) Oct. 6th 2014, (c) Nov. 14th 2014, (d) April. 2th 2015, and (e) April. 3th 2015. Only the values of Vs are changed, other parameters are fixed to their values of OAT level '0'. Solid black line stands for the OAT level "0" of Vs ; the dashed blue line stands for the OAT level "-1", and the dash-dotted red line stands for the OAT level "+1". Several peaks of TSS concentration are observed and simulated during each rainfall events.

3.4. What is the proper value of Settling Velocity for urban wash-off modelling ?

As discussed above, the settling velocity (V_s) is the key parameter for road wash-off processes. However, in this case, it is revealed that the value of V_s = 0.0001 m/s, which is calculated from the measured median diameter of particles (d50=15um), is not suitable for reproducing the continuous dynamics of the TSS concentration for the road catchment. Therefore, we conclude that using the single-class sediments assumption, where the particle size equals to median diameter, is not capable of accurately reproducing the dynamics of TSS concentrations at the outlet of a road

catchment, particularly for the later part of stormwater event. The application of the Particle Size Distribution with different classes of sediment could be suggested for more accurate simulations over the entire duration of a rainfall event. Nevertheless, since the single-class simplification could significantly reduce the computational time for such a physically-based and distributed model, this assumption could be used for specific objectives of water management. As shown in FIG. 12, the dynamics of the TSS concentration are generally well represented until the initial peaks, regardless of different values of settling velocity. We could therefore use the single class assumption in order to investigate water pollution limited to the first part of a rainfall event.

Besides, as observed by many researchers (Datry et al., 2003; Julien, 2010; Kafi et al., 2008), the existence of a cohesive layer beneath the deposited urban dust layer might also be a meaningful explication for the present issue, with which coarser particles and flocculated fine particles can be detached only in the latest part of a storm event when the top layer has already been washed off. This assumption could also be investigated using the H-R and FullSWOF models in future studies.

4. Perspectives

In the previous sections, we introduced a novel approach to model urban stormwater quality with the physically-based FullSWOF and Hairsine-Rose (H-R) model. This new method has good potential for future studies in the following two aspects: (1) a helpful research approach for increasing understanding of urban wash-off mechanisms; (2) a useful tool for designing innovative stormwater management technologies.

Current urban wash-off models rely on empirical, catchment-scale functions (Sartor et al., 1974), that did not achieve significant advances for the last 40 years. Using the physically-based model coupled with high precision and fully-distributed data, researchers can have an insight view of the spatial and temporal heterogeneities of the dynamics of urban pollutants as well as the driving forces for wash-off mechanisms. This information is helpful for designing advanced experimental measurements and settings, in order to improve the underlying theories as well as the mathematical equations of urban wash-off processes. Nevertheless, since the present approach requires highly precise input data and the simulations are quite time-consuming, this method may be not suitable for large urban catchments as a research tool yet. The detailed studies of urban wash-off behavious can nowadays only be focused on small-scale roads, buildings or greenlands.

On the other hand, accurate predictions of stormwater quality are very meaningful for planning and designing preventative measures. Benefitting from this physically-based approach, stormwater managers could have the knowledge of the spatial

distribution of particles and particulate pollutants on the road surface. The stormwater pre-entrance technologies such as filter systems and storage tanks can be applied at-source for certain areas where more sediments trend to be settled. This type of source-control techniques are easier to implement comparing with other facilities at-the-end of catchment (e.g. wastewater treatment plants, storage basin, etc.) and can reduce the costs.

There is considerable scope for discussing the computational feasibility of applying this type of detailed physically-based model for large urban catchments. For example, how much spatial detail is needed to robustly represent wash-off processes for an urban catchment; and what kind of input information is necessary for successful water quality simulations. Undoubtedly, there is a need for systematic works on the suitability of, and methods for, such up-scaling. These investigations may be helpful for spreading this detailed urban wash-off modelling. Meanwhile, we are currently working on a multi-processor version of the FullSWOF model. This advancement may help further studies by reducing drastically the simulation time.

5. Conclusion

In the current study, the monitoring survey coupled with a simulation approach by the physically-based FullSWOF model and the process-based Hairsine-Rose model (H-R) is applied to a road catchment near Paris, in order to model the dynamics of urban wash-off. Centimetric resolution of topographic data, continuous measurements of rainfall intensities, water flows and turbidity measurements, as well as road dust and stormwater samplings are used in the model in order to obtain realistic input data. A global sensitivity analysis of 6 input factors is performed by using the Elementary-Effects (EE) method. This is the first time that such a research approach is applied and discussed in the context of urban wash-off modelling.

From on-site experimental measurements, the particle samplings show that the total mass and the Particle Size Distribution (PSD) in stormwater samples are quite different from that found in road dust samples, only the finest particles of the urban dry stocks can be transferred to the sewer inlet of the road catchment during a rainfall event. Meanwhile, it confirmed that most PAHs are found in the particulate phase and associated with suspended particles.

In our study, the H-R model coupled with FullSWOF software is for the first time applied to urban wash-off modelling. The simulation results indicate that the combined use of the models and high spatial- and temporal-resolution data provides a good representation of both water flow and water quality modelling.

Sensitivity analysis indicates that the settling velocity (V_s) and the initial dry stock (S) are the most sensitive parameters for either overall or second-order effects. The

raindrop-driven detachment is revealed as the major force for detaching the sediment from the urban surface. However, the flow-driven detachment is more responsible for the fluctuations of TSS concentration in the latest part of the rainfall event.

The effects of settling velocity (V_s) on continuous TSS correlation are investigated throughout 5 different rainfall events. The value of V_s, which is calculated from the single-class sediments assumption with d50=15um, fell short of adequately reproducing the TSS dynamics, whereas coarser particles appear to be more adapted for modelling the TSS dynamics. Thus, a multi-class sediment perspective regarding the PSD is suggested for improving the model performance. Finally, the perspectives of using this new approach for increasing understanding of urban wash-off mechanisms, as well as for designing stormwater management technologies are discussed for future research and practical issues.

ACKNOWLEDGEMENT

The research work of PhD student Yi Hong is financed by ANR-Trafipollu project and Ecole des Ponts ParisTech. Firstly, the authors would like to thank OPUR (Observatoire des Polluants Urbains en Île-de-France) for providing the platform for changing idears and elaborating collaborations with different researchers from various institutions. The author would also want to thank B. Béchet (IFSTTAR) and B. Soheilian (IGN) for providing valuable experimental data which help to implement the model on the study site. Finally, we want to give a special thanks to the experimental team of ANR Trafipollu project for all collected necessary for this work, in particular David Ramier (CEREMA), Mohamed Saad (LEESU) and Philippe Dubois (LEESU).

References:

Aryal, R., Vigneswaran, S., Kandasamy, J., Naidu, R., 2010. Urban stormwater quality and treatment. Korean J. Chem. Eng. 27, 1343–1359. doi:10.1007/s11814-010-0387-0

Bechet, B., Bonhomme, C., Lamprea, K., Campos, E., Jean-soro, L., Dubois, P., Lherm, D., 2015. Towards a modeling of pollutant flux at local scale - Chemical analysis and micro-characterization of road dusts. Presented at the 12th Urban Environment Symposium, Oslo, Norway.

Bennett, N.D., Croke, B.F.W., Guariso, G., Guillaume, J.H.A., Hamilton, S.H., Jakeman, A.J., Marsili-Libelli, S., Newham, L.T.H., Norton, J.P., Perrin, C., Pierce, S.A., Robson, B., Seppelt, R., Voinov, A.A., Fath, B.D., Andreassian, V., 2013. Characterising performance of environmental models. Environ. Model. Softw. 40, 1–20. doi:10.1016/j.envsoft.2012.09.011

Beuselinck, L., Hairsine, P.B., Govers, G., Poesen, J., 2002. Evaluating a single-class net deposition equation in overland flow conditions: SINGLE-CLASS NET DEPOSITION EQUATION. Water Resour. Res. 38, 15–1–15–10. doi:10.1029/2001WR000248

Bressy, A., Gromaire, M.-C., Lorgeoux, C., Saad, M., Leroy, F., Chebbo, G., 2012. Towards the determination of an optimal scale for stormwater quality management: Micropollutants in a small residential catchment. Water Res. 46, 6799–6810. doi:10.1016/j.watres.2011.12.017

Campolongo, F., Cariboni, J., Saltelli, A., 2007. An effective screening design for sensitivity analysis of large models. Environ. Model. Softw. 22, 1509–1518. doi:10.1016/j.envsoft.2006.10.004

Cheng, N., 1997. Simplified Settling Velocity Formula for Sediment Particle. J. Hydraul. Eng. 123, 149–152. doi:10.1061/(ASCE)0733-9429(1997)123:2(149)

Datry, T., Malard, F., Vitry, L., Hervant, F., Gibert, J., 2003. Solute dynamics in the bed sediments of a stormwater infiltration basin. J. Hydrol. 273, 217–233. doi:10.1016/S0022-1694(02)00388-8

Delestre, O., Cordier, S., Darboux, F., Du, M., James, F., Laguerre, C., Lucas, C., Planchon, O., 2014. FullSWOF: A Software for Overland Flow Simulation, in: Gourbesville, P., Cunge, J., Caignaert, G. (Eds.), Advances in Hydroinformatics. Springer Singapore, Singapore, pp. 221–231.

Deletic, A., Maksimovic, [Cbreve]edo, Ivetic, M., 1997. Modelling of storm wash-off of suspended solids from impervious surfaces. J. Hydraul. Res. 35, 99–118. doi:10.1080/00221689709498646

Dotto, C.B.S., Mannina, G., Kleidorfer, M., Vezzaro, L., Henrichs, M., McCarthy, D.T., Freni, G., Rauch, W., Deletic, A., 2012. Comparison of different uncertainty techniques in urban stormwater quantity and quality modelling. Water Res. 46, 2545–2558. doi:10.1016/j.watres.2012.02.009

Duncan, H., 1995. A review of urban stormwater quality processes. Cooperative Research Centre for Catchment Hydrology, Clayton, Vic.

Egodawatta, P., Thomas, E., Goonetilleke, A., 2007. Mathematical interpretation of pollutant wash-off from urban road surfaces using simulated rainfall. Water Res. 41, 3025–3031. doi:10.1016/j.watres.2007.03.037

Elliott, A.H., Trowsdale, S.A., 2007. A review of models for low impact urban stormwater drainage. Environ. Model. Softw., Special section: Advanced Technology for Environmental Modelling 22, 394–405. doi:10.1016/j.envsoft.2005.12.005

Fletcher, T.D., Andrieu, H., Hamel, P., 2013. Understanding, management and modelling of urban hydrology and its consequences for receiving waters: A state of the art. Adv. Water Resour. 51, 261–279. doi:10.1016/j.advwatres.2012.09.001

Gasperi, J., Geara, D., Lorgeoux, C., Bressy, A., Zedek, S., Rocher, V., El Samrani, A., Chebbo, G., Moilleron, R., 2014. First assessment of triclosan, triclocarban and paraben mass loads at a very large regional scale: Case of Paris conurbation (France). Sci. Total Environ. 493, 854–861. doi:10.1016/j.scitotenv.2014.06.079

Gloaguen, C., Lavergnat, J., 1995. Raindrop size distribution near Paris. Electron. Lett. 31, 405–406. doi:10.1049/el:19950272

Grayson, R.B., Moore, I.D., McMahon, T.A., 1992a. Physically based hydrologic modeling: 1. A terrain-based model for investigative purposes. Water Resour. Res. 28, 2639–2658. doi:10.1029/92WR01258

Grayson, R.B., Moore, I.D., McMahon, T.A., 1992b. Physically based hydrologic modeling: 2. Is the concept realistic? Water Resour. Res. 28, 2659–2666. doi:10.1029/92WR01259

Gupta, H.V., Kling, H., Yilmaz, K.K., Martinez, G.F., 2009. Decomposition of the mean squared error and NSE performance criteria: Implications for improving hydrological modelling. J. Hydrol. 377, 80–91. doi:10.1016/j.jhydrol.2009.08.003

Hairsine, P.B., Rose, C.W., 1992a. Modeling water erosion due to overland flow using physical principles: 1. Sheet flow. Water Resour. Res. 28, 237–243. doi:10.1029/91WR02380

Hairsine, P.B., Rose, C.W., 1992b. Modeling water erosion due to overland flow using physical principles: 2. Rill flow. Water Resour. Res. 28, 245–250. doi:10.1029/91WR02381

Heng, B.C.P., Sander, G.C., Armstrong, A., Quinton, J.N., Chandler, J.H., Scott, C.F., 2011. Modeling the dynamics of soil erosion and size-selective sediment transport over nonuniform topography in flume-scale experiments. Water Resour. Res. 47, W02513. doi:10.1029/2010WR009375

Heng, B.C.P., Sander, G.C., Scott, C.F., 2009. Modeling overland flow and soil erosion on nonuniform hillslopes: A finite volume scheme. Water Resour. Res. 45, W05423. doi:10.1029/2008WR007502

Hervieu, A., Soheilian, B., 2013. Semi-Automatic Road/Pavement Modeling using Mobile Laser Scanning. ISPRS Ann. Photogramm. Remote Sens. Spat. Inf. Sci. II-3/W3, 31–36. doi:10.5194/isprsannals-II-3-W3-31-2013

Hogarth, W.., Rose, C.., Parlange, J.., Sander, G.., Carey, G., 2004. Soil erosion due to rainfall impact with no inflow: a numerical solution with spatial and temporal effects of sediment settling velocity characteristics. J. Hydrol. 294, 229–240. doi:10.1016/j.jhydrol.2004.02.014

Jomaa, S., Barry, D.A., Brovelli, A., Sander, G.C., Parlange, J.-Y., Heng, B.C.P., Tromp-van Meerveld, H.J., 2010. Effect of raindrop splash and transversal width on soil erosion: Laboratory flume experiments and analysis with the Hairsine–Rose model. J. Hydrol. 395, 117–132. doi:10.1016/j.jhydrol.2010.10.021

Julien, P.Y., 2010. Erosion and sedimentation, second. ed.

Kafi, M., Gasperi, J., Moilleron, R., Gromaire, M.C., Chebbo, G., 2008. Spatial variability of the characteristics of combined wet weather pollutant loads in Paris. Water Res. 42, 539–549. doi:10.1016/j.watres.2007.08.008

Kim, J., Ivanov, V.Y., Katopodes, N.D., 2013. Modeling erosion and sedimentation coupled with hydrological and overland flow processes at the watershed scale: HYDROLOGIC-

HYDRAULIC-MORPHOLOGIC MODEL AT WATERSHED SCALE. Water Resour. Res. 49, 5134–5154. doi:10.1002/wrcr.20373

Le, M.-H., Cordier, S., Lucas, C., Cerdan, O., 2015. A faster numerical scheme for a coupled system modeling soil erosion and sediment transport. Water Resour. Res. 51, 987–1005. doi:10.1002/2014WR015690

Massoudieh, A., Abrishamchi, A., Kayhanian, M., 2008. Mathematical modeling of first flush in highway storm runoff using genetic algorithm. Sci. Total Environ. 398, 107–121. doi:10.1016/j.scitotenv.2008.02.050

Mie, G., 1908. Beiträge zur Optik trüber Medien, speziell kolloidaler Metallösungen. Ann. Phys. 330, 377–445. doi:10.1002/andp.19083300302

Montgomery, M.R., 2008. The Urban Transformation of the Developing World. Science 319, 761–764. doi:10.1126/science.1153012

Morris, M.D., 1991. Factorial Sampling Plans for Preliminary Computational Experiments. Technometrics 33, 161–174. doi:10.1080/00401706.1991.10484804

Mutchler, C.K., Hansen, L.M., 1970. Splash of a Waterdrop at Terminal Velocity. Science 169, 1311–1312. doi:10.1126/science.169.3952.1311

Paparoditis, N., PAPELARD, J.-P., CANNELLE, B., DEVAUX, A., SOHEILIAN, B., DAVID, N., HOUZAY, E., 2012. Stereopolis II: A multi-purpose and multi-sensor 3D mobile mapping system for street visualisation and 3D metrology. Rev. Fr. Photogrammétrie Télédétection 69–79.

Proffitt, A.P.B., Rose, C.W., Hairsine, P.B., 1991. Rainfall Detachment and Deposition: Experiments with Low Slopes and Significant Water Depths. Soil Sci. Soc. Am. J. 55, 325. doi:10.2136/sssaj1991.03615995005500020004x

Rossman, lewis A., 2010. STORM WATER MANAGEMENT MODEL USER'S MANUAL Version 5.0. NATIONAL RISK MANAGEMENT RESEARCH LABORATORY OFFICE OF RESEARCH AND DEVELOPMENT U.S. ENVIRONMENTAL PROTECTION AGENCY, CINCINNATI, OH 45268.

Saltelli, A., Annoni, P., 2010. How to avoid a perfunctory sensitivity analysis. Environ. Model. Softw. 25, 1508–1517. doi:10.1016/j.envsoft.2010.04.012

Sartor, J.D., Boyd, G.B., Agardy, F.J., 1974. Water Pollution Aspects of Street Surface Contaminants. J. Water Pollut. Control Fed. 46, 458–467.

Shaw, S.B., Walter, M.T., Steenhuis, T.S., 2006. A physical model of particulate wash-off from rough impervious surfaces. J. Hydrol. 327, 618–626. doi:10.1016/j.jhydrol.2006.01.024

Song, X., Zhang, J., Zhan, C., Xuan, Y., Ye, M., Xu, C., 2015. Global sensitivity analysis in hydrological modeling: Review of concepts, methods, theoretical framework, and applications. J. Hydrol. 523, 739–757. doi:10.1016/j.jhydrol.2015.02.013

Torri, D., Sfalanga, M., Del Sette, M., 1987. Splash detachment: Runoff depth and soil cohesion. CATENA 14, 149–155. doi:10.1016/S0341-8162(87)80013-9

Tsihrintzis, V.A., Hamid, R., 1997. Modeling and management of urban stormwater runoff quality: a review. Water Resour. Manag. 11, 136–164.

Vaze, J., Chiew, F.H.S., 2003. Comparative evaluation of urban storm water quality models. Water Resour. Res. 39, 1280. doi:10.1029/2002WR001788

Wijesiri, B., Egodawatta, P., McGree, J., Goonetilleke, A., 2015. Incorporating process variability into stormwater quality modelling. Sci. Total Environ. 533, 454–461. doi:10.1016/j.scitotenv.2015.07.008

Zoppou, C., 2001. Review of urban storm water models. Environ. Model. Softw. 16, 195–231. doi:10.1016/S1364-8152(00)00084-0

Chapitre 6. New insights into the urban washoff process with detailed physical modelling

Yi Hong[1], Celine Bonhomme[1], Minh-Hoang Le[2], Ghassan Chebbo[1,3]

[1]LEESU, MA 102, École des Ponts, AgroParisTech, UPEC, UPE, Champs-sur-Marne, France, 6-8 Avenue Blaise Pascal, 77455 Champs-sur- Marne cedex 2, France.

[2] LHSV, Ecole des Ponts, CEREMA, EDF R&D, UPE, Chatou, France

[3]Université Libanaise, faculté de génie, campus rafic hariri, Hadat, Lebanon

* Corresponding author: yi.hong@leesu.enpc.fr

*(Article publié dans le journal "**Science of Total Environment**")*

DOI: 10.1016/j.scitotenv.2016.08.193

Abstract:

Current urban washoff models still rely on empirical catchment-scale functions, that have not been substantially updated during the last 40 years. This paper introduce a new approach using the physical model FullSWOF to evaluate urban washoff process. The modelling approach is performed for a Parisian road catchment. Water flow simulation is validated by outlet discharge measurements and local observations of water depth. Water quality modelling of three classes of particles (d50 = 7 µm, 70 µm, and 250 µm) is applied using the Hairsine-Rose model. Analysis of the washoff process at the catchment scale indicates that most (> 90%) of the finest particles are removed at the beginning of a rainfall event, about 10%–20% of medium-sized particles are moved over the latest part of the event, and almost no coarse particles can be transferred into the sewer inlet. Spatial analysis of washoff process reveals that the concentration of suspended solids on road and sidewalk surface is more sensitive to rainfall intensities than that on gutter surface, while coarser particles tend to accumulate in the gutter over the later part of a rainfall event. Investigation of the driving force behind the detachment process indicates that rainfall-driven effects are two orders of magnitude higher than flow-driven effects. Moreover, it is observed that rainfall-driven detachment is considerably decreased

with the rising water depth, while flow-driven detachment occurs only in gutter areas. Finally, several controversial arguments on the use of physical models for assessing the washoff process, and perspectives on development of physical urban washoff models are discussed.

Keywords: urban washoff modelling; physically based and distributed model; FullSWOF; Hairsine-Rose model; raindrop-driven detachment; flow-driven detachment.

1. Introduction

Stormwater runoff from road surfaces forms a major contribution to pollution loads in urban areas (Aryal et al., 2010; Fletcher et al., 2013; Zoppou, 2001). Since most of the problematic contaminants, such as heavy metals and polycyclic aromatic hydrocarbons (PAHs), are transported by adsorption to fine particles (Bressy et al., 2012; Gromaire et al., 2001; Kafi et al., 2008; Zgheib et al., 2012), the dynamics of suspended solids (SS) is regarded as one of the basic indicators of urban runoff pollution. Because of the difficulties in accurately monitoring the spatial and temporal variations of SS concentrations in urban catchments, urban stormwater modelling is increasingly usedfor the interpretation of urban build-up/washoff mechanisms.

Sartor et al. (1974) introduced the first sediment washoff model, which assumed that the rate of particle loss on a catchment scale is directly proportional to the water flow and the availability of pollutants on the surface. Since then, numerous urban stormwater quality models have been developed, assisted by the gradual increase in computing power. However, most current urban stormwater models, such as SWMM (Rossman, 2010) and MUSIC (Wong et al., 2002), are still based on the original exponential equations. Different research studies have shown that the empirical formulations, in models such as SWMM, cannot represent the spatial heterogeneities of urban particle distributions during stormwater events (Kanso, 2004; Sage et al., 2015). Conceptual models are therefore incapable of simulating urban non-point source pollutions (Fletcher et al., 2013; Merritt et al., 2003). Improved insights into washoff mechanisms are hence required to provide new theories and gain new understanding of the urban washoff process, allowing the development of novel models to improve management practices.

Physical modelling combined with highly detailed field data is a promising approach to better understand the urban washoff process (Beven, 1989; Fletcher et al., 2013). However, current physical models describing sediment transfers are mostly developed and applied to the natural environment, not to the field of urban

pollution. With assumptions that the physical theory of particulate pollutant transfer in urban areas is the same as sediment transfer in natural environments, this work focuses on the use of an erosion model (initially developed for the natural environment) to better explain and describe the washoff process occurring in an urban catchment. In this context, physical descriptions of particle washoff generally focus on two distinct physical process: the removal of particles by raindrop impacts, or shear stress from overland flow (Kinnell, 2009; Shaw et al., 2006; Vaze and Chiew, 2003).

It has been stated that particulate size is a crucial factor for transport of PAHs and heavy metals in urban stormwater flow (Herngren et al., 2010; Zhao and Li, 2013). Therefore, it is important to take into account the particle size distribution (PSD) of the sediments in urban pollutant modelling. On the contrary, conceptual formulations only considered the total pollutant flux. Among the numerous published size-selective erosion models (e.g. Deletic et al., 1997; Hairsine and Rose, 1992a, 1992b; Merritt et al., 2003; Shaw et al., 2006), the Hairsine and Rose (1992a, 1992b) model (H-R) best fits our needs. Unlike other process-based approaches, the H-R model treats detachment and deposition process independently, which makes a size-selective modelling possible. It also simulates a deposited layer that differs from the original soil in its composition and detachability, this allows us to distinctively model urban dust and road asphalt. Moreover, as the rainfall-driven and flow-driven detachments are calculated separately in the model, a greater insight into the washoff process can be achieved, by comparing the rate of detachment induced by different factors.

With the aim of physical modelling the washoff process in urban areas, Le et al. (2015) recently introduced a well-balanced and high-order finite volume implementation of the H-R model in the FullSWOF platform (Full Shallow-Water equations for Overland Flow, see Delestre et al., 2014). Latterly, Hong et al. (2016) applied the underlying system to a road catchment near Paris using single-class sediment assumptions. In this study, we recall the previous work, but using multi-class sediment assumptions. The simulated water depth is compared with local observations to ensure that the physical modelling is capable of accurately representing water distributions over precipitation events. The objective is to achieve better insights into the urban washoff process by analyzing the spatial and temporal variations of suspended solids, deposited particles, as well as the detachment rate driven by raindrops or water flow. Finally, issues with the use of physical models to assess the washoff process, and perspectives for this modelling approach, are also discussed.

2. Methods and Materials

2.1. Model description

The C++ code FullSWOF (Delestre et al., 2014) uses a finite volume scheme to solve bidimensional Shallow-Water (SW) equations using topographical and friction source terms. The water infiltration process is represented by the Green and Ampt (1911) model. Recently, Le et al. (2015) revisited the studies of Heng et al. (2011) and Kim et al. (2013), and introduced a faster numerical scheme for coupling the H-R model with the SW equations within the FullSWOF system, thus allowing the simulation of soil erosion and sediment transport process.

The H-R model allows any sediment particle to be present in one of three compartments: the flow itself (in the form of suspended solid), the deposited layer, or the original soil. Once sediments have been detached by the impact of raindrops, particles can be suspended or returned to the bed by deposition, forming a deposited layer from which they can be subsequently re-detached. Two types of washoff process are considered: the first is due to rainfall impact, while the second is due to the shear stress exerted on the bed surface by the water flow. When the detachment process continuously add sediment to water flow, the deposition process causes a continuous loss of sediments from the flow forming a deposited layer. Therefore, some fraction of the original soil surface is always covered by a layer of deposited sediment. This presumption allows the model to distinguish between the rates of detachment of the original cohesive soil and non-cohesive deposited sediments. In the case of the urban catchment, the road asphalt is considered as a non-erodible original soil, while the road dust is the deposited layer. This consideration leads to a simplification of the initial H-R model by neglecting the detachment for original soil (denoted e_i, r_i) in the urban context. The process represented in the H-R model are illustrated in Fig. 1.

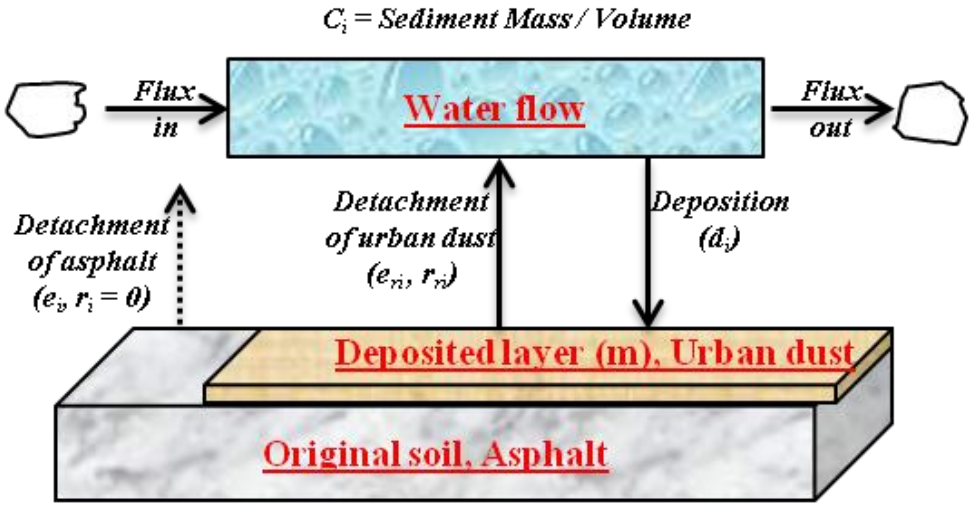

Fig. 1 Concept of the Hairsine-Rose model. For the ith class of particles, Ci represents the suspended solids concentration in mass per unit volume; mi refers to the deposited sediment mass per unit area; ei and ri stand for the rate of rainfall-driven and flow-driven detachment for original soil respectively (ei, ri = 0 in the case of asphalt); eri and rri mean, respectively, the rate of rainfall-driven and flow-driven detachment for the deposited layer; di is the rate of solid deposition from the water flow to the deposited layer.

The H-R model reflects the conservation of mass entering and leaving a cell (called the control volume). Using the simplification linked to the urban context, the mass balance equations can be written as:

$$\frac{\partial hc_i}{\partial t} + \frac{\partial qc_i}{\partial x} = e_{ri} + r_{ri} - d_i \qquad (1)$$

$$\frac{dm_i}{d_t} = d_i - e_{ri} - r_{ri} \qquad (2)$$

where for the i_{th} class of particles, c_i represents the suspended solids concentration in mass per unit volume; m refers to the deposited sediment mass per unit area; e_{ri} and r_{ri} mean the rate of rainfall-driven and flow-driven detachment for the deposited layer, respectively; ∂t is the partial derivative of time; ∂x is the partial derivative of distance; h is the water-depth, and q is the water flux, which are computed from the SW equations; *and* d_i is the deposition. The terms e_{ri} , r_{ri} and d_i can be determined by:

$$e_{ri} = \frac{m_i}{m_T}\, a_d P \qquad (3)$$

$$r_{ri} = \frac{m_i}{m_T}\, \frac{\Omega_e}{\frac{\rho_s - \rho_w}{\rho_s}\, gh} \qquad (4)$$

$$d_i = v_i\, c_i \qquad (5)$$

where,

- m_i is the deposited mass per unit area of the i^{th} class of particles (kg/m²);

- m_T is the total mass per unit area of the deposited particles (kg/m²);
- a_d is the detachability of the deposited sediment (kg/m^3);
- P is the rainfall intensity (m/s);
- Ω_e is the effective stream power (W/m²);
- ρ_s and ρ_w are the densities of sediment and water, respectively (kg/m^3);
- h is the water-height (m);
- g is standard gravity (m/s²);
- v_i is the settling velocity of the i_{th} class of particles in water *(*m/s).

According to Eq. 3, the rate of rainfall detachment (e_{ri}) is considered to be dependent on the rainfall rate (P). In Eq. 4, since the cohesive strength of this deposited sediment is considered negligible, the resisting force of flow-driven detachment only depends on the immersed weight of sediments. The power expended in lifting the sediment to some height in the flow is directly calculated by the rate of change of potential energy of the sediment. The detachability a_d and the effective stream power Ω_e can be written as:

$$a_d = \begin{cases} a_{d0}\,, & h \le h_0 \\ a_{d0}\left(\frac{h_0}{h}\right)^b\,, & h > h_0 \end{cases} \qquad (6)$$

$$\Omega_e = F(\Omega - \Omega_0) \qquad (7)$$

$$\Omega = \rho_w g S_f q \qquad (8)$$

where:

- a_{d0} is the initial detachability of deposited sediment (kg/m^3);
- h_0 is the threshold of flow depth, above which the detachability will decline (m);
- b is a positive constant;
- F is the effective fraction of excess stream power;
- Ω is the calculated total stream power (W/m²);

- Ω_0 is the threshold stream power below which there is no entrainment (W/m²);

- S_f is the friction slope which is calculated using Manning's equations.

Equation 6 illustrates that the raindrop impact detachability declines with rising flow depth beyond a certain threshold. This principle was originally proposed by Mutchler and Hansen (1970), and was revised by Proffitt et al. (1991) for the H-R model. Eqs. 7–8 show that the rate of flow-driven detachment is due to the effective stream power (Ω_e), while the source and sinks of stream power in overland flow are shown in Fig. 2.

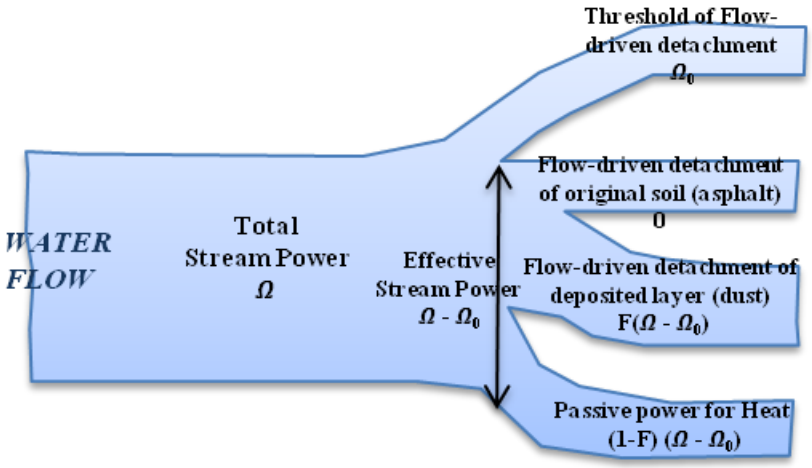

Fig. 2 Flow diagram of the redistribution of total stream power.

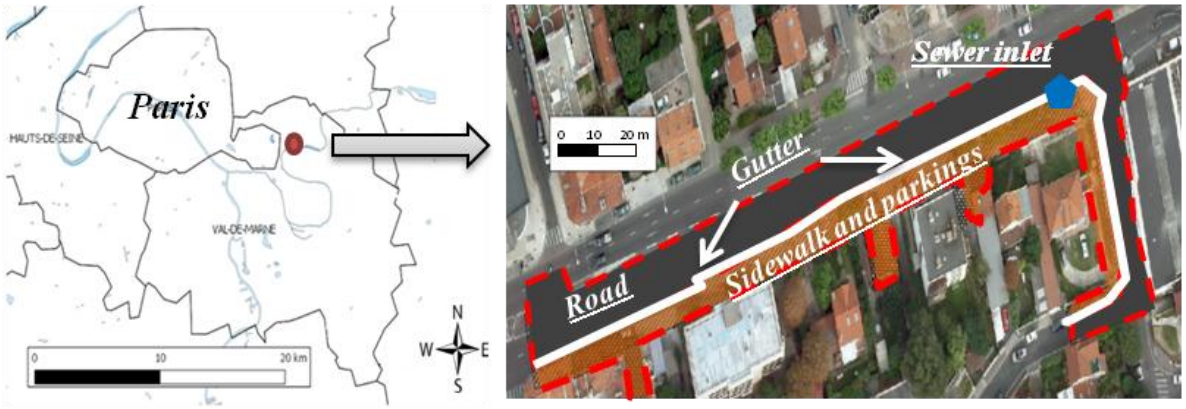

Fig. 3 Study area in eastern Paris, France. The catchment is delineated by dashed red lines; the sewer inlet is located at the northeast side of the catchment. In this image, the road area is marked in grey, gutter area in white, and sidewalk and parking areas in brown.

2.2. Study site

The model is applied to a small urban road catchment near Paris (Le Perreux sur Marne, Val de Marne, France). This study area consisted of a segment of busy road (more than 30,000 vehicles per day), and its adjacent sidewalk and parking zones. A gutter is located between the road and the sidewalk, directing water flow from the upper part of the catchment to the sewer inlet (Fig. 3). The total surface of the study basin is 2661 m², with approximately 65% of the surface being roads, 30% sidewalks, and 5% gutters and parking places. The western section had a higher incline than the eastern side, with an average slope of less than 2%.

2.3. Detailed input data

2.3.1. Rainfall data

A tipping-bucket rain gauge is installed on the roof of a building close to the urban catchment (less than 150 m). The pluviometer had a resolution of 0.1 mm. As the study area is quite small, rainfall is considered as homogeneous within the basin. In our previous work (Hong et al., 2016), 56 rainfall events were identified during the study period from September 20, 2014 to April 27, 2015; six typical events were selected for the model application with the assumption of single-class particles.In this study, we recall the same rainfall events for analyzing the urban washoff process with the assumption of three particle classes. Detailed analysis of the urban washoff process is performed for the event of October 7, 2014 and the February 28, 2015. With which, the event of October 7, 2014 has a single but significant peak of rainfall intensity (rainfall depth = 2 mm; max intensity = 20 mm/h), whereas the Feb 28, 2015 event contains several peaks of rainfall intensity in the later part of the rainfall event (rainfall depth = 4.6 mm; max intensity = 5 mm/h). Moreover, the duration of these two events is relatively short (only 40 min and 2.2 h, respectively), which results in shorter simulation times than with other precipitation events.

2.3.2. High resolution topographic data

In the framework of the ANR-Trafipollu project, particularly high-resolution topographic data (1 cm) is collected by an on-vehicle LiDAR with the collaboration of the French National Institute of Geography (IGN; Hervieu and Soheilian, 2013; Paparoditis et al., 2012). To apply the data to the model using an appropriate number of pixels, the 1-cm resolution is downscaled to a 10-cm resolution using the mean aggregation method (Fig. 4):

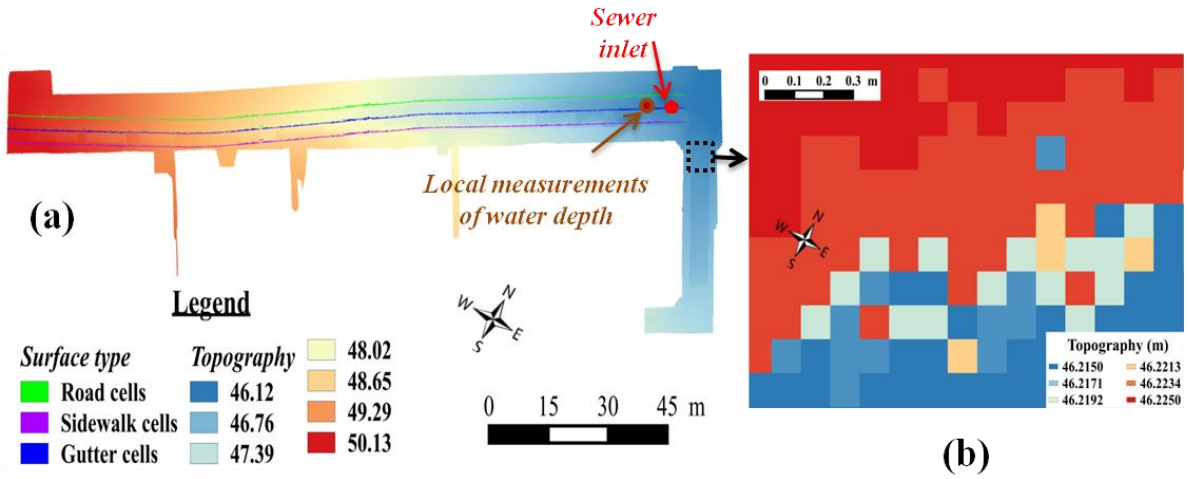

Fig. 4 (a) Topographic data of the road catchment; (b) Zoom-in on a rectangular area of the road surface topography.

2.3.3. Road dust and Particle Size Distribution (PSD) data

A series of road dust samples were collected within the studied area by Bechet et al. (2015), using a 2 m² vacuum. The PSD of the collected sediments was then determined by laboratory monitoring. According to the measurements of Hong et al. (2016), only particles of sizes below 400 µm could be transferred into the sewer inlet during average rainfall events. Based on the 10%, 50% and 90% (D10, D50 and D90) cumulative undersize PSD of 0–400 µm particles, the sediments can be categorized into three different classes (Fig. 5). Representing the finest (0-15 µm, 10%), medium-sized (15-125µm, 40%) and coarsest particles (125-400 µm, 50%). The settling velocity of is then calculated using Cheng's (1997) equation, according to the median size of each particle class (Table 1).

Table. 1 The three particle classes.

Particle classes	Diameter (d50)	Percentage	Settling velocity (cm/s)
0–15 µm	7 µm	10%	0.002
15–125 µm	70 µm	40%	0.192
125–400 µm	250 µm	50%	1.78

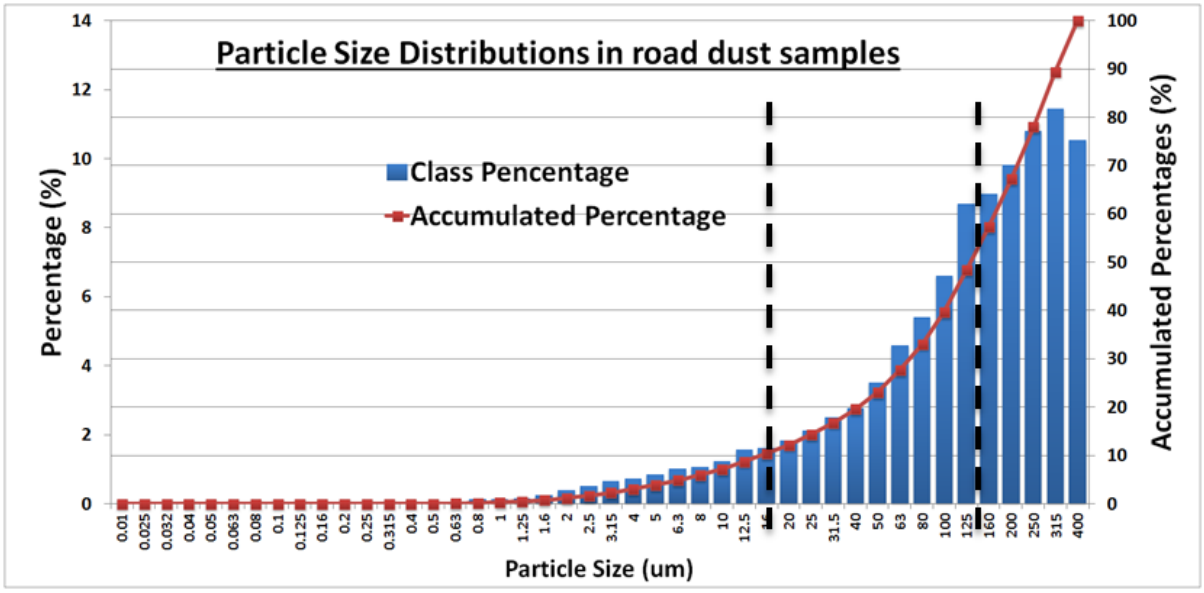

Fig. 5 Particle Size Distribution (PSD) of the finest part (< 400µm) of the dry deposited particles.

2.4. Validation of water flow modelling by outlet and local measurements

Reliable modelling of urban stormwater quality requires a detailed spatial and temporal description of water runoff characteristics. Therefore, the validation of water flow simulations is an essential preliminary step for the physical analysis of washoff mechanisms. In this context, Manning's n coefficient is calibrated and validated using measured hydrographs at the catchment outlet (road sewer inlet) for six rainfall events.

Spatial validation is a quite valuable, but rarely applied approach, for proving the reliability of such a physically-based and distributed model. However, experimental measurements are usually only available at the outlet of the catchment. In this study, in addition to the validation data from hydrographs at the catchment outlet, the water depth data is collected at the surface of the road catchment using a remote surface condition sensor (DSC111, Vaisaila). The measurement was performed in a 20-cm-diameter round area with a resolution of 0.01 mm. The monitoring location is shown in Fig. 4a. Therefore, the four correspond cells (10 cm) in the model can be identified, which allows comparison between the simulated water depth (averaged water depth of the four cells) and the observations.

2.5. Washoff behavior at the catchment scale

For the sediment transport simulation, the H-R model is implemented using the standard parameter values (a_{d0}, b, F, $\Omega 0$) obtained from Hong et al. (2016). The homogeneous initial dry stock (S) is considered as the mean mass of all the urban dust samples (Bechet et al., 2015), and the settling velocities of different particle classes (V_i) are calculated by considering the observed particle sizes (Table 2). Analysis of the washoff process at the catchment scale is focused on the evaluation of the concentration of suspended solids at the outlet and the ratio of remaining particles to initial deposits for each sediment class. The measured concentration of Total Suspended Solids (TSS) is derived from the continuous measurements of turbidity at the catchment outlet (Hong et al., 2016).

Table 2 Used parameter values.

a_{d0} (kg/m^3)	b	F	$\Omega 0$ (W/m^2)	S (g)	v_1 (cm/s)	v_2 (cm/s)	v_3 (cm/s)
2000	**0.8**	**0.02**	**0.2**	**0.002**	**0.002**	**0.192**	**1.78**

2.6. Spatial analysis of the washoff process

The evolution of the spatial distribution of suspended and deposited particles, as well as the dynamics of washoff mechanisms, can be evaluated according to different urban land uses. For the studied road catchment, the position of the narrow gutter, which is around 10–20 cm wide, could be delineated from the topographic data. The studied urban surface could then be divided into three distinct land uses, these being road, gutter, and sidewalk. Despite the fact that the surface material of these areas is equally impervious and non-erodible asphalt, the varying topography certainly affected the respective washoff behaviors. Thus, it is interesting to compare the water flow and washoff process according to the different types of land use. Therefore, we firstly defined the gutter cells, which have a clear road shoulder (> 5 cm) between gutter and sidewalk, and we then selected the same number of cells to represent the road and the sidewalk parallel to the cells of the gutter. A total of 2625 cells for each land use areidentified along the street, which well represented the gutter, road, and sidewalk (see Fig. 4a).

This allowed the spatial and temporal variations of the urban washoff process to be separately evaluated for gutter, road and sidewalk. Although the initial deposited layer is spatially uniform at the beginning of the simulation, the washoff process could lead to a heterogeneous distribution of particles over the course of a precipitation

event. In order to assess variations in the washoff process for different land uses, the mean concentration of suspended solids and the ratio of remaining particles to initial deposits for each sediment class (Eq. 9), are individually calculated for the gutter, road, and sidewalk.

$$ratio_{LU(i),particle(j)} = \frac{\sum_1^{n_{cell,LU(i)}} remaining\ mass\ (particle(j))}{\sum_1^{n_{cell,LU(i)}} initial\ mass\ (particle(j))} \quad (9)$$

where $ratio_{LU(i),particle(j)}$ is the ratio of remaining particles to initial deposits for the landuse *LU(i)* and the j^{th} class of particles; n_{cell} is the number of studied cells of *LU(i)* which is equal to 2625.

Moreover, since the calculation of the rainfall-driven and flow-driven detachment process in the H-R model is separated (eqs. 3–8), we can independently analyse the mass flux of detachment caused by raindrop energy (e_{ri}, *kg/m²s*) or flow energy (r_{ri}, *kg/m²s*) for each cell. The driving force (rainfall-driven or flow-driven) of the sediment detachment process for gutter, road, and sidewalk can therefore be distinctly evaluated. Furthermore, by considering the median, and lower and upper quartiles of the mass flux for the cells of each land use, we can also investigate the spatial heterogeneity of sediment detachment in the gutter, road and sidewalk.

3. Results

3.1. Validation of water flow simulation

Using the water flow measurements at the outlet of the catchment, an optimized Manning's n coefficient value of 0.05 was calibrated and validated for the study area (Hong et al., 2016). In addition to our previous work, this paper compares the simulated surface water depth with the observations (Fig. 6).

As presented in Fig. 6, the water depth simulations at the monitored location closely matched the in-situ measurements, even at a very fine scale with the water depth varying from 0–0.5 mm. This finding demonstrates that the application of the FullSWOF model with detailed input data, is a suitable approach to represent the spatial and temporal variations of water flows on urban catchments.

3.2. Urban particle washoff at the catchment scale

3.2.1. Concentration of suspended solids at the catchment outlet

The simulated concentration of total suspended solids (TSS), as well as the concentration of the 3 classes of particles (d50 = 7 µm, d50 = 70 µm and d50 = 250 µm), are compared with the measured TSS at the catchment outlet (Fig. 7).

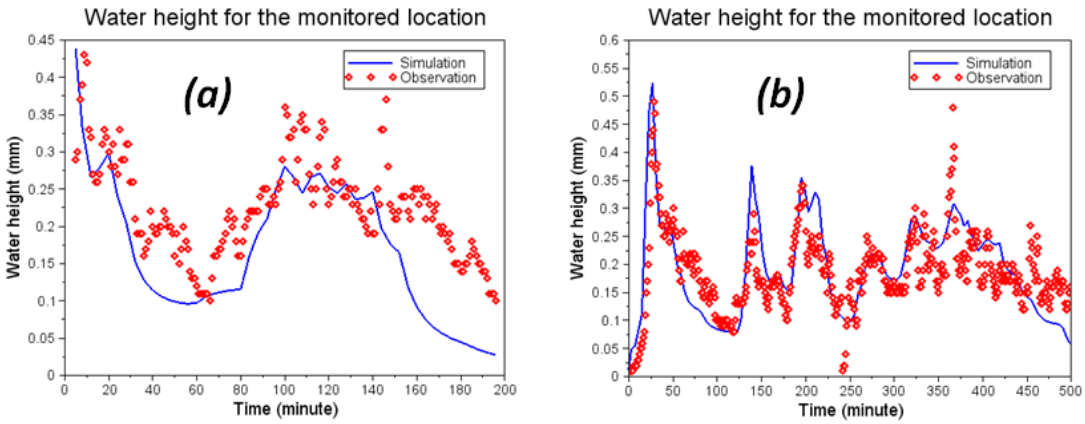

Fig. 6 Spatial validation of the water depth simulation (solid blue line) using measured local water depth data (red circles) from the monitoring location inside the urban catchment (see Fig. 4b). For the events of: (a) April 2, 2015 and (b) April 3, 2015.

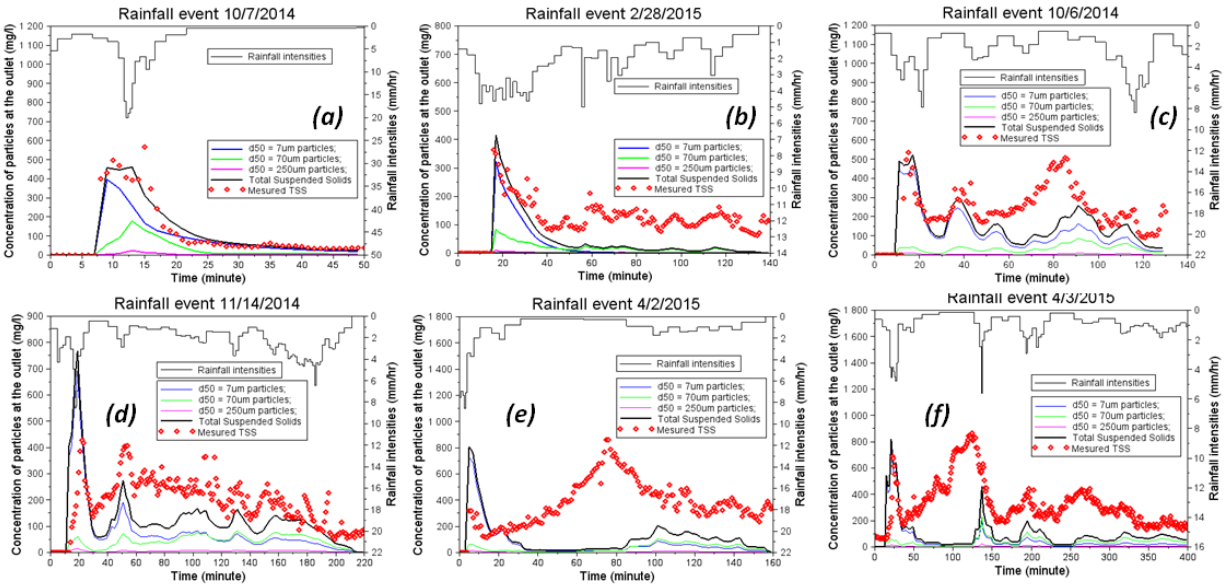

Fig. 7 Concentration of particles at the catchment outlet. The simulated concentration of total suspended solids (TSS; solid black line), d50 = 7-µm particles (solid blue line), d50 = 70-µm particles (solid green line), and d50 = 250-µm particles (solid magenta line), are compared with the measured TSS (red circles). Rainfall is plotted on the upper part. For events (a) October 7, 2014; (b) February 28, 2015; (c) October 6, 2014; (d) November 14, 2014; (e) April 2, 2015; (f) April 3, 2015.

Overall, it can be seen from the Fig. 7 that the physical model FullSWOF can correctly reproduce the TSS dynamics, especially the first peak of TSS concentration for all the studied rainfall events. However, the simulated TSS concentrations are generally underestimated for later TSS fluctuations (Fig. 7 b, c, d, e, f). This phenomenon is mainly because of the rough classification of urban particles into three classes (7um, 70um and 250um). Since the 7um particles can be easily removed at the beginning of the rainfall events, while the coarser particles (70um and 250um) are hardly transferred under the investigated rainfall intensities for forming the later TSS fluctuations. More elaborate classification of particles between 7 um and 70 um could be considered for improving the model performance on further studies. Nevertheless, as this paper aims to provide a physical insight into the urban washoff process, the categorization of three particle classes is proved to be an acceptable compromise between the simulation time and the modelling accuracy. In below sections, the results of detailed analysis of urban washoff process are presented for the rainfall events of October 7, 2014 (40 min duration) and February 28, 2015 (2.2 h duration).

3.2.2. Ratio of remaining particles to initial deposits at catchment scale

The ratios of remaining particles to initial deposits for each sediment class are presented in Fig. 8.

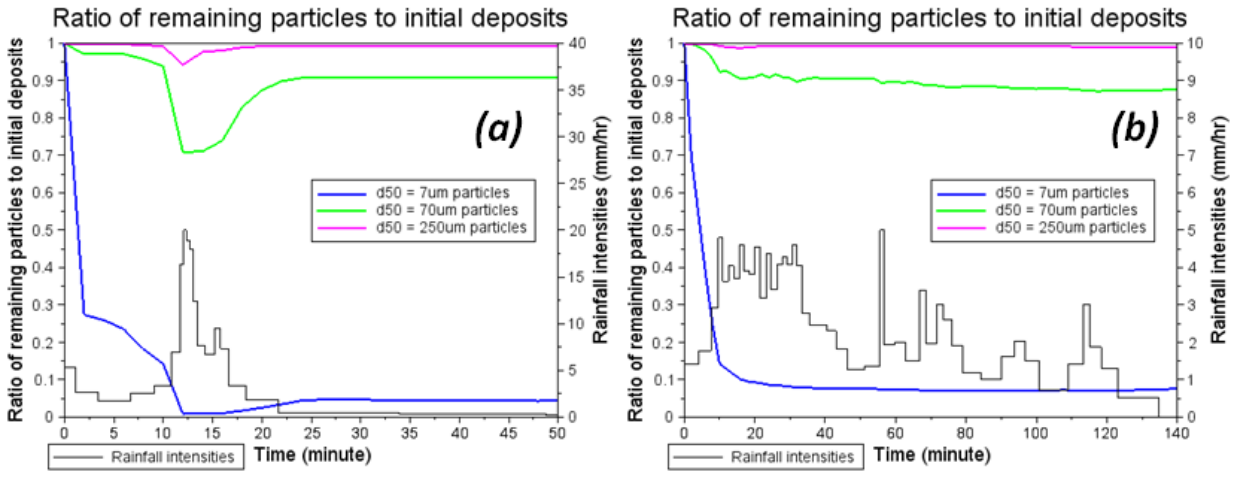

Fig. 8 Ratios of remaining particles to initial deposits on the catchment surface. The d50 = 7-µm particles (solid blue line), d50 = 70-µm particles (solid green line) and d50 = 250-µm particles (solid magenta line) are evaluated for the events of (a) October 7, 2014; (b) February 28, 2015. Rainfall is plotted on the lower part (black line).

As shown in Fig. 8, most (> 90%) fine particles (d50 = 7 µm), about 10%–20% of medium-size particles (d50 = 70 µm), and almost no coarse particles (d50 = 250 µm) are transferred into the sewer inlet. Whereas the fine particles are rapidly removed from the urban surface at the beginning of rainfall events, the other sediment sizes are only detached from the surface at high rainfall intensities, and are then re-deposited back to the surface when the rainfall weakens, causing a rise in the remaining proportions of these particles on the surface. These findings are in agreement with the concentrations of suspended solids recorded at the catchment outlet (Fig. 7). We also found that in both of the two studied events, there are always some fine particles (< 10%) remaining on the urban surface until the end of the rainfall. This phenomenon can be explained by surface depressions at the scale of the cell size (10 cm). As displayed in Fig. 4b, the topography of certain cells includes local depressions on the surface, where suspended particles may be trapped during rainfall events.

The simulated TSS concentration at the catchment outlet does not completely match the in-situ measurements, especially for the last part of the longer rainfall event (February 28, 2015). This discrepancy may be due to the inappropriate classification of the initial urban dry deposit. Since we manually attribute 10% of the total mass of dry deposits to d50 = 7-µm particles, all of these particles could easily be removed at the beginning of the rainfall events, causing a very high peak in the TSS concentration. Particles of 15–125 µm are also represented by a single class of d50 = 70 µm, which is not able to reproduce the later fluctuations in TSS concentrations.

3.3. Spatial analysis of the washoff process

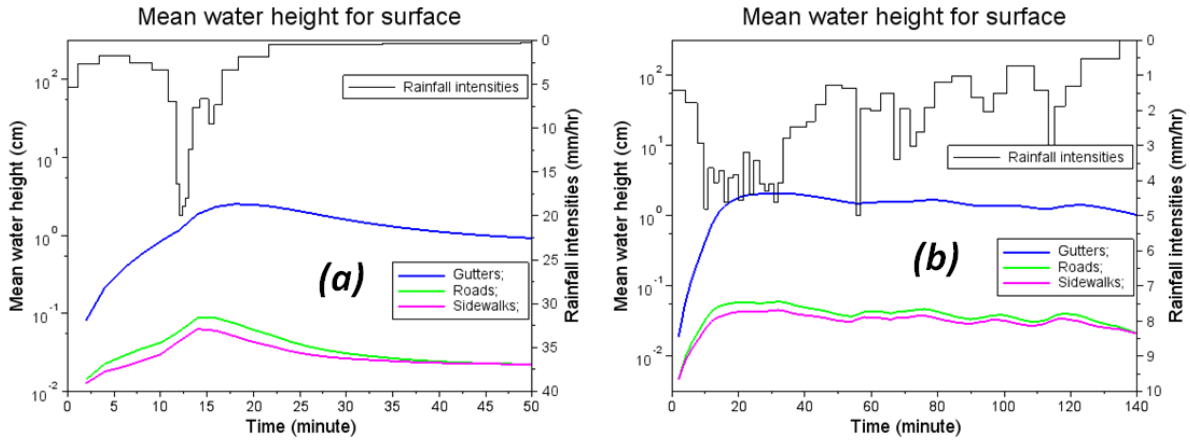

Fig. 9 Mean water depth for the cells of gutter (solid blue line), road (solid green line) and sidewalk (solid magenta line). For the events of (a) October 7, 2014; (b) February 28, 2015. Rainfall is plotted on the upper part (black line).

Since the cells of gutter, road, and sidewalk have been properly defined (section 2.6), the simulations of water depth, remaining particles, suspended solid concentration, and the mass flux of detachment by raindrop-driven or flow-driven effects, can be analysed according to the different land uses.

3.3.1. Spatial distribution of water depth

In Fig. 9, it is clear that the water depth in the gutter cells is much higher than that in the road or sidewalk cells. While the water depth in the gutter can reach 1–2.5 cm, it is always less than 0.1 cm in the road and sidewalk cells.

3.3.2. Spatial distribution of suspended solids concentration and the ratio of remaining particles to initial stocks

The spatial distributions of the mean concentration of the suspended solids and the remaining fraction of particles are presented in Fig. 10 and Fig. 11, respectively.

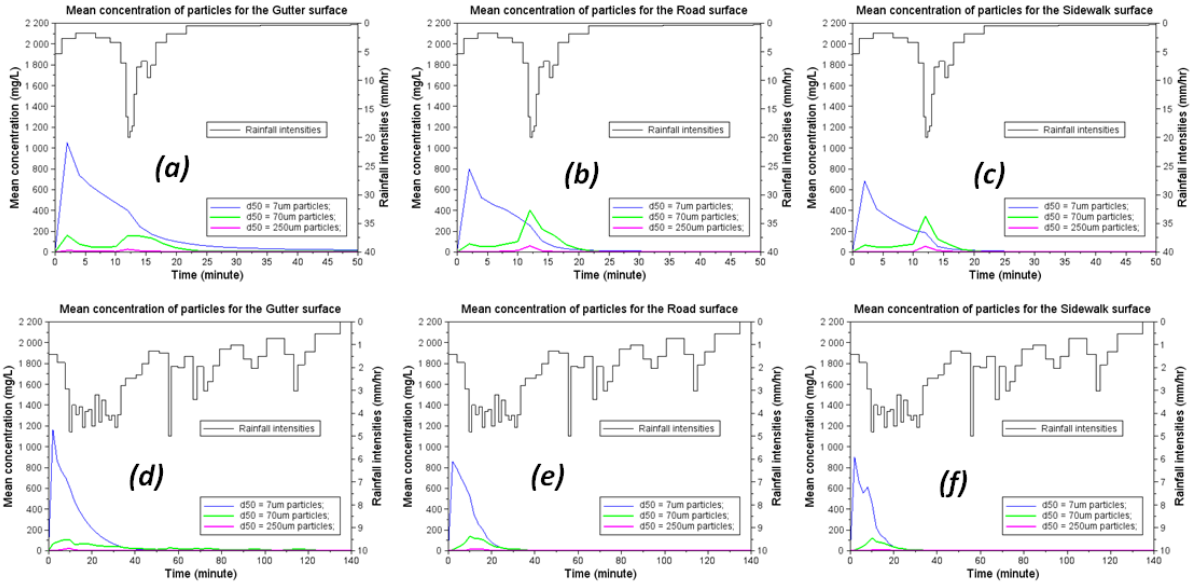

Fig. 10 Mean concentration of particles for the gutter (a, d), road (b, e) and sidewalk (c, f). The simulated concentrations of total suspended solids (TSS; solid black line), d50 = 7-µm particles (solid blue line), d50 = 70-µm particles (solid green line), and d50 = 250-µm particles (solid magenta line) are compared. Rainfall is plotted on the upper part. Events (a, b, c) are October 7, 2014; (d, e, f) February 28, 2015.

According to Fig. 10, the mean concentration of the finest particles (d50 = 7 µm) is similar in all studied conditions. When rainfall begins, the finest particles can immediately be detached and transferred to the sewer inlet. For the coarser particles,

the suspended solids concentration show significant peaks associated with high rainfall intensities for the road and sidewalk, but these are not apparent for the gutter area. This phenomenon can be explained by the behavior of water flows. As shown in Fig. 9, the gutter experience much more substantial water depths than the other land uses, and is therefore less sensitive to raindrop impacts.

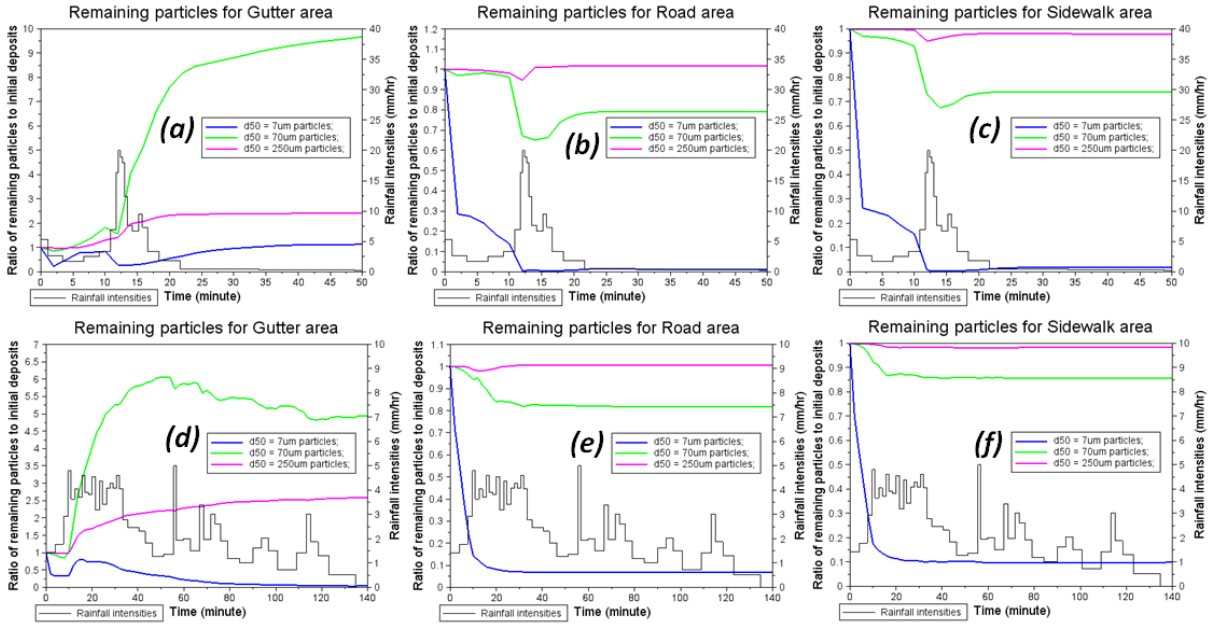

Fig. 11 The ratio of remaining particles to initial stocks for the gutter (a, d), road (b, e) and sidewalk (c, f). The evolution of d50 = 7-µm particles (solid blue line), d50 = 70-µm particles (solid green line), and d50 = 250-µm particles (solid magenta line) are evaluated for the events of (a, b, c) October 7, 2014; (d, e, f) February 28, 2015. Rainfall is plotted on the lower part (black line).

The results for the remaining particles in Fig. 11 support the above findings. As illustrated in the graphics, the great majority of the finest particles are instantly evacuated at the very beginning of rainfall events. However, coarser particles, particularly medium-sized (d50 = 70 µm) sediments, are removed from the surface of the road and sidewalk, but accumulate in the gutter. This fact suggests that with rising water depth during rainfall events, coarser particles can still be detached from the road and sidewalk, but that they are transferred to and deposited on gutter areas. As most of the finest particles are eroded at the beginning, and the total quantity of the coarsest particles appears stable during the entire rainfall period, the later fluctuations in TSS concentration at the sewer inlet are mainly generated by medium-size particles.

3.3.3. Rainfall-driven and flow-driven detachment on urban catchments

The spatial distributions of the detachment mass flux caused by raindrop energy (e_{ri}, *kg/m²s*) or water flow energy (r_{ri}, *kg/m²s*), are independently calculated for the areas of gutter, road and sidewalk. The mean mass fluxes of rainfall-driven and flow-driven detachment for the indicated surface areas are presented in Fig. 12.

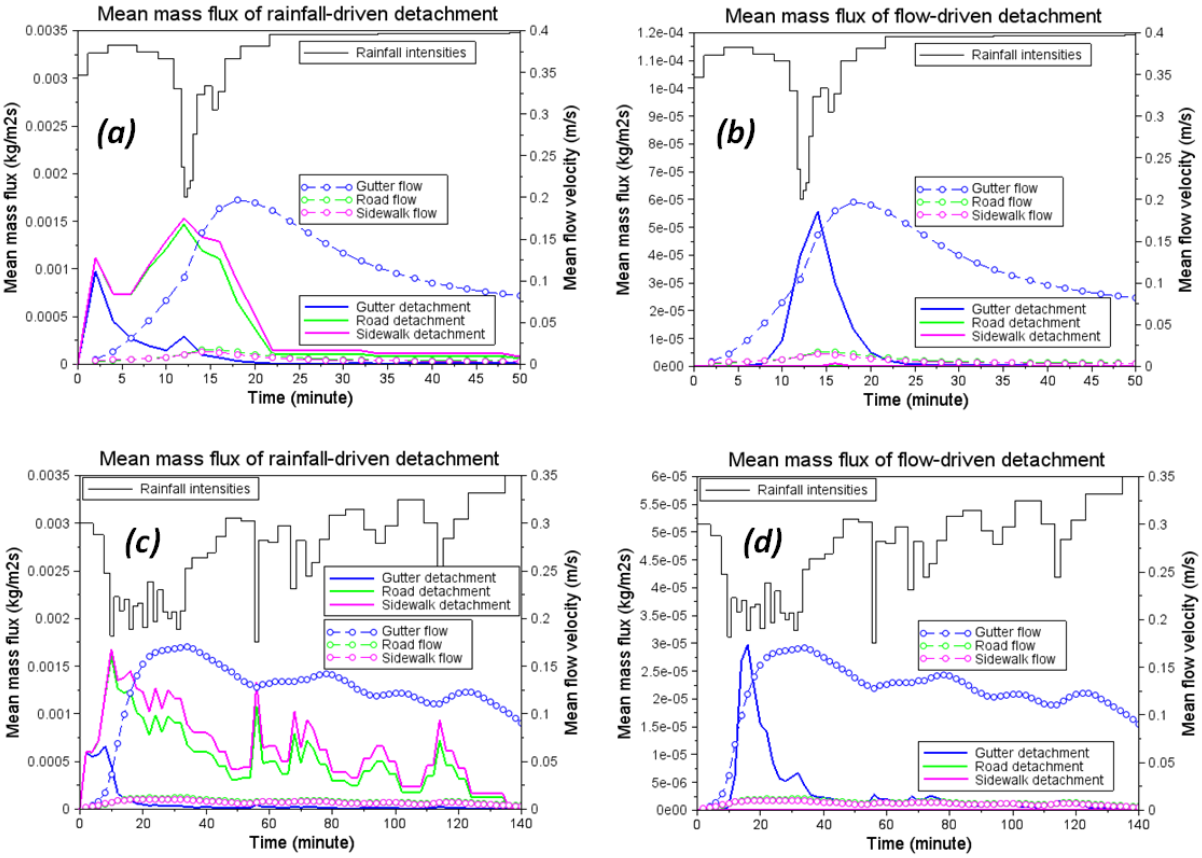

Fig. 12 Mean detachment mass flux by raindrop-driven (a, c) or flow-driven (b, d) effects, for the gutter (solid blue line), road (solid green line) and sidewalk (solid magenta line). Mean flow velocities are plotted as dashed-dotted lines for the gutter (blue), road (green) and sidewalk (magenta). Rainfall intensities are plotted on the upper part (black line). For the rainfall events of October 7, 2014 (a, b), and February 28, 2015 (c, d).

According to Fig. 12, for the two studied rainfall events over different land uses (gutter, road, and sidewalk), the mean mass flux of rainfall-driven detachment is larger than that of flow-driven detachment by 2 orders of magnitude (10^{-3} and 10^{-5} kg/m², respectively). This indicates that rainfall-driven detachment is much more important than flow-driven detachment in urban areas, and that the flow-driven effect

can be ignored most of the time. Moreover, it can be observed in Fig. 12(a) and (c), that the raindrop effects for gutter, road, and sidewalk are similar at the start of rainfall events, but decrease considerably in gutter areas afterwards. This phenomenon is due to the increase in water depth at the gutter surface during rainfall events. A comparison with the results presented in Fig. 9 shows that the water depth in the gutter is much higher than the road and the sidewalk. By using Eq. 6 given in section 2.1, it can be seen that the raindrop impact detachability in the gutter dramatically declines with the rise in flow depth beyond a certain threshold (0.7 mm). Otherwise, the water depth of the road and sidewalk cells rarely exceeds this limit; the rainfall-driven detachment therefore remains at a high level throughout the rainfall event. Moreover, the mean mass flux of rainfall-driven detachment on road areas is slightly lower than that on sidewalk areas. This may be caused by the road areas having a greater surface roughness than sidewalk areas; the greater number of depressions on road areas may reduce the general raindrop impact because of ponding water.

Fig. 12(b) and (d) indicate that the flow-driven detachment process occurs only in the gutter, where the water flow velocity is much higher than on the other types of surface. However, although the water flow velocity remains at a significant level through the later part of the rainfall event, the flow-driven detachment does not follow the dynamic of flow velocity, and declines much more quickly than the mean flow velocity. This phenomenon is due to the effects of fine particles available (d50 = 7 μm) on the surface. Comparisons with Fig. 11(a) and 11(d) show the decrease in flow-driven detachment comes after the decrease in the availably of fine particles on the gutter surface. This therefore indicates that the detachment caused by flow energy affects mainly the fine particles.

3.3.3. Spatial heterogeneity of sediment detachment in the gutter, road and sidewalk

In order to evaluate the heterogeneity of the washoff process within each land use, the median, and lower and upper quartiles of the mass flux (rainfall-driven and flow-driven) for the selected cells (2625 cells) of gutter, road, and sidewalk, are respectively presented in Fig. 13.

Similar to Fig. 12, Fig. 13 also shows that the rainfall-driven detachment is much more important than the flow-driven effects, and that the flow-driven detachment process only occurs in the gutter. It also reveals that the inter-quartile range for the mass flux in gutter cells is less significant than in the other land uses. This indicates that the lowest spatial heterogeneity in the washoff process occurs in gutter areas. Contrarily, the largest inter-quartile range for the mass flux, which occurs in road cells, illustrates the highest spatial heterogeneity for this land use. This finding suggests that the surface roughness for the study catchment follows road > sidewalk > gutter.

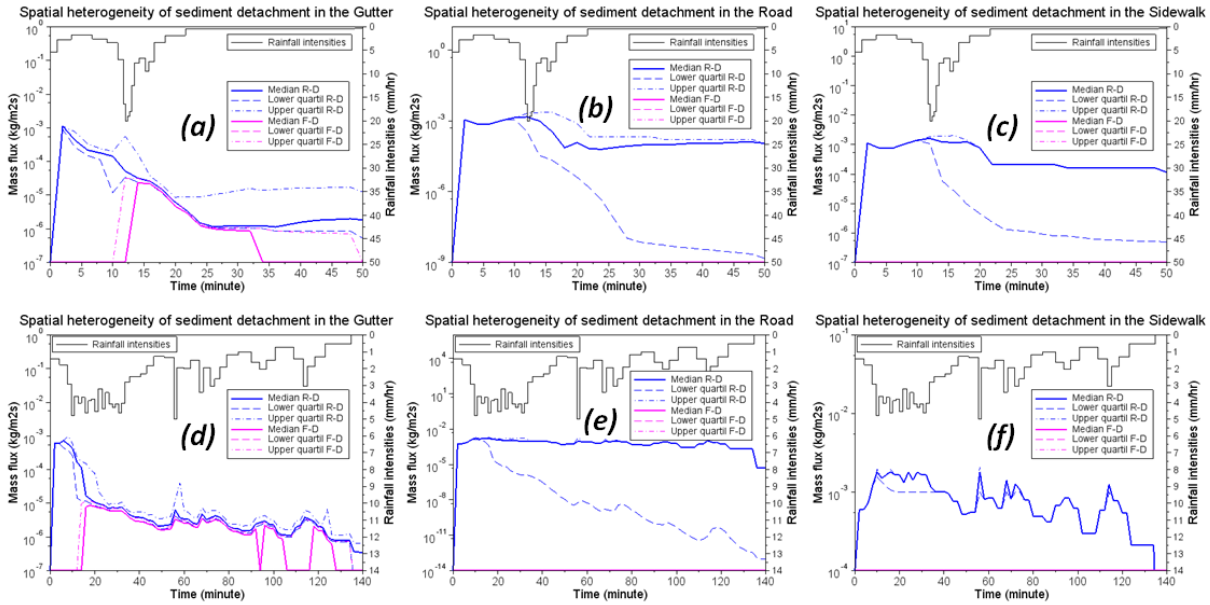

Fig. 13 Spatial heterogeneity of rainfall-driven (R-D; blue lines) or flow-driven (F-D; magenta lines) sediment detachment for the gutter (a, d), road (b, e), and sidewalk (c, f). The median values of the selected cells are represented by solid lines, the lower quartiles by dashed lines, and the upper quartiles by dashed-dotted lines. Rainfall intensities are plotted on the upper part (black line). For the events of October 7, 2014 (a, b, c), and February 28, 2015 (d, e, f).

Additionally, according to the results of the road and sidewalk areas, the lower quartiles of the mass flux caused by raindrops, is far from the median values, particularly during the latest part of the rainfall events. This phenomenon indicates that certain road and sidewalk cells represent local depressions on the surface, where relatively greater water depths can remarkably reduce the rainfall-driven detachment effects. Otherwise, as for the mass flux in gutter areas, intervals between the upper quartiles and the median values are more important than those of the lower quartiles. This fact implies that several gutter cells represent higher locations, where the water depth is lower, causing more significant detachment effects.

4. Discussion

4.1. On the use of physical models for assessing the urban washoff process

Use of physical models to assess real-world mechanisms assumes that the physical process can be represented in a deterministic way. In other words, it implies that the overall catchment response can be reproduced by the combined action of

the constituent process representations, and the spatial variability of a catchment can be displayed by distributed values at the model scale. These assumptions have been criticized by several researchers (Beck, 1987; Beven, 1989), who generally refer to the lack of totally distributed spatial data; the superficial input parameters being generally too sparse to allow realistic interpolation. However, the current study uses the 2D shallow-water equations with a particularly high-resolution (10 cm) topographic data, over an impervious urban catchment, which ensures an acceptable precision for overland flow modelling by equations governing fluid mechanics. The simulated water depth is also validated with local measurements at a very fine scale (0–0.5 mm), confirming that the spatial variations in water flow are well represented by the presented modelling approach. These findings demonstrate the relevance of using the given physically-based water quantity model to further investigate the washoff process.

Current urban washoff models still rely on empirical catchment-scale functions (Sartor et al., 1974) that have not advanced substantially over the last 40 years. This is mainly due to the shortage of experimental methods to provide basic information for model development, such as distributed measurements of flow depth and velocity. Use of the physical models can provide insights into the spatial and temporal heterogeneities of flow characteristics for sediment or nutrient modelling. In this study, we applied the H-R model to simulate washoff mechanisms, which allowed us to distinguish the different effects of rainfall-driven and flow-driven detachment. As the sediment characteristics (mass, PSD) are derived from measured data, and the model parameters have been widely discussed and validated by other authors (Beuselinck et al., 2002; Heng et al., 2011; Proffitt et al., 1991; Sander et al., 1996), we consider that the current modelling approach is reliable for assessing washoff process. The spatial analysis of the suspended solids concentrations, the particles remaining after the washoff process, and the detachment mass flux caused by raindrops or water flows, provide us with a basic view of washoff mechanisms within an urban catchment. Such information is helpful for designing advanced experimental measurements and settings, to improve the underlying theories and mathematical equations describing urban washoff process.

The development of physical models has two major objectives. The first is to improve the understanding of a particular theoretical construct, the second is to accurately reproduce a specific output for certain conditions (generally hydrographs or pollutographs for the catchment outlet). The present study is very valuable in the first regard; however, it may not yet be suitable for application issues. One reason for this is that the current approach requires very precise input data, and the simulations are quite time-consuming; this method may not be applicable for large urban catchments. Another reason comes from the fact that the spatial heterogeneities in system responses may not be well reproduced by catchment average parameters, such as the mass of dry deposits and particle size distributions. Similarly, the water flow calculation at each grid cell would suffer from insufficient resolution when te

model being applied at the urban catchment scale. And the particle settling/resuspension process at the catchment surface needs a high resolution to be well reproduced. Moreover, for larger urban catchments, the settling/resuspension process in the drainage network may play a role, which limits the applicability of the presented modelling approach. Nevertheless, it is expected that these drawbacks could be overcome in the near future using means such as up-scaling methods and integrated modelling with atmospheric deposition models and urban sewer network models. With such developments, urban physically-based washoff models will become very useful for application projects, helping stormwater managers design pre-entrance technologies such as filter systems and storage tanks to control urban non-point source pollutions.

4.2. Comparison of physically-based washoff modelling with washoff experiments: a historical perspective

Vaze and Chiew (2003) published one of the few papers in which the relative importance of the raindrop and runoff energies in the pollutant washoff process was investigated by field and laboratory experiments. In their paper, the authors stated that the energy of raindrops is very important for detaching surface pollutants at the beginning of an event, but is not so important later on. Their findings are similar to our simulation results for the gutter areas (Fig. 12). However, our simulations suggest that the raindrop impact is the essential force for detaching particles over the entire rainfall event for the road and sidewalk areas. This finding provides a new insight into the wash off process. This difference is mainly caused by the fact that the experimental setting of Vaze and Chiew (2003) used intense simulated rainfall events (26–50 mm/h for 8–17 min), which are much higher than our measured rainfall intensities (mean rainfall intensity is 2–3 mm/h). Therefore, the water depth in the underlying authors' experimental plots may have rapidly reached a high level, comparable to the simulated water depth in the observed gutter in our experiment, leading to a significant decrease in rainfall-driven detachment. Moreover, both Vaze and Chiew (2003) and ourselves, found that only the finer particles are removed during rainfall events, with most coarser sediments remaining on the surface.

Vaze and Chiew (2003) also conducted another group of experiments, where insect screens were placed above the surface to remove the rainfall energy. Nevertheless, the authors observed that the washoff process could also take place from the very beginning of the rainfall events. Considering that the detachment induced by water flow energy was shown to be negligible in the current study, use of only the flow energy-based equations may be insufficient for describing the flow-driven detachment in urban areas. Chebbo and Gromaire (2009) argued that certain urban particles have a quasi-nil settling velocity, which means that they will not be deposited on urban surfaces. In such cases, these suspended particles could be easily transferred into the sewer inlet under a very limited water flow. Therefore, energy-based flow-driven equations with a threshold of stream power would no

longer be appropriate for the underlying conditions. By studying the effects of these loose particles, more advanced flow-driven detachment equations may be derived, which would allow improvements to the understanding of urban washoff process.

4.3. Future outlook of physical urban washoff modelling

4.3.1. Taking the spatial distributions of input factors into consideration

Although the spatial variations of the washoff process are well represented in this study, we still use the uniform inputs of initial loads and the PSD of particles. These inputs are derived from the experimental data of Bechet et al. (2015), by averaging the measurements of samples from the gutter, road and sidewalk. However, the PSD of urban particles from different land uses are quite different (Fig. 14).

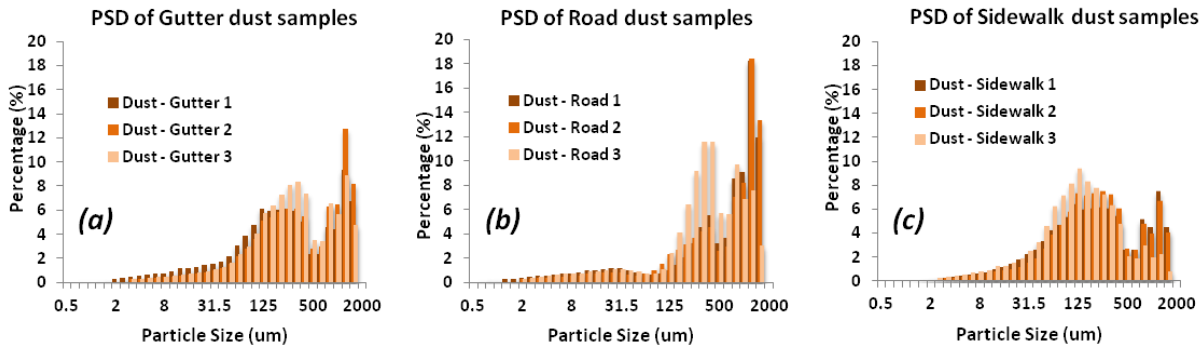

Fig. 14 Particle size distribution (PSD) for the dust samples of (a) gutter, (b) road, and (c) sidewalk at three different locations (1, 2, and 3).

According to Fig. 14, the PSD of gutter dust samples (Fig. 14a) and sidewalk (Fig. 14c) dust samples are similar, although both are different to road samples (Fig. 14b), with road dust containing less fine particles and more coarse sediments. This is due to the different sources of the urban dry deposits. Road dust chiefly comes from the direct abrasion of the road surface materials, whereas finer atmospheric depositions are more likely to remain on the sidewalk and gutter. Nevertheless, the homogeneous PSD input (see Fig. 5) in the current modelling approach hides this spatial heterogeneity. Since it is demonstrated that the first peak in the TSS concentration at the catchment outlet is caused mainly by the finest particles, and that the later fluctuations of the pollutograph are driven by medium-sized sediments, this misinterpretation of PSD may lead to an overestimate of TSS concentration at the beginning, but underestimate the TSS concentration during the later part of the rainfall. That is the case for the events shown in Fig. 7 (Fig. 7 b, c, d, e, and f), where the use of particles of d50 = 70-µm could not reproduce the moderate dynamics of the TSS concentration after all the d50 = 7-µm particles are removed. Therefore, it

would be interesting to continue to develop the FullSWOF model to assess the effects of the spatially distributed input factors (initial mass, PSD, H-R parameters), as well as the impacts of different particle size classes. Moreover, according to (Al Ali et al., 2016), the six investigated rainfall events in this paper are related to "first flush" events. However, as Métadier and Bertrand-Krajewski (2012) noted that an important number of rainfall events does not follow the "traditional" pattern for the TSS dynamics, advanced theories and urban washoff equations should be tested for our further studies in order to cope with these rainfall events.

4.3.2. Taking advantage of novel remote sensing techniques

Despite the very high-resolution topographic data and local measurements of water depth used in this study, limitations in the validation of physical urban washoff modelling still remain. This is mainly due to the shortage of suspended solids observations. For example, the measurements of TSS concentrations in the current study are based on turbidity observations (mini-probe OTT) at the sewer inlet, which require a certain depth of water to initialize the assessment. However, the most significant peak in TSS concentration in urban washoff usually occurs at the very beginning of the rainfall, yet it cannot be examined by this experimental method, as the water depth is quite limited during the initial stage. Moreover, without continuous PSD measurements of the suspended particles, the size-selective washoff modelling could not be approved by comparison with observations.

The newly developed digital particle image velocimetry (DPIV) technique shows potential for overcoming the underlying challenges in urban washoff modelling. Using a DPIV system, continuous measurement of the particle sizes and concentrations, as well as their spatial distributions, could be achieved. By establishing different experimental scenarios, advanced physical washoff models could be established and tested, in order to improve understanding of the washoff process.

5. Conclusion

In this paper, we introduce a new approach of using the physical model FullSWOF to evaluate urban washoff process. The Hairsine-Rose (H-R) water quality sub-model is able to independently simulate the rainfall-driven and flow-driven detachment, which allow us to have an insight into the urban washoff mechanisms. The water quantity simulation is validated with continuous and local measurements of water depth, which confirm that the present modelling approach is able to represent the spatial variations of the water flow on an urban surface.

Analysis of the washoff process at the catchment scale indicates that most (> 90%) of the finest particles are removed at the beginning of a rainfall event, with about

10%–20% of medium-size particles are removed over the later part of the event. Almost no coarse particles can be transferred into the sewer inlet.

The spatial analysis reveals that the water depth in the gutter is much more important than that on the road or on the sidewalk. Over the later part of a rainfall event, the concentration of coarser particles is more sensitive to rainfall intensities on the road and sidewalk, while the coarser particles tend to accumulate in the gutter.

Investigation of the driving force behind the detachment process indicates that the rainfall-driven effects is two orders of magnitude larger than the flow-driven effects. Moreover, it is observed that the rainfall-driven detachment on the gutter is considerably decreased with a rise in water depth, while flow-driven detachment occurs only on the gutter areas.

Although the physically-based modelling is still a simplification of the real world, it is currently the only method for analyzing the spatial and temporal variations of the washoff process. Moreover, the effectiveness of this research approach are confirmed by the high-resolution input data and the spatial validation of water depth . However, the comparison of this modelling approach with the published experimental results reveals a shortage of energy-based flow-driven equations for urban washoff modelling. Therefore, the application of advanced detachment equations considering the effects of loose particles, the integration of the spatial distributions of input factors, and the use of novel digital particle image velocimetry (DPIV) techniques, are essential perspectives for physical urban washoff modelling.

Acknowledgements

The research work of PhD student Yi Hong is financed by ANR-Trafipollu project and Ecole des Ponts, ParisTech. Firstly, the authors would like to thank OPUR (Observatoire des Polluants Urbains en Île-de-France) for providing the platform for discussion of ideas and facilitating collaborations with different researchers from various institutions. We also thank the computing center of Orleans for providing computational resources for the modelling. The authors wish to thank B. Béchet (IFSTTAR) and B. Soheilian (IGN) for providing valuable experimental data which helped to implement the model on the study site. Finally, we want to give a special thanks to the experimental team of ANR Trafipollu project for all the collected resources necessary for this work, in particular David Ramier (CEREMA), Mohamed Saad (LEESU), and Philippe Dubois (LEESU).

References

Al Ali, S., Bonhomme, C., Chebbo, G., 2016. Evaluation of the Performance and the Predictive Capacity of Build-Up and Wash-Off Models on Different Temporal Scales. Water 8, 312. doi:10.3390/w8080312

Aryal, R., Vigneswaran, S., Kandasamy, J., Naidu, R., 2010. Urban stormwater quality and treatment. Korean J. Chem. Eng. 27, 1343–1359. doi:10.1007/s11814-010-0387-0

Bechet, B., Bonhomme, C., Lamprea, K., Campos, E., Jean-soro, L., Dubois, P., Lherm, D., 2015. Towards a modeling of pollutant flux at local scale - Chemical analysis and micro-characterization of road dusts. Presented at the 12th Urban Environment Symposium, Oslo, Norway.

Beck, M.B., 1987. Water quality modeling: A review of the analysis of uncertainty. Water Resour. Res. 23, 1393–1442. doi:10.1029/WR023i008p01393

Beuselinck, L., Hairsine, P.B., Govers, G., Poesen, J., 2002. Evaluating a single-class net deposition equation in overland flow conditions: SINGLE-CLASS NET DEPOSITION EQUATION. Water Resour. Res. 38, 15–1–15–10. doi:10.1029/2001WR000248

Beven, K., 1989. Changing ideas in hydrology — The case of physically-based models. J. Hydrol. 105, 157–172. doi:10.1016/0022-1694(89)90101-7

Bressy, A., Gromaire, M.-C., Lorgeoux, C., Saad, M., Leroy, F., Chebbo, G., 2012. Towards the determination of an optimal scale for stormwater quality management: Micropollutants in a small residential catchment. Water Res. 46, 6799–6810. doi:10.1016/j.watres.2011.12.017

Chebbo, G., Gromaire, M.-C., 2009. VICAS—An Operating Protocol to Measure the Distributions of Suspended Solid Settling Velocities within Urban Drainage Samples. J. Environ. Eng. 135, 768–775. doi:10.1061/(ASCE)0733-9372(2009)135:9(768)

Cheng, N., 1997. Simplified Settling Velocity Formula for Sediment Particle. J. Hydraul. Eng. 123, 149–152. doi:10.1061/(ASCE)0733-9429(1997)123:2(149)

Delestre, O., Cordier, S., Darboux, F., Du, M., James, F., Laguerre, C., Lucas, C., Planchon, O., 2014. FullSWOF: A Software for Overland Flow Simulation, in: Gourbesville, P., Cunge, J., Caignaert, G. (Eds.), Advances in Hydroinformatics. Springer Singapore, Singapore, pp. 221–231.

Deletic, A., Maksimovic, [Cbreve]edo, Ivetic, M., 1997. Modelling of storm wash-off of suspended solids from impervious surfaces. J. Hydraul. Res. 35, 99–118. doi:10.1080/00221689709498646

Fletcher, T.D., Andrieu, H., Hamel, P., 2013. Understanding, management and modelling of urban hydrology and its consequences for receiving waters: A state of the art. Adv. Water Resour. 51, 261–279. doi:10.1016/j.advwatres.2012.09.001

Green, W.H., Ampt, G.A., 1911. Studies on Soil Phyics. J. Agric. Sci. 4, 1–24. doi:10.1017/S0021859600001441

Gromaire, M.., Garnaud, S., Saad, M., Chebbo, G., 2001. Contribution of different sources to the pollution of wet weather flows in combined sewers. Water Res. 35, 521–533. doi:10.1016/S0043-1354(00)00261-X

Hairsine, P.B., Rose, C.W., 1992a. Modeling water erosion due to overland flow using physical principles: 1. Sheet flow. Water Resour. Res. 28, 237–243. doi:10.1029/91WR02380

Hairsine, P.B., Rose, C.W., 1992b. Modeling water erosion due to overland flow using physical principles: 2. Rill flow. Water Resour. Res. 28, 245–250. doi:10.1029/91WR02381

Heng, B.C.P., Sander, G.C., Armstrong, A., Quinton, J.N., Chandler, J.H., Scott, C.F., 2011. Modeling the dynamics of soil erosion and size-selective sediment transport over nonuniform topography in flume-scale experiments. Water Resour. Res. 47, W02513. doi:10.1029/2010WR009375

Herngren, L., Goonetilleke, A., Ayoko, G.A., Mostert, M.M.M., 2010. Distribution of polycyclic aromatic hydrocarbons in urban stormwater in Queensland, Australia. Environ. Pollut. 158, 2848–2856. doi:10.1016/j.envpol.2010.06.015

Hervieu, A., Soheilian, B., 2013. Semi-Automatic Road/Pavement Modeling using Mobile Laser Scanning. ISPRS Ann. Photogramm. Remote Sens. Spat. Inf. Sci. II-3/W3, 31–36. doi:10.5194/isprsannals-II-3-W3-31-2013

Hong, Y., Bonhomme, C., Le, M.-H., Chebbo, G., 2016. A new approach of monitoring and physically-based modelling to investigate urban wash-off process on a road catchment near Paris. Water Res. 102, 96–108. doi:10.1016/j.watres.2016.06.027

Kafi, M., Gasperi, J., Moilleron, R., Gromaire, M.C., Chebbo, G., 2008. Spatial variability of the characteristics of combined wet weather pollutant loads in Paris. Water Res. 42, 539–549. doi:10.1016/j.watres.2007.08.008

Kanso, A., 2004. Evaluation des Modèles de Calcul des Flux Polluants des Rejets Urbains par Temps de Pluie. Apport de l'Approche Bayésienne. Ecole Nationale des Ponts et Chaussées.

Kim, J., Ivanov, V.Y., Katopodes, N.D., 2013. Modeling erosion and sedimentation coupled with hydrological and overland flow processes at the watershed scale: HYDROLOGIC-HYDRAULIC-MORPHOLOGIC MODEL AT WATERSHED SCALE. Water Resour. Res. 49, 5134–5154. doi:10.1002/wrcr.20373

Kinnell, P.I.A., 2009. The influence of raindrop induced saltation on particle size distributions in sediment discharged by rain-impacted flow on planar surfaces. CATENA 78, 2–11. doi:10.1016/j.catena.2009.01.008

Le, M.-H., Cordier, S., Lucas, C., Cerdan, O., 2015. A faster numerical scheme for a coupled system modeling soil erosion and sediment transport. Water Resour. Res. 51, 987–1005. doi:10.1002/2014WR015690

Merritt, W.S., Letcher, R.A., Jakeman, A.J., 2003. A review of erosion and sediment transport models. Environ. Model. Softw. 18, 761–799. doi:10.1016/S1364-8152(03)00078-1

Métadier, M., Bertrand-Krajewski, J.-L., 2012. The use of long-term on-line turbidity measurements for the calculation of urban stormwater pollutant concentrations, loads, pollutographs and intra-event fluxes. Water Res. 46, 6836–6856. doi:10.1016/j.watres.2011.12.030

Mutchler, C.K., Hansen, L.M., 1970. Splash of a Waterdrop at Terminal Velocity. Science 169, 1311–1312. doi:10.1126/science.169.3952.1311

Paparoditis, N., Papelard, J.-P., Cannelle, B., Devaux, A., Soheilian, B., David, N., Houzay, E., 2012. Stereopolis II: A multi-purpose and multi-sensor 3D mobile mapping system for street visualisation and 3D metrology. Rev. Fr. Photogrammétrie Télédétection 69–79.

Proffitt, A.P.B., Rose, C.W., Hairsine, P.B., 1991. Rainfall Detachment and Deposition: Experiments with Low Slopes and Significant Water Depths. Soil Sci. Soc. Am. J. 55, 325. doi:10.2136/sssaj1991.03615995005500020004x

Rossman, lewis A., 2010. STORM WATER MANAGEMENT MODEL USER'S MANUAL Version 5.0. NATIONAL RISK MANAGEMENT RESEARCH LABORATORY OFFICE OF RESEARCH AND DEVELOPMENT U.S. ENVIRONMENTAL PROTECTION AGENCY, CINCINNATI, OH 45268.

Sage, J., Bonhomme, C., Al Ali, S., Gromaire, M.-C., 2015. Performance assessment of a commonly used "accumulation and wash-off" model from long-term continuous road runoff turbidity measurements. Water Res. 78, 47–59. doi:10.1016/j.watres.2015.03.030

Sander, G.C., Hairsine, P.B., Rose, C.W., Cassidy, D., Parlange, J.-Y., Hogarth, W.L., Lisle, I.G., 1996. Unsteady soil erosion model, analytical solutions and comparison with experimental results. J. Hydrol. 178, 351–367. doi:10.1016/0022-1694(95)02810-2

Sartor, J.D., Boyd, G.B., Agardy, F.J., 1974. Water Pollution Aspects of Street Surface Contaminants. J. Water Pollut. Control Fed. 46, 458–467.

Shaw, S.B., Walter, M.T., Steenhuis, T.S., 2006. A physical model of particulate wash-off from rough impervious surfaces. J. Hydrol. 327, 618–626. doi:10.1016/j.jhydrol.2006.01.024

Vaze, J., Chiew, F.H.S., 2003. Study of pollutant washoff from small impervious experimental plots. Water Resour. Res. 39, 1160. doi:10.1029/2002WR001786

Wong, T.H.F., Fletcher, T.D., Duncan, H.P., Coleman, J.R., Jenkins, G.A., 2002. A Model for Urban Stormwater Improvement: Conceptualization. American Society of Civil Engineers, pp. 1–14. doi:10.1061/40644(2002)115

Zgheib, S., Moilleron, R., Chebbo, G., 2012. Priority pollutants in urban stormwater: Part 1 – Case of separate storm sewers. Water Res. 46, 6683–6692. doi:10.1016/j.watres.2011.12.012

Zhao, H., Li, X., 2013. Understanding the relationship between heavy metals in road-deposited sediments and washoff particles in urban stormwater using simulated rainfall. J. Hazard. Mater. 246–247, 267–276. doi:10.1016/j.jhazmat.2012.12.035

Zoppou, C., 2001. Review of urban storm water models. Environ. Model. Softw. 16, 195–231. doi:10.1016/S1364-8152(00)00084-0

PARTIE III. Modélisation distribuée à base physique à l'échelle du quartier

Dans cette partie, nous présentons la modélisation du transfert de l'eau et de polluants à l'échelle du quartier. Deux plateformes de modélisation sont développées dans la thèse: (a) la plateforme TRENOE qui couple les modèles TREX [1] et CANOE [2]; (b) la plateforme LISEM-SWMM qui couple les modèles LISEM [3] et SWMM [4]. Ces deux plateformes 2D-1D permettent de simuler la variabilité spatiale et temporelle des flux d'eau et de polluants sur les surfaces urbaines et également dans les réseaux d'assainissement.

Dans le cadre du projet ANR-Trafipollu, les modèles sont appliqués sur un petit bassin-versant urbain autour du boulevard d'Alsace Lorraine (RD 34), situé sur la commune du Perreux-sur-Marne dans le département du Val de Marne (12 km à l'est de Paris). Le bassin-versant est délimité en considérant les données topographiques (jusqu'au 20 cm de résolution) et les connections au réseau d'assainissement. La surface du bassin est égale à 0.12 km². Les chapitres 7 - 9 présentent les développements, les applications et les analyses de ces plateformes 2D-1D (TRENOE et LISEM-SWMM) sur le bassin-versant étudié.

- **Chapitre 7**

Dans le Chapitre 7, une plateforme de modélisation intégrée, 2D/1D, "TRENOE", est développée en couplant le modèle 2D à base physique TREX (Velleux et al., 2008) et le modèle de réseau 1D CANOE (Alison, 2005). L'objectif de la plate-forme est de simuler la quantité et la qualité des eaux pluviales urbaines à l'échelle d'un quartier.

Des mesures en continu et un nombre important de données détaillées collectées dans le cadre du projet ont permis d'évaluer l'influence sur les résultats du modèle de différents paramètres comme la structure du modèle, la précision numérique, les paramètres et les données d'entrée utilisés. En changeant différentes options de mise en œuvre et de configurations du modèle, la modification des codes sources en adaptant la précision numérique et l'utilisation des données détaillée de l'occupation du sol sont des étapes cruciales pour cette approche de modélisation Par contre, l'utilisation de données topographiques de haute résolution pour la route et la calibration usuelle de la conductivité hydraulique à saturation et du paramètre de Manning semblent être de second plan à l'échelle du petit bassin versant urbain.

En ce qui concerne la modélisation de la qualité de l'eau, notre travail montre que les équations USLE empiriques doivent être complétées par des processus de détachement des poussières urbaines par les gouttes de pluie. Même si les simulations de la qualité de l'eau doivent être améliorées, la prise en compte de la distribution de taille des particules se révèle être un facteur important pour modéliser le transport des polluants en surface sur un bassin versant urbain.

- **Chapitre 8**

Le Chapitre 8 présente les résultats obtenus concernant l'utilisation des données topographiques de haute résolution et les données détaillées d'occupation du sol sur les résultats de modélisation.

En utilisant la plateforme TRENOE présentée dans le chapitre précédent, des simulations des flux d'eau à l'exutoire du bassin versant urbain ont été redressées en faisant varier (a) les données topographiques (haute et basse résolution) et (b) les données d'occupations du sol (détaillées et grossières) provenant de différentes sources de données. Les résultats de ces comparaisons montrent que (i) en utilisant simplement les données topographiques de basse résolution, le modèle 2D-1D est capable de reproduire les dynamiques des flux d'eau à l'exutoire du bassin-versant à l'échelle du quartier du milieu urbain; (ii) par contre, les informations détaillées de l'occupation du sol sont nécessaires pour réaliser des simulations satisfaisantes des transferts des eaux en milieu urbain.

- **Chapitre 9**

En tenant compte des origines des problèmes résultant de l'utilisation de la plateforme TRENOE présenté dans les chapitres précédents, nous avons développé dans le Chapitre 9 une nouvelle plateforme de modélisation intégrant un modèle d'érosion en surface à base physique (LISEM) avec un code de modélisation du transfert en réseau bien connu (SWMM).

Par rapport aux outils précédemment utilisés, l'outil LISEM est particulièrement intéressant dans la mesure où le schéma numérique associé à ce code prend en compte les transferts d'eau et de particules pour les 8 cellules adjacentes à chaque pixel. De plus, ce modèle est basé sur le modèle d'Hairsine et Rose (1992) pour l'érosion, incluant le détachement des poussières urbaines par les gouttes de pluie en distribuant sur plusieurs classes de particules.

Le transfert de matières en suspension lors de plusieurs évènements de pluie est présenté dans ce chapitre en se basant sur deux scénarios types : un scénario qui consiste à prendre en compte les données granulométriques et les masses déposées sur les surfaces urbaines à partir des données collectées au sein même du projet ANR-Trafipollu, un deuxième scénario qui consiste à prendre en compte pour les particules les plus fines sur les surfaces urbaines (<10 µm) les sorties de modèles atmosphériques. La prise en compte de ces données de simulation permet ainsi de considérer la distribution spatiale des dépôts atmosphériques à l'échelle du quartier.

La prise en compte de la concentration en HAP et métaux des particules, selon leur taille, permet de tracer l'évolution de la concentration en HAP et métaux à l'exutoire de ce bassin versant urbain, tout en distinguant les classes de particules

concernées. En comparant avec les données de concentration moyennes obtenues à partir des prélèvements dans l'avaloir (cf. Chapitre 5 - 6) dans le cadre du projet, les résultats montrent que l’emploi de modèles totalement distribués peut arriver à reproduire de manière très fine les dynamiques des particules, des hydrocarbures et des métaux. Par contre, les résultats de simulations montrent que les données recueillies à l’exutoire ne permettent pas clairement de distinguer la pertinence de l’utilisation de données distribuées par rapport à des données moyennées spatialement. Même si à ce stade la plateforme développée nécessite des améliorations pour adapter aux utilisations dans le champ opérationnel, ceci constitue une avancée pour le domaine de modélisation du transfert hydrologique des polluants routiers en milieu urbain.

Chapitre 7. Development and assessment of the physically-based 2D/1D model “TRENOE” for urban stormwater quantity and quality modelling

Yi Hong [1,*], Celine Bonhomme [1] and Ghassan Chebbo [1,2]

[1] LEESU, MA 102, École des Ponts, AgroParisTech, UPEC, UPE, Champs-sur-Marne, France;

[2] Université Libanaise, faculté de génie, campus Rafic Hariri, Hadat, Lebanon;

***** Correspondence: yi.hong@leesu.enpc.fr; Tel.: +33-164-153-630

*(Article publié dans le journal "**Water**")*

DOI: 10.3390/w8120606

Abstract: The widespread use of separate stormwater systems requires better understanding of the interactions between urban landscapes and drainage systems. This paper describes a novel attempt of developing urban 2D-surface and 1D-drainage model “TRENOE” for urban stormwater quantity and quality modelling. The physically-based TREX model and the conceptual CANOE model are integrated into the TRENOE platform, highlighting that the roofs of buildings are represented separately from the surface model, but simulated as virtual “sub-basins” in the CANOE model. The modelling approach is applied to a small urban catchment near Paris (Le Perreux sur Marne, 0.12 km^2). Simulation scenarios are developed for assessing the influences of different “internal” (model structure, numerical issues) and “external” (parameters, input data) factors on model performance. The adequate numerical precision and the detailed information of land use data are identified as crucial elements of water quantity modelling. Contrarily, the high-resolution topographic data and the common variations of the water flow parameters are not equally significant at the scale of a small urban catchment. Concerning water quality modelling, particle size distribution is revealed to be an important factor, while the empirical USLE equations need to be completed by a raindrop detachment process.

Keywords: urban stormwater modelling; urban water quality; 2D/1D modelling; physically-based model; spatially distributed model; TREX model; CANOE model; integrated modelling;

1. Introduction

Separate sewer discharges are now widely recognized for their deleterious impact on receiving water bodies. Although combined sewer overflows were traditionally considered to be the major cause of water quality degradation in urban waterways, the impacts of stormwater discharges has been recently attracting more attention with separate networks taking over combined ones [1–3]. The high levels of pollution frequently observed in stormwater outflows are shown to significantly contribute to the environmental pressure of urban areas on water streams, from which the importance of a proper evaluation of these discharges emerges [4,5].

The modelling of urban stormwater can be split into two components: the simulation of water quantity and the simulation of water quality. Despite the rapid development of hydrological modelling during last decades, the water quality component of urban stormwater modelling remains far less studied. One of the main reasons is that accurate simulations of pollutant transport on urban surfaces require detailed spatial and temporal information on stormwater runoff [6,7]. For example, surface modules of the well-known SWMM [8] and MUSIC [9] models are respectively based on examining sub-catchments and land-use parcels to simulate overland flows in urban catchments. These approaches are based on a conceptual representation of routing processes governing pollutants' transport from their generation points to the sub catchment outlet [10]. Most of them are based on Sartor and Boyd formulations of build-up and wash-off on urban surfaces [11]. These conceptual equations have been criticized by several authors [7,12–14] for their poor performance in reproducing pollutant concentration dynamics. However, current urban stormwater quality models (e.g., SWMM, MUSIC, etc.) still rely on these empirical catchment-scale functions that have not substantially evolved over the last 40 years. An alternative way to improve their performance might be to even out their spatial dimension applications. In this respect, the 2D erosion model (TREX), which was initially developed for rural/agricultural catchments and largely tested by the scientific community to simulate particle transport in natural catchments, represents an interesting tool to apply to urban catchments. This novel modelling approach could lend itself to new ways of thinking in the field of urban stormwater quality modelling, and could potentially advance our modelling techniques.

Over the last few years, the modeling approach of combining 2D overland flow and 1D drainage sewer flow has received great attention [15,16]. Several research models [17–20] and commercial tools [21,22] have already been developed and applied to various case studies. These models are able to accurately represent the

spatial and temporal variations of surface runoffs and sewer flows on urban areas. The concept of these 2D/1D models is hence well adapted to introducing more reliable pollutant transport processes. However, present applications of these models are mostly focused on urban flood modelling, while being rarely investigated for urban pollutant transport simulations. On the other hand, existing publications on integrated 2D/1D models rarely compare the influences of different factors on model outputs [16,23,24]. In that case, the main drivers of the model outputs are still not sufficiently investigated, which decreases the reliability of the integration of new processes into the existing model, and restricts the transferability of the model to other case studies.

In this context, we coupled the physically-based 2D model TREX [25,26], which has been initially developed for watershed rainfall-runoff, sediment and contaminant transport modelling, with the 1D pipe routing and subbasin components of the CANOE model [27], resulting in the “TRENOE” platform. It is the first time that such a 2D physically-based erosion model, based on USLE equations, has been coupled with an urban model for the simulation of urban stormwater quality. Moreover, TREX is an open source code, well-documented, with a robust numerical scheme, which makes it suitable for modification in an urban context. The coupling between TREX and CANOE models is designed to be able to simulate the 2D overland flows and the 1D sewer network routing. Roofs are simulated separately from the 2D surface model in TRENOE. Since the roof gutters are connected directly to the sewer networks in the studied catchment, roofs are represented as the “subbasins” in the 1D CANOE model.

Within the framework of the ANR (French National Agency for Research) Trafipollu project, a detailed Geographic Information System (GIS) database is available for the study of urban catchments (Le Perreux sur Marne, 0.12 km^2), such as by using the high-resolution topographic data of LiDAR survey and the detailed land use data derived from ortho photos. Benefitting from this large dataset of detailed source data and continuous measurement at the sewage outlet, the influences of various inherent (model structure, numerical issues) and external (input-data, parameter values) factors on model performance are evaluated.

In general, this paper focus on two objectives: firstly, to apply the physically-based 2D/1D TRENOE platform to urban stormwater quantity and quality modelling; secondly, to rank the impacts of different factors on model outputs and to highlight the prerequisites for high performance simulations. The results of this study may be very useful for reducing the cost of urban stormwater management by avoiding some unnecessary data acquisition and modelling efforts (high-resolution topograhic data, calibration, etc.). Perspectives and propositions for improving urban stormwater quality modelling are presented as well..

2. Materials and Methods

2.1. Model description

The physically-based 2D model TREX and the 1D pipe routing and subbasin components of the CANOE model are integrated into the TRENOE platform. Within TREX, the catchment surface is divided into several rectangular meshes based on GIS topographic data. These grids are then categorized into several classes according to land use information. Different parameters are attributed to each grid point in accordance with the land use type. Interception, infiltration, water runoff and pollutant transfer processes are then calculated. Diffusive wave approximation of Shallow-Water equations (SW) is applied for simulating the surface runoff at the grid scale, which is able to represent the spatial and temporal variations of the water flow and the associated pollutants. With the 1D sewer system CANOE model, stormwater and pollutant routing processes are computed for each portion of pipes between pre-defined junction nodes using the kinematic approximation of SW equations and advection equations, respectively. The modelling processes in TRENOE are described in Table 1:

Table 1. Modelling processes in the 2D/1D TRENOE platform.

	2D overland modelling: TREX	**Conceptual roofs modelling: CANOE**	**1D sewer network modelling: CANOE**
Water flow	2D Shallow-Water equations; (Diffusive Wave)	Non-linear reservoir	1D Shallow-Water equations; (Kinematic Wave)
Infiltration	Green & Ampt	-	-
Interception	Volume loss	-	-
Sediment deposition	Settling velocity [29]	-	-
Sediment erosion	Modified form of Universal Soil Loss Equation (USLE)	Exponential washoff equations	-
Numerical method	Finite Difference	Finite Difference	Finite Difference

The “junction nodes” in 1D sewer network model are the connecting points between different parts of the TRENOE platform. From the grids of “sewer inlets” and “roofs”, water and pollutants flow directly into the sewer networks via these “junction nodes”. “Sewer inlets” are considered as “holes” in the 2D surface model, where surface runoff and the related pollutants disappear at these grid points. In contrast, “roofs” are represented as obstacles, where water flows cannot enter these grids from other types of land uses. As the buildings are not described in the Digital Elevation Model (DEM) data, the grids of “roofs” are increased by 5 m at the step of input data pre-treatment. Since most roofs are directly connected to the sewer networks in the studied urban catchment, we gather the grids of roofs which are linked to the same junction nodes (the nearest), to set the conceptual “sub-catchments” in CANOE model. The size of each “sub-catchment” is equal to the total area of the linking “roofs” grids. The non-linear reservoir method and the exponential washoff equations [13] are then applied to simulate the rainfall-runoff and the pollutant transport, respectively, for each conceptual “sub-catchment”. The model scheme is illustrated in Figure 1:

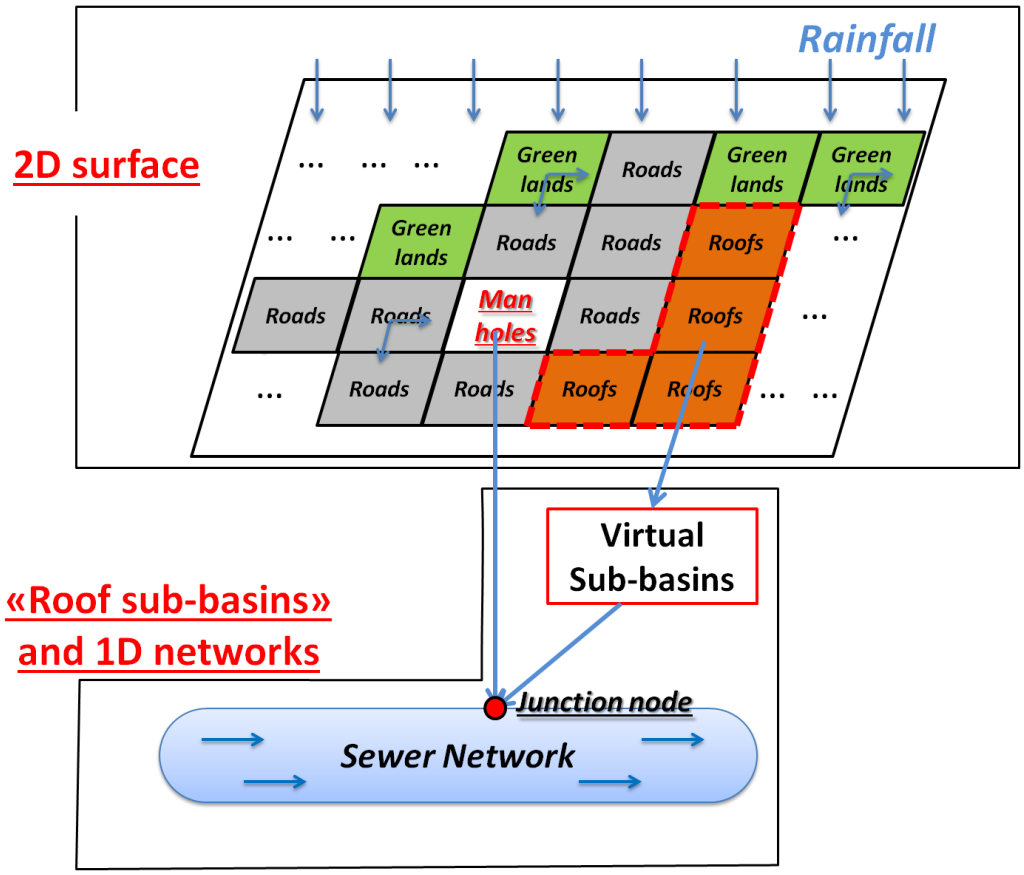

Figure 1. The scheme of the physically-based 2D/1D modelling platform TRENOE.

2.2. Study site and urban catchment delineation

The study site is located in the eastern suburb of Paris (Le Perreux sur Marne, Val de Marne, France). This research area is a typical residential zone in the Paris region, characterized by a highly trafficked main street of eastern Paris. A preliminary step is to delineate the urban catchment. Since this study aims at precisely modelling water flows and pollutant transport at small urban scales, a detailed delineation of the urban catchment is necessary. As it is well-known that the urban areas are complex because of various buildings and infrastructure that may influence the water flow path, our “hand-operated” delineation procedure is based on the complete knowledge of sewer network infrastructure, road high-resolution LiDAR data (20 cm), and the Digital Orthophoto Quadrangles (DOQs) (5 cm).

The detailed urban catchment is delimited by applying the following steps: (i) identifying the contributing sewage portions for the monitored drainage outlet using elaborate sewer network data; (ii) locating the sewer inlets; (iii) delimiting the “drainage basin” for each sewer inlet benefiting from the road high-resolution LiDAR data (20 cm); (iv) merging all the “drainage basins” defined by the precedent steps; (v) comparing data with the DOQs (5 cm), recognizing the buildings and infrastructure that should be included in the basin. The delimited urban catchment is presented in Figure 2:

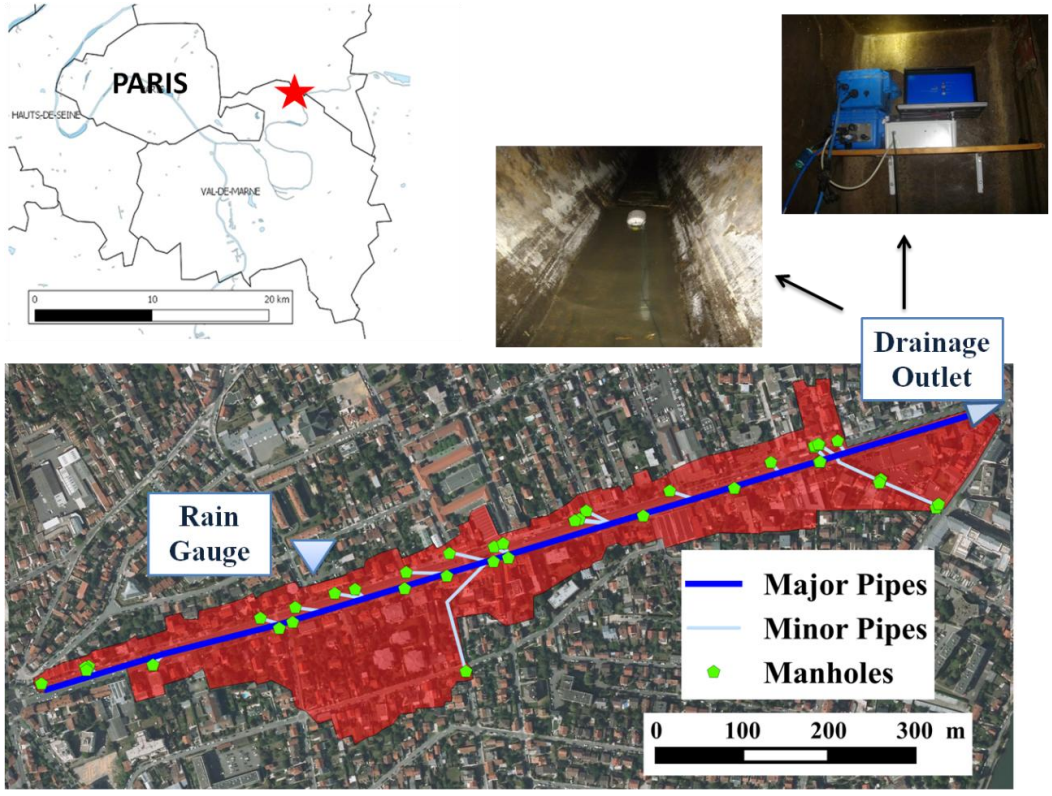

Figure 2. Delineated urban catchment of the study site, Le Perreux-sur-Marne, France.

2.3. Input data description

2.3.1. Rainfall data

A tipping-bucket rain gauge is installed on the roof of a building close to the urban catchment (less than 150 m). The pluviometer has a resolution of 0.1 mm. As the study area is quite small, rainfall is considered as homogeneous within the basin. Monitoring was conducted between 20 September 2014 and 27 April 2015. Different rainfall events are identified by the time intervals longer than 90 min between two tipping records and the total rainfall depth of each event should be more than 1 mm. At the end, 56 rainfall events have been recognized for the observed period. An analysis of rainfall depth, mean intensity, event duration and antecedent dry days is performed for all rainfall events in order to analyze their characteristics (Figure 3).

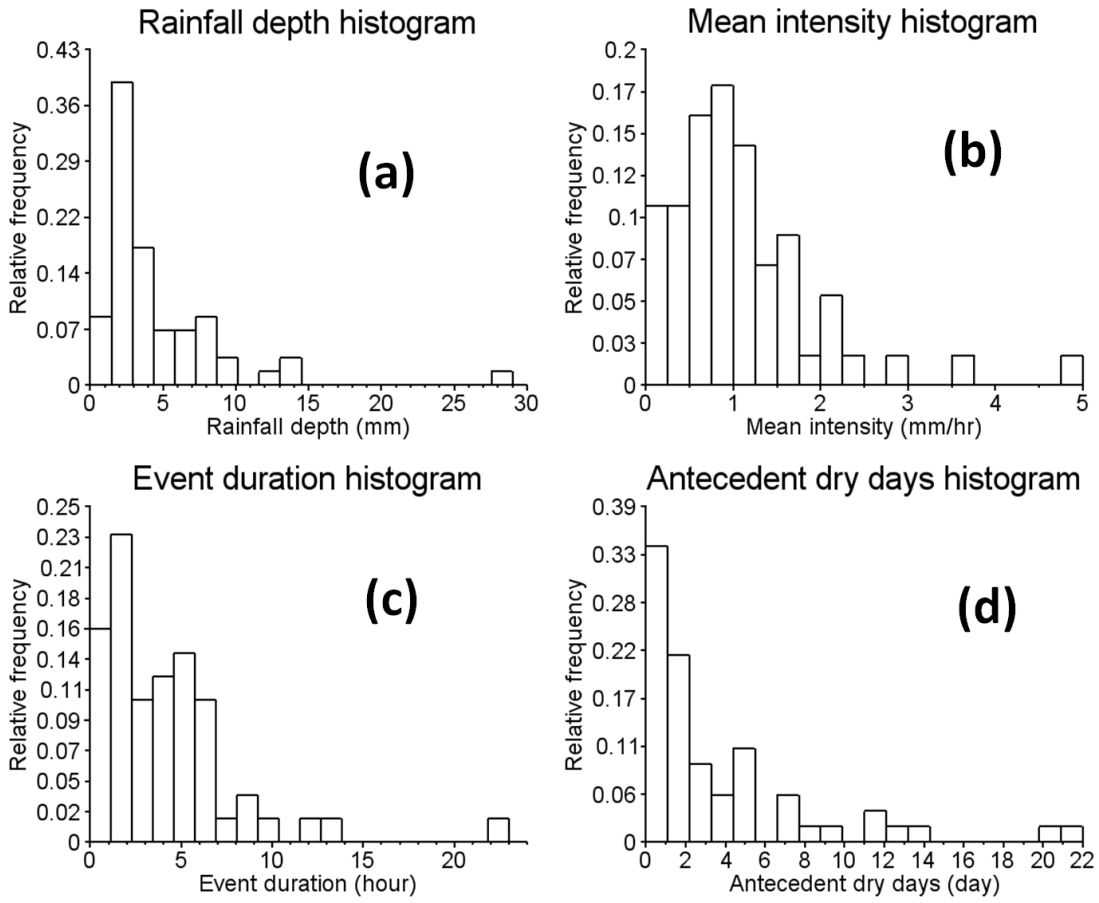

Figure 3. Histogram of rainfall event characteristics over the entire period. Where (a) Rainfall depth; (b) Mean intensity; (c) Event duration; (d) Antecedent dry days.

According to Figure 3a,b, we can observe that most rainfall events within the study area of eastern Paris are considered low. In fact, more than 88% of rainfall events have a rainfall depth of less than 8 mm, and nearly 89% of rainfall events have a mean intensity lower than 3 mm/h. Additionally, Figure 3c,d shows that event duration and antecedent dry days are a little more heterogeneous. However, most rainfall events observed are shorter than 7 h (87%), while 88% of the events are preceded by a previous rainfall event by less than 8 days. As the simulations are quite time-consuming, we have to select several rainfall events which contain different characteristics in order to characterize the overall performance of the TRENOE platform within an urban context. Among the rainfall events observed, we selected 6 typical events for model application and performance evaluation. A summary of selected rainfall events is listed in Table 2.:

Table 2. Summary of the 6 selected rainfall events.

Rainfall date	Rainfall depth (mm)	Mean intensity (mm/hr)	Duration (hour)	Antecedent dry days (day)
10/08/2014	4.86	1.51	3.22	0.4
10/12/2014	3.60	1.68	2.14	1.3
11/03/2014	4.6	1.33	3.46	12.9
11/15/2014	9.27	2.81	3.3	0.5
11/26/2014	2.86	1.1	2.6	9
12/12/2014	4.15	1.28	3.24	2.5

2.3.2. Topographic data

Topographic data is a crucial input for physically based modelling. In the GIS database of the Paris region, the 25 m-resolution DEM data is available (Figure 4a). Moreover, in the framework of the ANR-Trafipollu project, the LiDAR data of roads collected by IGN France have a horizontal resolution of 20 cm and a vertical precision of 1 cm. These data were collected by an on-vehicle laser (Figure 4b). The roads are essential flow pathways in the studied urban catchment, because the surrounding roofs are directly connected to the sewer network and the greenlands only represent a small part of the urban surface. Therefore, the topographic data of roads derived from high resolution LiDAR data improve the resolution and precision

of previously used DEM data. Nevertheless, the resolution used for the TREX-CANOE simulation platform needs to aggregate the Lidar data and thus to lower their original resolution. Following [29,30], the proper spatial resolution for 2D modelling of the urban surface can be set by considering the minimum distance between buildings and one third of the street width as well as the calculation time. For our case study, this distance can be estimated to 5 m. Compared with the DEM data at a 25 m resolution, the use of high resolution LiDAR is a significant improvement, even for the simulations performed at 5 m resolution. Thereupon, both 20 cm and 25 m resolution topographic data are firstly converted to 5 m resolution, and then merged to generate the input data. The merged topographic data of 5 m resolution is presented in Figure 4c, in which the study catchment is represented by a 224 × 85 rectangular grid.

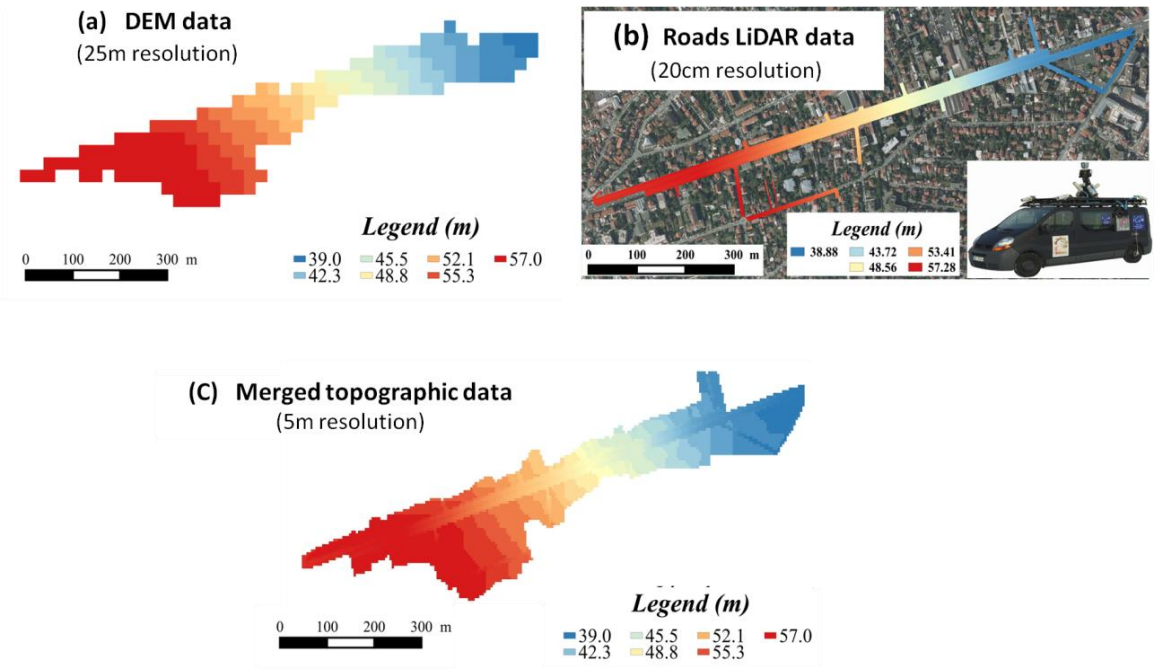

Figure 4. Topographic input data. (a) DEM data of 25m resolution; (b) Roads LiDAR data of 20 cm resolution; (c) Merged topographic input data of 5 m resolution.

2.3.3. Landuse and sewer network

In collaboration with the IGN France, we defined 13 classes of urban land uses which are derived from aerial photos. Besides, the locations of sewer inlets are identified from the GIS and AutoCAD sewer network data. Since sewer inlets should equally be presented in the surface part of the 2D/1D model, the “sewer inlets” are integrated into land use input as a specific type. The vectorial land uses are then transformed into grids using the same resolution as the topographic data. A specific order has to be defined for this transformation. As the “sewer inlets” are considered as the interface between the surface and sewer networks parts, it is undoubted that

the “Sewer inlet” is the first that should be considered, followed by roads, sidewalks, parking, various types of roofs, trees, grass and others. In general, 70% of catchment surfaces are impervious areas, within which the roof areas represent 35% of the total surface. The land use data and sewer network data are presented in Figure 5:

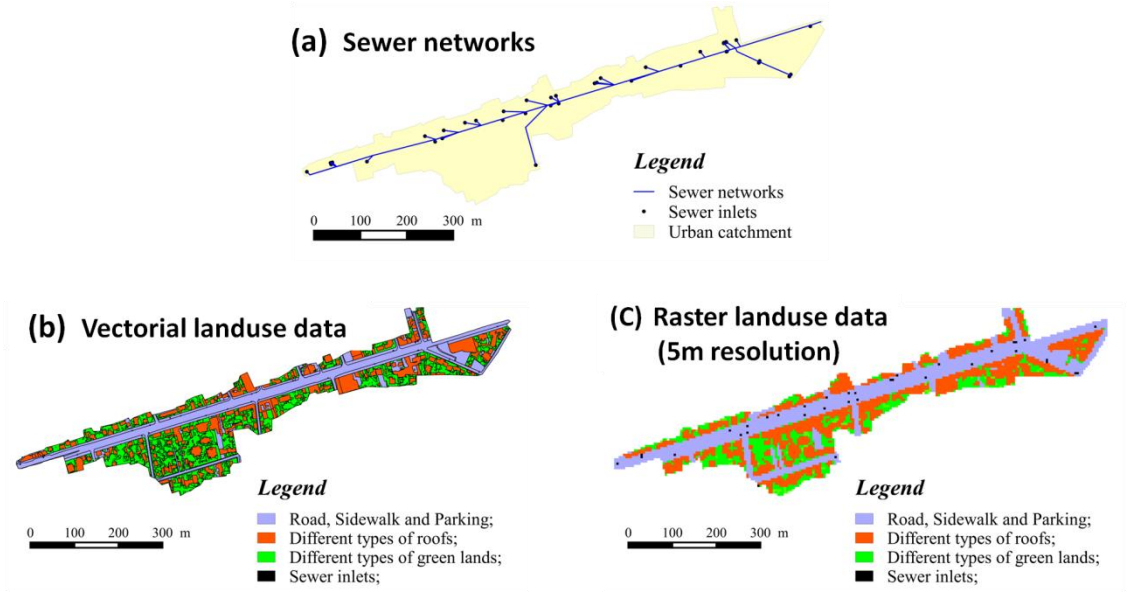

Figure 5. Input data for TRENOE: (a) Separate stormwater sewer networks, (b) Vectorial landuse data; (c) Raster landuse data with 5m resolution.

2.3.4. Urban surface dry stocks

Impervious urban surfaces are represented by two layers in TRENOE: the deposited layer (that can be detached in the form of particles) and the pavement (assumed to be non-detachable). The processes related to water quality modelling occur only in the deposited layer, while the parameters depend on the properties of the associated land use. Additionally, within the framework of the ANR-Trafipollu project, series of road dust samples were collected on the studied area using a 2 m^2 vacuum cleaner [31]. The collected road dust Particle Size Distribution (PSD) was then determined by laboratory monitoring. According to the measurements of dry stock samples over 3 different sites on the urban surface, it is assumed that the finest particles (PM10) are only generated by atmospheric dry deposits on all types of urban surfaces. The total dry stock on roads (coarse + fine particles) was estimated to 10 g/m^2. The mass of the finest part of the road dry deposits which represent the atmospheric dry depositions is then estimated to be 1 g/m^2. Therefore, it is considered that building roof accumulation is equal to the finest deposits on roads, and the chosen initial dry deposits on roofs are 1 g/m^2 in our simulations.

.

2.4. Model evaluation with scenario simulations

Due to time-consuming simulations with the physically-based TRENOE platform (using a computer core of 16 GB RAM, the model runtime is approximately 10 min for a 1-h rainfall event), the model assessment is performed by scenario simulations instead of complete sensitivity analysis. Model configurations are firstly calibrated by a trial and error method comparing with water flow measurements at the sewage outlet. The influences of various factors are then examined by analysing the simulation results using different model configurations, parameter values and input data.

The model performance is evaluated using different objective functions, including the Root Mean Square Deviation (RMSD), the Nash Sutcliffe Efficiency (NSE) criterion [32], and the Mean Relative Standard Deviation (MRSD). Using RMSD and MRSD coefficients, the bias between the simulation results and the continuous measurements could be represented, while the NSE coefficient is a well-known indicator for model performance. With these objective formulations, the accuracy and the variability of model outputs could be evaluated under different conditions.

Several scenario simulations are performed in order to assess (i) the suitability of numerical issues for applying a watershed model for small urban catchment; (ii) the influence of the saturated hydraulic conductivity (Kh) and the Manning's n values; (iii) the benefit of using high-resolution roads LiDAR data; (iv) the benefit of applying detailed land use data; (v) the impact of different choices of the particle size distributions.

2.4.1. Scenario 1: Internal numerical precision of the source code

As with the 2D surface part of TRENOE, TREX is a typical watershed model and usually applied for large areas [1,33]. The model uses the single-precision floating-point format in its source code for reducing computing times. This type of numerical precision has a limited internal representation at 10^{-7}, which means the model can only represent internal values that are greater than 10^{-7} at the end of each time-step. Concerning water volumes, it implies that a volume smaller than 10^{-7} cubic meters cannot be represented or taken into account. However, for the studied small urban catchment (0.12 km^2), we use a spatial resolution at 5 m and the time-step is less than 1 s.
In that case, the water depths are very low and the internal digital precision of the original source code (hereafter TREX) has to be adapted. Moreover, the amount of suspended particles to transfer from one grid point to the other one is far lower for urban water quality applications than for the erosion context. Therefore, scenario simulations of TRENOE are set for testing the suitability of the single-precision or double-precision floating-point format for the small urban catchment modelling, with the limit of the internal value being 10^{-14}. After that, we calibrate the hydrologic

components of the correct model by the trial and error method for the other scenario simulations described below.

.

2.4.2. Scenario 2: The influence of the calibration of typical model parameters

Saturated hydraulic conductivity and Manning's N coefficient are commonly considered as part of the most important parameters for water quantity modelling. The ranges of the parameter values have been extensively studied over the last decades [34–36]. In order to evaluate the impact of the parameter values on the water flow outputs, we perform 3 simulation configurations for every selected rainfall event, within which the parameters of configuration 2 are set to the optimized values, while the parameters of configurations 1 and 3 are set to their upper limits and lower limits, respectively. In Table 3, the parameter values are approximately categorized into two groups. The first represents the "Roads" areas, including roads, sidewalks and parking. The second indicates different types of greenlands, such as trees, gardens and grass. Since the buildings are considered as obstacles to runoffs in the 2D surface model, the parameters of different types of roofs are not discussed

Table 3. Different configurations of saturated hydraulic conductivity (Kh) and Manning's' N coefficient for scenario 2 simulations.

	N-manning		**Kh (m/s)**	
Landuse	Roads, Sidewalks, Parkings.	Trees, Gardens, Grass.	Roads, Sidewalks, Parkings.	Trees, Gardens, Grass.
Upper limits of parameters	0.02	0.05	$1\cdot 10^{-7}$	$1\cdot 10^{-4}$
Calibrated Parameters	0.015	0.03	$1\cdot 10^{-8}$	$1\cdot 10^{-5}$
Lower limits parameters	0.01	0.02	$1\cdot 10^{-10}$	$1\cdot 10^{-7}$

2.4.3. Scenario 3: Influence of the road LiDAR data in comparison with DEM data

Within the framework of the ANR-Trafipollu project, high-resolution topographic data of LiDAR survey are available for roads. The sensitivity of model outputs to the precision of altimetry will be tested, and also the need for costly GIS data will be

assessed. Therefore, 3 typical configurations are tested: (i) directly resampling the DEM data (25 m) to 5 m resolution; (ii) resampling the DTM data (25 m) to 5 m resolution, and then lowering the identified road grid cells by 20 cm; (iii) resampling the road LiDAR data (20 cm) and the DEM data (25 m) to 5 m resolution, then fusing the two types of data together.

2.4.4. Scenario 4: Influence of a fine knowledge of landuse based on ortho-photos

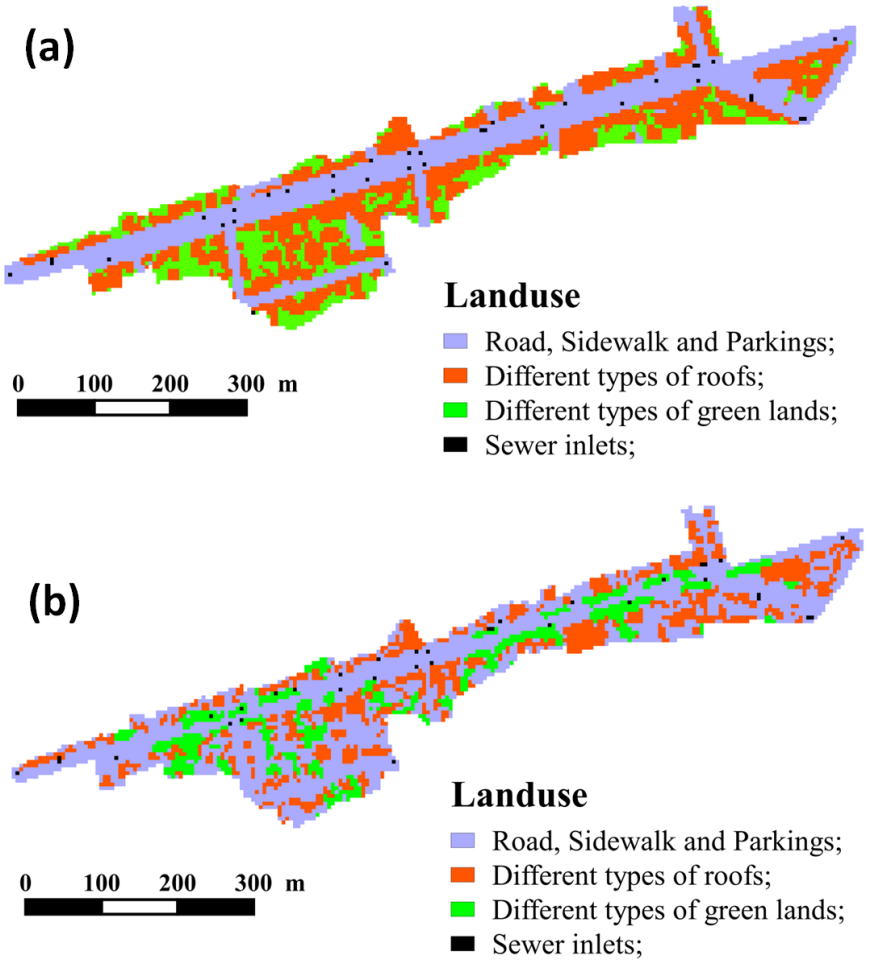

Figure 6. Landuse (LU) input map (5m) converted from different data sources: (a) from the detailed LU information which are derived from ortho photos; (b) from the coarser LU information which are used for urban plannings.

In the current study, we can benefit from detailed land use (LU) data which are derived from ortho-photos. In order to assess the model sensitivity to the fine knowledge of LU, we apply two simulation configurations: the first with detailed LU data derived from ortho-photos, and the second with regularly achieved LU data which contains only public buildings (stations, commercial centres, schools, etc.) and

green-lands, the undefined areas are considered as the roads and parking. These two types of data are illustrated in Figure 6. In general, the surface of urban roofs is largely underestimated with coarser LU information, while the road and parking surfaces are overestimated.

2.4.5. Scenario 5: Sensibility of the water quality module to different Particle Size Distributions (PSD)

For the water quality modelling, several stormwater samplings were performed at the outlet during rainfall events, and suspended solid measurements were then performed in the laboratory. Moreover, a series of road dust samples were collected on the studied urban surfaces using a 2 m^2 vacuum cleaner [31]. This experiment was carried out on 14 October 2014 during dry weather after a dry period of 2 days. The measurements of the deposit samples could be used to calculate the total mass of road dust in the basin (2661 m^2), by supposing that the sediments are uniformly distributed on the road surface. Granulometric analysis was then conducted in the laboratory for evaluating the PSD of the studied samples. Based on the PSD and the total mass of each sample, we could calculate the mass of each particle size class. The mass and the particle size in different wet and dry samples are represented in Figure 7.

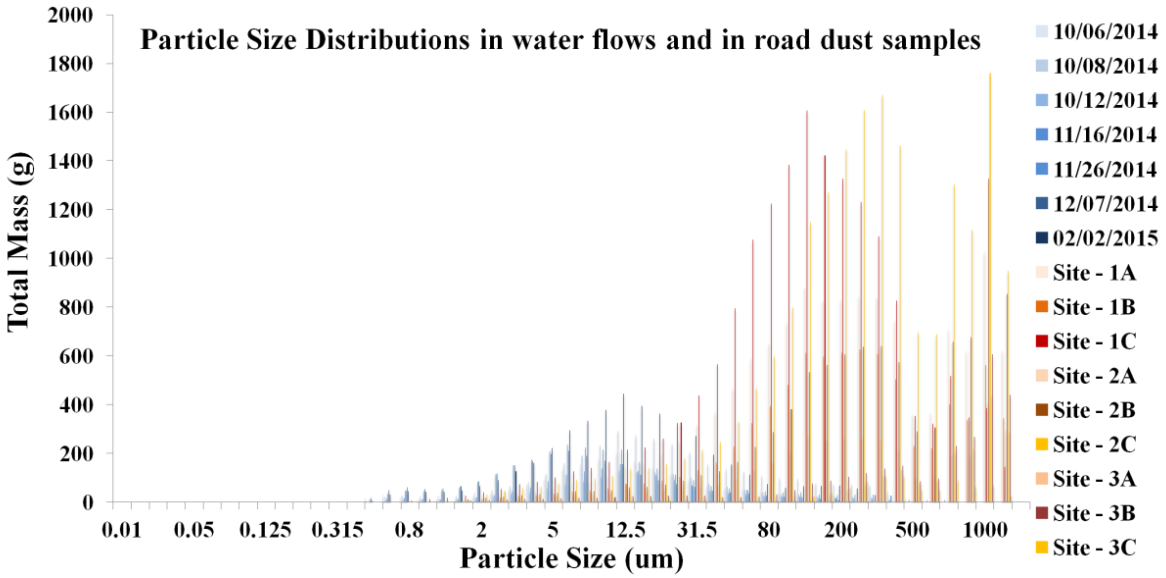

Figure 7. Particle Size Distributions of a stormwater samples (blue bars) and a road dust samples (yellow bars) during a dry weather sampling campaign (14 Oct. 2014).

In Figure 7, we observe that PSD in stormwater samples are quite different from that in road dust samples, where fine particles (<100 µm) are major compositions

(>90%) of Total Suspended Solids (TSS) in stormwater runoffs. Yet, it is contrary to the road dust samples (<10%). This phenomenon is caused by the fact that the finest particles of road dry deposits are transferred to the sewer network during typical rainfall events, whereas the coarser particles remain on the urban surface [37]. Based on these measurements, we tested two configurations for assessing the sensitivity to the characteristics of the road surface sediments (Table 4): (i) 3 particle classes based on dry deposit samples, which can represent all the available particles on the urban surfaces; (ii) 3 particle classes based on stormwater samples, which can only represent the removeable particles of the total dry stocks.

Table 4. Two configurations of different particle size classifications.

Particle Size (um)	Median Diameter (um)	Percentage	Settling velocity (cm/s)
Configuration 1, based on road dry deposit samples			
< 15	7	10%	0.002
15 - 125	70	40%	1.92
> 125	250	50%	1.78
Configuration 2, based on stormwater runoff samples			
< 7	3.5	30%	0.0005
7 - 25	15	40%	0.009
> 25	50	30%	0.1

3. Results and discussions

The results will be presented step by step in order to illustrate the influence of different factors on model outputs. To gain clarity in the following text, figures are only produced for the event of 15 November 2014. The results for all six studied events will be listed in the tables. The Root-Mean- Square-Error (RMSE) coefficient, Nash-Sutcliffe-Efficiency (NSE), and Mean-Root-Square-Deviation coefficient are used to evaluate the model performance. For assessing the model performance of different settings of model structures and input data, the most detailed configuration is

considered as the benchmark reference. In fact, the double precision, the high resolution topographic data, and the detailed land use data are systematically used when one of them is analyzed. By altering different options of model configurations, the influence of different factors on model performance can be evaluated. The results of this research can help practitioners identify the key factors in 2D-1D modelling at the district scale in order to avoid the collection of unnecessary and costly data.

3.1. Scenario 1: Internal numerical precision of the source code

Figure 8 shows the change of the hydrograph in response to the change of digital precision (single-precision or double-precision floating point format) for the rainfall event of 15 November 2014, while the results of all rainfall events are presented in Table 5.

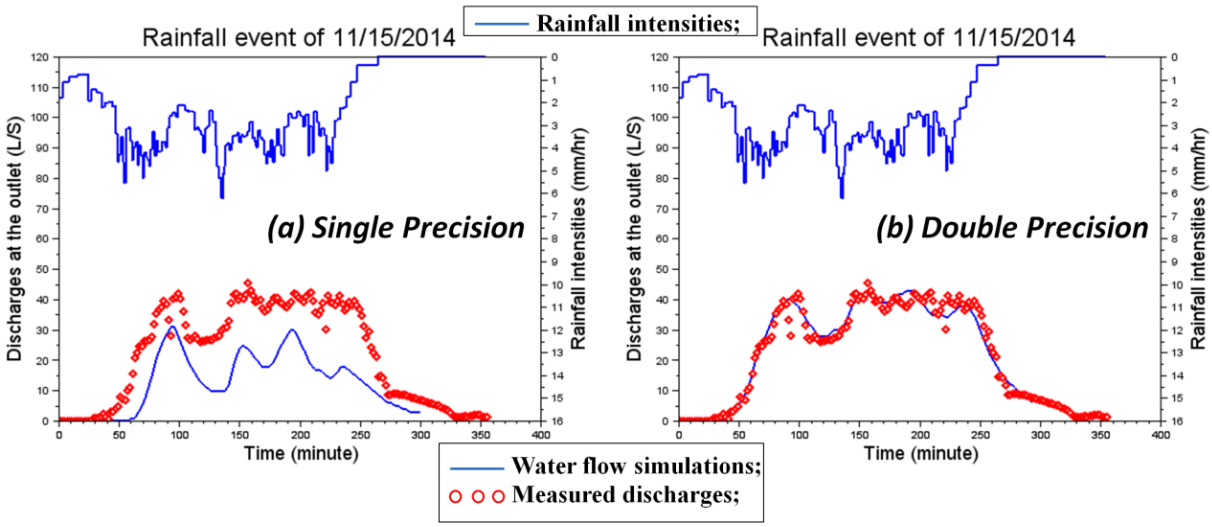

Figure 8. Change of the hydrograph due to the change from (a) single-precision to (b) double-precision floating-point format of the source code. The simulated discharges at the outlet (solid blue line) are compared with the measured data (red circles). Rainfall is plotted on the upper part.

As illustrated in Figure 8 and Table 5, simulations with single-precision floating-point format of the source code do not obtain acceptable results. Moreover, in practice, we have mentioned that, no matter what combinations of parameter values are taken, the dynamics of the simulation outputs are far from that of the measurements. As shown in Figure 8, model outputs with single-precision floating-point format are more sensitive to the change in rainfall intensity. As precipitation in the Paris region usually consists of light rainfall (<10 mm/h), the accumulation of water volume in a grid cell (25 m^2) during a calculation time-step (0.1 s) is sometime

less than 10^{-7} cubic meters, especially at the beginning of the rainfall event. In that case, the volume of water is not represented during these time-steps with the single-precision floating-point format of the source code. While for the double-precision floating-point format of the source code, the internal numerical limit is 10^{-14}, this problem will not arise. In Table 5, the results confirm that the model works well with the double-precision floating-point format of the source code. For these simulations, the distributed water quantity parameters are the "best-fit" parameters and the only change is the numerical precision of the source code. As can been seen in Figure 8, the water balance is not conservative when the numerical precision is not appropriate. Therefore, the first step of urban stormwater modelling is to ensure that the water balance is correct, and the water quantity parameters can be adjusted at a later stage. For the current study, we will use the double-precision floating-point format in further evaluations as presented below.

Table 5. Influence of numerical precision of the source codes on water flow at the outlet of the sewer system.

	NSE		**RMSE**		**MRSD**	
	Double	Single	Double	Single	Double	Single
Oct. 08. 2014	0.88	0.09	5.9	16.9	0.39	0.78
Oct. 12. 2014	0.89	0.41	3.21	7.48	0.54	0.82
Nov. 03. 2014	0.89	0.67	7.74	13.32	0.38	0.64
Nov. 15. 2014	0.97	0.06	2.69	14.7	0.14	0.53
Nov. 26. 2014	0.76	0.14	5.08	9.67	0.59	1.29
Dec. 12. 2014	0.28	-0.16	21.33	27.3	0.27	0.51

3.2. Scenario 2: The influence of the calibration of typical model parameters

As presented in the above section, we test three model configurations by using Kh and surface flow Manning's N value at their (i) upper limit; (ii) calibrated value and (iii) lower limit. The greatest Kh and Manning's N values assume that the surface are more pervious and rough, while the lower limit of these two parameters means that the imperviousness of the urban land uses are much higher with smoother surfaces.

The hydrograms of the event on 15 November 2014 are presented in Figure 9, while the outcomes of all six events are illustrated in Table 6.

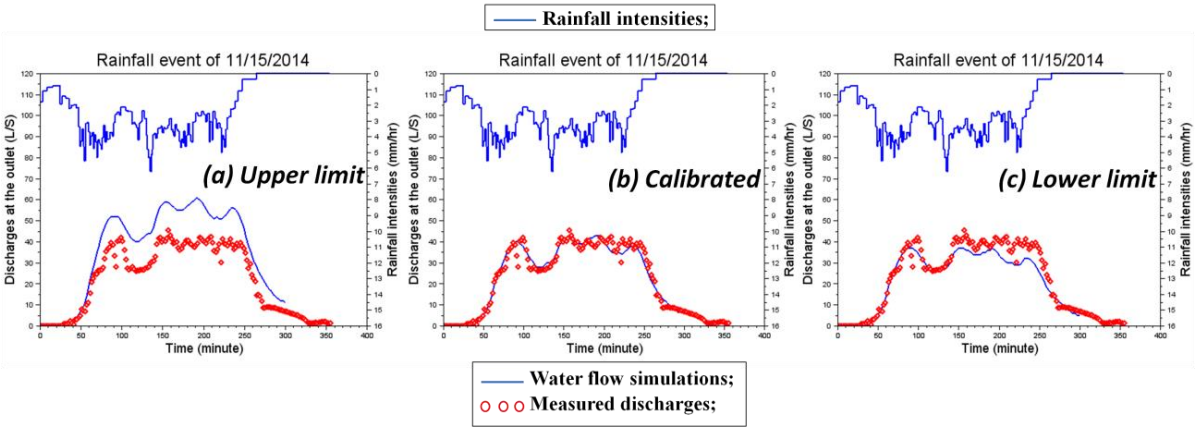

Figure 9. Hydrogram at the outlet of catchment using different values of water flow parameters. For (**a**) simulation using the upper limits of the parameter values; (**b**) simulation using the calibrated parameter values; (**c**) simulation using the lower limit of the parameter values. The simulated discharges at the outlet (solid blue line) are compared with the measured data (red circles). Rainfall is plotted on the upper part.

Table 6. Influences of parameter values on water flow at the outlet of the sewer system.

	NSE			RMSE			MRSD		
	Calibrated	Upper limit	Lower limit	Calibrated	Upper limit	Lower limit	Calibrated	Upper limit	Lower limit
Oct. 08. 2014	0.88	0.79	0.52	5.9	8.83	12.43	0.39	0.45	0.5
Oct. 12. 2014	0.89	0.78	0.33	3.21	5.12	9.43	0.54	0.68	0.72
Nov. 03. 2014	0.89	0.8	0.45	7.74	10.23	17.25	0.38	0.42	0.51
Nov. 15. 2014	0.97	0.9	0.19	2.69	4.67	13.6	0.14	0.18	0.46
Nov. 26. 2014	0.76	0.61	0.52	5.08	6.21	13.18	0.59	0.62	0.66
Dec. 12. 2014	0.28	0.15	0.16	21.33	23.12	23.54	0.27	0.31	0.32

Compared to the results of Scenario 1, simulations of Scenario 2 suggest that the impacts of parameters (Manning's N, saturated hydraulic conductivity (Kh)) on model outputs are less significant than that of the numerical precision in source codes. The dynamics of simulated water flow and the model performance remain acceptable under different parameter configurations, particularly for the simulations using the lower limit of the parameter values. The physical properties of the two parameters can explain these results. The Manning's equation is used to calculate the surface runoff velocity, since the studied urban catchment is relatively small (0.12 km^2) and the flow path from each grid cell to its nearest sewer inlet is short (less than 100 m). Surface runoffs can always rapidly enter the neighbouring sewer inlets regardless of the Manning's N values. Besides, Kh is the essential parameter in the Green-Ampt model for infiltration modelling. It influences the total quantity of water entering the sewer system, but it has limited impact on flow dynamics. As shown in Table 6, the simulated configurations for all six studied rainfall events display comparable results.

3.3. Scenario 3: Influence of the road LiDAR data in comparison with DEM data

In order to evaluate the impact of the merged high-resolution road LiDAR data, three different model configurations are established with different topographic input maps: (i) directly resampling the DEM data (25 m) to 5 m resolution; (ii) resampling the DEM data (25 m) to 5 m resolution, and then lowering the identified road grid cells by 20 cm; (iii) resampling the road LiDAR data (20 cm) and the DEM data (25 m) to 5 m resolution, then fusing the two types of data together. The simulation results are presented in Figure 10 and Table 7.

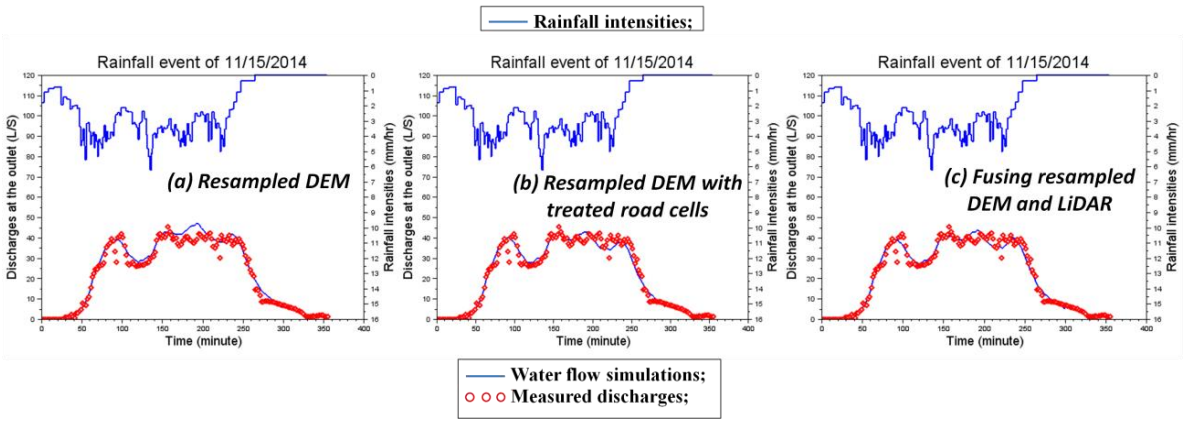

Figure 10. Hydrographs at the outlet of catchment using different topographic input maps. For (a) directly resampling the DEM data (25m) to 5m resolution; (b) resampling the DEM data (25m) to 5m resolution, and then lowing the identified road grid cells by 20cm; (c) resampling the road LiDAR data (20cm) and the DEM data

(25m) to 5m resolution, then fusing the two types of data together. The simulated discharges at the outlet (solid blue line) are compared with the measured data (red circles). Rainfall is plotted on the upper part.

Table 7. Influence of high-resolution road topographic data on water flow at the outlet of the sewer system.

	NSE			**RMSE**			**MRSD**		
	Fusing resampled DEM and LiDAR	Resampled DEM	Resampled DEM with dug roads	Fusing resampled DEM and LiDAR	Resampled DEM	Resampled DEM with dug roads	Fusing resampled DEM and LiDAR	Resampled DEM	Resampled DEM with dug roads
Oct. 08. 2014	0.88	0.85	0.87	5.9	6.14	6.04	0.39	0.42	0.4
Oct. 12. 2014	0.89	0.8	0.83	3.21	4.01	3.87	0.54	0.6	0.58
Nov. 03. 2014	0.89	0.78	0.8	7.74	9.04	8.55	0.38	0.49	0.44
Nov. 15. 2014	0.97	0.9	0.89	2.69	2.94	2.78	0.14	0.18	0.15
Nov. 26. 2014	0.76	0.7	0.71	5.08	6.12	5.66	0.59	0.65	0.62
Dec. 12. 2014	0.28	0.25	0.26	21.33	23.01	22.11	0.27	0.33	0.3

As can be seen in Figure 10, it seems that the high resolution data on the road altimetry has a weak influence on model outputs. In Table 7, the results confirm this observation for all six studied events, as model performance remains acceptable under different rainfall conditions. Moreover, simulations with DEM data with dug road appear to be slightly better than that only with DEM data, and they are similar in terms of performance to the model outputs with merged road LiDAR data and DEM data.

Since the major benefit of using high-resolution LiDAR data is to ensure that water flows in appropriate directions, the present study indicates that the flow directions in

the TRENOE model are generally well represented even with coarser resolution topographic data. Therefore, we can conclude that using high resolution altimetry data is not a key factor for water flow simulations at the outlet of an urban catchment. Considering only basic topographic data with lower streets is sufficient for simulations

.

3.4. Scenario 4: Influence of a fine knowledge of landuse based on ortho-photos

In collaboration with the French National Institute of Geography (IGN), detailed information on urban land use (LU) could be obtained. The vectorial land use data derived from the ortho photos can have a very high resolution even at the scale of centimetres, but transforming land use data into a reliable map of land uses is not straightforward. Because the urban environment is constituted of varied characteristics that have a typical size of less than 5 m (natural soil surrounding the trees next to the road, courtyards, etc.), and the analyses of the ortho photos are three dimensional. For example, the canopy has an extent on aerial photography which is not the land use at the ground level (in an urban catchment, this ground will be mainly pavement, for example). Therefore, when aggregating the land use classes at the scale of the mesh grid, it is very important to hierarchise the different land use types. The priority is based on the effect of the land use on the water quantity and quality. A specific priority between land uses has been defined for this transformation. In the current study, the priority land use is “sewer inlets”, followed by roads, sidewalks, parking lots, various types of roofs, trees, grass and others. As for the coarser LU information, the vectorial LU source data contains only public buildings and greenlands, and the undefined areas are considered as impermeable roads and parking areas. We followed the same priority order as mentioned before to generate LU input maps (5 m). The results of water flow simulation at the outlet of catchments using these two different LU input maps are presented in Figure 11 and Table 8.

As shown in Figure 11, the simulation outputs with LU input map converted from coarser LU information do not match the measurements. In fact, the simulated water balance is far less than the observed one and the simulated hydrographs seem to be insensitive to the variations in rainfall intensity. Since private buildings are not included in the low resolution LU source data, the infiltration is overestimated and the longer pathways of surface runoff result in longer time of concentration compared with the water from roofs.

On the other hand, the results in Table 8 indicate poor model performance with the input LU map converted from coarser LU information. This finding confirms that the land use information is an essential input data for this kind of urban stormwater 2D/1D modelling.

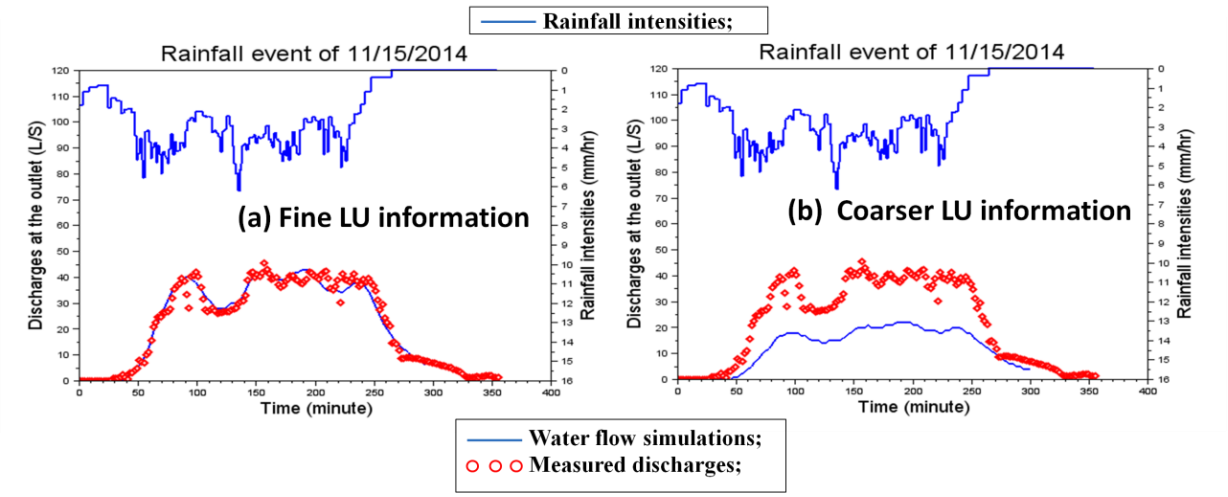

Figure 11. Hydrogram at the outlet of catchment using different landuse (LU) input maps. For (a) LU input map (5m) converted from fine LU information; (b) LU input map (5m) converted from coarser LU information. The simulated discharges at the outlet (solid blue line) are compared with the measured data (red circles). Rainfall is plotted on the upper part.

Table 8. Influence of fine landuse (LU) information on water flow at the outlet of the sewer system.

	NSE		RMSE		MRSD	
	Fine LU information	Coarser LU information	Fine LU information	Coarser LU information	Fine LU information	Coarser LU information
Oct. 08. 2014	0.88	0.16	5.9	16.14	0.39	0.65
Oct. 12. 2014	0.89	0.21	3.21	12.37	0.54	0.88
Nov. 03. 2014	0.89	0.14	7.74	21.2	0.38	0.67
Nov. 15. 2014	0.97	0.04	2.69	14.9	0.14	0.5
Nov. 26. 2014	0.76	0.07	5.08	19.67	0.59	0.87
Dec. 12. 2014	0.28	-0.5	21.33	32.1	0.27	0.42

As shown in Figure 11, the simulation outputs with LU input map converted from coarser LU information do not match the measurements. In fact, the simulated water balance is far less than the observed one and the simulated hydrogram seems insensitive to the variation of rainfall intensities. Since the private buildings are not included in the low resolution LU source data, the infiltration is overestimated and the longer pathways of surface runoff slows down the time of concentration compared with the water from roofs.

On the other hand, the results in Table. 9 indicate poor model performance with the input LU map converted from coarser LU information. This finding confirms that the landuse information is an essential input data for this kind of urban stormwater 2D/1D modelling.

3.5. Scenario 5: Sensibility of the water quality module to different Particle Size Distributions (PSD)

Since hydrological modelling is extensively discussed and calibrated in the above sections, we can now work on water quality simulations. As this is the first time that the USLE equation is adapted to an urban context, we fixed all the parameters to their maximum values which are equal to 1 in our first tests, including the rainfall erodibility factor (R), the soil erodibility factor (K), the topographic factors (L, S) and the cropping management factors (C, P). Because the PSD of stormwater samples are quite different from that of road dust samples (Figure 7), we analyse the impact of different PSD values on water quality simulations in order to know which choice is appropriate for the current 2D/1D model. The simulation results are presented in Figure 12.

According to Figure 12, we can note that the simulations of Total Suspended Solids (TSS) concentrations vary across the configurations of the three classes of particles derived from PSD of stormwater samples (3.5 µm, 15 µm, 50 µm) and that derived from PSD of dry stock samples (7 µm, 70 µm, 250 µm). Since coarser particles have greater settling velocities, simulated TSS concentrations using three classes of fine particles are much higher than the other ones. Nevertheless, as with the classification based on fine particles or coarser particles, the water quality simulations are unsatisfactory with the current version of the TRENOE platform. It cannot reproduce the first peak of TSS concentration at the beginning of the rainfall event.

Indeed, the current code of TRENOE platform uses a modified form of Universal Soil Loss Equation (USLE) for simulating sediment erosion, where the pollutant wash-off from a given land use is represented as a mass rate of particle removal from

the bottom boundary over time. Considering that the USLE method is originally designed to predict soil losses caused by runoff in agricultural areas, several adaptations are certainly needed to use it for urban areas, such as the alterations of USLE parameters according to different criterions, the definition of the appropriate initial dry deposits corresponding to various land uses, etc. Moreover, it is important to note that TRENOE does not include any detachment processes driven by raindrops, and the sediment erosion is only calculated from water flow detachment. Therefore, the actual version of TRENOE cannot simulate the first peak of TSS concentration when the water flow is still weak at the first part of the rainfall event. In agreement with the recent findings of [37,38] that the raindrop impacts are essential for wash off processes in urban areas, the raindrop-driven detachment should be taken into account for further studies.

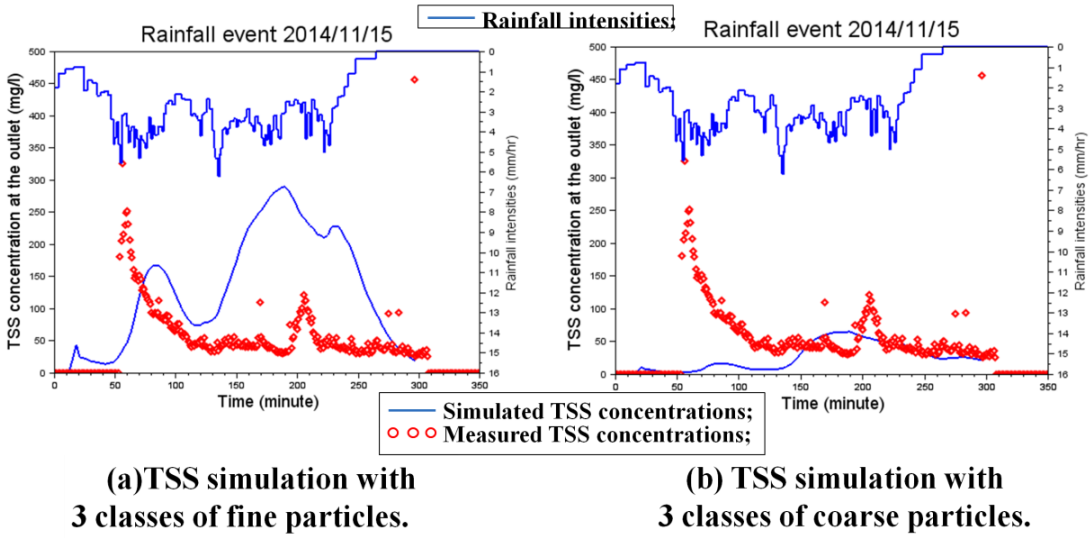

(a)TSS simulation with 3 classes of fine particles.

(b) TSS simulation with 3 classes of coarse particles.

Figure 12. Water quality simulations with different Particle Size Distributions. For (a) 3 classes of fine particles derived from PSD of stormwater samples: 3.5um, 15um, 50um; (b) 3 classes of coarse particles derived from PSD of dry stock samples: 7um, 70um, 250um. The simulated TSS concentrations at the outlet (solid blue line) are compared with the measured data (red circles). Rainfall is plotted on the upper part.

4. Conclusion and perspectives

In this study, we describe an attempt to develop an integrated 2D/1D modelling platform “TRENOE”, as well as the necessary modelling assumptions and adaptations to simulate both quantitative and qualitative hydrological processes for urban areas. The physically-based combined modelling system is established for water flow and water quality modelling by coupling urban surface and sewer networks.

Within the framework of the ANR (French National Agency for Research) Trafipollu project, TRENOE platform is applied to a small urban catchment near Paris (Le

Perreux sur Marne, 0.12 km^2). In collaboration with other partners within the project, high-resolution topographic data from LiDAR survey, detailed land use data derived from ortho-photos, and Particle Size Distributions (PSD) are obtained for the studied urban catchment. Benefitting from these elaborate sources of input data, this article tests the relative influence of various factors on the outputs of the model, particularly the influence of numerical precision on source code, the influence of common parameters on water quality, and the influence of having precise knowledge of the topography (more or less known with great precision) and land uses. By analysing the impacts of these internal and external factors on model outputs, the main objective of this work is hence not only to identify which factors are significant for urban 2D/1D stormwater modelling, because all of them are, but mainly to underline the necessary model configurations for appropriate simulations with limited availability of data sources and human modelling and simulation capabilities.

The numerical precision of source codes and the precise knowledge of land uses are proved to be the most influential factors in the model outputs, whereas the resolution of road topographic data and the model parameters have less impact. These findings can assist urban stormwater managers in better organising their efforts in data surveys to improve model accuracy from necessary field investigations. Besides, the present results emphasise the importance of considering the parameters' physical significance in the model calibration. In cases where the dynamics of model outputs greatly differ from measurements and cannot be explained by the effects of parameters, there may be internal issues with the model or problems with input data. Of course, these results need to be confirmed by applying this modelling approach to other urban catchments with different shapes and slopes.

Concerning water quality modelling, the present work fails to correctly reproduce the concentration of Total-Suspended-Solids (TSS) at the catchment outlet. However, the importance of taking into account the appropriate particle classification is highlighted. Using only empirical USLE equations is certainly responsible for the poor performance of the sediment erosion modelling. Taking into account the direct detachment by rain drops is essential for improving urban stormwater quality modelling. Testing the robustness of our main observations of an urban catchment showing different physical characteristics (larger, steeper, with more green spaces etc.) would also represent an interesting perspective in the future.

Acknowledgments: The research work of Ph.D. student Yi Hong was financed by ANR-Trafipollu project (ANR-12-VBDU-0002) and Ecole des Ponts ParisTech. Firstly, the authors would like to thank OPUR (Observatoire des Polluants Urbains en Ile-de-France) for providing the platform for changing idears and elaborating collaborations with diffrent researchers from various institutions. The authors would also like to thank B. Béchet (IFSTTAR), B. Soleilhan (IGN) and V. Bousquet (IGN-Conseil) for

providing invaluable measurements and GIS data. We also want to give a special thanks to the experimental team of ANR Trafipollu project for all collected necessary for this work, in particular David Ramier (CEREMA), Mohamed Saad (LEESU) and Philippe Dubois (LEESU).

Author Contributions: This study was designed by Yi Hong, Céline Bonhomme and Ghassan Chebbo. The manuscript was prepared by Yi Hong and revised by Céline Bonhomme and Ghassan Chebbo.

Conflicts of Interest: The authors declare no conflict of interest.

References

1. Walsh, C.J.; Fletcher, T.D.; Ladson, A.R. Stream restoration in urban catchments through redesigning stormwater systems: Looking to the catchment to save the stream. *J. N. Am. Benthol. Soc.* **2005**, *24*, 690–705.
2. Deffontis, S.; Breton, A.; Vialle, C.; Montréjaud-Vignoles, M.; Vignoles, C.; Sablayrolles, C. Impact of dry weather discharges on annual pollution from a separate storm sewer in Toulouse, France. *Sci. Total Environ.* **2013**, *452–453*, 394–403.
3. Bressy, A.; Gromaire, M.-C.; Lorgeoux, C.; Saad, M.; Leroy, F.; Chebbo, G. Efficiency of source control systems for reducing runoff pollutant loads: Feedback on experimental catchments within Paris conurbation. *Water Res.* **2014**, *57*, 234–246.
4. Hatt, B.E.; Fletcher, T.D.; Walsh, C.J.; Taylor, S.L. The influence of urban density and drainage infrastructure on the concentrations and loads of pollutants in small streams. *Environ. Manag.* **2004**, *34*, 112–124.
5. Clark, S.; Pitt, R.; Burian, S.; Field, R.; Fan, E.; Heaney, J.; Wright, L. *Annotated Bibliography of Urban Wet Weather Flow Literature from 1996 through 2006*; Environmental Engineering Program: Middleton, PA, USA, 2007.
6. Duncan, H. *A Review of Urban Stormwater Quality Processes*; Report 95/9 for Cooperative Research Centre for Catchment Hydrology: Clayton, Australia, 1995.
7. Vaze, J.; Chiew, F.H.S. Comparative evaluation of urban storm water quality models. *Water Resour. Res.* **2003**, *39*, 1280.
8. Rossman, L.A. *Storm Water Management Model User's Manual Version 5.0*; National Risk Management Research and Development, U.S. Environmental Protection Agency: Cincinnati, OH, USA, 2010.

9. Wong, T.H.F.; Fletcher, T.D.; Duncan, H.P.; Coleman, J.R.; Jenkins, G.A. *A Model for Urban Stormwater Improvement: Conceptualization*; American Society of Civil Engineers: Portland, OR, USA, 2002; pp. 1–14.

10. Elliott, A.H.; Trowsdale, S.A. A review of models for low impact urban stormwater drainage. *Environ. Model. Softw.* **2007**, *22*, 394–405.

11. Sartor, J.D.; Boyd, G.B.; Agardy, F.J. Water pollution aspects of street surface contaminants. *J. Water Pollut. Control Fed.* **1974**, *46*, 458–467.

12. Bonhomme, C.; Petrucci, G. Spatial representation in semi-distributed modelling of water quantity and quality. In Proceedings of the 13th International Conference on Urban Drainage, Kuching, Malaysia, 7–11 September 2014.

13. Kanso, A. Evaluation des Modeles de Calcul des Flux Polluants des Rejets Urbains par Temps de Pluie. Apport de L'Approche Bayesienne. Ph.D. Thesis, Ecole Nationale des Ponts et Chaussées, Champs-sur-Marne, France, 22 September 2004.

14. Sage, J.; Bonhomme, C.; Al Ali, S.; Gromaire, M.-C. Performance assessment of a commonly used "accumulation and wash-off" model from long-term continuous road runoff turbidity measurements. *Water Res.* **2015**, *78*, 47–59.

15. Bach, P.M.; Rauch, W.; Mikkelsen, P.S.; McCarthy, D.T.; Deletic, A. A critical review of integrated urban water modelling—Urban drainage and beyond. *Environ. Model. Softw.* **2014**, *54*, 88–107.

16. Vojinovic, Z.; Tutulic, D. On the use of 1D and coupled 1D-2D modelling approaches for assessment of flood damage in urban areas. *Urban Water J.* **2009**, *6*, 183–199.

17. Chen, A.S.; Djordjevic, S.; Leandro, J.; Savic, D. The urban inundation model with bidirectional flow interaction between 2D overland surface and 1D sewer networks. In Proceedings of the NOVATECH 2007—Sixth International Conference on Sustainable Techniques and Strategies in Urban Water Management, Lyon, Rhone-Alpes, France, 25–28 June 2007; pp. 465–472.

18. Djordjević, S.; Prodanović, D.; Maksimović, C.; Ivetić, M.; Savić, D. SIPSON—Simulation of interaction between pipe flow and surface overland flow in networks. *Water Sci. Technol.* **2005**, *52*, 275–283.

19. Kidmose, J.; Troldborg, L.; Refsgaard, J.C.; Bischoff, N. Coupling of a distributed hydrological model with an urban storm water model for impact analysis of forced infiltration. *J. Hydrol.* **2015**, *525*, 506–520.

20. Domingo, N.D.S.; Refsgaard, A.; Mark, O.; Paludan, B. Flood analysis in mixed-urban areas reflecting interactions with the complete water cycle through coupled hydrologic-hydraulic modelling. *Water Sci. Technol.* **2010**, *62*, 1386–1392.

21. DHI MIKE by DHI Software. Reference Manuals for MIKE FLOOD. 2008. Available online: https://www.mikepoweredbydhi.com/products/mike-flood (accessed on 19 December 2016).

22. Innovyze Ltd. InfoWorks 2D-Collection Systems Technical Review. 2011. Available online: http://www.innovyze.com/products/infoworks_cs/infoworks_2d.aspx (accessed on 19 December 2016).

23. McMichael, C.E.; Hope, A.S.; Loaiciga, H.A. Distributed hydrological modelling in California semi-arid shrublands: MIKE SHE model calibration and uncertainty estimation. *J. Hydrol.* **2006**, *317*, 307–324.

24. Thompson, J.R.; Sørenson, H.R.; Gavin, H.; Refsgaard, A. Application of the coupled MIKE SHE/MIKE 11 modelling system to a lowland wet grassland in southeast England. *J. Hydrol.* **2004**, *293*, 151–179.

25. Velleux, M.L. Spatially Distributed Model to Assess Watershed Contaminant Transport and Fate. Ph.D. Thesis, Colorado State University, Fort Collins, CO, USA, 2005.

26. Velleux, M.L.; England, J.F.; Julien, P.Y. TREX: Spatially distributed model to assess watershed contaminant transport and fate. *Sci. Total Environ.* **2008**, *404*, 113–128.

27. Lhomme, J.; Bouvier, C.; Perrin, J.-L. Applying a GIS-based geomorphological routing model in urban catchments. *J. Hydrol.* **2004**, *299*, 203–216.

28. Cheng, N.-S. Simplified settling velocity formula for sediment particle. *J. Hydraul. Eng.* **1997**, *123*, 149–152.

29. Gallegos, H.A.; Schubert, J.E.; Sanders, B.F. Two-dimensional, high-resolution modeling of urban dam-break flooding: A case study of Baldwin Hills, California. *Adv. Water Resour.* **2009**, *32*, 1323–1335.

30. Fewtrell, T.J.; Duncan, A.; Sampson, C.C.; Neal, J.C.; Bates, P.D. Benchmarking urban flood models of varying complexity and scale using high resolution terrestrial LiDAR data. *Phys. Chem. Earth ABC* **2011**, *36*, 281–291.

31. Bechet, B.; Bonhomme, C.; Lamprea, K.; Campos, E.; Jean-soro, L.; Dubois, P.; Lherm, D. Towards a modeling of pollutant flux at local scale—Chemical analysis and micro-characterization of road dusts. Presented at the 12th Urban Environment Symposium, Oslo, Norway, 1–3 June 2015.

32. Nash, J.E.; Sutcliffe, J.V. River flow forecasting through conceptual models part I—A discussion of principles. *J. Hydrol.* **1970**, *10*, 282–290.

33. England, J.F.; Julien, P.Y.; Velleux, M.L. Physically-based extreme flood frequency with stochastic storm transposition and paleoflood data on large watersheds. *J. Hydrol.* **2014**, *510*, 228–245.

34. Ayvaz, M.T. A linked simulation–optimization model for simultaneously estimating the Manning's surface roughness values and their parameter structures in shallow water flows. *J. Hydrol.* **2013**, *500*, 183–199.

35. Butler, T.; Graham, L.; Estep, D.; Dawson, C.; Westerink, J.J. Definition and solution of a stochastic inverse problem for the Manning's n parameter field in hydrodynamic models. *Adv. Water Resour.* **2015**, *78*, 60–79.

36. Coustau, M.; Rousset-Regimbeau, F.; Thirel, G.; Habets, F.; Janet, B.; Martin, E.; de Saint-Aubin, C.; Soubeyroux, J.-M. Impact of improved meteorological forcing, profile of soil hydraulic conductivity and data assimilation on an operational Hydrological Ensemble Forecast System over France. *J. Hydrol.* **2015**, *525*, 781–792.

37. Hong, Y.; Bonhomme, C.; Le, M.-H.; Chebbo, G. A new approach of monitoring and physically-based modelling to investigate urban wash-off process on a road catchment near Paris. *Water Res.* **2016**, *102*, 96–108.

38. Hong, Y.; Bonhomme, C.; Le, M.-H.; Chebbo, G. New insights into the urban washoff process with detailed physical modelling. *Sci. Total Environ.* **2016**, *573*, 924–936.

Chapitre 8. Are high-resolution topographic and landuse data really necessary for urban 2D-surface and 1D-sewer modelling ?

Yi Hong[1], Celine Bonhomme[1], Bahman Soheilian[2], Ghassan Chebbo[1,3]

[1]LEESU, MA 102, École des Ponts, AgroParisTech, UPEC, UPE, Champs-sur-Marne, France, 6-8 Avenue Blaise Pascal, 77455 Champs-sur- Marne cedex 2, France.

[2] Laboratoire MATIS, SRIG, 73 Avenue de Paris, 94165 Saint-Mande Cedex. France.

[3] Université Libanaise, faculté de génie, campus rafic hariri, Hadat, Lebanon

*(Article soumis dans le journal "**Water Science & Technologie**")*

Abstract

Remote sensing data is increasingly used in urban stormwater modelling. However, the collection of unnecessary and costly data may cause wastes of the experimental resources. In this context, this paper describes a new approach to assess the advantages of using high-resolution LiDAR data and detailed landuse data for urban 2D/1D stormwater modelling. The physically-based TREX model (Velleux, England, et al., 2008) and the conceptual CANOE model (Lhomme, Bouvier, et al., 2004) are integrated in TRENOE platform. The modelling approach is applied to a small urban catchment near Paris (Le Perreux sur Marne, 0.12 km²) over six studied rainfall events. According to the results, the detailed landuse information is a crucial factor for accurate simulations, but using the very high resolution altimetry

data is not equally significant for the water flow simulations at sewage outlet. Finally, we suggest that the "proper" modelling approach should be developed with "adequate" input data, depending on different management/research objectives. Testing the performance of more efficient modelling tools with more economical remote sensing technologies would represent an interesting perspective in the future.

Keywords

2D/1D modelling; detailed urban landuse; high-resolution LiDAR data; urban stormwater modelling; TRENOE platform;

Introduction

Over the past ten years, the increasing availability of distributed remote sensing data has led to a sudden shift of hydrological modelling from a data-sparse to a data-rich research (Di Baldassarre and Uhlenbrook, 2012; Bates, 2012). For instance, high-resolution topographic data and high resolution multi-view aerial images are accessible by using airborne laser altimetry of LiDAR (Light Detection and Ranging), flood extent maps are achievable by using satellites Synthetic Aperture Radar (SAR), accurate information on landuse is available by analyzing digital ortho-photos. Such new data sources allowed a significant breakthrough in urban spatially distributed modelling (Fewtrell, Bates, et al., 2008; Gallegos, Schubert, et al., 2009; Horritt, Di Baldassarre, et al., 2007).

Due to the high heterogeneity of urban surfaces, various city objects such as roads and buildings are hardly specified in urban hydrological models. Consequently, researchers often argue that more detailed remote sensing data should be considered for improving the accuracy of the simulation results (Fletcher, Andrieu, et al., 2013; Salvadore, Bronders, et al., 2015). Nevertheless, the acquisition of such data usually requires expensive ad hoc instruments, ample data storage capacity and post-treatments analysis. Therefore, the efficiency of using highly detailed remote

sensing data for common practices of urban hydrological modelling need to be discussed.

In order to support urban infrastructure design and to control urban non-point source pollutions, the integrated modelling of two-dimensional (2D) surface runoff and one-dimensional (1D) urban sewer network has received growing attention in recent years. Several research models (Djordjević, Prodanović, et al., 2005; Kidmose, Troldborg, et al., 2015; Sto Domingo, Refsgaard, et al., 2010; Vojinovic and Tutulic, 2009) and commercial tools (Mike-FLOOD,DHI, 2008; InfoWorks CS, Innovyze Ltd, 2011) have been developed and applied for various case studies. However, current applications of urban 2D/1D models focus on applying increasingly detailed remote sensing data (Di Baldassarre and Uhlenbrook, 2012; Bates, 2012). Yet few studies have attempted to quantify the gains made by using these high-resolution data compared to only using traditional low-cost data sources (for example, low-resolution topographic data and coarse landuse information). Such work is crucial for recognizing the real needs of collecting remote sensing data for improving urban stormwater modelling.

In this study, an urban 2D-surface and 1D-sewer model TRENOE is applied to a small urban catchment near Paris (Le Perreux sur Marne, Val de Marne, France), in order to assess the influence of high-resolution topographic data and detailed landuse information on model performance. The physically-based TREX model (Velleux, England, et al., 2008) and the conceptual CANOE model (Lhomme, Bouvier, et al., 2004) are integrated in TRENOE platform. In this platform, the building roofs are simulated separately from the surface module and represented as virtual "sub-basins" in the sewer module. This paper provides for the first time a discussion on the economical use of the detailed GIS (Geographic Information System) information for urban 2D/1D modelling.

Materials and methods

Model description

The physically-based 2D TREX model (Velleux, England, et al., 2008), the 1D pipe routing and sub-basin components of the CANOE model (Lhomme, Bouvier, et al., 2004) are integrated in the TRENOE platform. As for the land-phase hydrology, TRENOE uses the diffusive wave approximation of Shallow-Water equations (SW) for surface runoff modelling, the Green and Ampt (1911) method for infiltration calculations and the canopy storage for interception estimations. An explicit finite-difference scheme (Euler's method) is applied for numerical solution. Otherwise, the building roofs are represented separately from the 2D surface model. Since the real elevation of roofs are generally not described in Digital Terrain Model (DTM) data for urban areas, a realistic adaptation consists in raising the building elevations above the land surface at the step of input data pre-treatment. Besides, as most roofs are directly connected to the sewer network in the studied catchment, the grid-cells of roofs which are linked to the same sewer node (the nearest) are assembled as virtual sub-basins in the CANOE model. The areas of these sub-basins are equal to the total area of the connected roof cells. Non-linear reservoir method is then applied to simulate the rainfall - runoff relations for each conceptual sub-basin. These sewer nodes are the connecting points between the 2D surface module and the 1D network module in TRENOE platform, called "Junction nodes". At each time-step, TRENOE removes water from the grid-cells of "manholes" and simultaneously makes it enter into the corresponding "junction nodes". Additionally, flow routing process in the sewer networks is computed by the 1D kinematic wave approximation of the Shallow Water equations and solved by an implicit finite-difference scheme (six steps Preisman method). The model scheme is illustrated in Fig. 1.

Study site

The study site is located in the eastern suburb of Paris (Le Perreux sur Marne, Val de Marne, France). This area is a typical residential zone in the Paris region, characterized by a busy main street in the Eastern Paris (more than 30,000 vehicles per day). The total area of this catchment is 12 ha, about 70% of the surface is impervious, and the roofs represent about 35% of the entire catchment. The western

section has a higher incline than the eastern side, with an average slope of less than 2% (Fig. 2).

The stormwater sewer system consists of 1156 metres major pipes (vertical ellipse, 2.3m × 1.3m) along the main street, and nearly 1000 metres minor pipes (circular, 0.3m × 0.3m) used to connect manholes to the major pipes. In total, there are 35 manholes in the studied catchment. The sewage outlet is located at the North-Eastern edge of the presented sewer network, where the flow is continuously monitored by a Nivus Flowmeter with 2 minutes time interval.

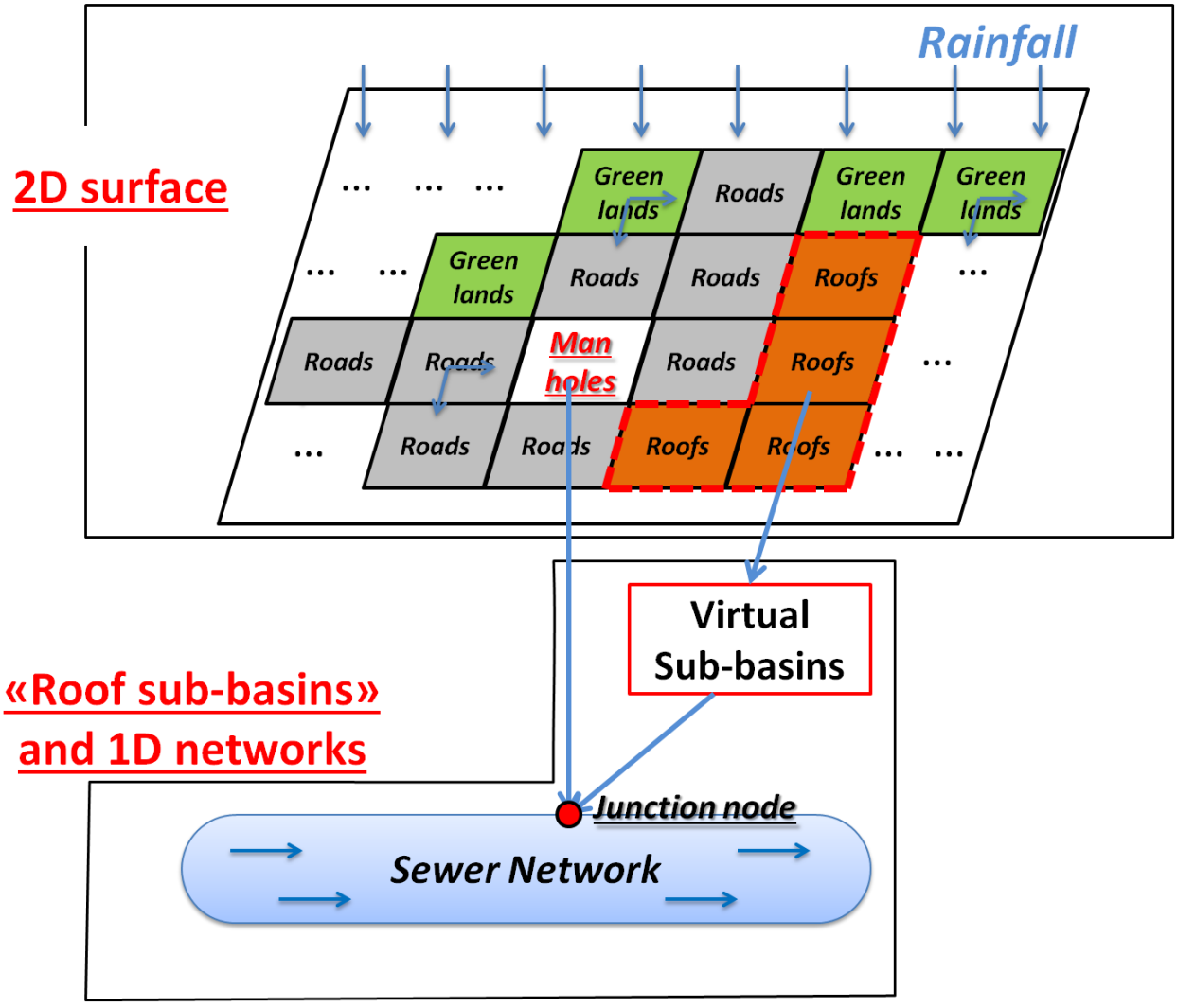

Fig. 1. The scheme of the 2D-surface and 1D-network modelling system TRENOE.

.

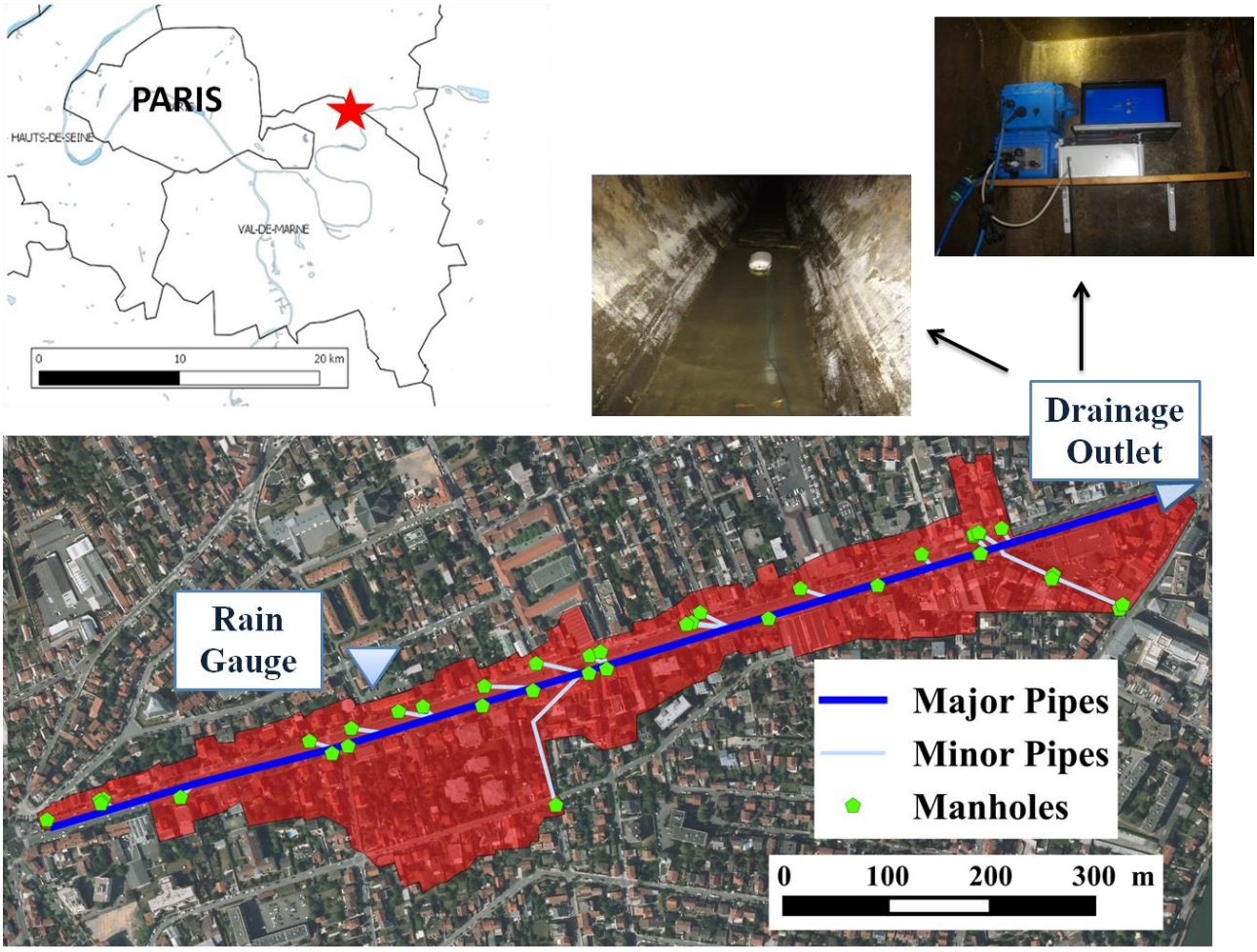

Fig. 2, Study area at Eastern Paris (Le Perreux sur Marne), and instrumental settings in the drainage network. Flow monitoring devices at the drainage outlet is also presented.

Rainfall event data

A tipping-bucket rain gauge is installed on the roof of a building close to the urban catchment (see Fig 2). The rain gauge has a resolution of 0.1 mm. As the study area is quite small, rainfall is considered as homogeneous within the basin. The monitoring was performed between the September 20, 2014 and the April 27, 2015. In our previous work of Hong, Bonhomme, et al., (2016), 56 rainfall events were identified during this study period, with more than 88% of the events had a rain depth of less

than 8 mm, nearly 89% of the events had a mean intensity smaller than 3 mm/h, and 87% of the events had a duration shorter than 7 h.

In this study, 6 typical rainfall events were selected for model assessment. These rainfall events can be considered as representative of various hydrological situtations on the catchment. The characteristics of the 6 selected rainfall events are illustrated in Table 1.

Table 1 Characteristics of the six studied rainfall events.

Rainfall date	Rainfall depth (mm)	Mean intensity (mm/h)	Max intensity (mm/h)	Duration (h)
10/08/2014	4.86	1.52	8.57	6.17
10/12/2014	3.60	1.68	7.50	2.14
11/03/2014	4.60	1.33	36.0	10.3
11/15/2014	9.27	2.81	6.21	4.41
11/25/2014	2.86	1.32	5.14	3.33
12/12/2014	4.15	1.28	40.0	22.6

LiDAR and topographic data

In Europe, thanks to the Inspire Directive (2007/2/EC) of the European Parliament and of the Council, Digital Terrain Model (DTM) databases are accessible for public research centres. In France, the National Institute of Geographic and Forestry Information (IGN) provides the large scale reference database (RGE®, http://professionnels.ign.fr/rge) containing DTM data of 25m resolution for the whole country. FIG. 3a shows a part of this data on our study site. This dataset is relatively easy to achieve and demands no extra cost, hence have evident value for operational purposes.

In addition to this available DTM data, a Mobile Mapping System (MMS) called Stereopolis (Paparoditis, Papelard, et al., 2012) has been applied over the study area in order to produce a 3D point cloud of the road topography with centimetric

resolution. Whereas, the measured 3D cloud not only contains the topography but also objects such as trees, urban furniture as well as moving objects such as vehicles and pedestrians. A semi-automatic modelling approach was then developed in order to filter out the non-terrain point (Hervieu and Soheilian, 2013). At the end, a 20cm resolution topographic data of road and sidewalks was accomplished (Fig. 3b).

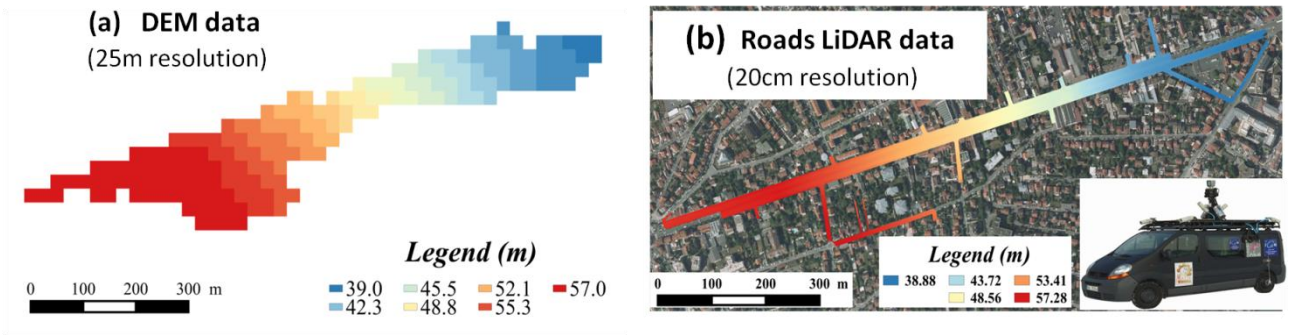

Fig. 3 Different sources of the topographic data. (a) coarse Digital Terrain Model (DTM) data of 25m resolution; (b) 20cm resolution LiDAR topographic data for roads and sidewalks.

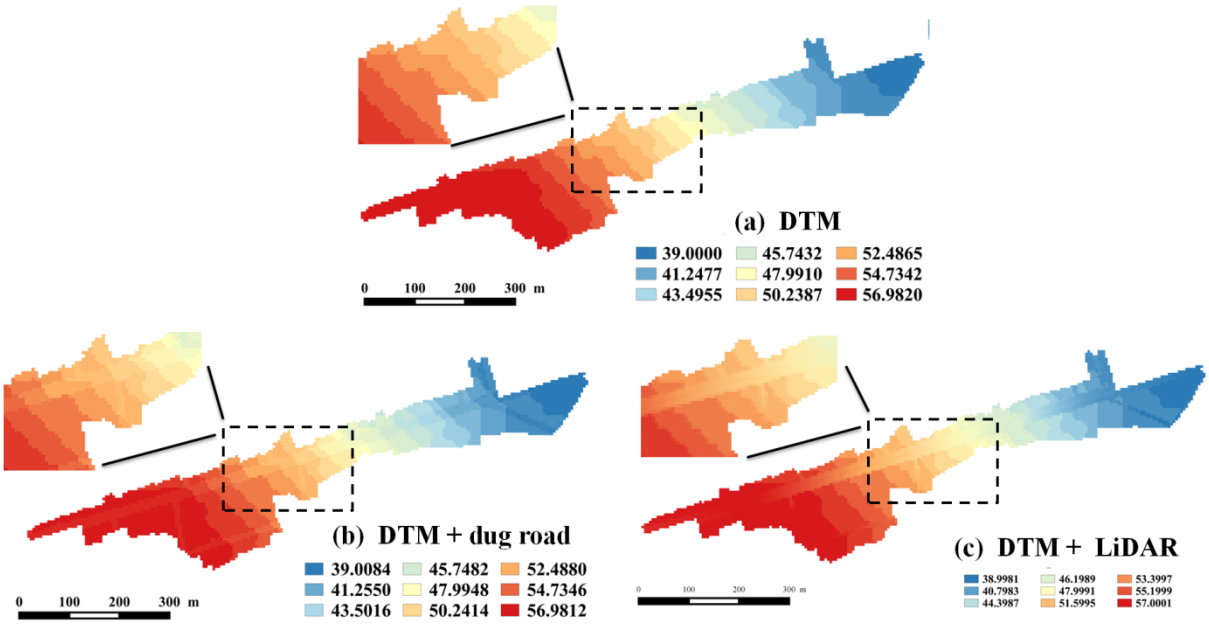

Fig. 4 Three different topographic input data. For (a) DTM, (b) DTM - dug road, and (c) DTM +LiDAR

Following Gallegos, Schubert, et al. (2009) and Fewtrell, Duncan, et al. (2011), the proper spatial resolution for 2D modelling of the urban surface can be set by considering the minimum distance between buildings and the one third of the street width. For our case study, this distance can be estimated to 5 meters. In order to assess the influence of high-resolution LiDAR data on urban 2D/1D modelling, 3 typical configurations are tested: (i) directly resampling the DTM data (25m) to 5m resolution, called "DTM"; (ii) resampling the DTM data (25m) to 5m resolution, and then lowering the identified road grid cells by 50 cm, called "DTM -dug road"; (iii) resampling the road LiDAR data (20cm) and the DEM data (25m) to 5m resolution, then fusing the two types of data together, called "DTM+LiDAR". The three different topographic scenarios are illustrated in Fig. 4.

Landuse information

In order to obtain a fine information of the urban landuse, different landuse classes can be identified by combining multiple data sources, such as aerial ortho-photos, LiDAR data and public accessible database. This is the first configuration of the input landuse data for TRENOE platform (FIG. 5a), noted "detailed landuse". In detailed landuse, the road surfaces are traced by using aerial ortho-photos, thus the sidewalks can be identified automatically as the areas between buildings and roads. Then inside every cadastral plot, the complement of buildings was considered. Ortho-photo identification was applied in order to classify those parts into different classes such as bituminous surface, lawn and vegetation. LiDAR data was used for recognizing low vegetation from trees. Moreover, an automatic image segmentation tool (Guigues, Cocquerez, et al., 2006) was applied on aerial ortho-photo for recognizing different types building roofs, such as flat, slopping and tiled roofs. As for the overlapped areas within different data sources, a specific priority order of landuses is defined by considering the hydrologic connectivity in urban landscape, followed by roads, sidewalks, parking lots, various types of roofs, trees, grass and others. Additionally, since the manholes have a key role in the coupling between the 2D surface and 1D network models, they are represented as a specific class of landuse in TRENOE model.

The second configuration of the input landuse data is simply extracted from the BD-TOPO® database, which is much easier to achieve than the multiple data sources, noted "coarse landuse" (FIG. 5b). The BD-TOPO® database only contains the information of buildings which are more than 20 m², and the urban public green spaces. The undefined areas are considered as impermeable zones such as roads, sidewalks and parkings.

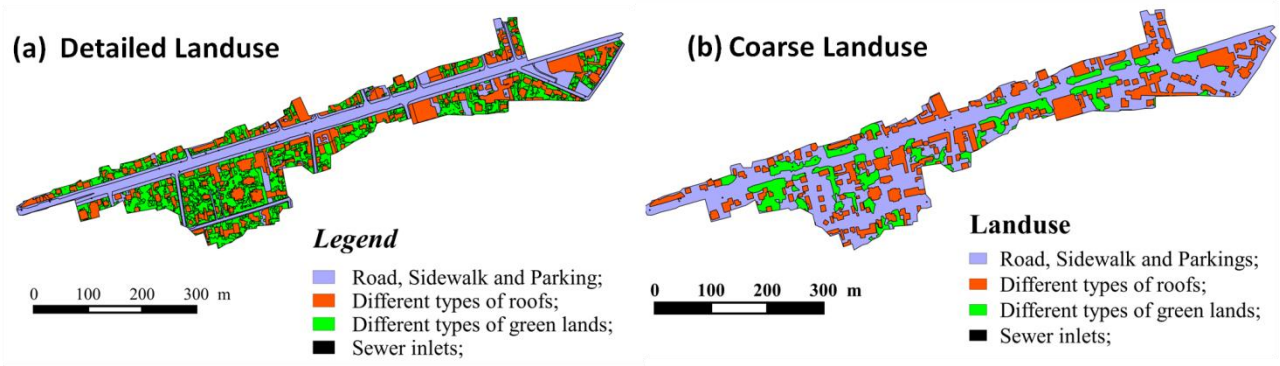

Fig. 5 Input landuse information. (a) Obtained by combining multiple data sources, (Multi-sources Landuse); (b) Extracted directly from the RGE® database (RGE Landuse).

Results and discussion

Parameter calibration and validation

In recent urban 2D/1D modelling studies, researchers widely investigated the physical meanings and the reliable ranges of different hydrological parameters (e.g. Kidmose, Troldborg, et al., 2015; Djordjević, Prodanović, et al., 2005; Leandro, Chen, et al., 2009), such as the infiltration parameters of Green and Ampt (1911) method, the friction coefficient for surface and pipes (Manning's N), as well as the interception loss. Considering the common parameter ranges which have been used by the above authors, the TRENOE parameters are firstly calibrated with a trial-and-error procedure using the DTM+LiDAR topographic data and the Detailed Landuse information. The Nash and Sutcliffe (1970) coefficient (NSE) are used to evaluate the

model performance. Optimisation is performed on the event of November 15, 2014, and the calibrated parameters (Table 2) are applied for the other five rainfall events. Compared to the continuous measurements of water flow at the network outlet, the performance of the urban 2D/1D modelling can be assessed. The simulation results are illustrated in Fig. 6.

Table 2 Calibrated parameter values of TRENOE model.

	Manning's n	**Saturated hydraulic conductivity (m/s)**	**Initial loss (mm)**	**Suction head at the wetting front (m)**	**Residual soil moisture content**
Roads	0.015	$1.0 * 10^{-8}$	0.5	0.01	0.1
Trees	0.2	$1.0 * 10^{-5}$	3	0.01	0.1
Grass	0.2	$1.0 * 10^{-5}$	2	0.01	0.1

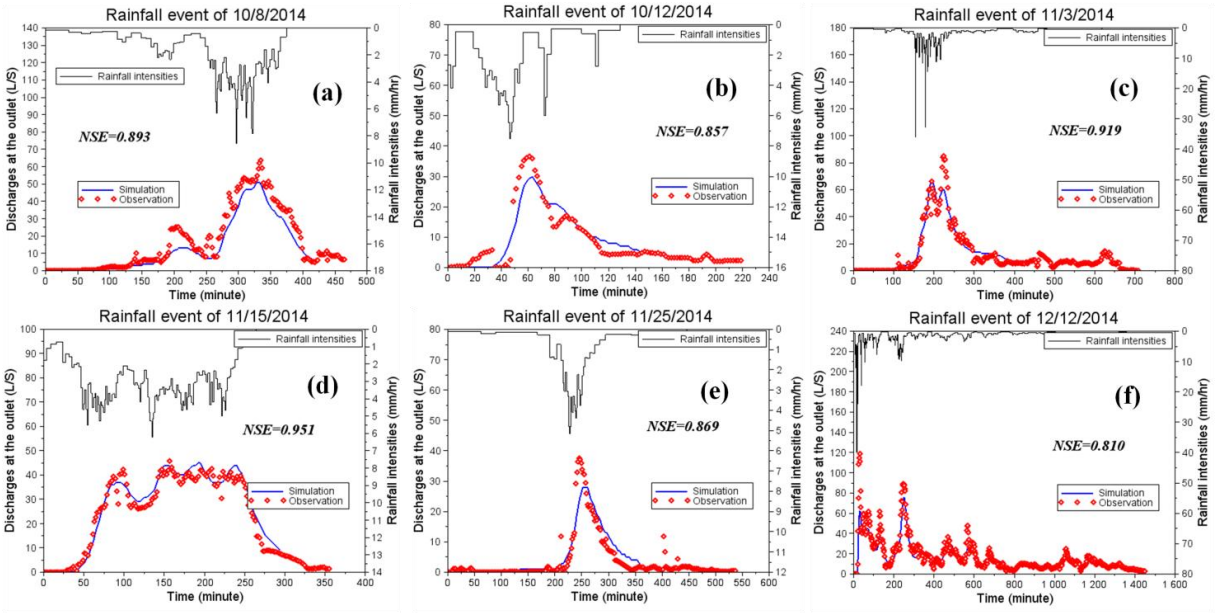

Fig. 6 Water flow simulations using urban 2D/1D TRENOE model with the detailed DTM + LiDAR topography and Multi-sources Landuse. The simulated discharges at the network outlet (solid blue lines) are compared with the measured data (red circles). Rainfall is plotted on the upper part. For events (a) October 8, 2014;

(b) October 12, 2014; (c) November 3, 2014; (d) November 15, 2014; (e) November 25, 2014; (f) December 12, 2014.

According to the simulation results in Fig. 6, the performance of the water flow simulation is quite satisfying with the DTM + LiDAR topographic data and Detailed Landuse information. The NSE values for all the six studied rainfall events are greater than 0.8, indicating a quite satisfactory modelling performance for the investigated urban catchment. This encouraging result confirms that the 2D-surface and 1D-sewer TRENOE model is a promising modelling approach for urban stormwater quantitative simulations.

Sensitivties of low-resolution topograhic data and coarse landuse information

Considering the simulations using "DTM + LiDAR topography" and detailed landuse (DTM_LiDAR + DL) as reference, the effects of applying low-resolution topographic data and coarse landuse information on model outputs can be respectively evaluated by comparing the reference simulations to simulations using (i) DTM topography and detailed landuse (DTM + DL); (ii) DTM - dug road topography and detailed landuse (DTM_dug + DL); (iii) DTM + LiDAR topography and coarse landuse (DTM_LiDAR + CL). The Mean Deviation (MD) and Relative Mean Deviation (RMD) coefficients are used as performance indicators to quantify the differences between the references and the scenario simulations (Eq. 1 - 2):

$$MD = \frac{1}{n}\sum_{i=1}^{n}\left|x_i - \overline{x_{ref,i}}\right| \qquad (1)$$

$$RMD = \frac{\frac{1}{n}\sum_{i=1}^{n}\left|x_i - \overline{x_{ref,i}}\right|}{\overline{x_{ref}}} * 100\ \% \qquad (2)$$

where n is the total number of simulated discharges during the rainfall events, x_i and $x_{ref,i}$ are the i_{th} output of the scenario and reference simulation, respectively, and $\overline{x_{ref}}$ is the mean discharge of the reference simulation.

The simulated sewer network discharges for the six studied rainfall events are presented in the Fig. 7, and their RMD coefficients are displayed in the Table 3:

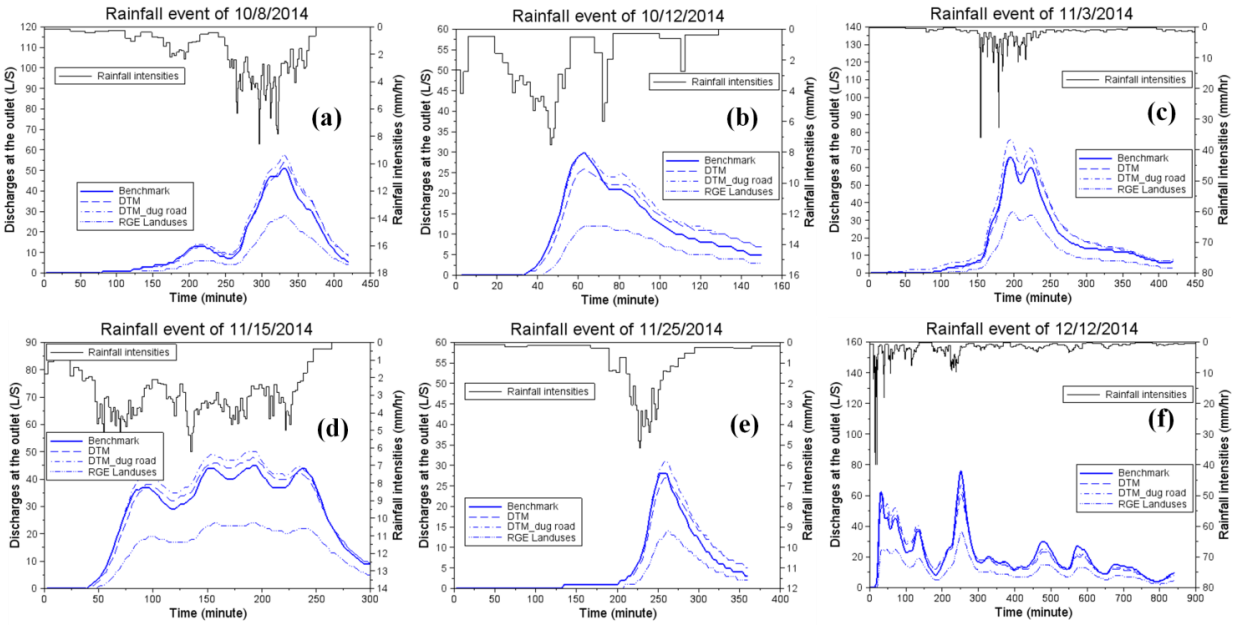

Fig. 7 Sensitivities of low-resolution topographic data and coarse landuse information. Simulations using DTM + LiDAR topography and Multi-sources Landuse (solid blue lines) are compared with simulations using (i) DTM topography and Multi-sources Landuse (dashed blue lines); (ii) DTM - dug road topography and Multi-sources Landuse (dash-dotted blue lines); (iii) DTM + LiDAR topography and RGE Landuse (dotted blue lines). Rainfall is plotted on the upper part. For events (a) October 8, 2014; (b) October 12, 2014; (c) November 3, 2014; (d) November 15, 2014; (e) November 25, 2014; (f) December 12, 2014.

As shown in Fig. 7 and Table 3, simulations using coarse landuse data (CL) are quite different from that using detailed landuse information (DL), with RMD values around 50%. This result reveals that the present 2D/1D modelling approach is very sensitive to landuse data on the studied urban catchment. Compared with the simulations using DL, scenarios using CL underestimate water discharges at the sewage outlet. This phenomenon is mainly due to the inappropriate description of the urban landuses for the adjoining areas of manholes in CL. Since the connecting areas of manholes are major water pathways for urban surface runoffs, the presence

of public green spaces surrounding the manholes (Fig. 5b) can lead an overestimation of infiltration. Contrarily, as the manholes are realistically surrounded by the impermeable roads and sidewalks in DL (Fig. 5a), the infiltration of surface runoffs can be correctly simulated by using detailed landuse information.

Table 3 MD and RMD between the reference simulations and simulations using low-resolution topographic data and coarse landuse information, respectively.

Input data	**DTM / Multi-sources Landuse**		**DTM - dug road / Multi-sources Landuse**		**DTM + LiDAR / RGE Landuse**	
Coefficients	**MD (L/S)**	**RMD**	**MD (L/S)**	**RMD**	**MD (L/S)**	**RMD**
10/08/2014	1.96	14.7 %	1.31	9.33 %	6.32	47.6 %
10/12/2014	1.72	16.5 %	1.70	16.3 %	5.34	51.3 %
11/03/2014	3.76	23.3 %	1.99	12.3 %	7.54	46.9 %
11/15/2014	2.80	10.5 %	1.94	7.30 %	12.5	47.1 %
11/25/2014	0.94	17.4 %	0.86	15.9 %	2.76	51.1 %
12/12/2014	2.32	11.3 %	2.31	11.2 %	9.58	46.6 %

On the other hand, the results surprisingly demonstrate that the gaps between the reference simulations and simulations using lower-resolution topographic data (DTM and DTM_dug) are not significant. The simulated water flows at the sewage outlet are hence not sensitive to the use of different resolutions of topographic data. This result is mainly related to the precisely defined and closely located manholes in the studied urban catchment. Since the distances between manholes are very short (generally less than 300 m), stormwater runoffs enter rapidly into the sewer networks. Thus the precision of the road topography does not influence notably the transfer time, as this time is very short in any case. Moreover, as the building roofs are directly connected to the sewer networks in TRENOE platform, the effects of using precise road topographic data has no effect for these landuses. Of course, this result

needs to be confirmed by applications of this modelling approach to other urban catchments with different shapes and slopes. It is important to notice that the resolution of road topographic data may not be a key factor for urban 2D/1D modelling.

Is the more detailed remote sensing data really necessary?

As presented in the above sections, by assessing the performance of the newly developed 2D/1D TRENOE platform on an urban catchment at the city district scale, detailed landuse information is required for accurate simulations of water flows at sewer outlet. On the contrary, urban stormwater managers are not recommended to apply expensive remote sensing techniques for measuring high-resolution altimetry data, while using only easily achieved topographic data with artificially dug streets seems to be a reasonable compromise to obtain acceptable simulations.

Nevertheless, this preliminary conclusion does not mean that the high-resolution topographic data is useless. In fact, detailed remote sensing data can be used for developing and analyzing physically-based models. As the descriptions of spatially-variable processes can be supported by spatial measurements, researchers will be able to test new theories and gain a new understanding of the physical mechanisms with higher-resolution data, helping to improve the modelling techniques. On the contrary, in the aspect of operational applications, lower-resolution images have the advantages of greater spatial and temporal coverage, lower costs and lack of copyright restrictions, hence are preferred by urban stormwater practitioners (Di Baldassarre and Uhlenbrook, 2012). However, in order to achieve an acceptable model performance, the necessity of detailed remote sensing data should be evaluated for new modelling applications.

Furthermore, based on the results of this paper, it can be noted that the precise description of manhole locations is also an important factor for the urban 2D/1D modelling. As the roads are the major water pathways for stormwater runoffs at the city district scale, the main benefit of using high-resolution road LiDAR data is to accurately simulate the surface runoffs over roads, particularly for representing the flow directions and velocities. However, this high-resolution data is no longer a key

factor when manholes are close from one another, implying the runoff time from road surface to the nearest manholes can be correctly simulated even with lower-resolution topography. Nevertheless, the landuse information, especially for the areas close to the manholes, needs to be appropriately described. Therefore, perspectives of using remote sensing technologies on urban 2D/1D modelling can focus on (i) the identification of the manhole locations, an automatic manhole detection algorithm (Hervieu, Soheilian, et al., 2015) can be an promising next step; (ii) the detailed characterizations of landuses close to manholes as well as on the adjoining urban surfaces. Meanwhile, new types of urban stormwater modelling tools, such as models based on manhole locations and the adjoining areas, can be tested for further studies.

Conclusion

In this paper, we proposed a new approach to assess the needs of high-resolution LiDAR data and detailed landuse data for urban 2D/1D stormwater modelling. The TRENOE platform was applied to a small urban catchment near Paris (Le Perreux sur Marne, 0.12 km²). According to the results, we can conclude that detailed landuse information is a crucial factor for accurate simulations, but the effect of using very high resolution altimetry data is limited for the simulations of water flows at sewer outlet. Only considering basic topographic data with dug streets seems to be a reasonable compromise to obtain acceptable model results.

Certainly, identification of the real needs of high-resolution and detailed input data for urban hydrological modelling is a challenge for practitioners to avoid the collection of unnecessary and costly data. Depending on different management/research objectives, the "proper" modelling approach should be developed with "adequate" input data. This study described a benchmark for assessing the gains made by using the high-resolution topographic data and detailed landuse information compared to only using traditional low-cost data sources. Testing the performance of more efficient modelling tools (for example, based on manhole locations) with more economical remote sensing technologies (for example, automatic manhole detection algorithm) would represent an interesting perspective in the future.

ACKNOWLEDGEMENT

The research work of PhD student Yi Hong was financed by ANR-Trafipollu project (ANR-12-VBDU-0002) and Ecole des Ponts ParisTech. The authors would like to thank the experimental team of ANR Trafipollu project for all collected necessary for this work, in particular David Ramier (CEREMA), Mohamed Saad (LEESU) and Philippe Dubois (LEESU).

Reference

Bates, P.D., 2012. Integrating remote sensing data with flood inundation models: how far have we got? Hydrol. Process. 26, 2515–2521. doi:10.1002/hyp.9374

DHI, 2008. MIKE by DHI Software. Reference Manuals for MIKE FLOOD.

Di Baldassarre, G., Uhlenbrook, S., 2012. Is the current flood of data enough? A treatise on research needs for the improvement of flood modelling. Hydrol. Process. 26, 153–158. doi:10.1002/hyp.8226

Djordjević, S., Prodanović, D., Maksimović, C., Ivetić, M., Savić, D., 2005. SIPSON--simulation of interaction between pipe flow and surface overland flow in networks. Water Sci. Technol. J. Int. Assoc. Water Pollut. Res. 52, 275–283.

Fewtrell, T.J., Bates, P.D., Horritt, M., Hunter, N.M., 2008. Evaluating the effect of scale in flood inundation modelling in urban environments. Hydrol. Process. 22, 5107–5118. doi:10.1002/hyp.7148

Fewtrell, T.J., Duncan, A., Sampson, C.C., Neal, J.C., Bates, P.D., 2011. Benchmarking urban flood models of varying complexity and scale using high resolution terrestrial LiDAR data. Phys. Chem. Earth Parts ABC, Recent Advances in Mapping and Modelling Flood Processes in Lowland Areas 36, 281–291. doi:10.1016/j.pce.2010.12.011

Fletcher, T.D., Andrieu, H., Hamel, P., 2013. Understanding, management and modelling of urban hydrology and its consequences for receiving waters: A state of the art. Adv. Water Resour. 51, 261–279. doi:10.1016/j.advwatres.2012.09.001

Gallegos, H.A., Schubert, J.E., Sanders, B.F., 2009. Two-dimensional, high-resolution modeling of urban dam-break flooding: A case study of Baldwin Hills, California. Adv. Water Resour. 32, 1323–1335. doi:10.1016/j.advwatres.2009.05.008

Green, W.H., Ampt, G.A., 1911. Studies on Soil Phyics. J. Agric. Sci. 4, 1–24. doi:10.1017/S0021859600001441

Hervieu, A., Soheilian, B., 2013. Semi-Automatic Road/Pavement Modeling using Mobile Laser Scanning. ISPRS Ann. Photogramm. Remote Sens. Spat. Inf. Sci. II-3/W3, 31–36. doi:10.5194/isprsannals-II-3-W3-31-2013

Hong, Y., Bonhomme, C., Le, M.-H., Chebbo, G., 2016. A new approach of monitoring and physically-based modelling to investigate urban wash-off process on a road catchment near Paris. Water Res. 102, 96–108. doi:10.1016/j.watres.2016.06.027

Horritt, M.S., Di Baldassarre, G., Bates, P.D., Brath, A., 2007. Comparing the performance of a 2-D finite element and a 2-D finite volume model of floodplain inundation using airborne SAR imagery. Hydrol. Process. 21, 2745–2759. doi:10.1002/hyp.6486

Innovyze Ltd, 2011. InfoWorks 2D - Collection Systems Technical Review.

Kidmose, J., Troldborg, L., Refsgaard, J.C., Bischoff, N., 2015. Coupling of a distributed hydrological model with an urban storm water model for impact analysis of forced infiltration. J. Hydrol. 525, 506–520. doi:10.1016/j.jhydrol.2015.04.007

Leandro, J., Chen, A.S., Djordjević, S., Savić, D.A., 2009. Comparison of 1D/1D and 1D/2D Coupled (Sewer/Surface) Hydraulic Models for Urban Flood Simulation. J. Hydraul. Eng. 135, 495–504. doi:10.1061/(ASCE)HY.1943-7900.0000037

Lhomme, J., Bouvier, C., Perrin, J.-L., 2004. Applying a GIS-based geomorphological routing model in urban catchments. J. Hydrol., Urban Hydrology 299, 203–216. doi:10.1016/j.jhydrol.2004.08.006

Paparoditis, N., Papelard, J.-P., Cannelle, B., Devaux, A., Soheilian, B., David, N., Houzay, E., 2012. Stereopolis II: A multi-purpose and multi-sensor 3D mobile mapping system for street visualisation and 3D metrology. Rev. Fr. Photogrammétrie Télédétection 69–79.

Salvadore, E., Bronders, J., Batelaan, O., 2015. Hydrological modelling of urbanized catchments: A review and future directions. J. Hydrol. 529, Part 1, 62–81. doi:10.1016/j.jhydrol.2015.06.028

Sto Domingo, N.D., Refsgaard, A., Mark, O., Paludan, B., 2010. Flood analysis in mixed-urban areas reflecting interactions with the complete water cycle through coupled hydrologic-hydraulic modelling. Water Sci. Technol. J. Int. Assoc. Water Pollut. Res. 62, 1386–1392. doi:10.2166/wst.2010.365

Velleux, M.L., England, J.F., Julien, P.Y., 2008. TREX: Spatially distributed model to assess watershed contaminant transport and fate. Sci. Total Environ. 404, 113–128. doi:10.1016/j.scitotenv.2008.05.053

Vojinovic, Z., Tutulic, D., 2009. On the use of 1D and coupled 1D-2D modelling approaches for assessment of flood damage in urban areas. Urban Water J. 6, 183–199. doi:10.1080/15730620802566877

Chapitre 9. Integrating atmospheric deposition, soil erosion and sewer transport models to assess the transfer of traffic-related pollutants in urban areas

Yi Hong[1*], Celine Bonhomme[1], Bastian Van den Bout[2], Victor Jetten[2], Ghassan Chebbo[1,3]

[1]LEESU, MA 102, École des Ponts, AgroParisTech, UPEC, UPE, Champs-sur-Marne, France.

[2] ITC-ESA, Department of Earth Systems Analysis, Enschede, Netherlands

[3]Université Libanaise, faculté de génie, campus Rafic Hariri, Hadath, Lebanon

* Corresponding author: yi.hong@leesu.enpc.fr

*(Article soumis, en cours de révision, dans le journal "**Environmental Modelling & Software**")*

Abstract

For the first time, this paper develops an integrated and spatially-distributed modelling approach, linking atmospheric deposition, soil erosion and sewer transport models, to assess the transfer of traffic-related pollutants in urban areas. The modelling system is applied to a small urban catchment near Paris. Two modelling

scenarios are tested by using experimentally estimated and simulated atmospheric dry deposits. Simulation results are compared with continuous measurements of water flow and total suspended solids (TSS) at the catchment outlet. The performance of water flow and TSS simulations are satisfying with the calibrated parameters; however, no significant difference can be noticed at the catchment outlet between the two scenarios due to the "first flush" effects. Considering the Cu, BaP and BbF contents of different particle size classes, simulated event mean concentration of each pollutant is compared with local in-situ measurements. Finally, perspectives to improve model performance and experimental techniques are discussed.

Keywords:

Integrated modelling; Atmospheric deposition; Soil erosion model; Sewer transport; Traffic-related pollutants; Spatially-distributed modelling; OpenLISEM; SWMM; Urban stormwater;

1 Introduction

Urban traffic emission is a major cause of nonpoint source pollution in cities and near high-ways (Fletcher et al., 2013; Petrucci et al., 2014; Shorshani et al., 2015). Key pollutants such as total suspended solids (TSS), heavy metals and polycyclic aromatic hydrocarbons (PAHs) are first accumulated in the atmosphere with traffic activities (Gunawardena et al., 2013). With time, these atmospheric phase pollutants can be transported and settle to urban surfaces forming dry or wet depositions (Huston et al., 2009). Finally, these nonpoint source pollutants are entrained by urban stormwater runoffs from separated sewer systems to water bodies, causing the degradation of aquatic environments and ecosystems (Shirley Clark, 2007). In the context of the European Water Framework Directive (2000), the mitigation of diffuse urban pollutions such as heavy metals and PAHs is one of the main objectives. Therefore, it is essential to understand the transport of such contaminants in urban air-surface-sewer systems during rainfall events.

According to the chemical nature and the source of contaminants, heavy metals and PAHs in urban stormwater runoff can be partitioned into solid and liquid phases (particulate contaminants and dissolved contaminants, respectively). Several investigations of the chemical and physical properties of these pollutants have been reviewed by (Aryal et al., 2010; Pant and Harrison, 2013; Tsihrintzis and Hamid, 1997). Generally, the authors conclude that most of the PAHs, Cu, Pb, Fe, and Ni are associated with fine particles. By assuming that such pollutants are in particulate phase and distributed in different sizes of suspended solids (SS), the transport of such nonpoint source pollutants can be simulated with physically-based and distributed soil erosion models. Using that type of model, the spatial and temporal variations of water flow and pollutants washoff can be precisely described.

Up to now, a large amount of integrated systems linking traffic flow, pollutant emission and atmospheric dispersion models have been developed (Lim et al., 2005; Oxley et al., 2013). However, very limited attention has been paid to couple atmospheric deposition and stormwater quality models. (Shorshani et al., 2015, 2013) firstly proposed the concept of integrated traffic, air and stormwater modelling for urban areas. Nevertheless, the stormwater model in their modelling chain still relies on exponential, catchment scale washoff functions (Sartor et al., 1974). Moreover, the resolution of their model is restricted by the size of subcatchments. By assuming that the rate of pollutant loss on a sub-catchment is directly proportional to the water flow at the outlet and to the averaged dry deposits, the (Sartor et al., 1974) functions are inadequate to represent the spatial heterogeneities of the urban nonpoint source pollutions, accompanying with the high variability of urban surfaces.

In this paper, we linked for the first time a physically-based 2D erosion model (De Roo et al., 1996; Jetten and Roo, 2001) to an air quality model (Soulhac et al., 2011) and a sewer network model (Rossman, 2010). In order to simulate the transport of multi-class sediments and their associated contaminants in urban areas. The integrated modelling approach separately simulates the transfer of different sizes of particles, allowing the distribution of contaminants among various particle classes possible. Moreover, this integrated model independently calculates the detachment process caused by rain splash impacts and by shear stress effects, which is confirmed to be a crucial factor for accurate modelling of urban washoff process (Hong et al., 2016a). Finally, the coupling of spatially-distributed atmospheric

depositions and the 2D surface models, emphasizes a promising potential for the improvement of the urban nonpoint source pollution management.

The following sections will provide details on model development, configurations, and the application of the integrated modelling system to a small urban catchment near Paris (12 ha, Le Perreux sur Marne). In this study, two modelling scenarios are tested by using experimentally estimated and simulated atmospheric dry deposits. The performance of the simulations are evaluated by comparing the simulated water flow and TSS concentrations with continuous measurements at the catchment outlet. The simulated event mean concentrations of traffic-related pollutants are compared with local in-situ measurements. Finally, perspectives to improve model performance and experimental techniques are discussed.

2 Materials and methods

2.1 Development of the integrated modelling system

This paper describes an integrated modelling approach which links three separated modelling components: the air quality component, the 2D surface component, and the roof and sewer network component. The scheme of the integrated model is presented in Fig. 1:

2.1.1 Air quality component

The air quality component of the integrated modelling system uses the SIRANE model (Soulhac et al., 2011) to simulate the dispersion and deposition of urban atmospheric pollutants. In the framework of the ANR (French National Agency for Research) Trafipollu project, the collection of the input data and the simulations were performed by the association AirParif (http://www.airparif.asso.fr/). The outputs of the air quality component are adapted and connected to the 2D surface component in this study.

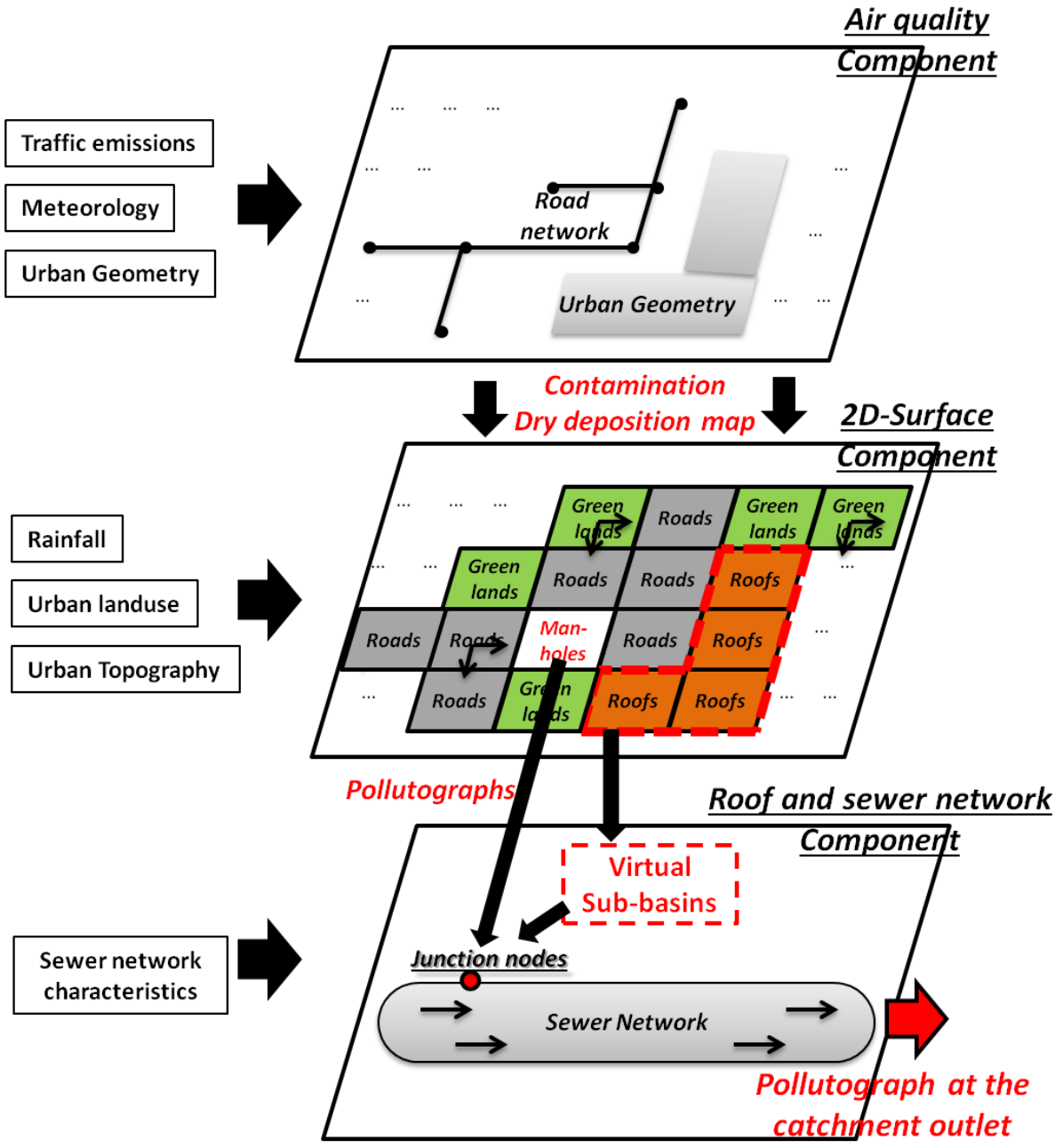

Fig. 1 Conceptual scheme of the integrated modelling framework for the simulation of the transfer of traffic-related pollutant on air-surface-sewer networks.

Within the SIRANE model, the streets are modelled as a network of connected road segments. Traffic emissions are firstly assumed to be uniformly mixed within each segment of street, the model then simulates the transport of pollutants in and out of the street segments by three main mechanisms: (i) advection along the street due to the mean wind along their axis, (ii) diffusion across the interface between the

street and the overlying atmospheric boundary layer, and (iii) exchange with other streets at street intersections. The simulation at street level is then complemented by a standard Gaussian plume model for atmospheric transport and dispersion above roof level. Assuming that the deposition velocity is 0.1 cm/s, the deposition rates for different types of pollutants are calculated for the bottom layer of the atmospheric columns, forming spatially-distributed dry and wet deposits at the urban surface.

The input data for the air quality component is the traffic emissions, the meteorological situations (wind, precipitation, temperature), and the urban geometries. In the framework of the Trafipollu project, the hourly counting traffic data and the characteristics of vehicles were collected for the studied urban catchment over several weeks, in order to simulate realistic average daily traffic intensities. The emission of the traffic-related pollutants is then calculated by considering the vehicle types, traffic speeds, road characteristics (slope, material, etc.), engine power and temperature. The weather data is offered by Meteo-France (http://www.meteofrance.com/), and the urban geometry data is provided by the National Institute of Geography of France (IGN).

The air quality component simulates the dispersion and deposition processes of PM10 (< 10μm particles), Cu, Zn, Cd, benzo (a) pyrene (BaP) and benzo (b) fluoranthene (BbF). The hourly deposition rates for such contaminants are calculated at regular points with 10 meters distance. The total mass of the atmospheric deposition at each point between two rainfall events can be calculated by accumulating the hourly dry deposits during the dry period. Moreover, in accordance with the commonly used assumption that the dry deposits dominate the atmospheric depositions (Gunawardena et al., 2013; Sabin et al., 2006), the wet deposition loads are neglected in this study.

In order to link the air quality component with the 2D surface component, the accumulated atmospheric dry deposits at regular points (10 m) are then transformed into 5m-resolution dry deposit maps by using the triangle interpolation method. Since the deposition of Cd is not significant in the studied urban catchment, and the Zn is mainly present in the dissolved form in urban stormwater runoff (Herngren et al., 2005; Huston et al., 2009), the present modelling approach focuses on the simulations of PM10, Cu, BaP and BbF.

2.1.2 2D surface component

The physically-based, two-dimensional model openLISEM (stand for Limburg Soil Erosion(De Roo et al., 1996; Jetten and Roo, 2001) is used for simulating water flow and pollutant transport in the 2D surface component. OpenLISEM is a raster-based model that simulates the surface water and sediment balance for every grid-cell. It is event based and has great spatial and temporal resolution.

The process within openLISEM can be separated into two categories: the hydrological part and the sediment transport part. In the hydrological part, openLISEM uses the kinematic wave 2D approximation of shallow-water equations for the surface runoff modelling, the (Green and Ampt, 1911) method for infiltration calculations and the canopy storage for interception estimations. A finite volume scheme is applied for numerical solution. As for the sediment transport part, the detachment and deposition processes are simulated at steady state. Within each time-step, particles eroded by the rainfall splash detachment ($det_{splash,i}$) are firstly added to the concentration of suspended solids (C_i); the updated concentration is then compared with the transport capacity of the water flow (T_i). The flow-driven detachment ($det_{flow,i}$) takes place when the updated concentration falls below T_i, while the deposition (dep_i) occurs when the T_i is exceeded. Eq. 1 represents the calculations of the final concentration of the *i-th* class of particles (E_i) in a grid-cell at the end of a time-step:

$$\begin{cases} \mathrm{E_i} = C_i + \dfrac{dt}{A\,h}\left(det_{splash,i} + det_{flow,i}\right); & \text{if} \quad C_i + \dfrac{dt}{A\,h}\, det_{splash,i} < T_i, \\ \mathrm{E_i} = C_i + \dfrac{dt}{A\,h}\left(det_{splash,i} - dep_i\right); & \text{if} \quad C_i + \dfrac{dt}{A\,h}\, det_{splash,i} > T_i, \end{cases} \tag{1}$$

Where:

- E_i *is* the final concentration of the *i-th* class of particles in a grid-cell at the end of a time-step (*kg/m*^{3});

- C_i *is* the concentration of the *i-th* class of particles in a grid-cell at the beginning of a time-step (*kg/m*^{3});

- *dt* is the time step (*s*);

- A is the surface area of a grid-cell (m^2);

- h is the water depth (m);

- $det_{splash,i}$ is the rainfall splash detachment rate of the *i-th* class of particles (kg/s);

- $det_{flow,i}$ is the flow detachment rate of the *i-th* class of particles (kg/s);

- dep_i is the deposition rate of the *i-th* class of particles (kg/s);

- T_i is the transport capacity for the *i-th* class of particles (kg/m^3);

For each class of particles, the (Hairsine and Rose, 1992) model (H-R) is used to calculate the T_i (Eq. 2). The $det_{splash,i}$ is simulated as a function of the sediment aggregate stability (A_s), rainfall kinetic energy (Ke) and the water depth (h) (Eq. 3-4, derived from unpublished test data). The $det_{flow,i}$ is calculated by assuming that the T_i deficit becomes detachment (Eq. 5), where the (Rauws and Govers, 1988) erosion efficiency factor (γ) is used to limit the detachment by the cohesion of the sediment material (Eq. 6). Finally, the dep_i is calculated by assuming that the T_i surplus becomes depositions (Eq. 7), and the settling velocity ($v_{s,i}$), is calculated by the Stoke's equations (Eq. 8).

$$T_i = F_r \left(\frac{\rho_{s,i}}{\rho_{s,i} - \rho_w}\right)\left(\frac{\omega - \omega_{cr}}{\omega}\right) S_f \, \rho_w \quad (2)$$

$$det_{splash,i} = P_i \left(\frac{2.82}{A_s} \, K_e \, e^{(-1.48\, h)} + 2.96\right) \frac{A\, h}{dt} P_h \quad (3)$$

$$K_e = 8.95 + 8.44 \, Log(I) \quad (4)$$

$$det_{flow,i} = \gamma \, (T_i - C_i) \, v_{s,i} \, A \quad (5)$$

$$\gamma = \min\left(1, \quad \frac{1}{0.89 + 0.56 \, coh}\right) \quad (6)$$

$$dep_i = (C_i - T_i) \left(1 - \exp\left(dt \frac{v_{s,i}}{h}\right)\right) v_{s,i} \, A \quad (7)$$

$$v_{s,i} = \frac{2}{9} \frac{(\rho_{s,i} - \rho_w)}{\mu} \, g \, R^2 \quad (8)$$

where:

- F_r is the re-entrainment parameter of the H-R equations;

- $\rho_{s,i}, \rho_w$ are the mass densities of the *i-th* class of particles and water, respectively (*kg/m*^{3});

- ω, ω_{cr} are the flow velocity and the critical flow velocity for sediment erosion, respectively (*m/s*);

- S_f is the friction slope;

- P_i is the fraction of available sediment that lies within the *i-th* class of particles;

- A_s is the aggregate stability (median number of raindrops to decrease the aggregate by 50%);

- K_e is the kenetic energy of the rainfall (*J/m² mm*);

- P_h is the rainfall depth in the time-step (*m*);

- *I* is the rainfall intensity (*mm/hr*)

- γ is erosion efficiency coefficient;

- *coh* is the surface cohesion coefficient *(k Pa)*.

- v_s is the settling velocity of the *i-th* class of particles *(m/s)*.

- *g* is gravitational acceleration, = 9.8 *m/s²*;

- μ is the dynamic viscosity (http://en.wikepedia.org/wiki/Dynamic_viscosity), (= 0.001 *kg/m*s*);

- *R* is the radius of the particle (*m*);

As shown in the above equations, the transport capacity (Eq. 2) is calculated for each class of particles, allowing the simulation of size-selective erosion possible. Besides, since the characteristics of the sediment material are different from one rainfall event to another, the cohesion coefficient (*coh*) may need calibrations for

different rainfall events. The values of other parameters can be fixed according to published literature.

Generally, the inputs for the 2D surface component consist of rainfall data, urban landuse information and urban topographic data. Details of these input data will be presented in the sections below. Otherwise, the outputs of this modelling component are hydrographs and pollutographs for the cells representing manholes, which will be linked to the roof and sewer network component.

2.1.3 Roof and Sewer network component

The building roofs in this modelling approach are represented separately from the 2D surface component. Contrarily, the grid-cells of roofs are assembled as different virtual sub-basins connecting to their nearest sewer nodes. For representing the fact that the roof drains are directly connected to the sewer networks in the studied catchment. The areas of each virtual sub-basin is equal to the total area of all the connected roof cells. These sub-basins are treated as the non-linear reservoirs, surface runoff occurs when the depth of water in the "reservoir" exceeds the loss of initial wetting for roofs. The outflow of each sub-basin is given by the Manning's equation. The washoff process is simulated by using exponential equations, where the eroded mass is proportional to the water flow and the remaining particles on roofs.

The sewer network part of the integrated modelling approach is based on SWMM model (Rossman, 2010). Interactions between the 2D surface component and the roof and sewer network component is modelled through flow exchange at identified linking points, named "junction nodes". These "junction nodes" can receive water and pollutant flows from the virtual sub-basins and the manholes. The water flow in sewer networks is computed by the 1D kinematic wave approximation of the Shallow Water equations and solved by the finite-difference scheme. Otherwise, water quality routing within conduits assumes that the conduit behaves as a continuously stirred tank reactor (CSTR). Using the CSTR method, the concentration of a constituent exiting the conduit at the end of a time step is calculated by integrating the conservation of mass equation. The sewer network module only requires the characteristics (connections, slope, length, etc.) of the urban drainage network as the input information, while the outputs are hydrographs and pollutographs at the sewerage outlet, which could be further compared with the in-situ observations.

2.2 Study site

The modelling system is applied to a small urban catchment near Paris (Le Perreux sur Marne, Val de Marne, France). This study area is a typical residential zone in the Paris region, characterized by a highly trafficked main street in the Eastern Paris (more than 30,000 vehicles per day). The total area of this catchment is 12 ha, about 70% of the surface is impervious, and the building roofs represent approximately 35% of the entire catchment. The western section has a higher altitude than the eastern side, with an average slope of less than 2% (Fig. 2).

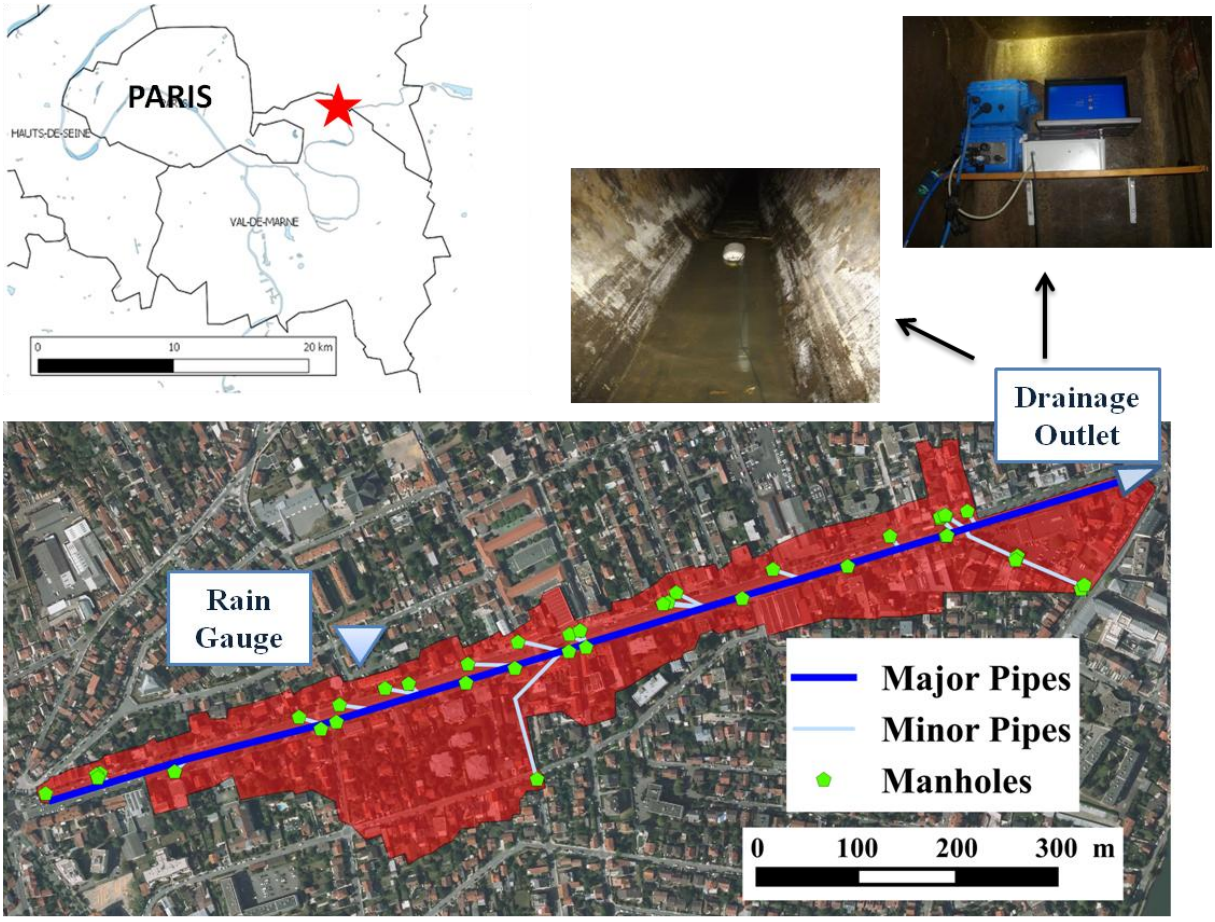

Fig. 2 Study area at Eastern Paris (Le Perreux sur Marne). Instrumental settings for measuring water flow and turbidity at the drainage outlet, as well as rainfall intensities.

The stormwater drainage system consists of 1156 metres major pipes (vertical ellipse, 2.3m height and 1.3m large) along the main street, and nearly 1000 metres minor pipes (circle, 0.3m diameter) for connecting manholes to the major pipes. In total, there are 35 manholes in the studied catchment. The sewerage outlet is located at the North-Eastern edge of the presented drainage network, where the flow is continuously monitored by a Nivus Flowmeter with 2 minutes time interval, and the turbidity is consistently measured by a multi-parameter probe (mini-probe OTT). The total suspended solids (TSS) - turbidity relationship is therefore established based on samplings during 16 studied rainfall events. That follows a linear regression TSS = 0.8533 x Turbidity, with the R^2 equal to 0.97.

2.3 Input data and model configurations

2.3.1 Rainfall events

Table 1 Summary of the studied rainfall events.

Rainfall date		Rainfall depth (mm)	Mean intensity (mm/hr)	Duration (hour)	Antecedent dry days (day)
10/08/2014		4.86	1.51	3.22	0.4
10/12/2014		3.60	1.68	2.14	1.8
11/15/2014		9.27	2.81	3.3	0.5
11/26/2014		2.86	1.1	2.6	9
Summary of the 56 rainfall events	D10	1.55	0.51	0.70	0.24
	D50	3.35	1.18	3.29	1.82
	D90	8.65	3.15	7.51	10.18

A tipping-bucket rain gauge is installed on the roof of a building close to the urban catchment (see Fig 2). The pluviometer has a resolution of 0.1 mm. As the study area is quite small, homogeneous rainfall is considered for the entire urban catchment.

The monitoring was performed between the 20th of September 2014 and the 27th of April 2015. In our previous works (Hong et al., 2016a, 2016b), 56 rainfall events were identified during this study period, more than 88% of the studied events had a rain depth less than 8 mm, nearly 89% of the events had a mean intensity smaller than 3 mm/h, and 87% of the events had a duration shorter than 7 h.

In this study, 4 typical rainfall events are selected for model assessment, with the rainfall depths varying from 2.9 to 9.3mm, and the mean intensities differing from 1.3 to 2.8 mm/hr. The characteristics of selected rainfall events and the summary of the entire 56 rainfall events are listed in Table 1.

2.3.2 Topography and landuse

High-resolution topographic data is essential for the accurate simulations of physically-based models. In Europe, thanks to the Inspire Directive (2007/2/EC) of the European Parliament and of the Council, Digital Terrain Model (DTM) databases are accessible for public research centres. In France, the large scale reference database (RGE®, http://professionnels.ign.fr/rge) containing DTM data of 25m resolution is available for the whole country. In addition to this DTM data, a Mobile Mapping System (MMS) called Stereopolis (Hervieu and Soheilian, 2013; Paparoditis et al., 2012) has been applied around the study area in order to produce a 20cm resolution topographic data (LiDAR) of the roads and sidewalks. Following Gallegos, Schubert, et al. (2009) and Fewtrell, Duncan, et al. (2011), the proper spatial resolution for 2D modelling of the urban surface can be set by considering the minimum distance between buildings, which is approximately 5 meters for the studied urban catchment. Therefore, we firstly resample the LiDAR data (20cm) and the DTM data (25m) to 5m resolution, then merge the two types of data. With this final topographic data (Fig. 3a), the urban catchment is represented by 224 x 85 rectangular grids.

One of the most significant benefits of using such a spatially-distributed model is to be able to accurately simulate the impacts of urban landuses. In collaboration with the IGN France, detailed landuse data is applied in this study, with manholes added as a specific type (FIG. 3b). The locations of manholes are identified from the GIS and AutoCAD sewer network data. Afterward, the vectorial landuse data are transformed into 5 m resolution grid-cells following a specific hierarchy of different

landuse types. The priority is based on the effect of the landuse on the water quantity and quality. In the current study, the prior landuse is the "manhole", followed by road, sidewalk, parking, various types of roofs and green lands. In general, 70% of the catchment surfaces are impervious areas, within which the roof areas represent 35% of the total surface.

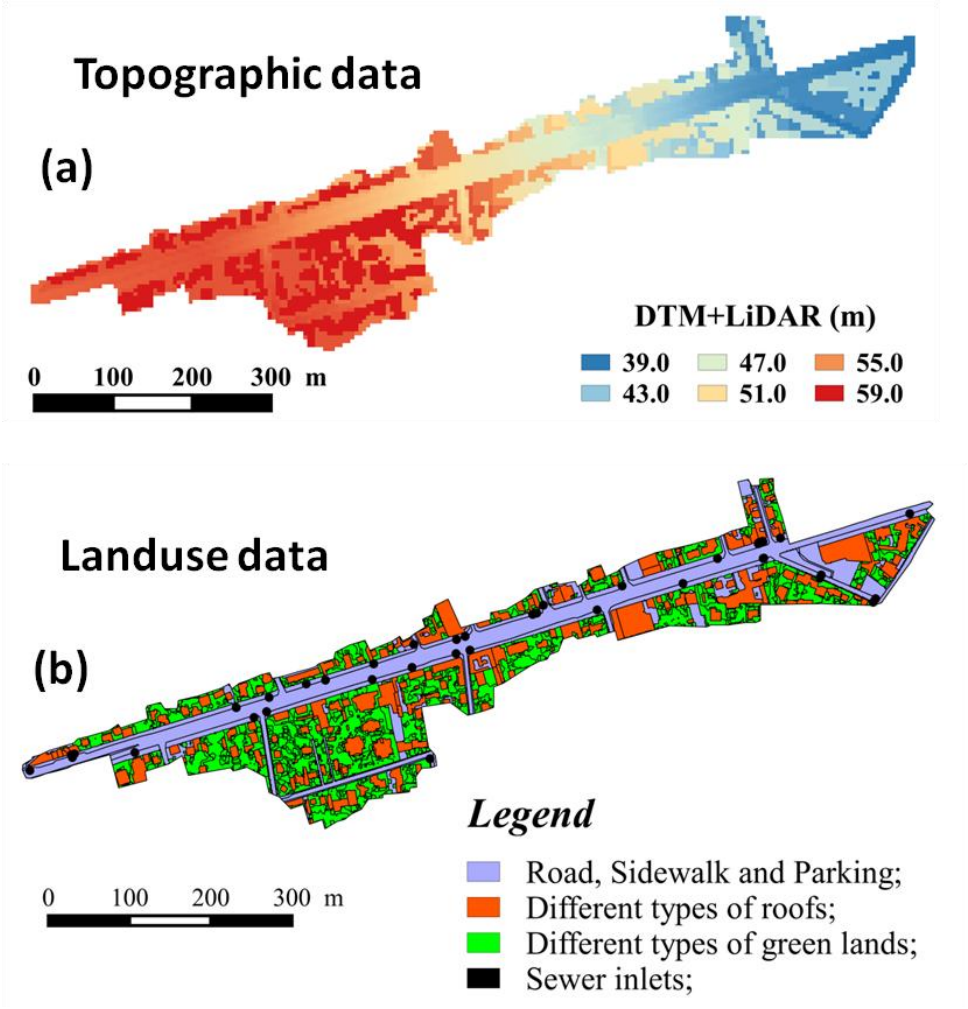

Fig. 3 (a) Input topographic data; (b) input landuse data.

2.3.3 Atmospheric dry depositions of PM10, Cu, BaP and BbF

As presented in the above sections, the atmospheric dry deposition maps can be simulated for each studied rainfall event. Taking the event of 26th of November 2014

as an example, the deposition maps for PM10, Cu, BaP and BbF are presented in Fig. 4.

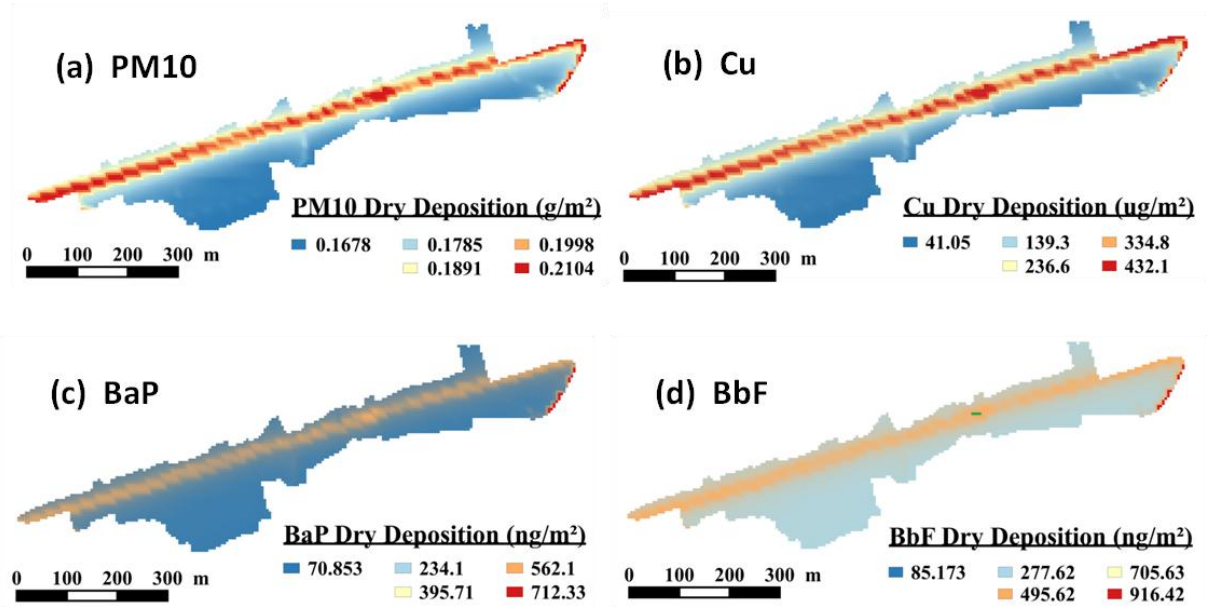

Fig. 4 Simulation of the accumulated atmospheric dry depositions for the event of 26th of November 2014. The dry deposition maps of (a) PM10, (b) Cu, (c) BaP, (d) BbF.

Since the studied urban catchment is highly urbanized, the atmospheric dispersion of traffic-related pollutants can be constrained by obstacles such as buildings or vegetation at around the road. Therefore, the atmospheric contaminants are generally accumulated and deposited on the main streets, nearby their sources.

2.3.4 Characteristics of detachable particles in surface runoffs

Water flow samples have been collected at a manhole in the studied urban catchment using a peristaltic pump (Watson Marlow), which pumped 250 mL of water at regular volume intervals entering the manhole (Hong et al., 2016b). For each rainfall event, the measured TSS concentration in the stormwater sample can be considered the same as the mean TSS concentration in the total surface runoff. By assuming that the initial dry deposits is equal to the amount of detachable particles

which can be afterward found in stormwater runoffs, the surface dry deposits can be estimated by Eq. 9:

$$Deposit_{dry} = \frac{Conc_{TSS} * Volume_{manhole}}{Area_{manhole}} \qquad (9)$$

Where $Deposit_{dry}$ is the experimentally estimated initial dry deposits for the urban catchment (g/m^2); $Conc_{TSS}$ is the mean TSS concentration of the stormwater runoff sample (g/L); $Volume_{manhole}$ is the total volume of stormwater runoffs collected in the sampling manhole (L); and $Area_{manhole}$ is the drainage area of the urban surface contributing to the sampling manhole (m^2).

The experimentally estimated urban dry deposits for the sampled rainfall events are presented in Fig. 5a, the average value is 1 g/m². Granulometric analysis was performed in the laboratory to evaluate the Particle Size Distribution (PSD) of the suspended particles (Bechet et al., 2015). The PSD and the accumulated percentage of suspended solids are presented in Fig. 5b. Since the air quality component only simulates the dispersion and depositions of PM10 (< 10µm particles), particles are separated into two different classes. That the first represents the PM10 (noted fine particles), with the median size (D50) equals to 5 μm; while the second stands for the > 10µm particles (noted coarse particles), which D50 is equal to 25 μm.

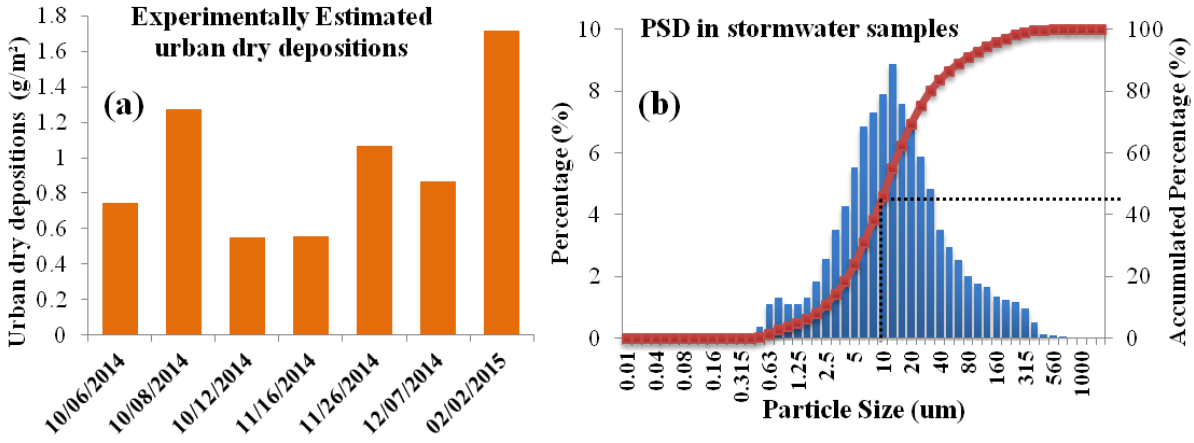

Fig. 5 (a) Experimentally estimated urban dry deposits of detachable particles (for both fine and coarse particles). (b) Particle Size Distribution (PSD) of the suspended particles in urban stormwater runoffs.

2.3.5 Cu, BaP and BbF Contents of different particle classes

Based on the simulated mass of atmospheric dry depositions of different pollutants (Fig. 4), the Cu, BaP and BbF contents of fine particles can be calculated (Eq. 10). In order to assess the concentration of such pollutants in urban stormwater samples, Cu was analyzed by an inductively Coupled Plasma – Mass Spectrometry (ICP-MS), while the PAHs were determined by a high performance liquid chromatography (HPLC) coupled with UV fluorescence assay. Therefore, the Cu, BaP and BbF contents of TSS (average sized) can be calculated (Eq. 11). Considering that the fine particles and coarse particles represent 45% and 55% of the TSS, respectively (Fig. 5b), the pollutants content of coarse particles can be calculated with Eq. 12. The Cu, BaP and BbF contents of different classes of particles are represented in Table 2.

Table 2 Mean Cu, BaP and BbF contents of fine particles (< 10µm), TSS (all particle sizes mixed), and coarse particles (> 10µm).

	Cu Content (µg/g)	BaP Content (ng/g)	BbF Content (ng/g)
Fine particles (< 10µm)	936.08	1734.80	1981.01
TSS (All particle sizes mixed)	541.82	920.84	1176.05
Coarse Particles (> 10µm)	219.24	254.88	517.44

$$Content_{fine,pollut} = \frac{depot_{pollut}}{depot_{PM10}} \quad (10)$$

$$Content_{TSS,pollut} = \frac{conc_{pollut}}{conc_{TSS}} \quad (11)$$

$$Content_{coarse,pollut} = \frac{\left(Content_{TSS,pollut} - 45\% * Content_{fine,pollut}\right)}{55\%} \quad (12)$$

Where $Content_{fine,pollut}, Content_{coarse,pollut}, Content_{TSS,pollut}$ are the pollutant (Cu, BaP, BbF) content of fine particles, coarse particles and TSS (All particle sizes mixed), respectively; $conc_{pollut}, conc_{TSS}$ are the measured concentration of pollutants (Cu, BaP, BbF) and TSS in stormwater samples, respectively; $depot_{pollut}, depot_{PM10}$

are the atmospheric dry depositions of pollutants (Cu, BaP, BbF) and PM10, respectively.

2.3.6 Configuration of parameters for urban areas

Table 3 Parameter values for the integrated air-surface-sewer modelling

Water quantity parameters		
	Impervious surface (road, sidewalk, etc...)	Pervious areas (grass, trees, etc...)
Rainfall interception (Smax, mm)	0	1
Random roughness (cm)	0.3	0.7
Initial moisture content (cm^3/cm^3)	0.1	0.4
Porosity (cm^3/cm^3)	0.1	0.5
Critical stream power for erosion (cm/s)	0.4	0.4
Initial loss of roof wetting (mm)	1	
Manning's N for sewer networks	0.014	
Manning's N for virtual sub-basins	0.012	
Manning's N values for surface runoffs	1 calibrated value for all the rainfall events	Idem
Saturated conductivities (mm/hr)	1 calibrated value for all the rainfall event	Idem
Water quality simulations		
Re-entrainment parameter	0.013	None
Critical flow velocity for detachment (m/s)	0.004	None
Washoff coefficient for virtual sub-basins	0.32	
Washoff exponent for virtual sub-basins	0.43	
Cohesion coefficient	1 calibrated value for every rainfall event	Idem

In order to reduce the calibration efforts, several parameter values are determined from bibliographic works. As for water quantity simulations, the rainfall interceptions for different urban landuses are defined by considering the canopy interception

values of (Xiao et al., 1998); the random roughness values are defined as (Zobeck and Onstad, 1987); besides, in accordance with (Rossman, 2010), we fixed three parameters for (Green and Ampt, 1911) method such as porosity, initial moisture content and average suction at wetting front, as well as three parameters used in the sewer network module, including the initial loss of roof wetting, the Manning's N for conduits and virtual sub-basins. As for the water quality part, the aggregate stability is defined following (Jetten and Roo, 2001); the re-entrainment parameter of the H-R equations is decided the same as (Hairsine and Rose, 1992); the critical flow velocity for detachment is explained as (Rauws and Govers, 1988); and two washoff-coefficients of the virtual sub-basins are determined from (Rossman, 2010).

Contrarily, calibrations are performed for three parameters using the trial-and-error method. For the water quantity modelling, the Manning's N value for surface runoffs and the saturated conductivities (Ksat) are calibrated for the event of 26th of November 2014, and then validated for the other studied rainfall events. While for the water quality modelling, the cohesion coefficient (*coh*) is calculated for each rainfall event. The parameter values are listed in Table 3

2.4 Simulation scenarios

Table 4, Initial dry deposits of the two scenarios.

	Scenario 1 (experimentally estimated)	Scenario 2 (simulated)
Initial deposits of fine particles on roads (g/m²)	0.45	Atmospheric simulations
Initial deposits of fine particles on roofs (g/m²)	0.45	Atmospheric simulations
Initial deposits of coarse particles on roads (g/m²)	0.55	0.55
Initial deposits of coarse particles on roofs (g/m²)	0	0

Since the dry deposits of coarse particles are usually caused by direct depositions, such as surface abrasion and tyre wear. The air quality component only simulates the atmospheric dry depositions of fine particles (PM10). Therefore, the experimentally estimated dry deposits (Fig. 5) of coarse particles are used in the model as the input data. Consequently, two modelling scenarios are tested in this study: Scenario 1 uses the experimentally estimated urban dry deposits for both fine and coarse particles; Scenario 2 uses the simulated atmospheric dry depositions for the fine particles, while the dry deposits of coarse particles follow the experimentally estimated values. The initial dry deposits of the two scenarios are presented in Table 4.

3. Results and discussions

3.1. Water flow simulations

Accurate water quantity simulations are required for reliable water quality modelling. The trial and error procedure is performed for calibrating the Manning's N and the saturated conductivities (K_{sat}), in order to precisely reproduce the dynamics of water flow at the catchment outlet. Parameters are calibrated for the event of 26th of November 2014, and then validated for the other studied rainfall events. The Root-Mean-Square-Error (RMSE) coefficient (Eq. 12) is used to evaluate the model performance. The optimized Manning's N is equal to 0.012 and 0.2 for the impervious and pervious surfaces, respectively. The calibrated K_{sat} is equal to 0.1 and 25 mm/hr for the impervious and pervious surfaces, respectively. The simulated water flow is compared with the continuous measurements at the catchment outlet (Fig. 6).

$$RMSD = \sqrt{\frac{\sum_{t=1}^{n}(Sim_t - Obs_t)^2}{n}} \qquad (12)$$

where n is the simulation duration, Sim_t and Obs_t are the simulated and observed TSS concentration at the *t-th* minute.

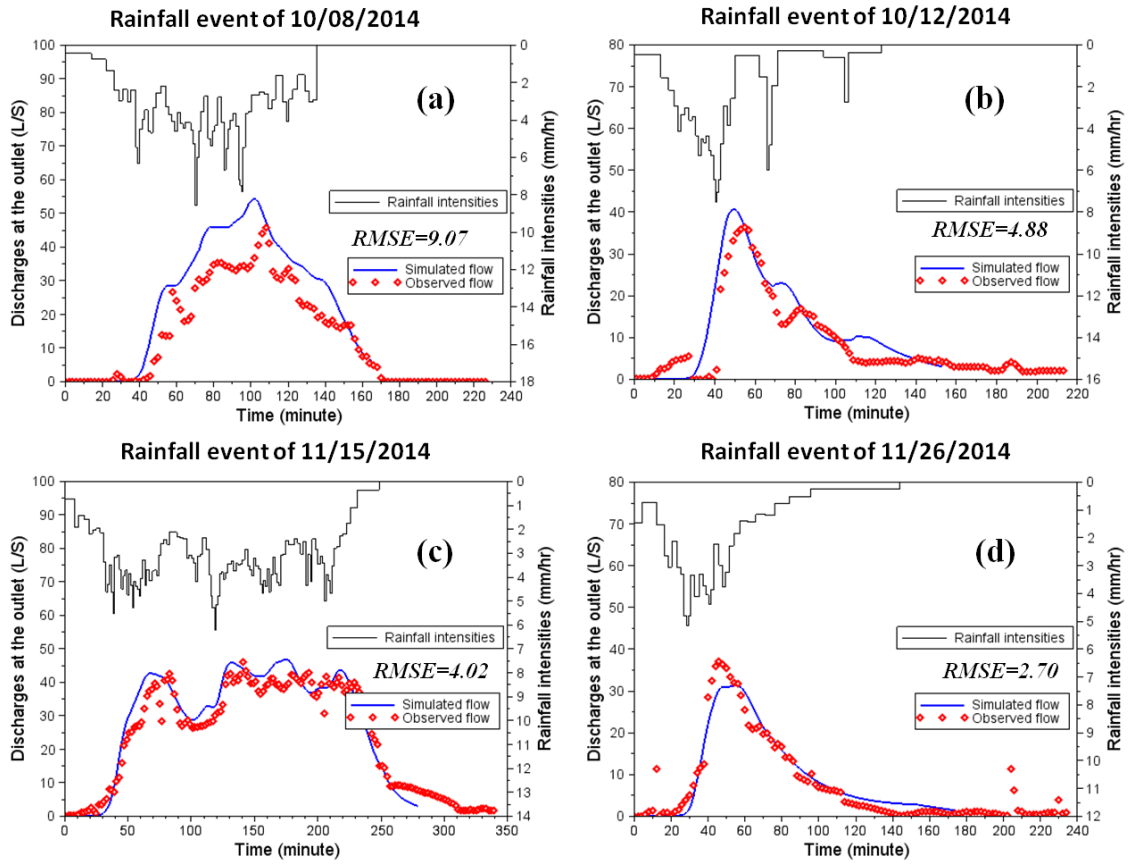

Fig. 6 Water flow simulations using the integrated modelling approach. The simulated discharges at the network outlet (solid blue lines) are compared with the measured data (red circles). Rainfall is plotted on the upper part. For events (a) 8th of October 2014; (b) 12th of October 2014; (c) 15th of November 2014; (d) 26th of November 2014.

As shown in Fig. 6, the performance of the quantitative simulations is quite satisfying with RMSE varying between 2.70 and 9.07. This result confirms that using such a spatially-distributed, integrated model is accurate for the water flow simulations at the scale of a small urban catchment.

3.2. Simulations of Total Suspended Solids (TSS)

Simulations using different initial dry deposits (Scenario 1 and 2) are performed for the four studied rainfall events. Since the surface conditions (humidity, heat, etc.) of

the urban catchment can be different from one event to another, the cohesion coefficient (*coh*) is calibrated for each studied rainfall event using the trial-and-error method. The simulated TSS concentrations are compared with the measurements at the catchment outlet. Simulations of Scenario 1 and Scenario 2 are shown in Fig. 7 - 8, respectively. The calibrated values of *coh* are presented in Table 5.

Table 5 Calibrated cohesion coefficient (*coh*) values (*kPa*).

coh (kPa)	Oct. 8 2014	Oct. 12 2014	Nov. 15 2014	Nov. 26 2014
Scenario 1	13	10	13	13
Scenario 2	12	10	10	12

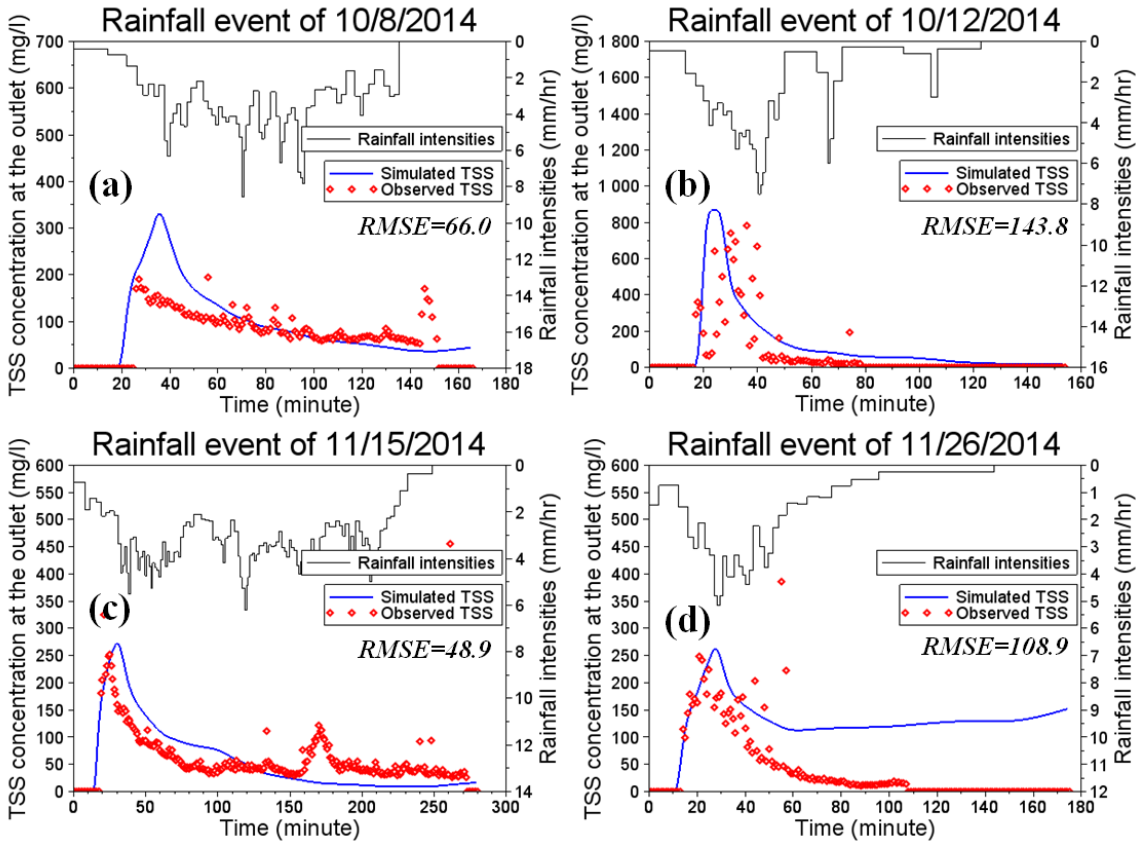

Fig. 7 Total Suspended Solids (TSS) concentration of Scenario 1 simulations (measured initial deposits). The simulated TSS concentrations at the network outlet (solid blue lines) are compared with the measured data (red circles). Rainfall is

plotted on the upper part. For events (a) 8th of October 2014; (b) 12th of October 2014; (c) 15th of November 2014; (d) 26th of November 2014.

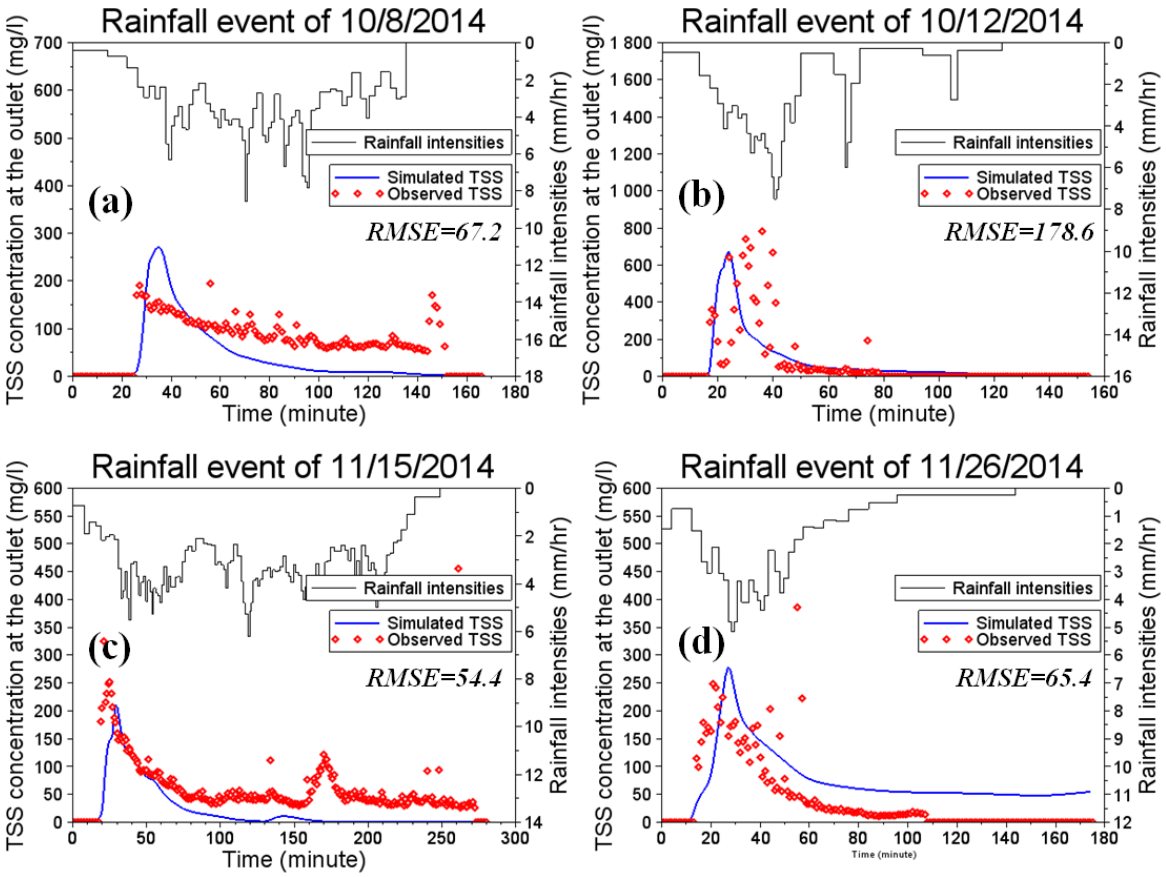

Fig. 8 Total Suspended Solids (TSS) concentration of Scenario 2 simulations (simulated initial deposits). The simulated TSS concentrations at the network outlet (solid blue lines) are compared with the measured data (red circles). Rainfall is plotted on the upper part. For events (a) 8th of October 2014; (b) 12th of October 2014; (c) 15th of November 2014; (d) 26th of November 2014.

As can be seen in Fig. 7 and Fig. 8, simulated concentrations of TSS generally fit well with the continuous measurements, especially for the amptitude and the time to the first peak. The RMSE values vary from 48.9 to 178.6, being of the same order as the uncertainty of the experimental measurements. These results confirm the good performance of using the presented modelling approach to simulate TSS dynamics in the urban context. Comparing with our previous work which used the USLE

equations (Kinnell, 2010) to simulate urban sediment erosions (Hong et al., 2015a, 2015b), this paper is undoubtly an improvement of stormwater quality simulations for urban areas.

In spite of the good performance of the TSS simulations, it should be mentioned that the calibrated *coh* values are not steady between the different scenarios and rainfall events. Generally, the calibrated *coh* for Scenario 2 are lower than that of Scenario 1. This phenomenon is due to the fact that the simulated atmospheric deposits are lower than the experimentally estimated dry depositions. As a consequence, lower *coh* values are calibrated for Scenario 2 simulations. Nevertheless, the calibrated *coh* for the both two scenarios correspond with the typical values of the non-cohesive solids (Geotechdata.info, 2014). Considering the uncertainties of the parameter values related to water quality simulations (Dotto et al., 2012; Fletcher et al., 2013), the present study provides encouraging results in the field of urban stormwater quality modelling.

It should be indicated that although the spatial distribution of the atmospheric dry deposits is different from Scenario 1 to Scenario 2, however, quite similar simulations of TSS concentration are obtained at the outlet of the urban catchment. This phenomenon may be explained by the "first flush" effects of the studied rainfall events. Since most pollutants are eroded at the beginning of the rainfall events, the impacts of the spatially-distributed dry deposits are not significant at the scale of the catchment outlet. Nevertheless, the effects of the spatial distribution of atmospheric dry depositions may be further assessed by experimental measurements by sampling manholes at different locations of the urban catchment. That model assessment can lead to develop advanced stormwater management strategies, such as filter systems located at the determined locations of the urban catchement, to reduce the traffic-related pollutants entering the sewer networks. This type of source-control techniques are easy to implement and can be effective and cheap.

Furthermore, in order to assess the dynamics of the two classes of particles for different scenarios, the evolution of the fractions of the fine and coarse particles of TSS for Scenario 1 and 2 are compared in Fig. 9:

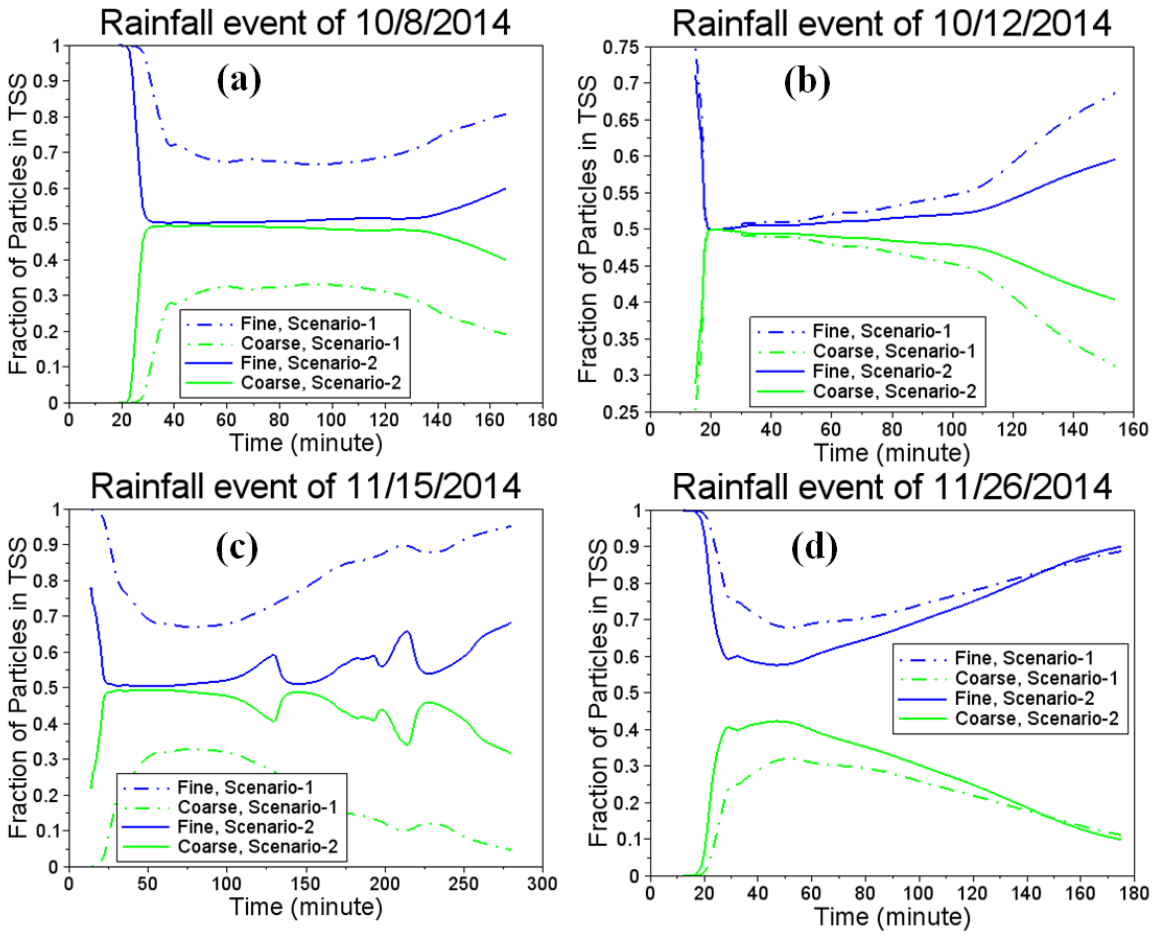

Fig. 9 Proportion of the fine particles (D50 = 5um, blue lines) and the coarse particles (D50=25um, green lines) in Total Suspended Solids. Scenario 1 is plotted in dash-dotted lines, and Scenario 2 is plotted in solid lines. For events (a) 8th of October 2014; (b) 12th of October 2014; (c) 15th of November 2014; (d) 26th of November 2014.

The fraction of fine particles in TSS in Scenario 1 is higher than in Scenario 2. This result is in agreement with the above findings, that the simulated dry deposits of PM10 are lower than the experimentally estimated values. For both scenarios, the fine particles are firstly eroded at the beginning of the rainfall events, while the fraction of coarse particles in TSS rapidly increases with the rise of rainfall intensities. For the events of 8th of October 2014 and 15th of November 2014 (Fig. 12 a, c), due to the steady rain throughout the rainfall event, the fractions of the different particle classes in TSS remain stable. On the contrary, for the events of 12th of October 2014

and 26th of November 2014 (Fig. 12 b, d), the fraction of coarse particles in TSS significantly decreases with the reduction of rainfall intensities.

It should also be mentioned that in both scenarios, the dry deposits used in the model cannot completely represent the real conditions of the urban surface. On the one hand, it is quite difficult to assess the exact mass of initial dry deposits on urban surfaces. In fact, (Bechet et al., 2015) showed that the variation range of the total mass of different road deposit samples is close to a factor 10. Therefore, our first scenario which takes into account the averaged deposit mass, has to be questioned regarding to the spatial variability of the urban catchment. On the other hand, atmospheric model outputs are also affected by large uncertainties, such as the atmospheric concentrations, the climate data and the dry deposition velocities. The simulated dry deposits of Scenario 2 are therefore not representative of the precise mass of particles for each grid-cell. In spite of all these uncertainties and approximations, this paper challenges for the first time the new field of integrated 2D air-surface-sewer urban stormwater quality modelling with reasonable assumptions. Moreover, the model performance can be further discussed by comparing the simulated concentrations of traffic-related pollutants (Cu, BaP and BbF) for the two studied scenarios as well as the local measurements.

3.3. Simulations of Cu, BaP and BbF

Considering the Cu, BaP and BbF contents of fine and coarse particles (Table 2), the dynamics of pollutant concentrations at the catchment outlet can be evaluated. The simulated pollutant concentrations (Cu, BaP and BbF) of Scenario 1 and Scenario 2 are presented in Fig. 10-11. Benefitting from the measurements of event mean concentrations of Cu, BaP and BbF in stormwater runoff samples (section 2.3.5), the simulated concentrations of such pollutants can be compared with the observed values (Fig. 12).

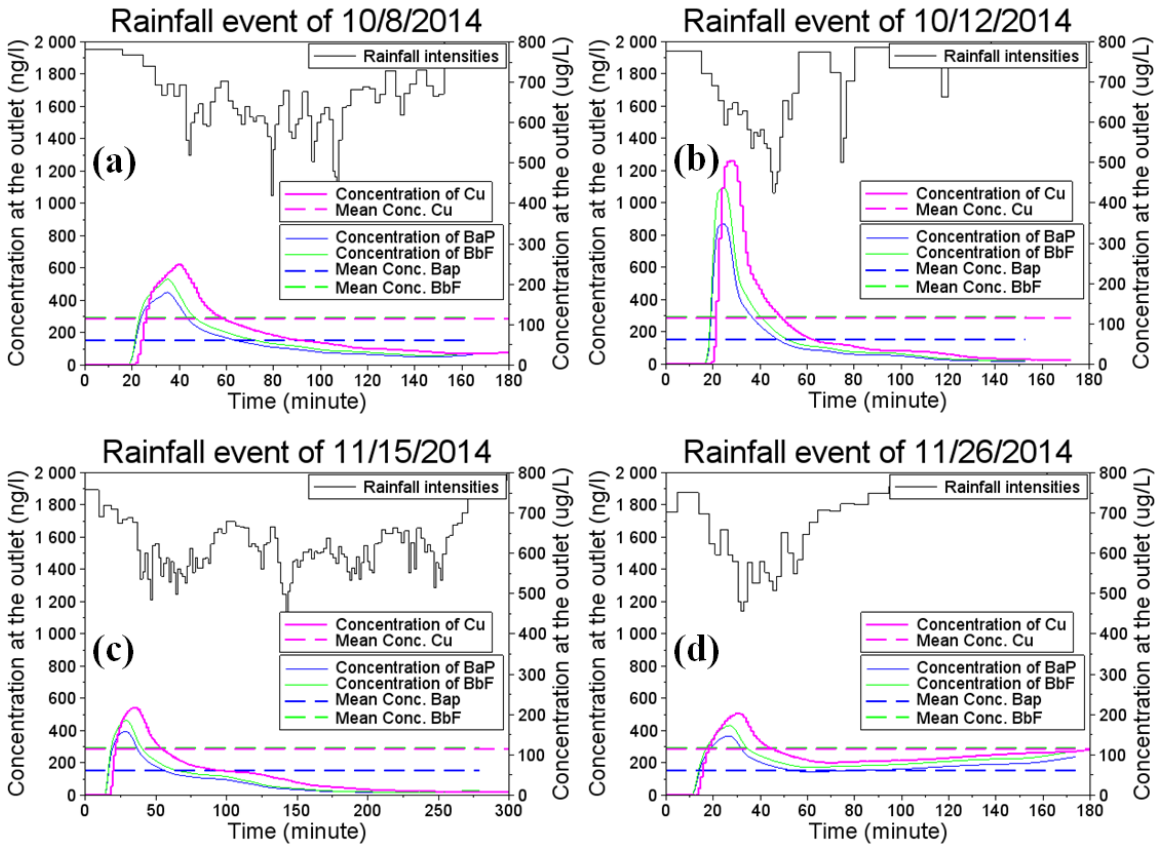

Fig. 10 Concentrations of Cu (µg/L, right y-axis), BaP (ng/L, left y-axis) and BbF (ng/L, left y-axis) for Scenario 1. The simulated Cu (solid magenta lines), BaP (solid blue lines) and BbF (solid green lines) concentrations are compared with the measured mean concentration of Cu (dashed magenta lines), BaP (dashed blue lines) and BbF (dashed green lines) (ng/L). Rainfall is plotted on the upper part. For events (a) 8th of October 2014; (b) 12th of October 2014; (c) 15th of November 2014; (d) 26th of November 2014.

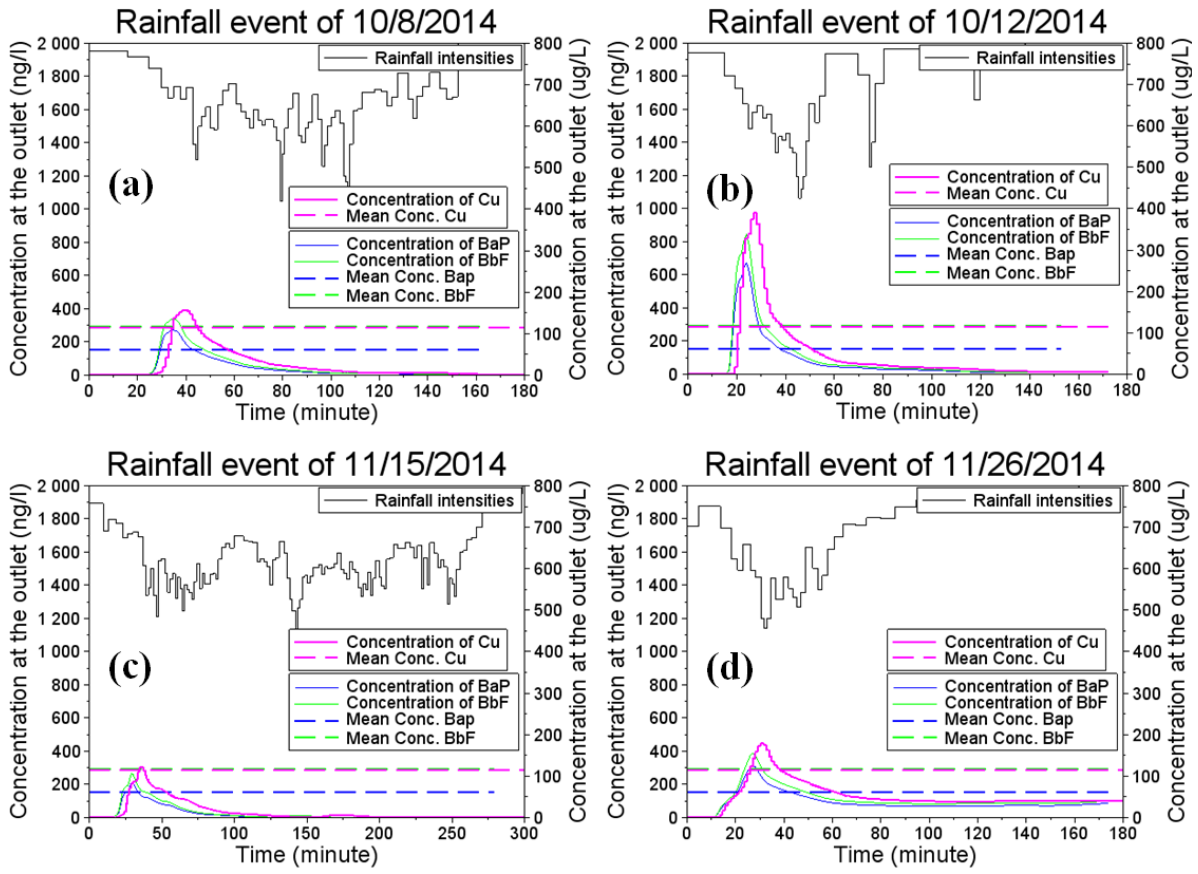

Fig. 11 Concentrations of Cu (µg/L, right y-axis), BaP (ng/L, left y-axis) and BbF (ng/L, left y-axis) for Scenario 2. The simulated Cu (solid magenta lines), BaP (solid blue lines) and BbF (solid green lines) are compared with the measured mean concentration of Cu (dashed magenta lines), BaP (dashed blue lines) and BbF (dashed green lines) (ng/L). Rainfall is plotted on the upper part. For events (a) 8th of October 2014; (b) 12th of October 2014; (c) 15th of November 2014; (d) 26th of November 2014.

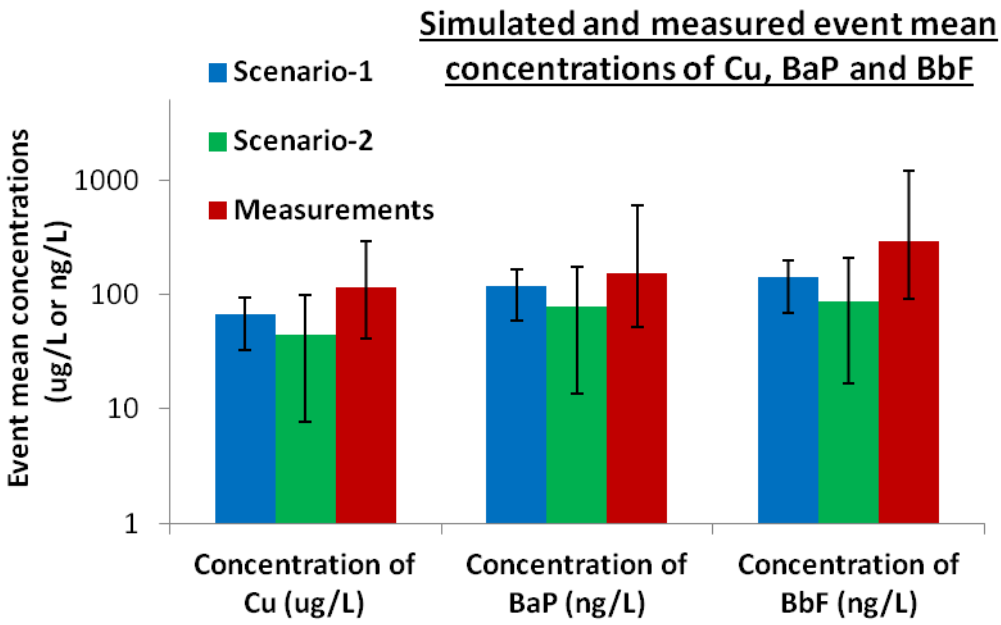

Fig. 12 Simulated and measured event mean concentrations of Cu, BaP and BbF (all particle size mixed)

Considering the large uncertainties in measurements of heavy metals and PAHs (Bechet et al., 2015), the Fig. 10-12 show that both scenarios give realistic results comparing with the measurements of pollutants in stormwater runoff samples. These encouraging results confirm the validity of using the presented modelling approach for simulating the transfer of traffic-related pollutants from air to the sewer outlet.

Nevertheless, it should be noted that the simulated concentrations of pollutants in Scenario 2 are always less than that in Scenario 1. This can be explained by the higher fractions of fine particles in TSS for Scenario 1 (Fig. 8). Since the pollutants are preferred to attach to fine particles (Table. 2), TSS of Scenario 1 can transport more associated pollutants. Analyzing the outputs of the air quality component (used in Scenario 2) for the four studied rainfall events, the averaged atmospheric dry deposits of PM10 for the entire urban catchment is equal to 0.055 g/m². This value is far below the estimated mass of the fine particles from the stormwater runoff samples (used in Scenario 1), which is equal to 0.45 g/m². This result can be mainly explained by three reasons: (i) Stormwater runoff samples are collected in a manhole along the road. Since there are more deposited particles on roads than on other types of urban landuses, the experimentally estimated dry deposits for the entire urban catchment is

hence overestimated for Scenario 1. (ii) The air quality simulations do not take into account the background atmospheric pollution, the PM10 deposits in Scenario 2 are certainly underestimated in this study. (iii) The precipitation inputs used in the air quality component are based on a prediction model of MeteoFrance (AROME model, www.meteofrance.fr). With such a meteorological model, insignificant precipitations (< 1mm), which are usually not recorded by the rain gauge, are considered as wet weather periods. These wet weather simulations further decrease the simulated dry deposits in Scenario 2.

Finally, uncertainties for the pollutants content of PM10 (Table. 2) should also be mentioned. Due to the uncertainties in rainfall event simulations, deposition velocities, and particle size distributions, the variation range for the simulated atmospheric deposits of pollutants can easily reach a factor 2 to 4 (Shorshani et al., 2015). Therefore, the results in Fig. 12 are quite acceptable for the modelling of heavy metals and PAHs in the urban context.

4. Conclusion and perspective

In this paper, an integrated air-surface-sewer modelling approach is for the first time developed to assess the transfer of traffic-related pollutants in urban areas during rainfall events. The modelling system consists of three separated components, including the air quality component, the 2D surface component, and the roof and sewer network component. For the air quality component, the SIRANE model (Soulhac et al., 2011) is coupled with realistic traffic data to generate spatially-distributed atmospheric dry depositions; in the 2D-surface component, the openLISEM model (De Roo et al., 1996; Jetten and Roo, 2001) is applied to simulate the transfer of water and particulate pollutants on roads and green areas; in the roof and sewer network component, building roofs are considered as virtual sub-basins which are directly connected to the sewer networks, the SWMM model (Rossman, 2010) is used to simulate the transport of water and pollutants from roofs and manholes to the outlet of drainage networks.

The integrated modelling platform is applied to a small urban catchment near Paris (12 ha, Le Perreux sur Marne, Val de Marne, France). Simulation results are

compared with continuous measurements of water flow and total suspended solids (TSS) at the catchment outlet. The performance of the quantitative simulation is highly satisfying with calibrated and validated parameter values of Manning's N and saturated conductivity (K_{sat}). As for the water quality modelling, two modelling scenarios are performed: Scenario 1 uses experimentally estimated dry deposits, which are homogenously distributed on the urban catchment; Scenario 2 uses simulated atmospheric dry depositions, which are spatially-distributed. With a simple calibration of the surface cohesion coefficient (*coh*), the TSS concentration simulations fit well with the observations for both scenarios. Nevertheless, no significant difference can be noticed at the catchment outlet between the two scenarios. This phenomenon is mainly due to the "first flush" effects of the urban catchment. For the studied rainfall events, since most pollutants are eroded at the beginning of the rainfall events, the spatially-distributed dry deposits have little effect at the scale of the catchment outlet. Therefore, specific experimental surveys such as sampling manholes, should be considered in order to test the modelling performance at different locations of the urban catchment.

Considering the Cu, BaP and BbF contents of different particle classes, the pollutographs of such pollutants are evaluated for each studied rainfall event. The simulated event mean concentrations of pollutants are compared with local in-situ measurements. For the first time, realistic simulations of traffic-related pollutants are achieved at the catchment outlet. Additionally, the differences between the two scenarios as well as the measurements are due to the modelling assumptions and the uncertainties of the atmospheric dry deposits simulations. As a perspective, sensitivity and uncertainty analysis should be considered for this modelling approach.

For the purpose of improving the model performance, the atmospheric background concentration of pollutants and the direct deposition of traffic activities, such as surface abrasion and tyre wear should be simulated. In order to evaluate the model performance in transporting different particle classes and the associated pollutants to the catchment outlet, the sampling at the sewer outlet with granulometric separation would be an important next step. Moreover, since Zinc (Zn) is not significantly associated with suspended particles, the modelling of soluble pollutants with adsorption/desorption processes can be integrated in the future studies.

The main interest in developing such an integrated modelling approach is undoubtedly to be able to understand and to predict the transfer of traffic-related pollutants in urban areas. This innovative work proves the effectiveness of using erosion models for the modelling of urban stormwater quality. Moreover, the present integrated modelling approach could be further coupled with traffic models and pollutant emission models, in order to assess the impacts of different traffic management strategies on urban separate sewer discharges.

Acknowledgement

The research work of PhD student Yi Hong was financed by ANR-Trafipollu project (ANR-12-VBDU-0002) and Ecole des Ponts ParisTech. Firstly, the authors would like to thank F. Mahe and F. Dugay (AirParif) for kindly providing simulation results of atmospheric depositions. The authors would also like to thank B. Béchet (IFSTTAR), B. Soleilhan (IGN) and V. Bousquet (IGN-Conseil) for providing invaluable measurements and GIS data, as well as C. Seigneur and L. Thouron (CEREA) for their helpful advices in the air quality modelling. We also want to give a special thanks to the experimental team of ANR Trafipollu project for all collected necessary for this work, in particular David Ramier (CEREMA), Mohamed Saad (LEESU) and Philippe Dubois (LEESU). Finally, the authors would like to thank OPUR (Observatoire des Polluants Urbains en Ile-de-France) for being a place for exchanging ideas and elaborating collaborations with different researchers from various institutions.

Reference

Aryal, R., Vigneswaran, S., Kandasamy, J., Naidu, R., 2010. Urban stormwater quality and treatment. Korean J. Chem. Eng. 27, 1343–1359. doi:10.1007/s11814-010-0387-0

Bechet, B., Bonhomme, C., Lamprea, K., Campos, E., Jean-soro, L., Dubois, P., Lherm, D., 2015. Towards a modeling of pollutant flux at local scale - Chemical analysis and

micro-characterization of road dusts. Presented at the 12th Urban Environment Symposium, Oslo, Norway.

De Roo, A.P.J., Wesseling, C.G., Ritsema, C.J., 1996. Lisem: A Single-Event Physically Based Hydrological and Soil Erosion Model for Drainage Basins. I: Theory, Input and Output. Hydrol. Process. 10, 1107–1117. doi:10.1002/(SICI)1099-1085(199608)10:8<1107::AID-HYP415>3.0.CO;2-4

Dotto, C.B.S., Mannina, G., Kleidorfer, M., Vezzaro, L., Henrichs, M., McCarthy, D.T., Freni, G., Rauch, W., Deletic, A., 2012. Comparison of different uncertainty techniques in urban stormwater quantity and quality modelling. Water Res. 46, 2545–2558. doi:10.1016/j.watres.2012.02.009

Fewtrell, T.J., Duncan, A., Sampson, C.C., Neal, J.C., Bates, P.D., 2011. Benchmarking urban flood models of varying complexity and scale using high resolution terrestrial LiDAR data. Phys. Chem. Earth Parts ABC, Recent Advances in Mapping and Modelling Flood Processes in Lowland Areas 36, 281–291. doi:10.1016/j.pce.2010.12.011

Fletcher, T.D., Andrieu, H., Hamel, P., 2013. Understanding, management and modelling of urban hydrology and its consequences for receiving waters: A state of the art. Adv. Water Resour. 51, 261–279. doi:10.1016/j.advwatres.2012.09.001

Gallegos, H.A., Schubert, J.E., Sanders, B.F., 2009. Two-dimensional, high-resolution modeling of urban dam-break flooding: A case study of Baldwin Hills, California. Adv. Water Resour. 32, 1323–1335. doi:10.1016/j.advwatres.2009.05.008

Geotechdata.info, 2014. Cohesion. http://www.geotechdata.info/parameter/cohesion.

Green, W.H., Ampt, G.A., 1911. Studies on Soil Phyics. J. Agric. Sci. 4, 1–24. doi:10.1017/S0021859600001441

Gunawardena, J., Egodawatta, P., Ayoko, G.A., Goonetilleke, A., 2013. Atmospheric deposition as a source of heavy metals in urban stormwater. Atmos. Environ. 68, 235–242. doi:10.1016/j.atmosenv.2012.11.062

Hairsine, P.B., Rose, C.W., 1992. Modeling water erosion due to overland flow using physical principles: 2. Rill flow. Water Resour. Res. 28, 245–250. doi:10.1029/91WR02381

Herngren, L., Goonetilleke, A., Ayoko, G.A., 2005. Understanding heavy metal and suspended solids relationships in urban stormwater using simulated rainfall. J. Environ. Manage. 76, 149–158. doi:10.1016/j.jenvman.2005.01.013

Hervieu, A., Soheilian, B., 2013. Semi-Automatic Road/Pavement Modeling using Mobile Laser Scanning. ISPRS Ann. Photogramm. Remote Sens. Spat. Inf. Sci. II-3/W3, 31–36. doi:10.5194/isprsannals-II-3-W3-31-2013

Hong, Y., Bonhomme, C., Chebbo, G., 2015a. Using 2D/1D model for urban stormwater pollution, in: Proceedings-Oral Presentations Part II. Presented at the 10th International Urban Drainage Modelling Conference, Québec, Canada, pp. 229–234.

Hong, Y., Bonhomme, C., Le, M.-H., Chebbo, G., 2016a. New insights into the urban washoff process with detailed physical modelling. Sci. Total Environ. 573, 924–936. doi:10.1016/j.scitotenv.2016.08.193

Hong, Y., Bonhomme, C., Le, M.-H., Chebbo, G., 2016b. A new approach of monitoring and physically-based modelling to investigate urban wash-off process on a road catchment near Paris. Water Res. 102, 96–108. doi:10.1016/j.watres.2016.06.027

Hong, Y., Giangola-Murzyn, A., Bonhomme, C., Chebbo, G., Schertzer, D., 2015b. Urban water-quality modelling: implementing an extension to Multi-Hydro platform for real case studies, in: EGU General Assembly Conference Abstracts. Presented at the EGU General Assembly Conference Abstracts.

Huston, R., Chan, Y.C., Gardner, T., Shaw, G., Chapman, H., 2009. Characterisation of atmospheric deposition as a source of contaminants in urban rainwater tanks. Water Res. 43, 1630–1640. doi:10.1016/j.watres.2008.12.045

Jetten, V.G., Roo, A.P.J. de, 2001. Spatial Analysis of Erosion Conservation Measures with LISEM, in: Harmon, R.S., III, W.W.D. (Eds.), Landscape Erosion and Evolution Modeling. Springer US, pp. 429–445.

Kinnell, P.I.A., 2010. Event soil loss, runoff and the Universal Soil Loss Equation family of models: A review. J. Hydrol. 385, 384–397. doi:10.1016/j.jhydrol.2010.01.024

Lim, L.L., Hughes, S.J., Hellawell, E.E., 2005. Integrated decision support system for urban air quality assessment. Environ. Model. Softw. 20, 947–954. doi:10.1016/j.envsoft.2004.04.013

Oxley, T., Dore, A.J., ApSimon, H., Hall, J., Kryza, M., 2013. Modelling future impacts of air pollution using the multi-scale UK Integrated Assessment Model (UKIAM). Environ. Int. 61, 17–35. doi:10.1016/j.envint.2013.09.009

Pant, P., Harrison, R.M., 2013. Estimation of the contribution of road traffic emissions to particulate matter concentrations from field measurements: A review. Atmos. Environ. 77, 78–97. doi:10.1016/j.atmosenv.2013.04.028

Paparoditis, N., Papelard, J.-P., Cannelle, B., Devaux, A., Soheilian, B., David, N., Houzay, E., 2012. Stereopolis II: A multi-purpose and multi-sensor 3D mobile mapping system for street visualisation and 3D metrology. Rev. Fr. Photogrammétrie Télédétection 69–79.

Petrucci, G., Gromaire, M.-C., Shorshani, M.F., Chebbo, G., 2014. Nonpoint source pollution of urban stormwater runoff: a methodology for source analysis. Environ. Sci. Pollut. Res. Int. 21, 10225–10242. doi:10.1007/s11356-014-2845-4

Rauws, G., Govers, G., 1988. Hydraulic and soil mechanical aspects of rill generation on agricultural soils. J. Soil Sci. 39, 111–124. doi:10.1111/j.1365-2389.1988.tb01199.x

Rossman, lewis A., 2010. Storm water management model user's manual version 5.0. National risk management research and development U.S. environmental protection agency, Cincinnati, OH 45268.

Sabin, L.D., Hee Lim, J., Teresa Venezia, M., Winer, A.M., Schiff, K.C., Stolzenbach, K.D., 2006. Dry deposition and resuspension of particle-associated metals near a freeway in Los Angeles. Atmos. Environ. 40, 7528–7538. doi:10.1016/j.atmosenv.2006.07.004

Sartor, J.D., Boyd, G.B., Agardy, F.J., 1974. Water Pollution Aspects of Street Surface Contaminants. J. Water Pollut. Control Fed. 46, 458–467.

Shirley Clark, R.P., 2007. Annotated Bibliography of Urban Wet Weather Flow Literature From 1996 Through 2006.

Shorshani, M.F., André, M., Bonhomme, C., Seigneur, C., 2015. Modelling chain for the effect of road traffic on air and water quality: Techniques, current status and future prospects. Environ. Model. Softw. 64, 102–123. doi:10.1016/j.envsoft.2014.11.020

Shorshani, M.F., Bonhomme, C., Petrucci, G., André, M., Seigneur, C., 2013. Road traffic impact on urban water quality: a step towards integrated traffic, air and stormwater modelling. Environ. Sci. Pollut. Res. 21, 5297–5310. doi:10.1007/s11356-013-2370-x

Soulhac, L., Salizzoni, P., Cierco, F.-X., Perkins, R., 2011. The model SIRANE for atmospheric urban pollutant dispersion; part I, presentation of the model. Atmos. Environ. 45, 7379–7395. doi:10.1016/j.atmosenv.2011.07.008

Tsihrintzis, V.A., Hamid, R., 1997. Modeling and management of urban stormwater runoff quality: a review. Water Resour. Manag. 11, 136–164.

Xiao, Q. (University of C., McPherson, E.G., Simpson, J.R., Ustin, S.L., 1998. Rainfall interception by Sacramento's urban forest. J. Arboric. USA.

Zobeck, T.M., Onstad, C.A., 1987. Tillage and rainfall effects on random roughness: A review. Soil Tillage Res. 9, 1–20. doi:10.1016/0167-1987(87)90047-X

PARTIE IV. Conclusions et Perspectives

Cette thèse s'inscrit dans le cadre du projet ANR Trafipollu. Elle a pour objectif de développer et d'exploiter de nouveaux outils de modélisation de flux de polluants afin d'améliorer la connaissance des processus liés aux polluants par temps de pluie, mais aussi de contribuer au développement d'une chaine de modélisation dédiée au transfert des polluants liés au trafic routier en zone urbaine (chaine de modélisation Trafic-Emission-Air-Eau). Pour répondre à ces objectifs, nous avons collaboré avec des chercheurs de multiples domaines : modélisation du trafic, des émissions, de l'air et nous avons utilisé des modules préalablement conçus pour modéliser l'érosion des bassins versants naturels. Le travail a été effectué à l'Ecole des Ponts, en lien aussi avec l'Université d'Orléans (MAPMO) et l'Université de Twente (ITC, Pays-Bas).

Conclusions

La première étape du travail a consisté en un travail de modélisation à l'échelle locale, en utilisant des données géographiques très détaillées (résolution spatiale centimétrique), ce qui a permis d'améliorer les connaissances des processus physiques liés au lessivage des polluants sur les surfaces urbaines par temps de pluie. La deuxième étape a permis le développement d'une plateforme de modélisation hydrologique de la qualité des eaux urbaines à l'échelle du quartier, couplant un modèle 2D de surface à un modèle 1D de réseau d'assainissement.

A l'échelle locale et du quartier, nous avons réussi à développer dans un contexte urbain des modèles distribués à base physique du transfert des particules et des contaminants associés. Les contaminants étudiés ont été les métaux et les HAP. Au niveau de la modélisation hydrologique quantitative, la performance aux deux échelles est très satisfaisante. Pour la modélisation des matières en suspension, les résultats ont été très satisfaisants à l'échelle locale, et d'un niveau de performance variable d'un évènement à un autre à l'échelle du quartier. La prise en compte des teneurs en polluants a permis de calculer des pollutogrammes en métaux et HAP à partir des concentrations en matières en suspension.

Les différentes analyses de sensibilité conduites aux deux échelles ont mis en évidence l'influence des caractéristiques granulométriques et de vitesses de chute des particules, ainsi que du stock initial des particules mobilisables. A l'échelle du quartier, l'occupation du sol apparait comme le facteur le plus important vis-à-vis des résultats de sortie.

Pour ce qui concerne l'analyse des résultats obtenus par les modèles, le détachement par les gouttes de pluie est prépondérant sur les surfaces urbaines observées (facteur 100 en masse entre le détachement par la pluie et par l'advection liée au ruissellement). L'analyse spatiale de la mobilisation des contaminants sur le

bassin versant étudié montre que le processus dominant sur la bande roulée et le trottoir est l'arrachage par les gouttes de pluie alors que dans le caniveau l'entrainement par le flux en deuxième partie d'évènement pluvieux est dominant.

L'analyse de la mobilité des différentes classes de taille modélisées montre que les particules fines sont mobilisées en priorité et transportées en suspension sur tout le bassin versant au début de l'évènement pluvieux, tandis que les particules grossières sont mobilisées puis accumulées dans le caniveau.

Au niveau du quartier, l'utilisation de données entièrement distribuées provenant de sorties de modèles atmosphériques n'est pas déterminante pour la dynamique des polluants à l'exutoire du bassin versant.

Perspectives

Les travaux réalisés relèvent d'un certain nombre de questions qui pourraient faire l'objet de recherches futures. Tout d'abord, il faudrait approfondir l'évaluation de ce type de modèle en acquérant des données sur la variabilité spatiale et temporelle des particules (tailles, vitesses de chute). L'acquisition de données concernant les teneurs en polluants des particules à l'intérieur d'un évènement pluvial permettrait d'améliorer la qualité de reproduction des pollutogrammes en métaux et HAP.

De plus, à l'échelle du quartier, il serait important d'évaluer les résultats de concentrations en micropolluants obtenue, sur des sites de caractéristiques différentes du site étudié et pour lesquels on dispose des données sur la dynamique des MES et de micropolluants pour reconstituer un pollutogramme.

La comparaison des résultats obtenus dans cette thèse à ceux qu'on pourrait obtenir avec d'autres modèles distribués plus conceptuels permettrait d'identifier la réelle plus-value du travail et l'intérêt pour répondre à des questions liées aux changements de longs termes affectant les bassins versants urbains.

Compte tenu de la longueur des calculs et de la quantité de données nécessaires pour la mise en œuvre, il serait important d'évaluer l'intérêt de ce type de modèles à l'échelle des agglomérations urbaines. Dans le cadre du programme OPUR, observatoire des polluants urbains en Ile de France, des réunions de concertation entre chercheurs et opérationnels devraient permettre d'identifier les adaptations et les simplifications à apporter éventuellement pour passer à plus grande échelle. Actuellement, la lourdeur associée à l'utilisation de ce type de modèles pourrait constituer un obstacle à une utilisation opérationnelle, sans la mise en place d'une expertise des chercheurs qui ont participé au développement.

Enfin, les résultats concernant la prise en compte de la contribution spatiale laissent penser à une contribution peu importante des retombées sèches aux flux de polluants dans l'eau. Une exploitation plus profonde des résultats de Trafipollu devrait permettre de préciser la voie de transfert effective de la contamination des eaux de ruissellement. Ce résultat ne doit pas être interprété hâtivement comme un désaveu vis-à-vis des modèles intégrés parce que le trafic peut manifestement être à l'origine d'une part conséquente des particules fines qui se déposent sur les chaussées, par transfert direct en dehors de la voie atmosphérique. Une origine de la dynamique des particules fines sur la chaussée s'impose.